



National Library
of Canada

Bibliothèque nationale
du Canada

Acquisitions and
Bibliographic Services Branch

Direction des acquisitions et
des services bibliographiques

395 Wellington Street
Ottawa, Ontario
K1A 0N4

395, rue Wellington
Ottawa (Ontario)
K1A 0N4

Your file Votre référence

Our file Notre référence

NOTICE

The quality of this microform is heavily dependent upon the quality of the original thesis submitted for microfilming. Every effort has been made to ensure the highest quality of reproduction possible.

If pages are missing, contact the university which granted the degree.

Some pages may have indistinct print especially if the original pages were typed with a poor typewriter ribbon or if the university sent us an inferior photocopy.

Reproduction in full or in part of this microform is governed by the Canadian Copyright Act, R.S.C. 1970, c. C-30, and subsequent amendments.

AVIS

La qualité de cette microforme dépend grandement de la qualité de la thèse soumise au microfilmage. Nous avons tout fait pour assurer une qualité supérieure de reproduction.

S'il manque des pages, veuillez communiquer avec l'université qui a conféré le grade.

La qualité d'impression de certaines pages peut laisser à désirer, surtout si les pages originales ont été dactylographiées à l'aide d'un ruban usé ou si l'université nous a fait parvenir une photocopie de qualité inférieure.

La reproduction, même partielle, de cette microforme est soumise à la Loi canadienne sur le droit d'auteur, SRC 1970, c. C-30, et ses amendements subséquents.

THE UNIVERSITY OF ALBERTA

THE RYCROFT LANDSLIDE DAM ON THE SADDLE RIVER, ALBERTA

BY

TIMOTHY R. KEEGAN



A THESIS

SUBMITTED TO THE FACULTY OF GRADUATE STUDIES AND RESEARCH

IN PARTIAL FULFILMENT FOR A DEGREE OF

MASTER OF SCIENCE

GEOTECHNICAL ENGINEERING

DEPARTMENT OF CIVIL ENGINEERING

EDMONTON, ALBERTA

FALL, 1992



National Library
of Canada

Bibliothèque nationale
du Canada

Canadian Theses Service Service des thèses canadiennes

Ottawa, Canada
K1A 0N4

The author has granted an irrevocable non-exclusive licence allowing the National Library of Canada to reproduce, loan, distribute or sell copies of his/her thesis by any means and in any form or format, making this thesis available to interested persons.

The author retains ownership of the copyright in his/her thesis. Neither the thesis nor substantial extracts from it may be printed or otherwise reproduced without his/her permission.

L'auteur a accordé une licence irrévocable et non exclusive permettant à la Bibliothèque nationale du Canada de reproduire, prêter, distribuer ou vendre des copies de sa thèse de quelque manière et sous quelque forme que ce soit pour mettre des exemplaires de cette thèse à la disposition des personnes intéressées.

L'auteur conserve la propriété du droit d'auteur qui protège sa thèse. Ni la thèse ni des extraits substantiels de celle-ci ne doivent être imprimés ou autrement reproduits sans son autorisation.

ISBN 0-315-77297-2

Canada

ABSTRACT

A 40 million m³ landslide dammed the Saddle River 12 km northeast of Rycroft on or about June 17, 1990. The Saddle River valley is 1 km wide and 100 m deep at the landslide, the walls of the valley slope at 11° down to the river which is 30 to 40 m wide. About 13 hectares of tilled land were lost at the prairie level as the valley crest retrogressed up to 200 m to a 1 km long, 15 to 25 m high scarp. The landslide dam was formed by upward rotation at the toe of the slope. By October, 1990 a 4 km long lake, up to 22 m deep and containing 4 Mm³ of water was impounded. Overtopping of the dam began in April, 1991 as a result of spring run off and has continued intermittently through the first year with some erosion. The river at the landslide is degrading close to the thalweg of a buried preglacial channel. The displaced mass involves glacial lake deposits, till and preglacial lake clay. The preglacial lake clay, seen as a weak layer at depth, is the main factor accounting for the large size and mobility of the landslide. The reactivated, retrogressive, compound earth-slide followed an intense rainstorm which produced 1 in 50 year flows in the Saddle River of 667 m³/sec at midnight on 11 June. The river profile shows that the post-glacial Saddle River is still actively degrading. The landslide occurred as the river cut into preglacial lake clays and is the result of a transition from a stable slope governed by the strength of the till, to one governed by the weaker strength of the preglacial lake clay. Laboratory tests indicate the till is medium plastic, normally consolidated and stiff to very stiff and the preglacial lake clay is normally consolidated and anisotropic in strength, highly plastic, stiff and fissured and exhibits significant strain softening. General slip surface limit equilibrium stability analyses confirm the assumed parameters of the pre-slide slope by indicating a factor of safety near unity for the initial rupture surface. The initial rupture surface formed a scarp 50 m back of the valley crest and then retrogressed to form the present main scarp. A 3-D stability analysis shows there is a 6% increase in the factor of safety due to 3-D effects. A post-slide stability analysis indicates that the displaced mass is now more stable.

ACKNOWLEDGEMENTS

This M.Sc. thesis received considerable assistance from many individuals and organizations. Firstly I am indebted to my supervisors Dr. Dave Cruden and Dr. Stan Thomson. Without their ongoing support, constructive criticism and encouragement this thesis would never have gotten off the ground. It is worth mentioning that it is the enthusiasm of these individuals along with their good standing in the geotechnical community that drives research efforts on significant landslide issues in Alberta like the Rycroft Landslide. I would like to also thank Dr. D. Cruden for suggesting this project and for teaching me the powerful use of careful observation in approaching geotechnical problems. Field work expenses were funded by NSERC funds granted to Dr. D. Cruden and research assistance for the 1991- 1992 spring sessions was funded by an NSERC grant awarded to Dr. S. Thomson.

Special thanks to Mr. A. Peterson of the University of Alberta who professionally completed a very tough EDM survey of the Rycroft Landslide in July 1991. My external examiner Dr. R. Rains, and the other members of my defence committee, Dr. D. Cruden, Dr. S. Thomson and Mr. A. Peterson are thanked for their thorough reading and constructive criticism of the thesis.

I would like to thank Alberta Environment for the enormous assistance and keen interest afforded this project throughout. The 1991 field work and subsequent laboratory testing was funded and supported by Alberta Environment Development and Operations and Hydrogeology Divisions and special mention is required for the following individuals. Norm Weimer and John McClung for arranging the funding and their ongoing support in the project. Ron Hansen in the Peace River office for the friendship and support offered in the field work. Fred Aitkin and Don Hopp and their crews for their work in arranging and completing the difficult test drilling at the site in July 1991 and Larry Kolody and his staff at the Alberta Environment geotechnical laboratories for their supervision, assistance and friendship in completing the laboratory testing program.

Additional appreciation is offered to Trudi, Don and the rest of the Durda family for their hospitality, assistance and friendship for the time I spent on their farm completing the field work. I would like to thank Bill MacDonald of Alberta Forestry for arranging the helicopter trip over the landslide, Glen Edwards of Nova for the very useful aerial photographs of the landslide, the

Faculty of Graduates Studies for their assisting me to present the Rycroft Landslide at the Canadian Geotechnical conference in Calgary and, last but not least, Dr. J.D. Mollard who took the time to send his very useful observations, suggestions and support regarding the Rycroft Landslide.

TABLE OF CONTENTS

	Page
Chapter 1: INTRODUCTION	1
Chapter 2: SITE DESCRIPTION AND CLASSIFICATION	4
2.1 Introduction	4
2.2 Site Layout	4
2.3 Landslide Description.....	8
2.4 Reservoir Description.....	12
2.5 Landslide Classification	12
2.6 Summary	16
Chapter 3 GEOLOGY.....	17
3.1 Introduction	17
3.2 Bedrock Geology	17
3.3 Preglacial History	19
3.4 Glacial History.....	22
3.5 Post Glacial History.....	26
3.6 Site Stratigraphy	26
3.7 Summary	29
Chapter 4: SADDLE RIVER HYDROLOGY	30
4.1 Introduction	30
4.2 Saddle River Flood Frequency	30
4.3 June 1990 Rainstorm Event.....	30
4.4 Summary	32

Chapter 5:	SADDLE RIVER MORPHOLOGY AND PHYSIOGRAPHY.....	34
5.1	Introduction	34
5.2	River Profile	34
5.3	Slope Physiography	36
5.4	Overtopping of the Landslide Dams.....	43
5.5	Summary	45
Chapter 6:	LABORATORY TESTING.....	46
6.1	Introduction	46
6.2	Classification Tests.....	46
6.3	Material Properties of the Till.....	49
6.4	Material Properties of the Preglacial Lake Clay	51
6.5	Summary	52
Chapter 7:	STABILITY ANALYSIS	56
7.1	Introduction	56
7.2	Geometry	57
7.3	Mechanism	62
7.4	Strength Parameters.....	65
7.5	Pore Pressure Distribution	67
7.6	Pre-slide Stability	67
7.7	Three-Dimensional Analysis.....	71
7.8	Sensitivity Analysis	73
7.8.1	Erosion of Material at the Toe	73
7.8.2	The Residual Shear Strength in the Preglacial Lake Clay	75

7.8.3	Effective Shear Strength in the Till.....	75
7.8.4	The Phreatic Surface.....	78
7.8.5	Location of the Transition from Peak to Residual Strength in the Preglacial Lake Clay	78
7.9	Post-slide Stability	82
7.10	Summary	84
Chapter 8.	CONCLUSION.....	87
8.1	General	87
8.2	Further Work	88
References	90
APPENDIX A:	Detailed log of testholes RS-1and RS-2	94
APPENDIX B:	Geophysical log testhole RS-1	126
APPENDIX C:	Flood Frequency Analysis	139
APPENDIX D:	Topographic survey of the Rycroft Landslide, July 1991.....	155
APPENDIX E:	Laboratory Test Results	181

LIST OF TABLES

	Page
Table 6.1	Summary of classification test results, Rycroft Landslide Dam 47
Table 7.1	Summary of soil properties used in stability analysis. 66
Table 7.2	Summary of stability analysis. 69

LIST OF FIGURES

	Page
Figure 1.1 Rycroft Landslide Dam location.	3
Figure 2.1 Rycroft Landslide Dam site plan.	5
Figure 2.2 Alberta Government panchromatic air photo AS4088-135 taken at a nominal scale of 1:25,000 on 17 October, 1990 Geographic Air Survey Ltd., Edmonton.	6
Figure 2.3 Overlay on Alberta Government panchromatic air photo AS1996- 76 taken at a nominal scale of 1:15000 on 23 June, 1979. Legend follows Dearman (1972). The 1990 scarp location is from Figure 2.4.	7
Figure 2.4 Overlay on Alberta Government panchromatic air photos AS4088-102, 103 & 104 taken at a nominal scale of 1:5000 on 17 October, 1990. Legend as on Figure 2.3. Within the hatched area, trees are upright and old landslide scarps have not been react	9
Figure 2.5 Dark brown-grey material in the foreground is debris scattered on the riverbed downriver of the landslide dam.	11
Figure 2.6 Classification of landslide movements.	13
Figure 2.7 Histogram of landslide volumes from the Alberta Landslide Inventory.	15
Figure 3.1 Bedrock geology, NTS 83M Map Sheet, Alberta.	18
Figure 3.2 Location of major buried valleys of the Grande Prairie-Peace River area.	20
Figure 3.3 Bedrock topography of the northeast quadrant of NTS 83M, Alberta.	21
Figure 3.4 Preglacial lake clay exposure in the displaced mass near the tip of the landslide.	25
Figure 3.5 Combined simplified borehole log from RS-1 and RS-2. (see Figure 2.4 for location)	27

Figure 4.1	Maximum annual discharges of the Saddle River near the Rycroft Landslide.	31
Figure 4.2	Saddle River Hydrograph	33
Figure 5.2	Typical downstream view of bed armour on river bed, downstream of the landslide.	37
Figure 5.3	Saddle River slope angles, valley crest to river level.	39
Figure 5.4	Oblique aerial photograph downstream of landslide.	40
Figure 5.5	Plan of Saddle River downstream of landslide showing location of dipping clay beds in river bed and identified river terraces.....	41
Figure 5.6	Oblique aerial photograph downstream of confluence of the Spirit River.	42
Figure 5.7	Sketch of river bank exposing post-glacial Saddle River terrace deposits downstream of the Rycroft Landslide Dam.	44
Figure 6.1	Plasticity chart showing range of plasticity at Rycroft Slide.	48
Figure 6.2	Standard and Modified Mohr diagrams for the till.	50
Figure 6.3	Mohr diagram for preglacial lake clay.	54
Figure 6.4	Stress path for consolidated undrained triaxial compression test on preglacial lake clay.	55
Figure 7.1	Pre-slide plan view of the slide area from an overlay on Alberta Government panchromatic air photo taken at a nominal scale of 1:5000 in October, 1990.	59
Figure 7.2	Pre-slide configuration reconstruction along A-A'.	61
Figure 7.3	Configurations along Section A-A' used in the stability analysis of the pre-slide slope.....	64
Figure 7.4	Stability analysis of various potential initial scarp locations for the pre-slide configuration.	70
Figure 7.5	Simplified 3-D configuration of the rupture surface for the 3-D stability analysis.	72

Figure 7.6	Sensitivity analysis: lateral removal of material at the toe.	74
Figure 7.7	Sensitivity analysis: preglacial lake clay, horizontal residual shear strength	76
Figure 7.8	Sensitivity analysis: till, effective shear strength	77
Figure 7.9	Sensitivity analysis: variation of the phreatic surface	80
Figure 7.10	Sensitivity analysis: location of the transition from peak to residual strength in the preglacial lake clay.	81
Figure 7.11	Configuration along section A-A' used in stability analysis of the post-slide slope.	83

CHAPTER 1: INTRODUCTION

With the deglaciation of the Interior Plains occurring less than 9,000 years B.P., the re-established river systems are still mainly degrading. Degradation is the lowering of the surface of land by erosive processes, especially by the removal of material through erosion and transportation by flowing water. Processes of over-steepening, stress release and valley rebound, associated with degradation, and the presence of weak layers, such as bentonite-rich seams in the bedrock of southern Alberta or preglacial lake clays in the Peace River lowlands, result in widespread slope instability in the river valley walls of Alberta. The resulting landslides are a natural step in valley formation during the Quaternary. In Alberta, the river valleys are the site of major industry and cities which depend on the river as a water source and are the location of numerous transportation and pipeline route crossings. An understanding of the processes associated with degradation of Alberta rivers is an essential mandate of the geotechnical engineer.

The study of the Rycroft Landslide Dam is part of an ongoing study of landslides along Alberta rivers undertaken jointly by the University of Alberta and Alberta Environment (Thomson and Morgenstern, 1977) and dedicated to enhancing knowledge of the factors that control the numerous landslides in Alberta's river valleys.

The landslide that dammed the Saddle River, referred to as the Rycroft Landslide Dam, occurred within a day or two of June 17th, 1990, at a location 12 km northeast of Rycroft in northwestern Alberta (Figure 1.1) on the north wall of the Saddle (Burnt) River, a tributary to the Peace River. The volume of the landslide, estimated at 40 million cubic metres, ranks as the largest historic landslide in Alberta. Because the displaced mass dams the river it is also the first historic landslide dam in the Interior Plains of Canada.

The landslide occurred four or five days following a 1 in 50 year rainstorm event in the Saddle River catchment. Approximately 12 hectares of freshly seeded wheat field dropped 15 to 25 metres due to the slide movement. Horizontally, the landslide measures 850 metres from scarp to the toe and it is 1,000 metres wide. The maximum depth to the rupture surface is 100 metres below prairie level. The dam, formed when the toe of the landslide was thrust upward by the slide movement, is 23 metres high at the spillway crest and approximately 800 metres long. By October of 1990, the nearly full reservoir extended 4 kilometres, with a maximum width of 200 metres and depth of 23 metres. Overtopping of the dam occurred with the annual

snowmelt in April, 1991, forming a channel where the displaced mass met the right bank of the river. Only minor erosion of the dam occurred over the first season.

Field reconnaissances of the site were completed by J. McClung of Alberta Environment and S. Thomson and D. Cruden of the Department of Civil Engineering, University of Alberta in July of 1990. The author was made aware of the landslide in April, 1991, and carried out a detailed field mapping in June, July and August, 1991, supported by the University of Alberta and Alberta Environment. A topographic survey of the landslide was conducted in July, 1991 by A. Peterson of the Department of Civil Engineering, University of Alberta. Two testholes, 187 and 120 metres deep were drilled behind the crest of the landslide, by Alberta Environment in July, 1991. Laboratory testing on samples recovered from the site were performed under the supervision of L. Kolody at Alberta Environment's geotechnical laboratories in the autumn of 1991.

The goals of this study of the Rycroft Landslide Dam are to determine the set of conditions that resulted in the large magnitude landslide, establish how these conditions fit into the ongoing interactive processes of the post-glacial Saddle River degradation and test the validity and sensitivity of assumed conditions and the appropriateness of laboratory strength test results and methods of stability analysis. The intended result is an increased understanding of the phenomena and an increased confidence in the prediction and mitigation of these large scale landslides that plague the Peace River lowlands.

The format chosen follows the sequence of the investigation. The thesis initially describes the physical setting of the landslide through a terrain analysis of the landslide and surrounding area. The geology of the site is established by investigating the bedrock geology and topography, the preglacial and glacial history and the test drilling at the site. The degradation processes of the river, as they relate to the Rycroft Landslide, are presented through a study of the hydrology, morphology and physiography of the Saddle River. The classification and material properties of the relevant soil units in the landslide are presented as obtained from the laboratory test program. Finally, the mechanics of the landslide are analyzed using limit equilibrium analyses of the reconstructed pre-slide slope and the post-slide displaced mass.

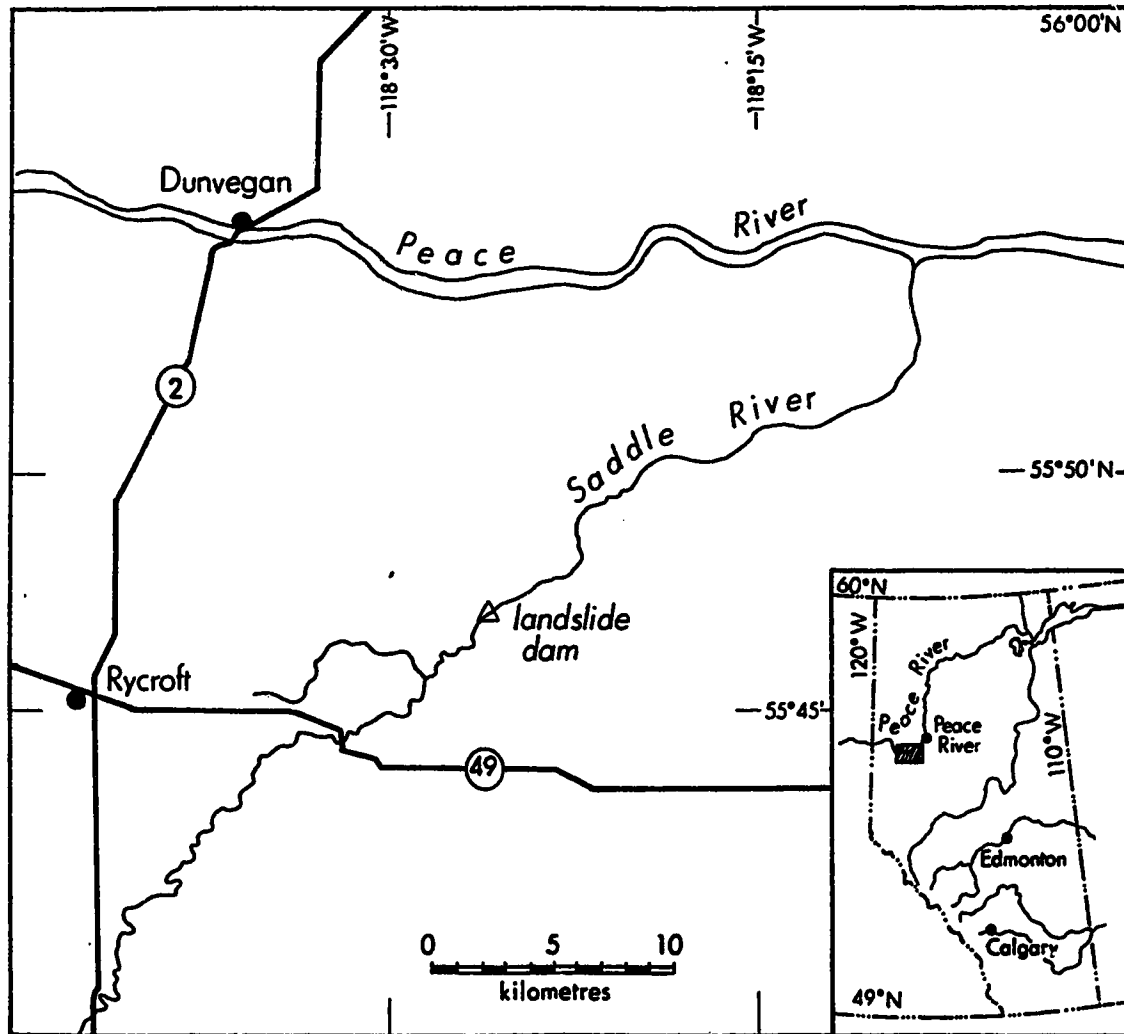


Figure 1.1 Rycroft Landslide Dam location map.

CHAPTER 2: SITE DESCRIPTION AND CLASSIFICATION

2.1 Introduction

A terrain analysis of the Rycroft Landslide site is presented in this chapter to provide a frame of reference for study of the relevant aspects of the landslide in subsequent chapters and to classify the magnitude and character of the landslide. The terrain analysis is performed from black and white vertical aerial photographs, oblique aerial photographs, topographic maps and field reconnaissance. This chapter starts with a general description of the terrain in the locality of the Rycroft Landslide, then narrows to describe the landslide, the landslide dam and the ensuing reservoir. Using the description of the site, the landslide is then classified according to mobility, size and character.

2.2 Site Layout

The Rycroft Landslide is contained in the Peace River Lowland physiographic region. The general layout of the site is illustrated in Figure 2.1. The landslide occurred on the left or north wall of the Saddle River about 6 km upstream of its confluence with the Spirit River. The post-slide air photo (Figure 2.2) shows the landslide dam and impounded reservoir as it looked in October, 1990. The only structure downstream of the landslide dam on the Saddle River is the secondary highway bridge approximately 6.5 kilometres down river (Figure 2.1).

The prairie level behind the Rycroft Landslide has a mean elevation of 575 metres above sea level. At prairie level the surficial deposits are mapped as glacial lake deposits (Liverman, 1990). The lake deposits are seen on air photos (Figure 2.2) as distinctive, mottled, dark to medium tones. On the ground, low hummocks form a rolling topography with a relief of 2 to 3 metres, a diameter of 80 to 200 metres and spaced 120 to 220 metres apart. The majority of the land at prairie level is cultivated with wheat and canola being the main crop types. Clearing of the land for agriculture took place during the 1960's. There is a large ephemeral slough 2.5 kilometres west of the site (Figure 2.1). Dark tones in depressions seen on air photos (Figure 2.2) behind the

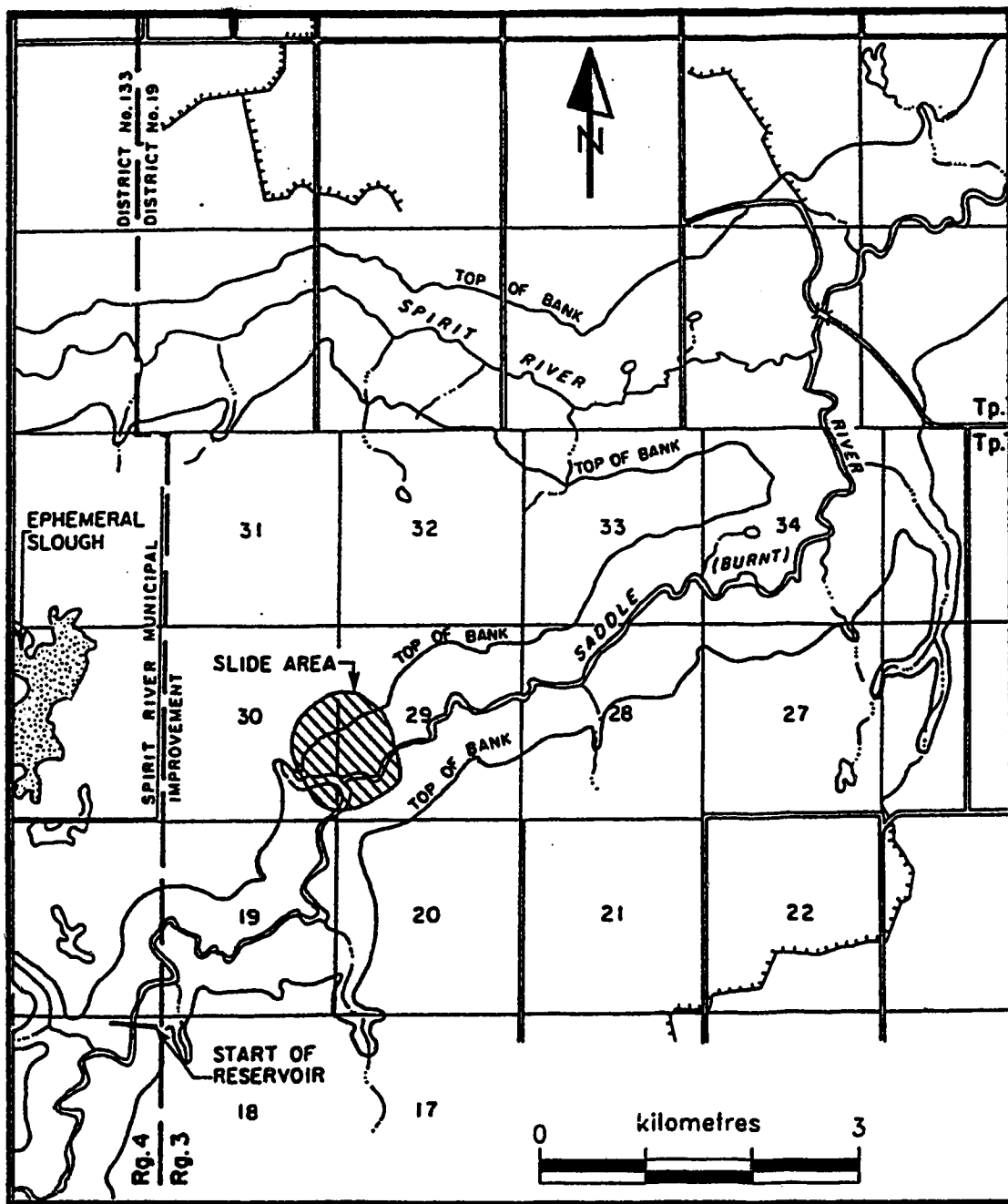


Figure 2.1 Rycroft Landslide Dam site plan.



Figure 2.2 Alberta Government panchromatic air photo AS4088-135 taken at a nominal scale of 1:25,000 on 17 October 1990, Geographic Air Survey Ltd., Edmonton.

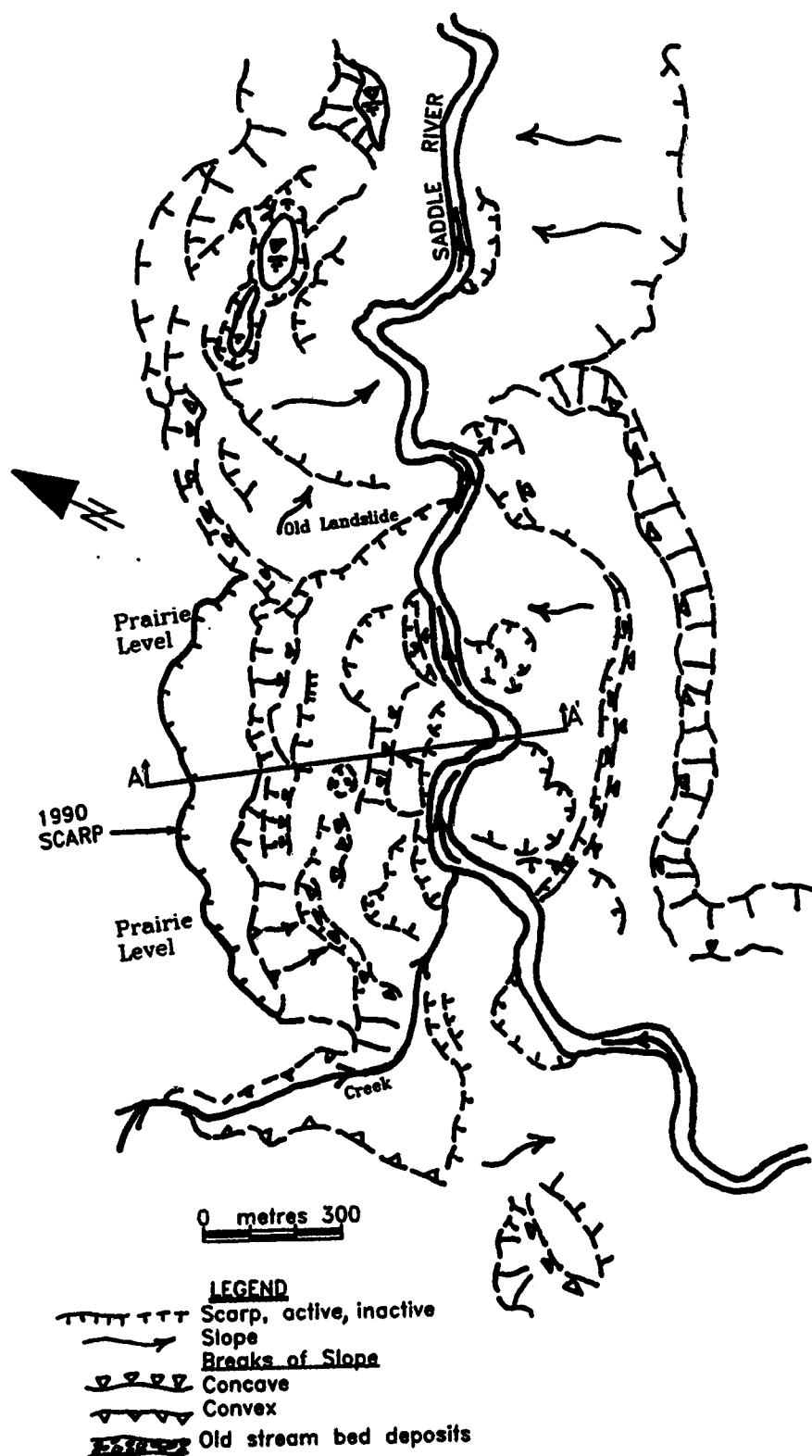


Figure 2.3 Overlay on Alberta Government panchromatic air photo AS1996-76 taken at a nominal scale of 1:15000 on 23 June, 1979. Legend follows Dearman (1972). The 1990 scarp location is from Figure 2.4.

scarp of the landslide are indications of wet conditions. These areas drain by a series of V-ditches which direct the runoff into the ravine that forms the right flank of the landslide.

The river valley terrain is mapped as colluvium (Liverman, 1990). An overlay of 1979 airphotos (Figure 2.3) shows numerous semi-circular and elongated scarps and sag ponds characteristic of the river valleys in the area. On air photos the colluvium is seen as dark uneven tones. The general channel pattern of the river is irregular having confined meanders controlled by landslides in the valley walls. Prior to the landslide, measurements from topographic maps (Alberta Forestry, 1985) indicated the valley walls sloped at an average of 11° . At prairie level the valley is about 1 km wide and at river level it is as wide as the river bed, 30 to 40 m. The valley depth is close to 100 m. The walls are densely forested with, poplar being the major tree type.

2.3 Landslide Description

The features of the post-slide site are illustrated on an overlay of low level (1:5,000) air photos flown in October, 1990 (Figure 2.4). In plan the landslide is roughly square with rounded corners. The displaced mass has an approximate length of 800 m and width of 1,000 m. On the left or north valley wall, the scarp forms a gentle arc about 1 kilometre long, starting at a small ravine on the right or southwest flank, traversing a cultivated field and curving abruptly toward the river tangent to an old landslide of similar character and size on the left or northeastern flank. The lateral scarps are parallel and sub-vertical. The loss of land at prairie level was 12 hectares. As the over-steep scarp retrogresses, a further 10 hectares may be lost.

The back portion of the displaced mass was downdropped and broken into a series of wedges. The main scarp varies from 15 to 25 m high and has an average dip of 57° . The main scarp formed at a maximum distance of 200 m behind the tree line that marked the original valley crest. This distance was stretched longitudinally during the landslide to approximately 300 m. The down-dropped area was broken into a number of blocks (or horsts and grabens) which backdip between 0° and 20° . This portion of the slide mass is evidence of the retrogression of the reactivated landslide whose scarp formed the original valley crest. Faults within this area have dips between 45° and 90° , both up and down slope (Figure 2.4). Exposures in this

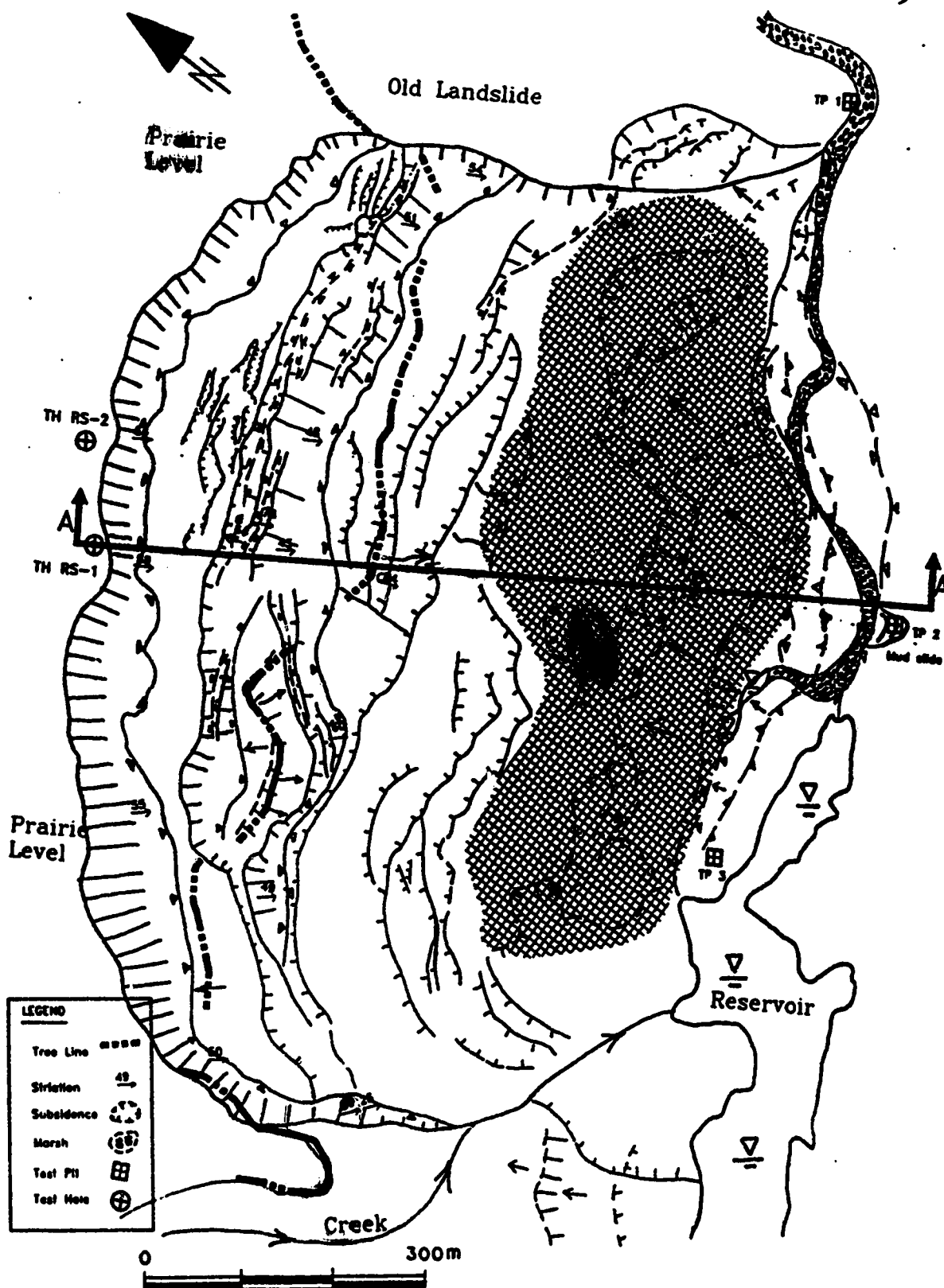


Figure 2.4 Overlay on Alberta Government panchromatic air photos AS4088-102, 103 & 104 taken at a nominal scale of 1:5000 on 17 October, 1990. Legend as on Figure 2.3. Within the hatched area, trees are upright and old landslide scarps have not been reactivated.

area of the slide mass reveal glacial lake deposits extending to depths of 15 to 25 m below the original prairie level and are underlain exclusively by till. A full description of these soils is given in Section 3.5.

There is little deformation within the central portion of the slide even though it moved approximately 100 m. The hatched area is included on Figure 2.4 to emphasize the extent of the undisturbed area. Within the hatched area, trees are upright and the old landslide scarps have not been reactivated. There is a circular shaped subsidence area indicated within the hatched area just west of line A-A' and is also present on the 1979 airphotos (Figure 2.3). On the ground the area of subsidence appears to collect drainage from the surrounding area but lacks evidence of ponding, suggesting the area drains vertically through an opening in the slope. It is suggested the opening is a remnant crack formed during a previous movement of the slope. Open cracks in the pre-existing slide area are significant if they have the potential of filling with water during periods of high surface runoff and affecting the slope stability. This is discussed further in Chapter 7. Till is the only soil found in exposures in the central portion of the slide mass.

The dam formed by the river bed being thrust upward by the slide movement. There is significant deformation at the toe of the displaced mass where the forest cover shows substantial rotation and thrusting. The riverbed was heaved upward and thrust over the right bank, a distance of some 60 m horizontally. This movement raised the river bed as much as 30 m above its original elevation 800m along the thalweg. Soil exposures within the toe area are primarily till. Exposures at test pits TP 1,2 and 3 (Figure 2.4) of stiff, fissured, rhythmited clay are discussed in detail in Section 3.6. The locations of uplifted riverbed deposits, also found in the toe area, are shown on Figure 2.4. A small mudflow at the tip of the slide (Figure 2.4) contains completely remoulded clay which apparently flowed out from the rupture surface ahead of the debris during the movement. Debris up to 1 metre in diameter is scattered on the riverbed downstream of the toe of the slide (Figure 2.5). These pieces were picked up and transported hydraulically by the high flows in the river valley (approximately 40 m³/sec.) at the time the channel was being constricted by the slide. The original spillway crest over the dam is at the tip of the landslide debris, 24 m above the pre-existing river bed elevation about 200 m from the upstream end of the displaced mass. There were no signs of seepage through the toe of the displaced mass in the first year following the landslide.

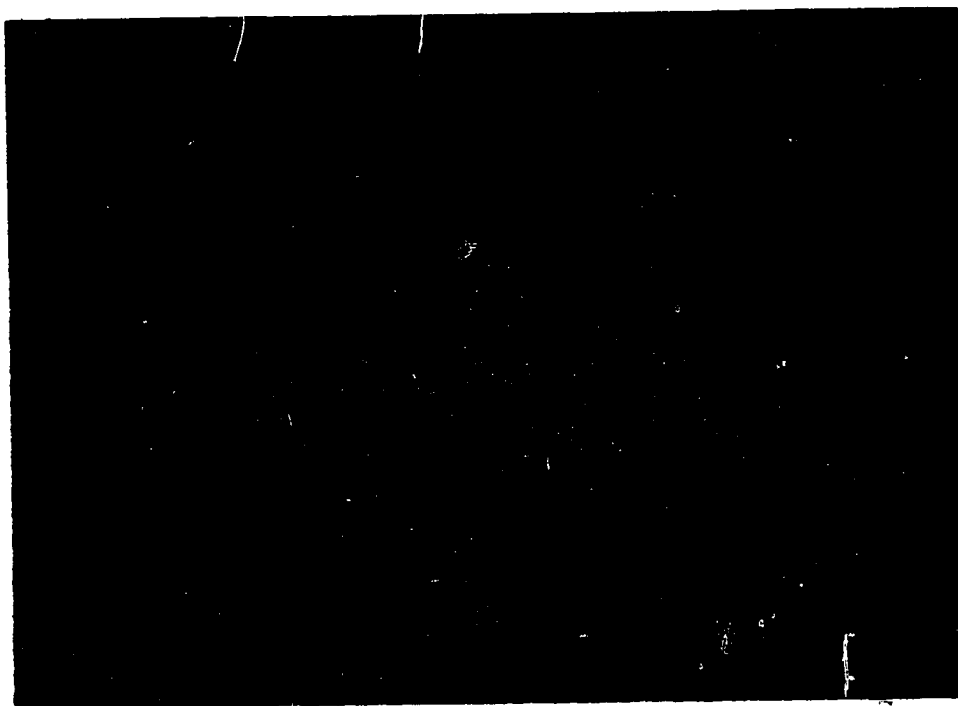


Figure 2.5 Dark brown-grey material in the foreground is debris scattered on the riverbed downriver of the landslide dam.

From the physical description of the landslide given above the landslide type is a reactivated, retrogressive, compound earth-slide (WP/WLI,1990).

2.4 Reservoir Description

The impounded reservoir in August, 1991 was 4 kilometres long, a maximum of 100 m wide and with an estimated volume of 4 million cubic metres (McClung, 1990). Soundings taken July, 1991, in the reservoir just upstream of the blockage indicated a maximum depth of 22 m. Small slumps are common and ongoing where the new banks rise steeply from the reservoir. Numerous drowned trees line the edges of the reservoir making boat navigation difficult. One year after the slide there is a thriving beaver community in the reservoir and numerous schools of minnows were sighted.

2.5 Landslide Classification

The Rycroft Landslide Dam is classified according to its mobility, size and character. There is limited evidence as to the speed at which the movement occurred since there were no witnesses to the movement. Based on the daily site visits by the farmer, however, it is known the movement occurred within a 24 hour period. The appearance of landslide debris scattered downstream of the dam, discussed in Section 2.4, suggests the movement did not occur so suddenly that the stream flow was instantly cut off. Assuming the movement occurred in a minimum of 1 hour and a maximum of 24 hours, and the maximum distance travelled by the main part of the slide mass was 100 m then the range of estimated velocities for the landslide is 0.03 to 0.001 m/sec . From Hungr (1981), the landslide movement is therefore ranked as rapid to very rapid and is placed in response class 3 or 4 (Figure 2.6).

To determine the volume of the landslide the method suggested by WP/WLI,(1990) to standardize the reporting of landslides is used. In this method the volume of the debris mass is computed by using the major axis of half an ellipsoid;

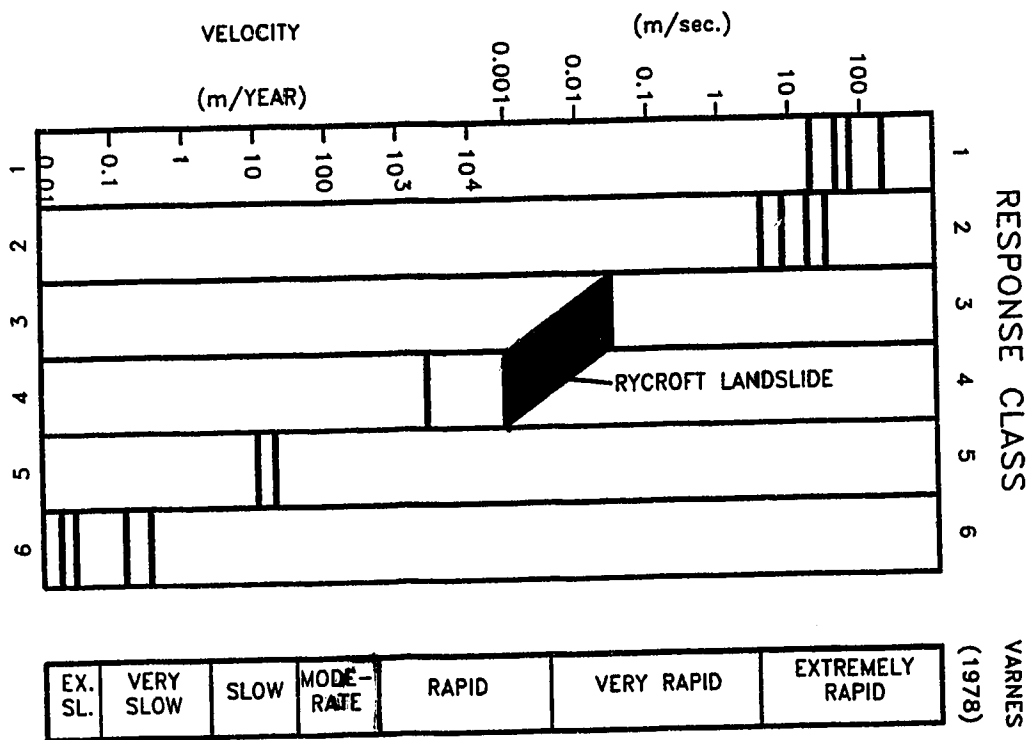


Figure 2.6 Classification of landslide movements.

$$\text{Volume of displaced mass} = 1/6 \pi L_d D_d W_d$$

L_d = length of displaced mass = 784m

D_d = depth of displaced mass = 98m

W_d = width of displaced mass = 1000m

$$\text{Volume} = \underline{40.2} \text{ Mm}^3$$

Figure 2.7 is a volume histogram generated from the Alberta Landslide Inventory in preparation by Dr. D. Cruden at the University of Alberta. The histogram indicates the Rycroft landslide is presently the largest historic landslide in Alberta and, aside from Frank Slide, is an order of magnitude larger than other landslides in Alberta.

This is the first historic landslide dam in the Interior Plains of Canada and because the rupture surface extends under the riverbed and emerges on the opposite valley side this slide can be added to the very few Type 6 Landslide Dams in the extensive United States Geological Survey catalogue (Costa and Schuster, 1988). Type 6 Landslide Dams involve one or more failure surfaces that extend under the river valley and emerge on the opposite valley side from the landslide.

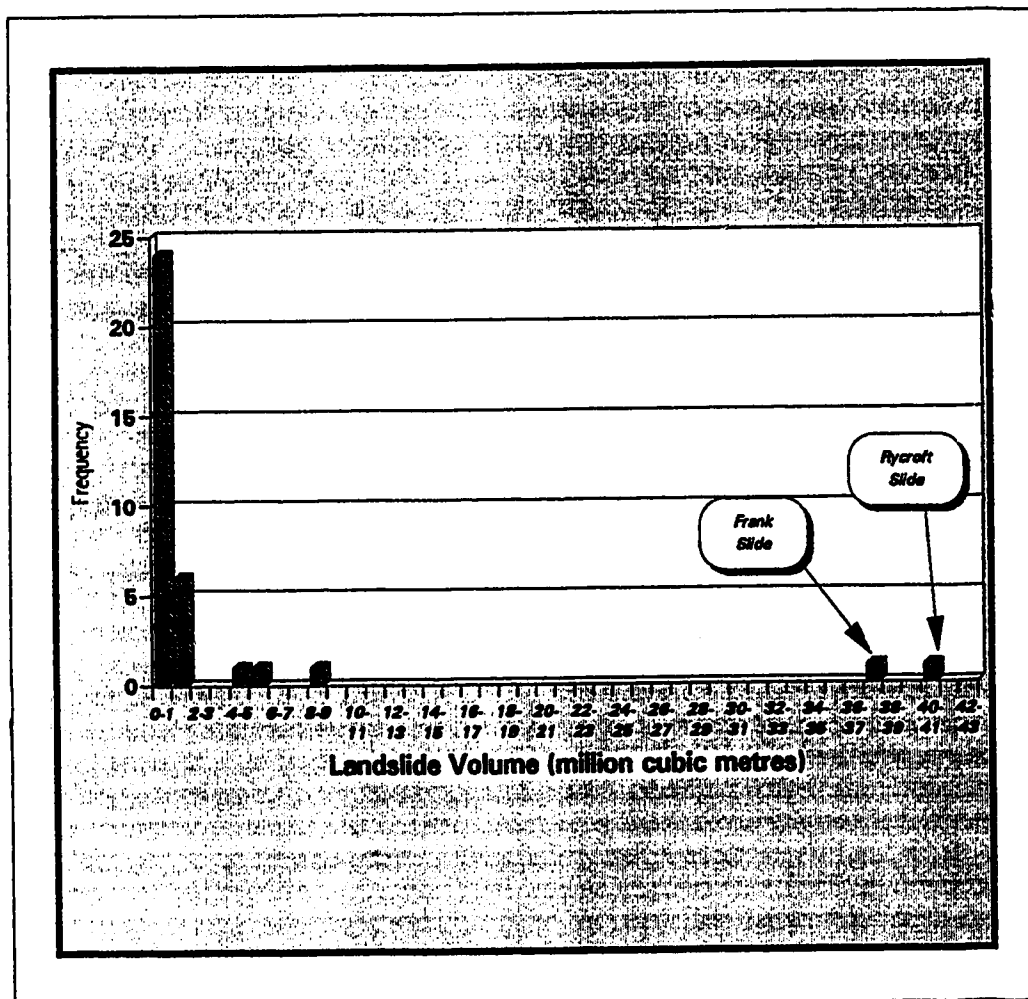


Figure 2.7 Histogram of landslide volumes from the Alberta Landslide Inventory.

2.6 Summary

The landslide occurred on the north slope of the Saddle River 6 kilometres upstream of its confluence with the Spirit River. At the slide the valley is one kilometre wide and 100 m deep. At prairie level the terrain is gently rolling. The valley has a confined, meandering channel pattern controlled by landslides on the valley sides. The Rycroft Landslide is a reactivated, retrogressive compound earth-slide, with downdropped grabens formed in the scarp area, sub-translational block movement in the middle and thrust uplift at the toe. The reservoir which formed was 4 kilometres long and contained 4 Mm³ in October, 1990. The estimated speed of the landslide movement is rapid to very rapid, placing it in response class 3 or 4. The Rycroft Landslide is the largest historic landslide in Alberta, is the only historic landslide dam in the interior plains of Canada and is a Type 6 Landslide Dam.

CHAPTER 3 GEOLOGY

3.1 Introduction

This chapter discusses the geology in the area of the landslide as it relates to the occurrence of the Rycroft Landslide. From Carlson and Hackbarth (1974) it is apparent that the Saddle River at the Rycroft Landslide is downcutting through a thick sequence of buried channel deposits of preglacial and glacial origin. The relevant geologic history at the landslide is developed by investigating the various sedimentary environments that resulted in the filling and subsequent erosion of the preglacial channel beneath the Saddle River. These environments then provide a frame of reference for interpreting the stratigraphy using testhole and field mapping information at the site. Topics covered include the bedrock geology and topography, the preglacial fluvial environment, the glacial and post-glacial history and a summary of the stratigraphy at the site.

3.2 Bedrock Geology

The Cretaceous sedimentary bedrock strata in the Grande Prairie map sheet (83M), which contains the Saddle River, dip at 2° to 10° to the south and are exposed along the major river valleys and on the tops of the Saddle Hills (Figure 3.1, after Liverman, 1989). The oldest rocks, exposed in the north, are the early Late Cretaceous carbonaceous sandstones and shales of the Dunvegan Formation. Overlying the Dunvegan Formation is the Smoky Group which makes up most of the bedrock north of the Saddle Hills and underlies the landslide site. The Smoky Group is composed mainly of marine shales of the Kaskapau, Badheart and Puskwasau Formations which are well exposed along the Smoky River. The Smoky Group grades upwards into the Wapiti Formation which, exposed in the south of the map sheet, is mainly continental sandstone with shale and coal and abundant ironstone concretions.

The preglacial bedrock topography of central Alberta, including the Peace River area, was formed by erosion during Tertiary and early Pleistocene times and has been preserved beneath glacial deposits except where postglacial rivers like the Peace River have cut through the glacial material and eroded the bedrock (Liverman, 1989).

Note : Permission to use this previously copyrighted material in this thesis was not obtained prior to the final submission of this thesis and is not shown. The figure shows the bedrock geology of the NTS 83M Map Sheet using a reproduction of a part of the Geological Highway Map of Alberta published by The Canadian Society of Petroleum Geologists.

Figure 3.1 Bedrock geology, NTS 83M Map Sheet, Alberta.

Figure 3.2 shows the thalwegs of buried and existing channels in the Grande Prairie-Peace River Area (Alberta Environment, 1991). The landslide site is close to the thalweg of a buried channel beneath the present Saddle River about 30 km upstream of where it joins the thalweg of the Shaftesbury Channel. The approximate bedrock topography where the two thalwegs join is shown in Figure 3.3. The contours are modified from Carlson and Hackbarth (1974) to include the known depth to bedrock in a testhole drilled at the landslide site in July 1991 discussed in Section 3.5. The landslide site is contained within the buried preglacial channel beneath the Saddle River in a widening basin close to where it joins the buried Shaftesbury channel.

3.3 Preglacial History

The preglacial drainage system, which largely parallels modern systems, flowed generally northeast across the area (Figure 3.2). The preglacial pattern of drainage had established trough downcutting through the Tertiary peneplain and was described as mature, broad valleys with gentle walls, and moderate gradient (Carlson and Hackbarth 1974).

Liverman et al, (1989) discussed a conformable sequence of buried channel deposits at Watino in the Smoky River valley. The Smoky River occupies the preglacial buried Bezanson channel which joins the preglacial Shaftesbury Channel downstream of the buried channel beneath the Saddle River (Figure 3.2) and may have a similar preglacial and glacial history to the buried channel beneath the Saddle River. The Watino section showed that a moderate- to low-energy braided stream system, flowing to the north down the Bezanson Channel, existed during the Middle Wisconsinan. The sequence fined upward from stratified sand and gravel at the base into silt and clay layers. Liverman et al.(1989) concluded this was produced by channel abandonment rather than by a change in the regional base level. None of the fluvial deposits contain clasts of Laurentide provenance, and the materials have been dated as Middle Wisconsinan, deposited during the Watino Nonglacial Interval (Fenton, 1984). The climate during this time, determined from fossil records, was a temperate boreal climate similar to today (Westgate et al. 1972). Preglacial fluvial sedimentation continued until at least 27,400 B.P.(Westgate et al. 1972).

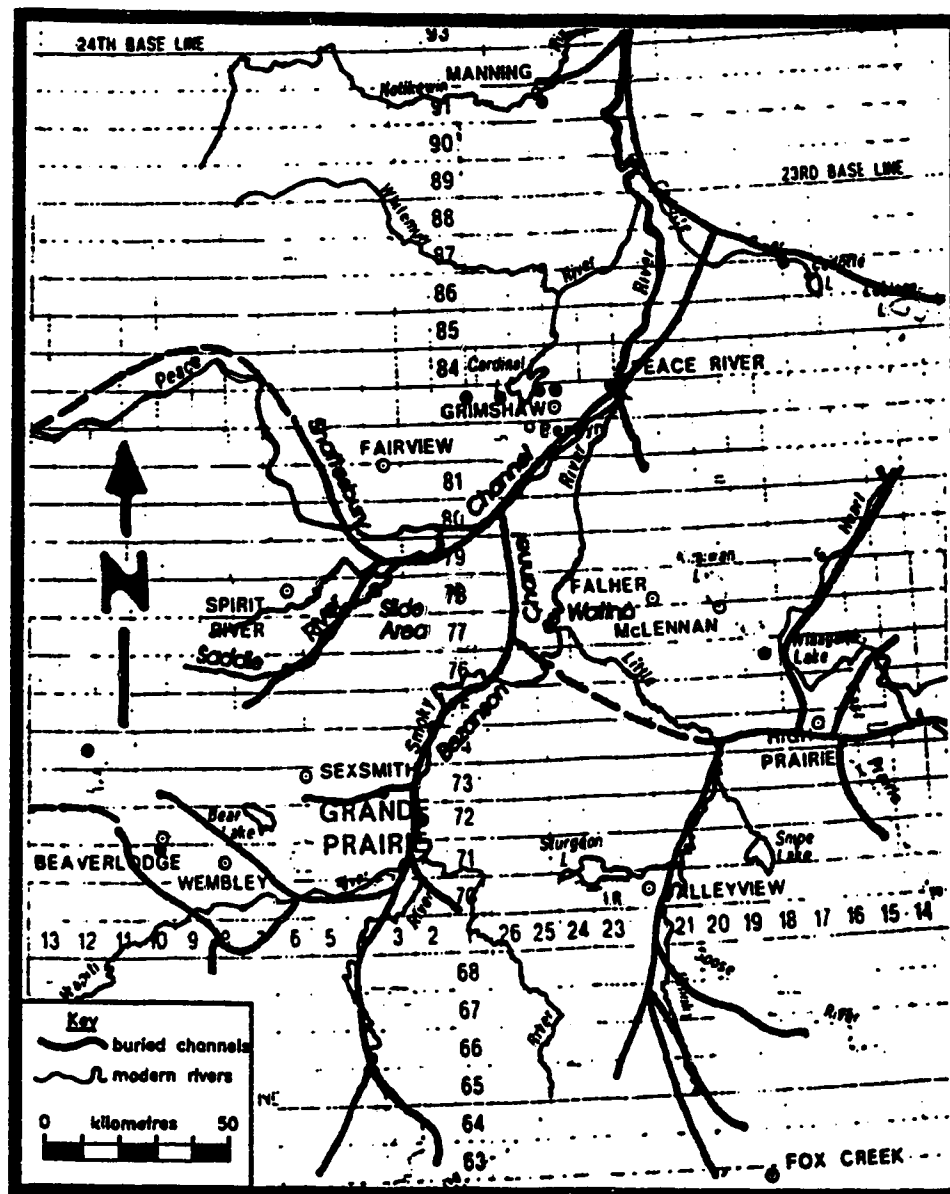


Figure 3.2 Location of major buried valleys of the Grande Prairie-Peace River area.

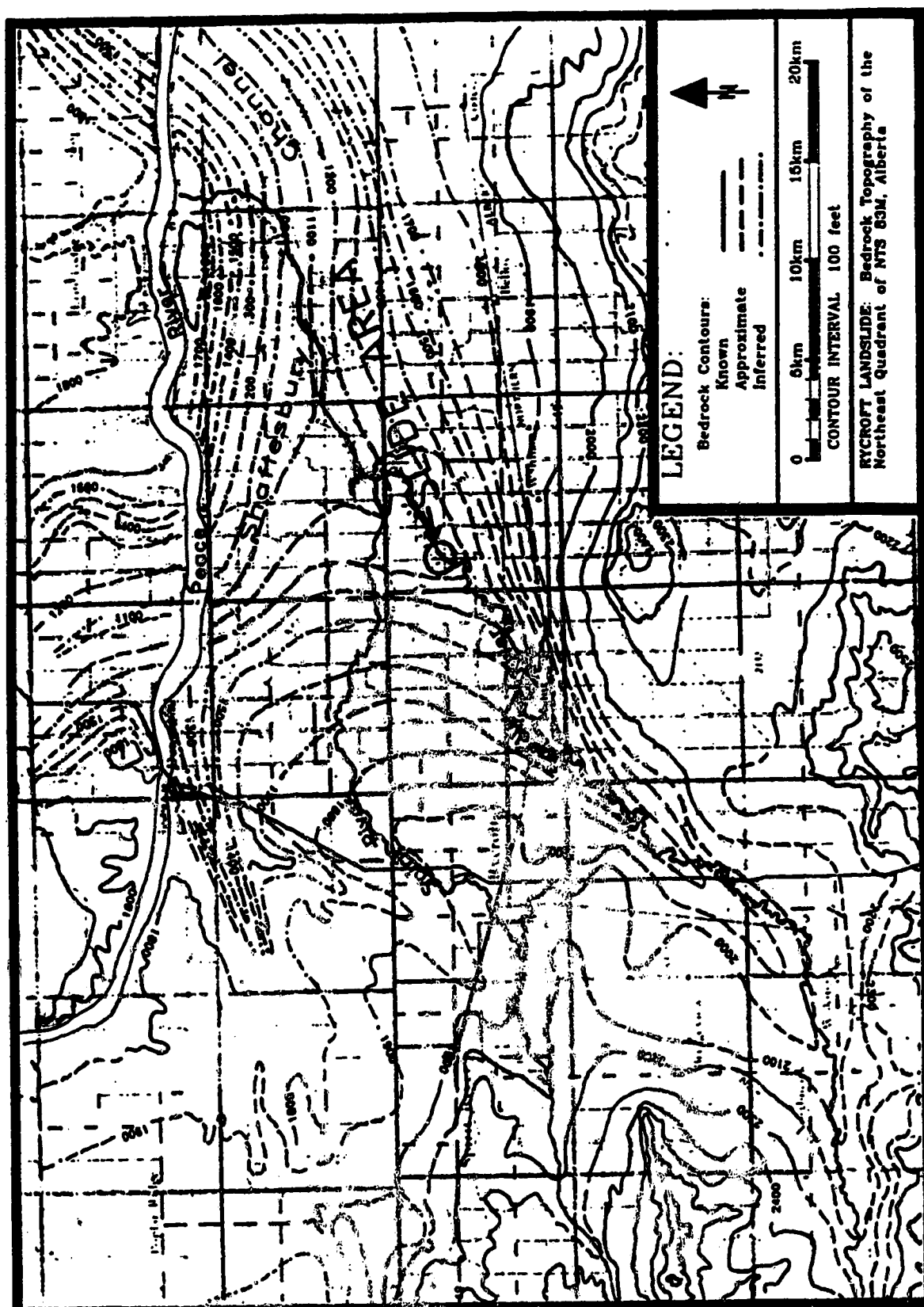


Figure 3.3 Bedrock topography of the northeast quadrant of NTS 83M, Alberta.

The regional proximity of Watino to the landslide site (Figure 3.2) suggests the fluvial environments of the two sites had similar base level, climate and geologic controls. This assumption is backed by information from testholes RS 1& 2 drilled behind the Rycroft Landslide and discussed in Section 3.6.

3.4 Glacial History

The Wisconsin glacial history of the Interior Plains of western Canada possibly included several Laurentide glacial advances (Fulton and Prest, 1987). Fenton (1984) outlined four separate events with the oldest dating to approximately 2 Ma B.P. In west-central Alberta, Liverman et al. (1989) have shown that only a single Late Wisconsin till of Laurentide provenance is widespread throughout the Grande Prairie - Watino region. Rutter's (1976, 1977a) investigation of the upper Peace River showed that, of the four Cordilleran ice advances which are thought to be Late Wisconsin, none reached the northeast quadrant of the Grande Prairie sheet (83M). Therefore the glacial history of the Landslide site directly involves only the advance and retreat of the Late Wisconsin Laurentide ice sheet.

Rains et al. 1990 interpret a minimum of 800 m of Laurentide ice over the Dunvegan area. As the Laurentide ice advanced up the regional gradient in a general southwest direction pro-glacial lakes formed at its margin. It is likely that due to the bedrock being easily deformed that the ice sheet in this area had a low gradient (Fisher et al. 1985) and was susceptible to topographic influence.

Evidence of lacustrine sedimentation in the pro-glacial lakes is provided in the Watino section introduced in Section 3.3. At the top of the section underlying till were 3 to 5.5 meters of clay (W-7) containing clasts derived from the Canadian Shield, indicating Laurentide provenance. The grainsize, mineralogy and stratigraphic position of the W-7 unit suggested that the sediment was deposited in a pro-glacial lake developed during the advance of the Late Wisconsin Laurentide ice sheet (Liverman et al, 1989).

A deposit of clay, similar in grainsize, composition, character and stratigraphic position to the W-7 clay is observed at the Rycroft Landslide as discussed in Section 3.6. This clay has significant relevance as it is inferred to contain the rupture surface of the Rycroft Landslide (Section 7.2).

It is suggested that the Laurentide ice, coming from the northeast flowed up the Shaftesbury Channel causing a blockage in the regional drainage and the formation of pro-glacial lakes in the elongated topographic lows of the preglacial valleys. Significant thicknesses of highly plastic lacustrine clay like the W-7 unit were deposited in these lakes. Although there was a mixture of Cordilleran and Laurentide sediments, it is inferred that the main sediment load of these lakes came from the active ice margin from which the pro-glacial lake carried away material entrained by the glacier. The high plasticity of the clay reflects the source of the material which in northwestern and western Alberta includes soft, clay-rich marine shales of the Dunvegan Formation and Smoky Group.

As the Late Wisconsinan Laurentide ice advanced over the area, the ice flow was directed into the topographic low of the Shaftesbury channel as proposed by Mathews (1980) who also suggested that this strong topographic control indicated that the ice sheet was thin, perhaps in the order of 600 m, and the surface slope was low. The advancing ice sheet easily eroded and deformed the weak pro-glacial lake clays in the preglacial valleys and possibly produced the numerous normal and reverse, highly slickensided shears observed in the remaining clay at both the Watino and Rycroft Slide sites. These shears could also be the result of Holocene mass-movement deformation. Figure 3.4 is a photo of the preglacial lake clay near the tip of the Rycroft Landslide showing the numerous shears as well as the rhythmited nature of the clay. The shears are laterally spaced at 5 to 20 cm intervals characterized by small offsets of 0.1 to 5 cm and dips from 40° to 60°. The rhythmites vary from non-existent to 0.5 mm thick and are discontinuously marked by silt laminae.

The till deposited by the Late Wisconsinan ice sheet in the buried channels is characterized by a low stone count and clay rich matrix. The major buried channels such as the Shaftesbury and Bezanson (Figure 3.1) contain deposits of clayey till which reach thicknesses of 120 m (Carlson and Hackbarth, 1974). Liverman (1989) identified the till sheet by its lithology, a mostly unstratified diamicton containing all grain sizes from boulders to clay, and also by its geometry, a tabular sheet with little lateral variability. The clasts contained in the till include igneous and high grade metamorphic rocks from the Canadian Shield, quartzites from either the Athabasca quartzite on the margins of the Canadian Shield or Cordilleran quartzites, carbonates from dolomite and limestone exposed throughout the Cordillera or from the Devonian limestones found at the margin of the Canadian Shield and finally local clasts such as poorly consolidated claystone, siltstone and sandstone, concretionary ironstone, and coal derived from the

local bedrock. The matrix of the till, classed as sand sizes and smaller, was well graded with a high clay size content of

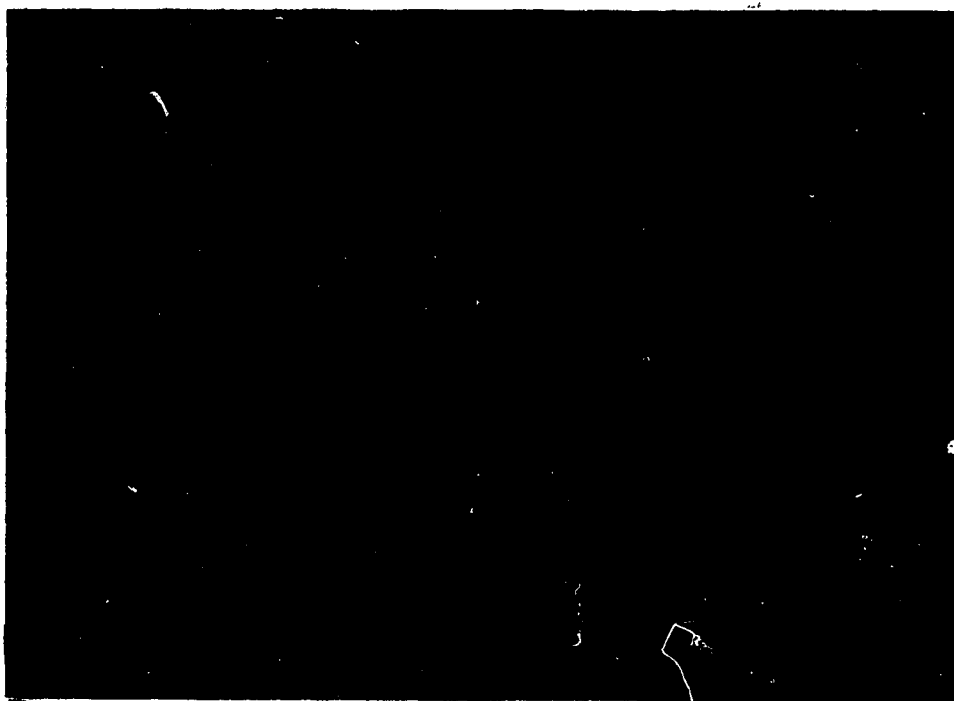


Figure 3.4 Preglacial lake clay exposure in the displaced mass near the tip of the landslide.

between 20 and 50 %. The main clay mineral was primarily illite with minor amounts of montmorillonite.

As the Laurentide ice retreated, pro-glacial lakes again formed in the topographic lows. The thickest deposits of glaciolacustrine silt and clay are found along the preglacial valleys including the Shaftesbury channel and the channel beneath the Saddle River. At the Rycroft Landslide, the glaciolacustrine deposits are 20 to 25 m thick. White et al. (1985) estimate deglaciation to have taken place over the Saddle Hills about 12,000 B.P..

3.5 Post Glacial History

Liverman (1989) suggested that after drainage of the glacial lakes in the area, entrenchment of major streams and rivers occurred early with series of paired terraces developed. Erosion of major rivers to their present levels, associated colluviation of steep slopes in river valleys, and the infilling of depressions with clay and organic sediments has continued to the present day. The development of the post-glacial Saddle River valley is discussed in detail in Chapter 4.

3.6 Site Stratigraphy

The stratigraphy at the site shown on the simplified log in Figure 3.5 is based on testholes RS 1 and 2 drilled by Alberta Environment, Hydrogeology's rotary drill rig in July, 1991 behind the crest of the landslide (Figure 2.4) and from correlating observations within the landslide and in the river valley. A detailed combined log of RS 1 and 2 is contained in Appendix A. Invaluable in the assessment of the stratigraphy were the down-hole geophysical logs completed by Alberta Environment Hydrogeology Division (Appendix B) in testhole RS 1. Correlating the characteristic signature on these logs with the test borings provides a complete picture of the stratigraphy. The stratigraphy is described in the order of deposition, from the bottom up and is divided into buried channel deposits, preglacial lake clay and glacial units.

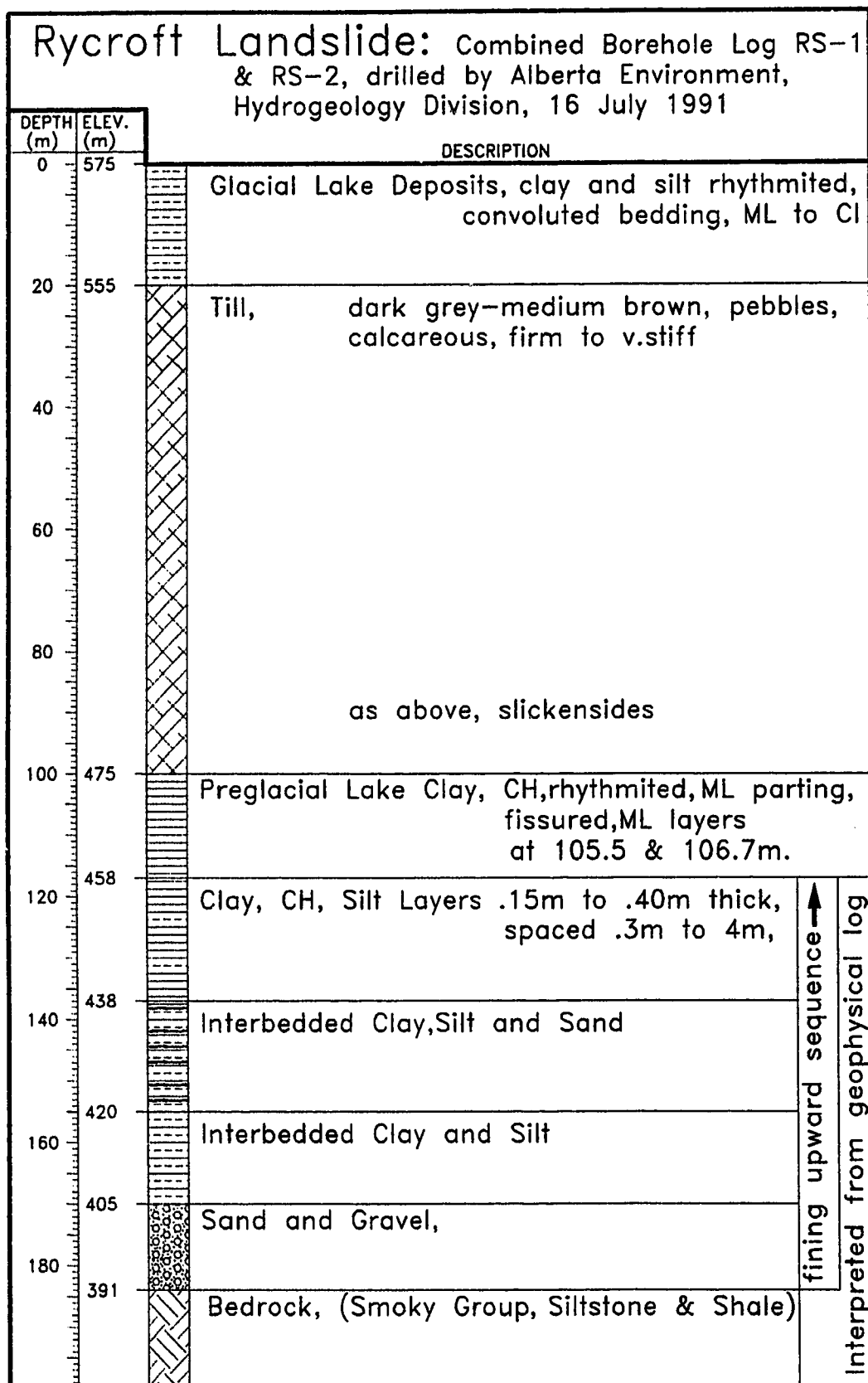


Figure 3.5 Combined simplified borehole log from RS-1 and RS-2. (see Figure 2.4 for location)

The preglacial buried channel deposits are a fining upward sequence contained by bedrock at the base and preglacial lake clay at the top. Although thicker, the buried channel succession described here is similar to the Middle and Late Wisconsinan section at Watino discussed in Section 3.3. The bedrock, inferred to be shale and siltstone of the Upper Cretaceous Smoky Group, is at a depth of 184 m below prairie level or 80 m below river level. Above the bedrock is a 10 metre layer of interlayered sand and gravel indicative of a high energy stream. Above this is a 53 metre thick, fining-upward, sequence of interbedded sand, silt and clay which has been interpreted as a moderate- to low- energy braided stream system flowing to the north down the preglacial channel (Liverman et al. 1989). These deposits are consistent with the preglacial fluvial environment expected in a preglacial channel.

A weak preglacial lake clay is identified between depths 117 and 100 m in testhole RS 1 overlying the buried channel deposits described above. The term "preglacial" is used here because the deposition of the clay is believed to predate the Late Wisconsinan ice advance which is the only Laurentide Ice advance that reached the site (Liverman et al. 1989). The term is not to imply that deposition predated the Laurentide Glaciation of the Interior Plains. As discussed in Section 3.4, the preglacial lake clay was deposited in a pro-glacial lake ponded against the advancing Late Wisconsinan Laurentide ice in the preglacial valley beneath the Saddle River. The clay is highly plastic, stiff, rhythmited and fissured containing slickensides in both outcrop and core. The macro-structure is as described in Section 3.4 in comparison with the W-7 clay of the Watino section (Liverman et al. 1989). Five metres below the top of this layer are two 0.3 m thick silt layers about 1.5 m apart. The same two marker beds are observed, at the same elevation, in a relatively undisturbed outcrop of the preglacial lake clay in the valley wall downstream of the toe of the landslide (TP 1 on Figure 2.4, Figure 5.7) indicating the preglacial lake clays are laterally continuous and flat-lying in the locality of the landslide.

The glacial deposits, left by the Late Wisconsinan ice advance and retreat over the site, are till and glacial lake deposits. Above the preglacial lake clay is 80 m of medium to highly plastic, till common to the buried channel fills of the Peace River area (Cruden et al. 1990). In the dried, weathered zone, the till is characterized by vertical joints spaced from 0.3 to 2.0 m. The depth of the weathered zone varies from 2 to 6 m. The till, below the dried weathered zone, is seen in outcrop in the slide mass and in samples from testholes RS 1, to be non- stratified and non-fissured. Samples recovered from testhole RS 1 exhibit an increase in stiffness ranging from firm to stiff samples taken near the top of the till to very stiff to hard samples taken near the base.

Slickensided surfaces are seen in till samples recovered in the bottom 10 m of the layer. There are minor, discontinuous silt and sand layers observed in outcrops of the till. Above the till to prairie level are 15 to 25 m of medium to high plastic, glacial lake deposits of clay and silt. The sediments are commonly rhythmited and in the scarp areas have a low moisture content. The glacial lake deposits are seen in outcrop to be non-homogeneous and non-fissured with variation in character due to layering and convolution of bedding. Collapse structures and convoluted bedding within the glacial lake sediments resulted from differential consolidation in combination with melting out of remnant glacial ice.

3.7 Summary

A study of the sedimentary environments in the preglacial river valley beneath the Saddle River leads to an interpretation of the geologic setting at the Rycroft Landslide. The Rycroft Landslide is located in a widened portion of a preglacial river valley close to where it joins the Shaftesbury buried valley beneath the present Saddle River. The stratigraphy at the site is typical of what is expected in the preglacial channel environment of the Peace River area where Laurentide ice sheets advanced up the regional gradient. A section of buried channel deposits at Watino studied by Liverman et al.(1989), similar in character to the lower stratigraphy at the Rycroft Landslide site, is used to interpret the preglacial history. The Middle Wisconsinan preglacial fluvial environment at the site resulted in a 63 metre unit of sand and gravel at the base fining upward to layered silt and clay near the top. The advance of the glaciers in the Late Wisconsinan blocked the regional drainage resulting in deposition of rhythmited preglacial lake clay in lakes contained in the preglacial river valleys. A similarity is drawn between the W-7 clay unit at Watino and the 17 metre preglacial lake clay at the Rycroft Landslide. Late Wisconsinan ice advanced over the recently deposited preglacial lake clay removing some and possibly consolidating and shearing the remainder. The Late Wisconsinan ice sheet deposited an 80 metre unit of till. The retreating glaciers caused pro-glacial lakes to form resulting in deposition of 15 to 25 m of glacial lake deposits, completing the stratigraphy at the Rycroft Landslide.

Having established the geologic setting of the landslide this study can now turn to the interactive processes involved in the post-glacial downcutting of the Saddle River and the relation between these processes and the large-magnitude landslides like the Rycroft Landslide.

CHAPTER 4: SADDLE RIVER HYDROLOGY

4.1 Introduction

The hydrology of the Saddle River is significant as it represents the main driving force behind the degradation processes of the river. The occurrence of the Rycroft Landslide, four to five days after an unusually intense rainfall, cannot be dismissed as a coincidence and a study of the Rycroft Landslide is not complete without a review of the river hydrology. This chapter covers a summary of available hydrometric data for the river including the details of the 11 June, 1990, flood and a back-calculation of the time of blockage.

4.2 Saddle River Flood Frequency

A flood frequency analysis for the Saddle River, conducted by the Hydrology Branch of Alberta Environment after the occurrence of the Rycroft Landslide, was used to assess the safety of the natural dam at the site. The report summarizing this analysis is contained in Appendix C. Hydrometric data for the river since 1967 are available from a station near Woking, approximately 25 km upstream of the landslide site. Figure 4.1 was produced from the hydrometric data accounting for the additional catchment between the gauge at Woking and the Rycroft Landslide. Figure 4.1 illustrates the highly variable and infrequent flood flows of the river. For the majority of the year there is no flow in the Saddle River.

4.3 June 1990 Rainstorm Event

On 11 and 12 June, 1990 a rainstorm of unusual intensity occurred in the Saddle River catchment area. Rainfall records from the three nearest stations recorded 160, 77 and 165 mm of precipitation during this period (McClung, 1990).

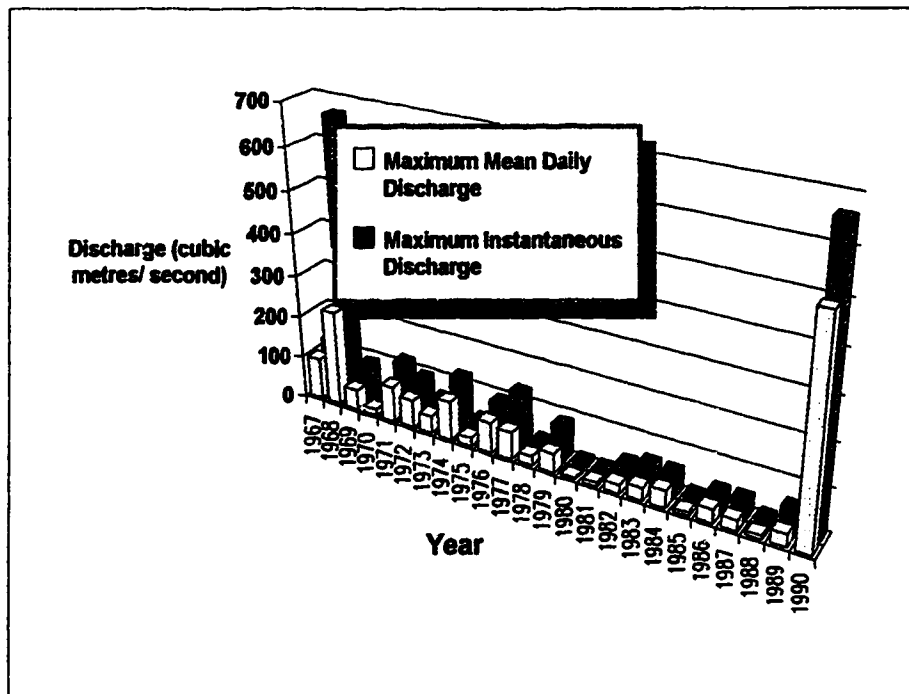


Figure 4.1 Maximum annual discharges for the Saddle River near the Rycroft Landslide. Hydrometric data for the Saddle River near Woking are scaled up to account for the additional catchment area between the gauge and the landslide.

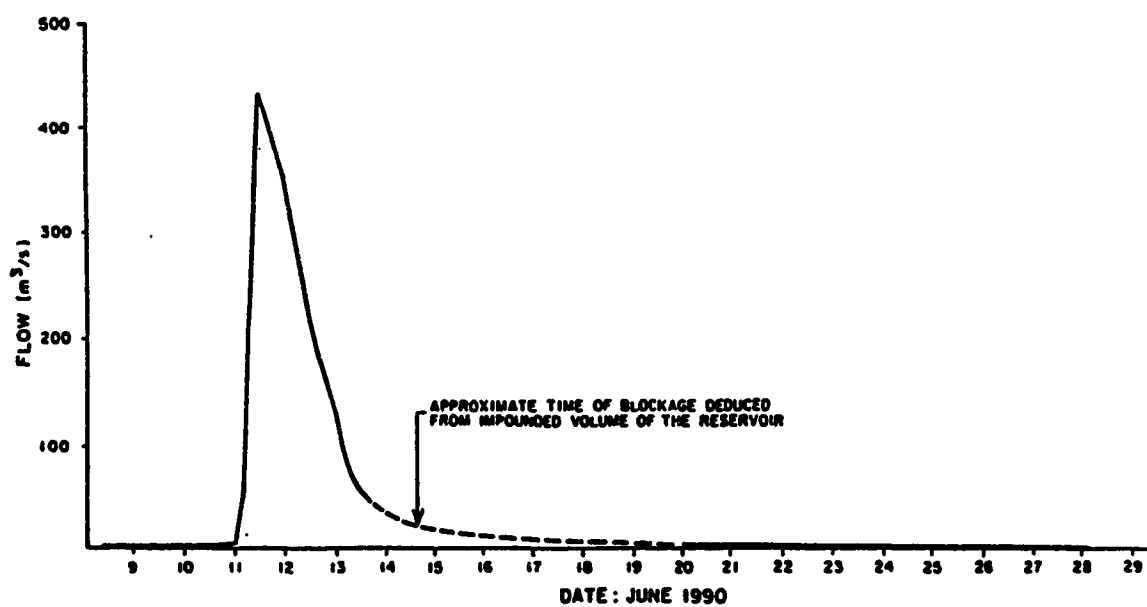
The rainfall resulted in a maximum flow in the Saddle River at the Woking gauge of $432 \text{ m}^3/\text{sec.}$ from 2300 to 2400 hours on 11 June, 1990 (Figure 4.1). The flow at the landslide is estimated at $667 \text{ m}^3/\text{sec.}$ obtained by scaling up to account for the additional catchment between the Woking gauge site and the landslide. This is a 1 in 50 year event and produced a 12 day flood volume of some 55 Mm^3 (Appendix C).

In October, 1990, some depth and width measurements were made by Alberta Environment of the lake created by the landslide dam which enabled the impounded volume of water to be roughly estimated at 4 Mm^3 . Using the river flows, back calculations indicate that the blockage of the river occurred within a day or so of 17 June, 1990, 4 or 5 days after the peak flood. The volume estimate also indicates that approximately 50 Mm^3 of the flood volume had flowed past the landslide site prior to the blockage.

4.4 Summary

The flood flows of the Saddle River are variable and infrequent. The high intensity rainstorm in the Saddle River catchment on 11 June, 1990, produced flows in the river at the landslide of $667 \text{ m}^3/\text{sec.}$ From the hydrometric data the time of blockage is calculated to be within a day or so of 17 June, 1990, and approximately 50 Mm^3 of the flood volume had flowed past the site prior to the blockage.

The hydrology of the Saddle River is the driving force behind the degradation of the post-glacial Saddle River of which the Rycroft Landslide is a single event. In the following chapter, the interactive degradation processes of the Saddle River are studied.



RYCROFT LAND SLIDE
WOKING GAUGE HYDROGRAPH

Figure 4.2 Saddle River Hydrograph

CHAPTER 5: SADDLE RIVER MORPHOLOGY AND PHYSIOGRAPHY

5.1 Introduction

The post-glacial entrenchment of the present day Saddle River is an interactive process of degradation involving the downcutting of the river and the development of the valley slopes. To better understand how the occurrence of the Rycroft Landslide Dam is involved in the entrenchment of the Saddle River this chapter investigates the interactive processes occurring in the Saddle River. This includes a discussion of the river profile, the slope physiography and the overtopping of landslide dams in the Saddle River.

5.2 River Profile

The site of the landslide dam on the Saddle River is approximately 30 km upstream of the confluence of the Saddle and Peace Rivers. The general channel pattern is irregular with entrenched meanders controlled by landslides on the valley sides. There are no significant paired terraces on the valley walls indicating the river has been actively downcutting without interruption since its re-entrenchment after deglaciation.

The longitudinal profile of the Saddle River is illustrated in Figure 5.1. The river and prairie level profiles were taken from Alberta Forestry 1:20,000 provincial base maps compiled from aerial photographs taken in 1981 (Alberta Forestry, 1985). The bedrock profile was taken from the revised bedrock topography of the Saddle River shown in Figure 3.3. As shown in Figure 5.1, the upper length of the Saddle River flows above a buried tributary channel of the buried Shaftesbury channel. The lower length cuts across the Shaftesbury channel before joining the Peace River. The stratigraphic section on Figure 5.1 is interpreted from the stratigraphy determined at the site and assumptions about the preglacial fluvial history discussed in Section 3.3.

The outstanding characteristic of the profile is its convex-up shape which implies the river is above its equilibrium level and actively downcutting. This convex-up shape of tributary rivers/creeks of large rivers in Alberta is very common (Rains and Welch, 1988). The Saddle river was apparently left behind by the rapid post-glacial downcutting of the Peace River leaving the convex shape of the river profile.

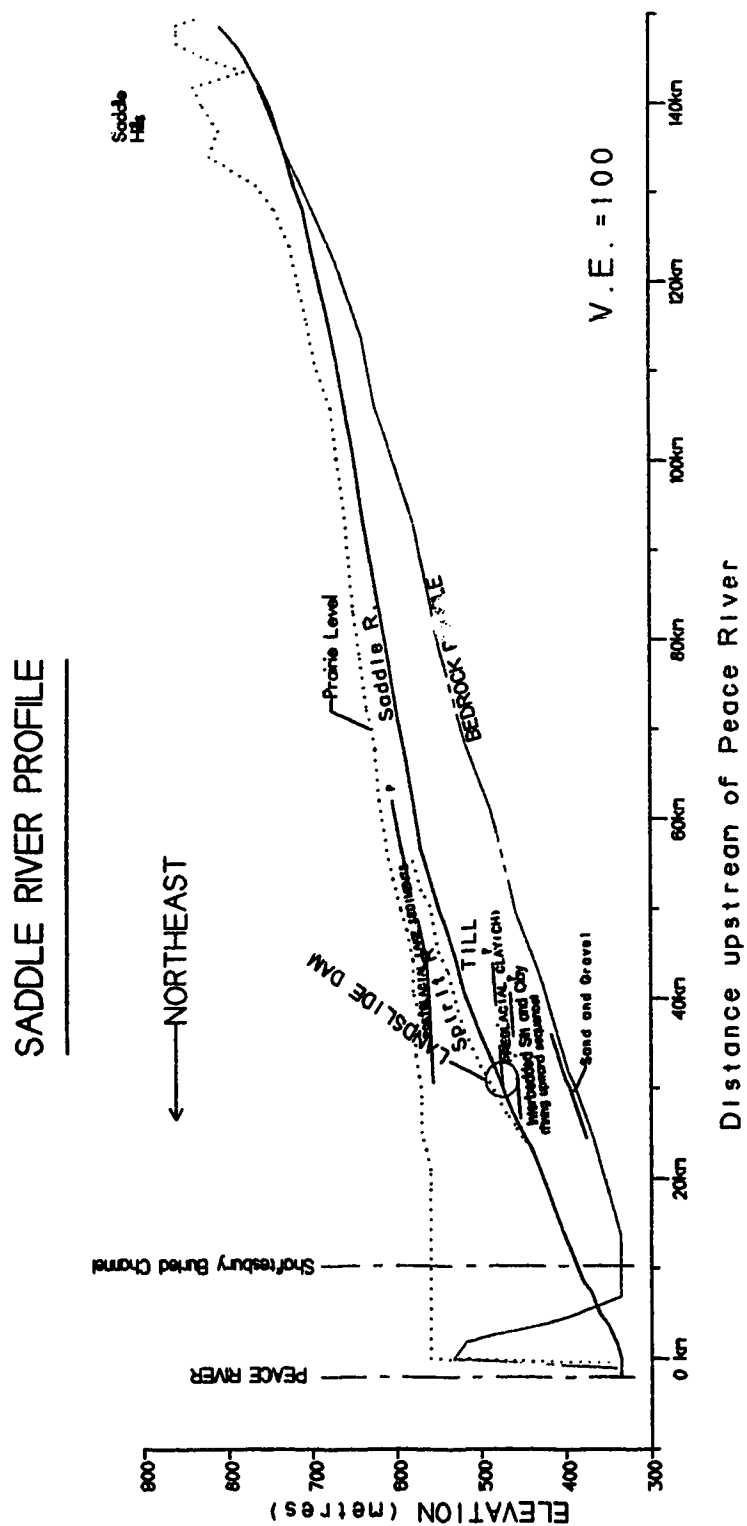


Figure 5.1 Saddle River Profile

Liverman (1989) stated that entrenchment of the major streams and rivers such as the Peace and Smoky rivers in the Grande Prairie map sheet area occurred early in the post-glacial history reaching close to their modern gradients and levels approximately 7,000 years B.P.

On the steeper downstream reach of the river the channel maintains a continuous bed armour, in pools and riffles, of medium to coarse gravels (Figure 5.2). In this reach the coarse clasts have been locally derived from erosion of the Laurentide till. It is suspected, but not investigated, that the coarse clasts are absent in the upstream shallower reach of the river where the source till is locally absent.

5.3 Slope Physiography

Slope physiography is the study of the genesis and evolution of slopes. In this section, the slopes of the Saddle River in the proximity of the landslide are studied to identify recognizable trends that can be associated with the ~~River~~ Landslide.

A significant observation from Figure 5.1 is that the ~~landslide~~ occurred at the ~~point where the river started~~ exposing the preglacial lake clay. A similar observation is made ~~in the river valley~~ on a relatively undisturbed outcrop downstream of the toe of the slide (TP 1, Figure 2.4) where the unconformable contact between the till and preglacial lake clay is approximately two metres above the existing riverbed.

There is evidence that rapid erosion of the riverbed at the toe of the slide immediately preceded the landslide movement. Comparison of the riverbed elevations, shown in Figure 5.1 compiled from 1981 aerial photographs (Alberta Forestry, 1985), with the land survey completed as part of this research in July, 1991, indicates the river bed incised between 1 and 2 metres in the past 10 years. Based on the significant recent erosion observed in the riverbed and from the flood flow records from this river in the past ten years (Section 4.2), it is assumed that most of the downcutting occurred during the flood flow brought on by the 1 in 50 year storm event that occurred on June 11, 1990. This was five times larger than any other storm event in this time period. It is interpreted that the slide movement was initiated in conjunction with the river rapidly eroding through the last remnants of till and into the preglacial lake clay.

The preglacial lake clay is a significant unit in the stratigraphy because it represents a weaker layer overlain by a thick layer (100 m) of stiffer glacial deposits, a condition often associated with lateral spreads where the movement may involve

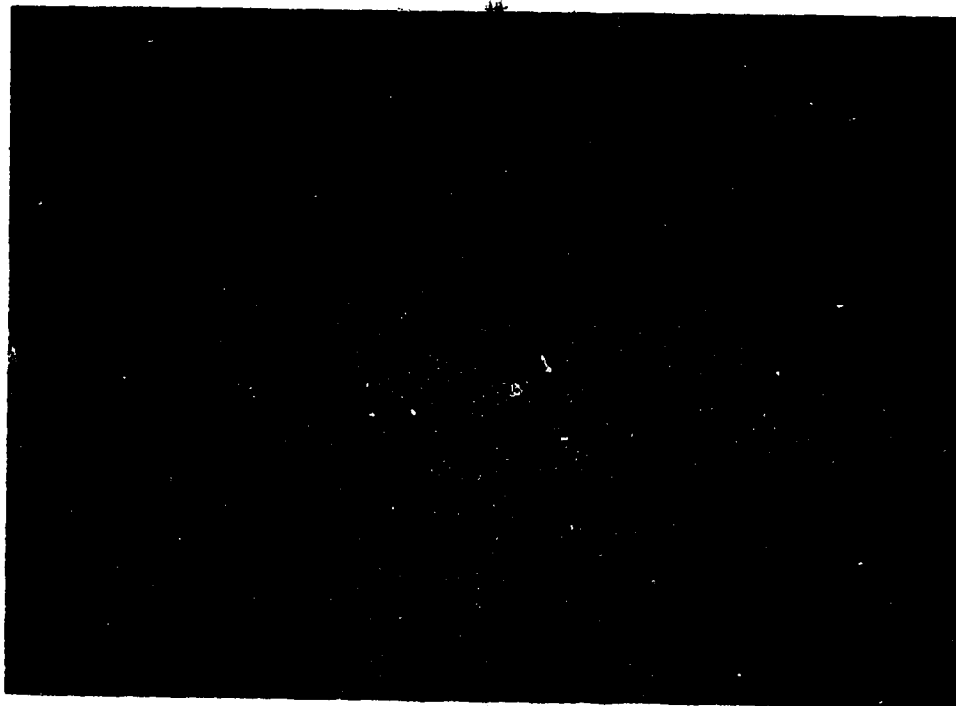


Figure 5.2 Typical downstream view of bed armour on river bed, downstream of the landslide.

fracturing and extension of coherent material owing to plastic flow of underlying weak material (Varnes, 1978). It is hypothesized that the main factor controlling the occurrence of deep-seated, large landslides like the Rycroft Landslide is the location of contact between the river level and the top of the preglacial lake clay, that this marks a transition between a stable slope angle governed by the shear strength of the till to one governed by the lower shear strength of the preglacial lake clay.

To investigate this hypothesis, slope angles for slopes on the Saddle River upstream and downstream of the landslide are measured from the 1:20,000 provincial base maps (Alberta Forestry, 1985) and shown on Figure 5.3. Although the plot has considerable scatter, there is a reduction in the average slope angle from 13° to 10° downstream of the landslide. Further downstream, below the confluence with the Spirit River, the average slope angle drops to 8° . The middle portion on Figure 5.3 downstream of the landslide, which averages 10° , may represent a transition zone between the apparently stable upstream slopes of 13° and stable downstream slopes of 8° .

In the transition zone, slopes have presumably moved out on a rupture surface formed in the preglacial lake clay, but due to the buttressing effect as the toe was pushed into the opposite bank and the time-dependent removal of the colluvium at the toe by river erosion, there is a delay in obtaining the ultimate 8° slope angle.

To illustrate this point further, Figure 5.4 is a photograph looking downstream from the landslide showing the river valley apparently squeezing in on the river bed in the transition zone described above. Investigation in the river bed along this length indicates steep sub-vertical river banks (Figure 5.4) and numerous backdipping clay layers pushed up through the riverbed (Figure 5.5). The uplifted riverbed has resulted in a distorted channel pattern with numerous pot holes in the riverbed.

Downstream of the confluence with the Spirit River (Figure 5.6), the average slope angle of 8° is relatively consistent (Figure 5.3) and the slopes appear stable. The river banks are no longer sub-vertical and back dipping clay layers in the riverbed are not seen (Figure 5.5). It is suggested that because the additional flow from the Spirit River resulted in earlier removal of the colluvium from the riverbed and because the river has finished cutting through the weak clay layers, the slopes and riverbed along this length have had time to reach their equilibrium level determined generally by the available shear strength of the preglacial lake clay.

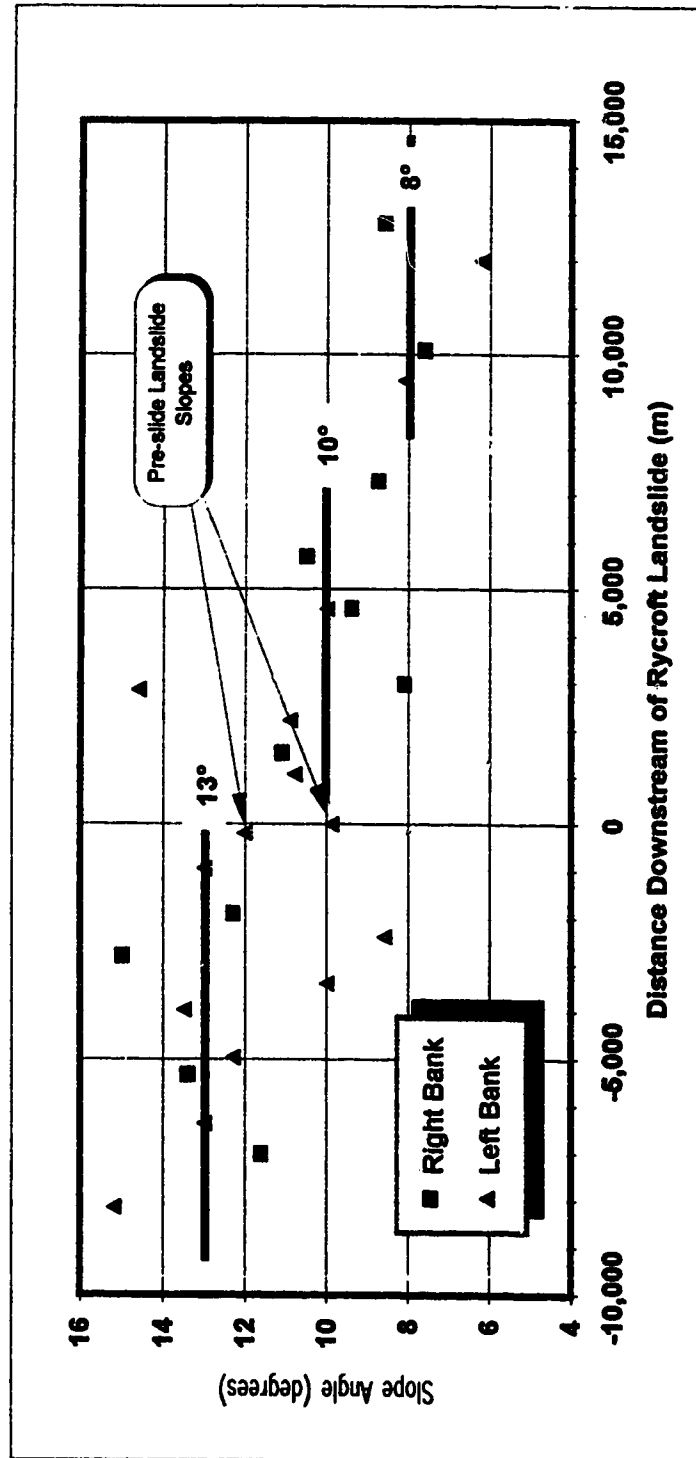


Figure 5.3 Saddle River slope angles, valley crest to river level.

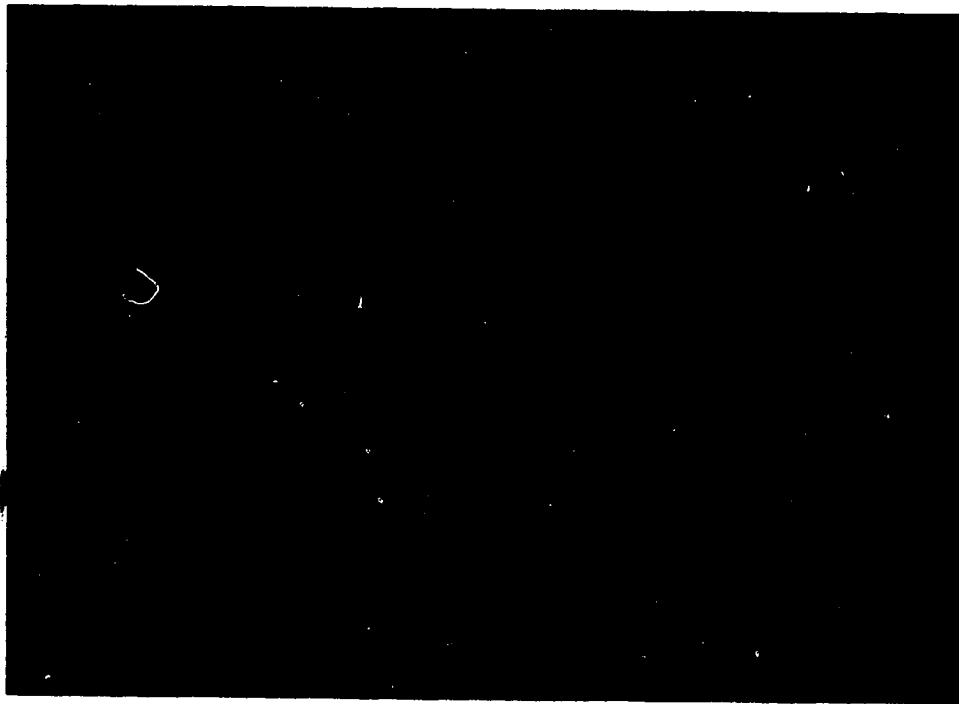


Figure 5.4 Oblique aerial photograph downstream of landslide.

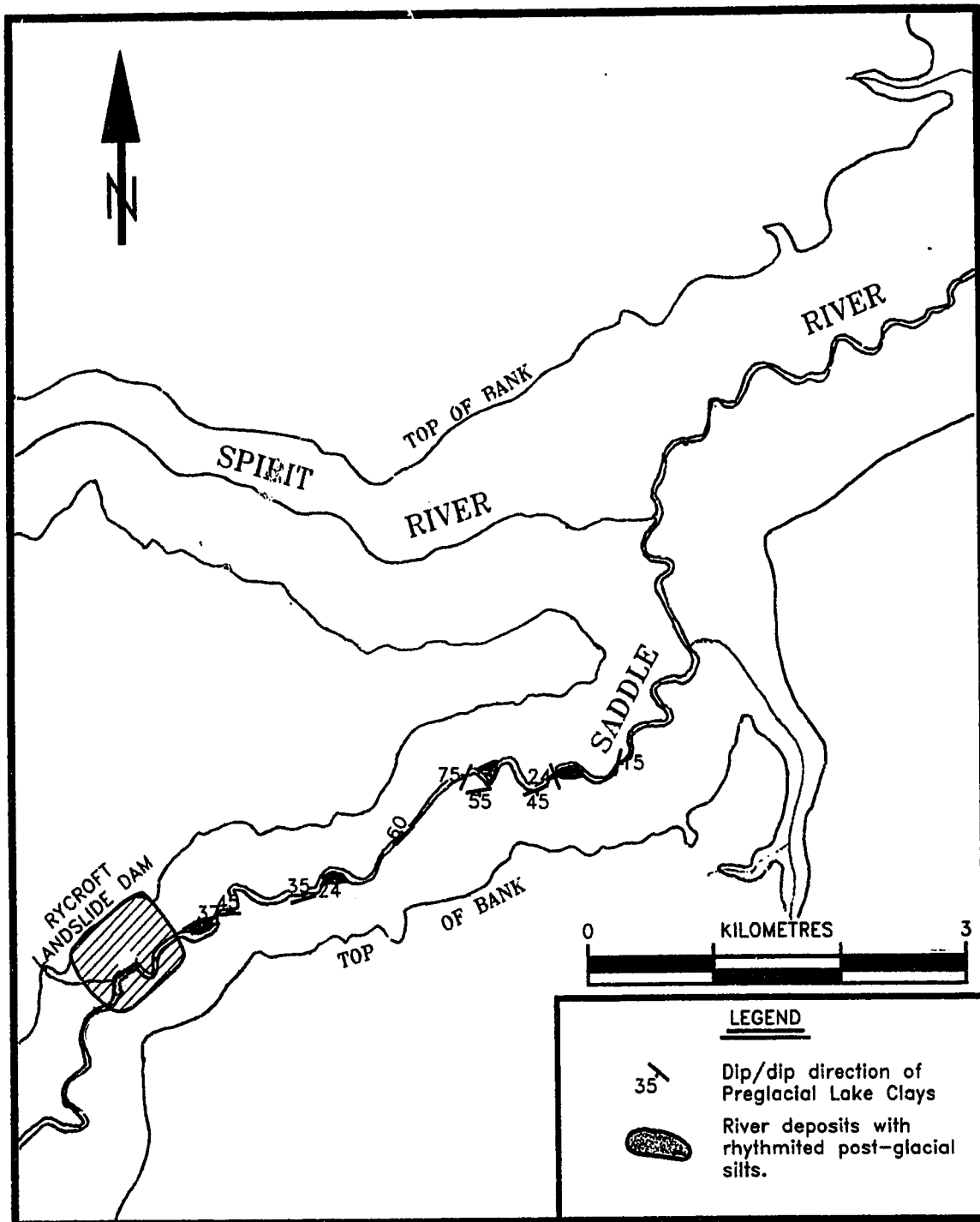


Figure 5.5 Plan of Saddle River downstream of landslide showing location of dipping clay beds in river bed and identified river terraces.

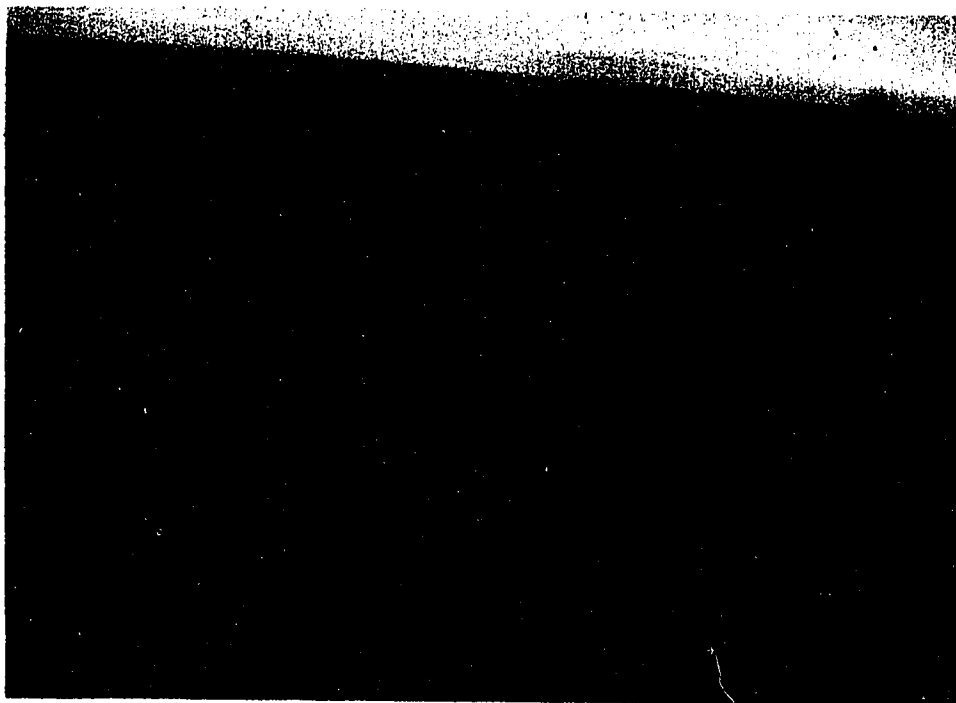


Figure 5.6 Oblique aerial photograph downstream of confluence of the Spirit River.

5.4 Overtopping of the Landslide Dams

Evidence of previous blockages in the Saddle River is used in conjunction with observations of the current blockage to estimate the behavior of the Rycroft Landslide Dam. Evidence of earlier blockages of the Saddle River is provided in a number of post-glacial deposits cut through by the current river channel observed downstream of the landslide (Figure 5.5). Figure 5.7 is a sketch of a cut bank where these deposits are exposed. The exposure shows a cross-section of a post-glacial buried channel containing rhythmited silt layers, indicators of ponded water deposition. This particular cut bank is at the location of TP 1 shown in Figure 2.4 and indicates three beds of rhythmited silt. Because the Saddle River has been actively downcutting since deglaciation, the only process that would result in the formation of this sequence of deposits is the blockage in the river valley resulting from landslides.

The highest number of rhythmites counted in one unit was 30. The formation of a single rhythmite is associated with a rainstorm or snowmelt event which for this river is infrequent and highly variable (Section 4.2) and therefore the rhythmites are only an order of magnitude indicator of the duration of previous blockages. These terraces indicate that previous similar landslides had blocked the river in the past but without producing any enduring lakes.

The current landslide dam is approximately 24 m above the original river bed at the spillway crest and has a length along the river bed of about 800 m. The material which forms the dam consists mostly of till, preglacial lake clay and coarse granular material of the pre-slide river bed. Overtopping began with runoff from the annual snow melt in 1991. On April 11, 1991, flows of about $2 \text{ m}^3/\text{sec.}$ eroded a new channel into the displaced mass where the landslide debris meets the opposite bank of the river. By the end of April, severe erosion was occurring at the downstream end of the displaced mass where a 50 metre long chute sloping at approximately 18° had developed. Upstream of the chute, a pond 40 m wide and 200 m long had formed and a smaller chute above it accounted for a further 5 m rise to the spillway crest and main reservoir. The upper chute is armored with uplifted coarse granular river bed deposits (Figure 2.4). Overtopping of the landslide toe continued intermittently through the remainder of 1991 with an approximate overall drop in the spillway crest elevation of about 1.5 metres.

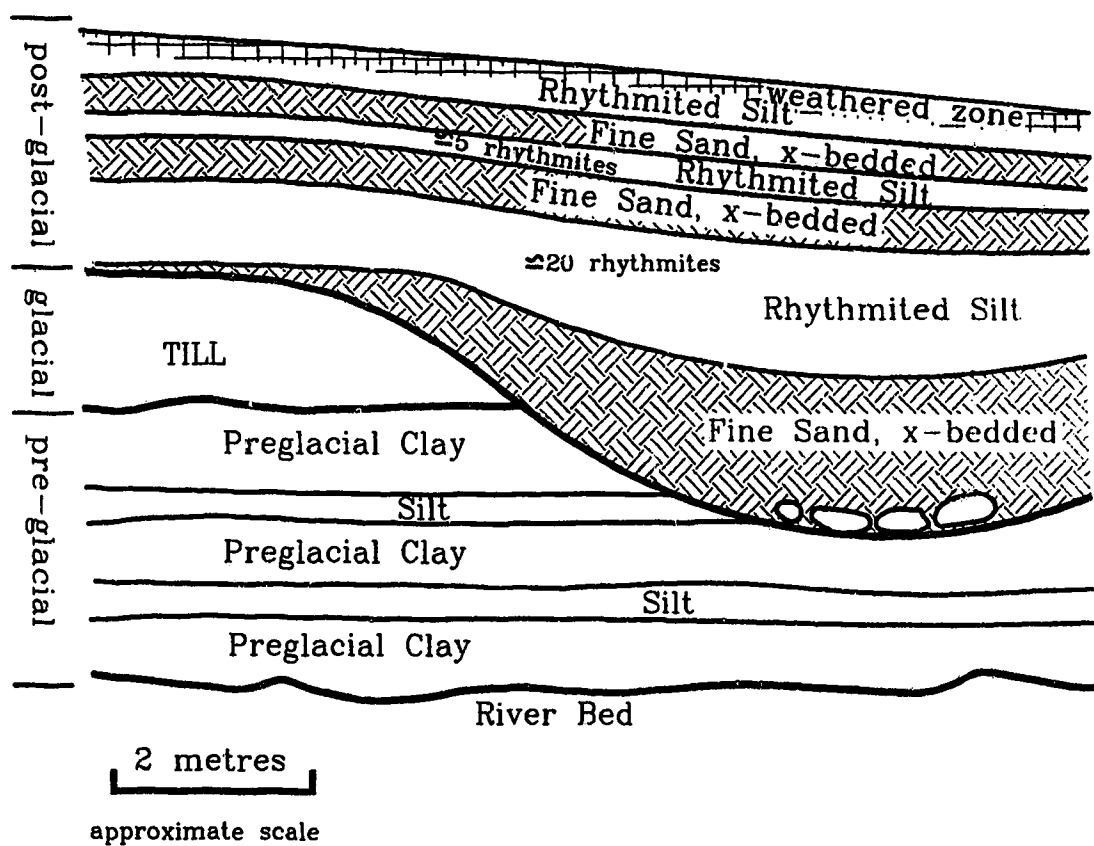


Figure 5.7 Sketch of river bank exposing post-glacial Saddle River terrace deposits downstream of the Rycroft Landslide Dam.

The displaced blocks that make up the dam appear relatively intact with no open cracks observed between them. This is not surprising assuming the toe of the slide mass was compressed against the right bank by the slide movement. The dam is hence capable of providing some resistance to erosion as overtopping occurs. The length of the dam along the thalweg, some 800 m, the lack of any seepage through the dam and the small amount of erosion observed in the first season suggest that a sudden, total breach of the dam is unlikely. It is anticipated that, over a period of years, the river will erode through the toe mass to its original level. The erosion rate, and the time to regain the pre-slide profile will depend on the magnitude of the variable and infrequent flood flows of the river.

If, by some chance, the level of the impounded lake is lowered sufficiently rapidly, drawdown failures are likely to occur on both sides of the reservoir. These, in turn, may generate slides involving the entire valley wall. Such slides could result in a significant displacement of water causing a surge of flow over whatever is left of the dam.

5.5 Summary

The Saddle River profile is convex shaped due to being left behind by the rapid entrenchment of the post-glacial Peace River and the erosion resistance in the till. The Rycroft Landslide Dam occurred at a location and time when the river was cutting through till and into preglacial lake clay. Downstream of the landslide there is a transition zone where the average slope angle of the valley walls drops from 13° and 8° . Field evidence supports the hypothesis that this zone marks a transition from a stable slope angle governed by the available shear strength in the till to a stable slope governed by the lower available shear strength in the preglacial lake clay. Evidence in post-glacial deposits downstream of the Rycroft Landslide suggests that previous landslides had blocked the river in the past but without forming any enduring lakes. The current landslide dam is reasonably competent and a sudden, total breach is unlikely. If the drawdown in the reservoir is sufficiently rapid then slope movements in the sides of the reservoir may be induced.

CHAPTER 6: LABORATORY TESTING

6.1 Introduction

The objective of the testing program is to establish the characteristic physical parameters of the soils which are fundamental to an understanding of the conditions which led to the Rycroft Landslide. The three geological units, involved in the landslide, are the glacial lake deposits, the till and the preglacial lake clay. This chapter covers a presentation and discussion of the classification tests and material properties of these geological units. Classification tests are conducted on soils from all three units while tests are conducted to obtain material properties of the two main units principally involved in the slide movement, that is, the till and preglacial lake clay.

Samples recovered for testing include disturbed and undisturbed shelby tubes, and double tube core barrel cores from testholes RS-1 and RS-2 drilled by Alberta Environment's mud rotary drill rig behind the crest of the landslide (Figure 2.4) at depths indicated in the detailed log in Appendix A. In addition, block samples of the preglacial lake clays were recovered from testpits at the toe of the landslide and at outcrops downstream of the toe (Figure 2.4). All tests were conducted at Alberta Environment, Development and Operations Division's geotechnical laboratories under the supervision of Larry Kolody, in accordance with ASTM standards generally following methods outlined by Lambe (1951).

6.2 Classification Tests

Classification tests including Atterberg Limits, natural moisture content, grain size analysis and bulk density were completed on the three units. Results of natural moisture content and Atterberg limits versus depth are illustrated in Appendix A and a summary of classification tests is given in Table 6.1. The glacial lake deposits are usually classed as inorganic clay of high plasticity (CH) but vary from medium-plastic silty clay to highly plastic clay (Figure 6.1). The till is usually classed as a well graded medium plastic silty clay (CI) but ranges from medium to high plasticity (Figure 6.1) with an increase in plasticity and clay content in the lower 30 m. Classification tests on block and core samples of preglacial lake clay indicate the material is consistently a

TABLE 6.1 Summary of classification test results, Rycroft Landslide Dam

Property	SOIL		
	Glacial Lake 0-20 m n = 5	Till 20 - 100m n = 10	Preglacial Clay 100 - 117m n = 12
Natural Water Content (%)	37 {31-40}	27 {18-40}	31 {24-35}
Liquid Limit (%)	56 {39-66}	45 {36-59}	73 {69-78}
Plastic Limit (%)	22 {20-23}	18 {14-21}	25 {22-29}
Plasticity Index (%)	34 {19-44}	28 {22-38}	48 {44-52}
% sand sizes	-	12 {3-21}	1 {0-2}
% silt sizes	45 {32-67}	51 {45-57}	32 {26-40}
% clay sizes	55 {32-68}	37 {30-45}	68 {59-74}
Activity	0.62 {.61-.65}	0.64 {.5-.73}	0.72 {.65-.88}
Bulk density (Kg/m³)	1915	2079	1943

Average value in heavy print

Range of values in brackets

n=number of samples tested

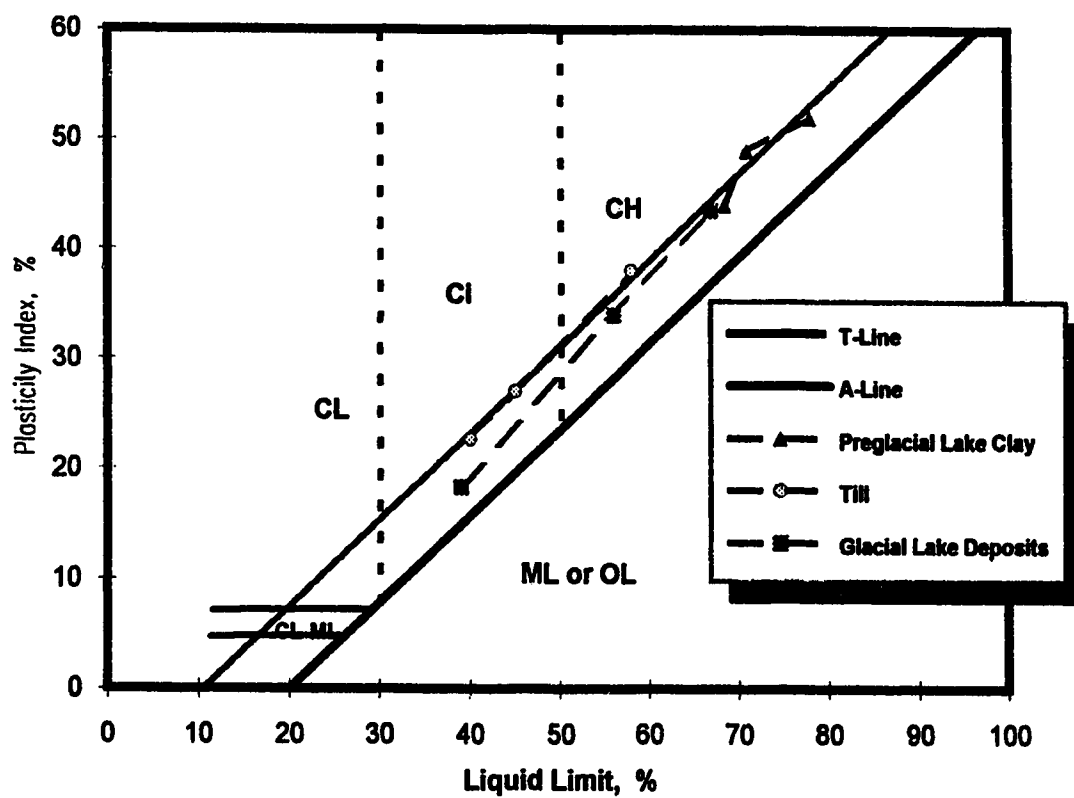


Figure 6.1 Plasticity chart showing range of plasticity at Rycroft Slide.

highly plastic clay (Figure 6.1) with clay content averaging 68%. The varving in the preglacial lake clay would suggest there is a gradation in plasticity and clay content vertically within the rhythmites. This gradation would not be apparent from the Atterberg Limits and grainsize analysis due to the complete mixing associated with these tests.

Drawn on Figure 6.1 is the T-line defined by Boulton and Paul (1976). These researchers discovered that unaltered englacial debris or lodgement till plotted on the plasticity chart on a line parallel to the A- line. These soils varied along this line according to clay content. The grain-size changes which commonly occurred in flow tills due to sorting processes, and the mixing of lodgement tills with other subjacent sediments due to subglacial deformation moved points away from the T-line (Boulton and Paul, 1976). The proximity of the till from the Rycroft Landslide site to the T-line indicates it can be characterized as englacial debris or undisturbed lodgement till with little to no disturbance of its grain-size. Note the deviation of the glaciolacustrine material and preglacial lake clay from the T- line which is consistent with the sorting processes these materials have undergone.

The activities of the three soils range from 0.5 to 0.9 indicative of an illite-rich clay (Skempton, 1953). It is possible, however, that thin, montmorillonite-rich layers may be present in the rhythmitic preglacial clays, partially controlling the unusually low peak and residual shear strengths measured parallel to the rhythmites as discussed in Section 6.3. No tests were completed to confirm this suspicion.

6.3 Material Properties of the Till

From observations in outcrops, below the weathered zone, and in core, the till lacked a recognizable macro-structure or layering and it is assumed the till is strength isotropic. Observations of the displaced mass indicate that the shears that formed in the till were first-time shears through intact till and it is therefore assumed the dominant mobilized shear strength in the till is its peak shear strength. On this basis the principal goal of the testing program on the till is to determine the effective peak shear strength parameters.

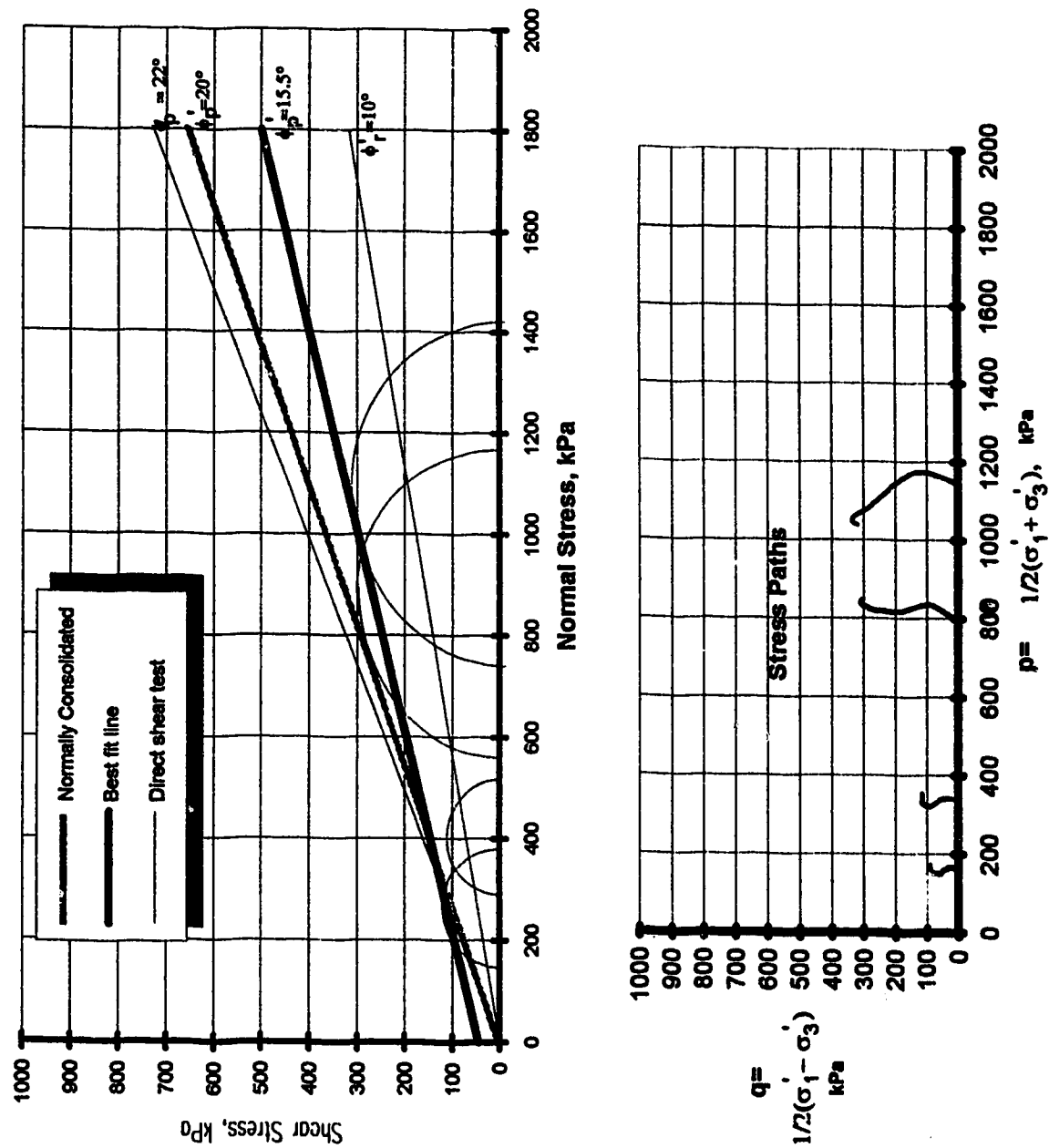


Figure 6.2 Standard and Modified Mohr diagrams for the till.

The primary tests conducted were consolidated undrained (CU) triaxial compression tests on shelly tube samples recovered from testhole RS-1. One direct shear test was conducted to corroborate the results and determine an estimate of the residual shear strength for the till for use in the post-slide analysis. Samples tested are from depths ranging from 50 to 100 m. The results are presented in Standard and Modified Mohr diagrams in Figure 6.2. Strain rates were maintained at a maximum 1×10^{-5} m/min. in an attempt to allow dissipation of localized pore pressures within the sample. Stress paths are shown for each of the triaxial tests. Using the results of all tests the best fit line gives $\phi'_p = 15.5$ with a cohesion intercept of 45 kPa. Using only tests conducted at stress ranges greater than their assumed preconsolidation pressure ($P_c > 500$ to 900 kPa) or, that is, in the normal consolidation range, yields $\phi'_p = 20^\circ$ with a zero cohesion intercept. The lone reverse direct shear test conducted on the till indicates $\phi'_p = 22^\circ$ assuming a zero cohesion intercept and $\phi'_r = 10^\circ$. The average pore pressure parameter A at failure is 0.7 which is consistent with a normally consolidated fine grained soil (Lamb and Whitman, 1969). Stress paths shown in Figure 6.2 all have shapes typical of a normally consolidated clay with the possible exception of one sample which is slightly to the right of vertical typical of a lightly overconsolidated clay (Lamb and Whitman, 1969). Which of the above effective strength parameters appropriate for the stability analysis is discussed in Section 7.4.

6.4 Material Properties of the Preglacial Lake Clay

Primarily because of the rhythmed nature of the preglacial lake clay, its effective shear strength, both peak and residual, is assumed to be anisotropic. This is based on the premise that horizontal shear bands preferentially form through the weaker, high clay content portion of the rhythmite. Shear bands that form vertically result in a mixing of the clay content across the rhythmite resulting in a slightly lower clay content and higher strength in the shear band. In the preglacial lake clay both the residual and peak effective shear strengths are important in the analysis because a portion of the rupture surface in the preglacial lake clay is pre-existing. Along the pre-existing surface the residual strength is assumed to be mobilized while back of this the peak strength is assumed.

Strength tests on the preglacial lake clay were performed on intact block samples taken from test pits TP 2 and TP 3 (Figure 2.4) and from double tube core barrel samples taken from testholes RS-1 and RS-2. Tests include consolidation tests in the oedometer, reverse direction direct shear tests both parallel and perpendicular to

bedding to determine peak and residual effective shear strength parameters and one consolidated, undrained triaxial compression test to confirm peak effective shear strength and obtain an estimate of the pore pressure parameters. A Mohr envelope plot for the preglacial lake clay is presented in Figure 6.3. Consolidation tests conducted on samples taken from testpit #2 (Figure 2.4) in the toe of the landslide, and from RS-1, resulted in maximum preconsolidation pressures of 300 kPa at the toe and 900 kPa at a depth of 105 m in RS-1. The soil exhibits anisotropic strength with peak effective angles of 14.3° and 20.1° and residual effective angles of 6.7° and 9.3° parallel (horizontal) and perpendicular (vertical) to the rhythmites respectively. There are no cohesion intercepts from these results suggesting that the samples tested are in their fully softened state and are behaving normally consolidated (Yoshida et al. 1990). Strain rates of 1×10^{-6} m/min. for peak strength and 5×10^{-4} m/min. for residual strength were used in the direct shear tests. The lone CU triaxial test conducted on the preglacial lake clay is on a core sample taken from RS-2 at a depth of 105 m (Figure 6.4). Assuming a zero cohesion intercept this test yields $\phi'_p = 19.4^\circ$ consistent with the peak effective strength perpendicular to bedding obtained from the direct shear tests. Measurements from the CU triaxial test indicated a pore pressure parameter A at failure of 0.75, and a stress path shown in Figure 6.4 which is left of vertical. These results are consistent with a normally consolidated clay (Lamb and Whitman, 1969).

6.5 Summary

The glacial lake deposits are usually classed as inorganic clay of high plasticity (CH) but vary from medium-plastic, silty clay to highly plastic clay. The till matrix is usually classed as a well graded, medium plastic, silty clay (CI) but ranges from medium to high plasticity. The preglacial lake clay is consistently a high plastic clay with clay content averaging 68%. The proximity of the till to the T-line on a plasticity chart indicates it can be characterized as englacial debris or undisturbed lodgement till with little to no disturbance of its grain-size. The activities of the soils of the three units range from 0.5 to 0.9 indicative of an illite rich clay.

The till assumed to be strength isotropic has $\phi'_p = 15.5$ with a cohesion intercept of 45 kPa, $\phi'_r = 10^\circ$ and behaves normally consolidated.

Consolidation tests on the preglacial lake clay indicate it behaves like a normally consolidated clay. The preglacial lake clay exhibits anisotropic strength with $\phi'_p = 14.3^\circ$ and 20.1° and $\phi'_r = 6.7^\circ$ and 9.3° parallel and perpendicular to the rhythmites

.respectively. No cohesion suggests the samples tested are in their fully softened state and are behaving normally consolidated.

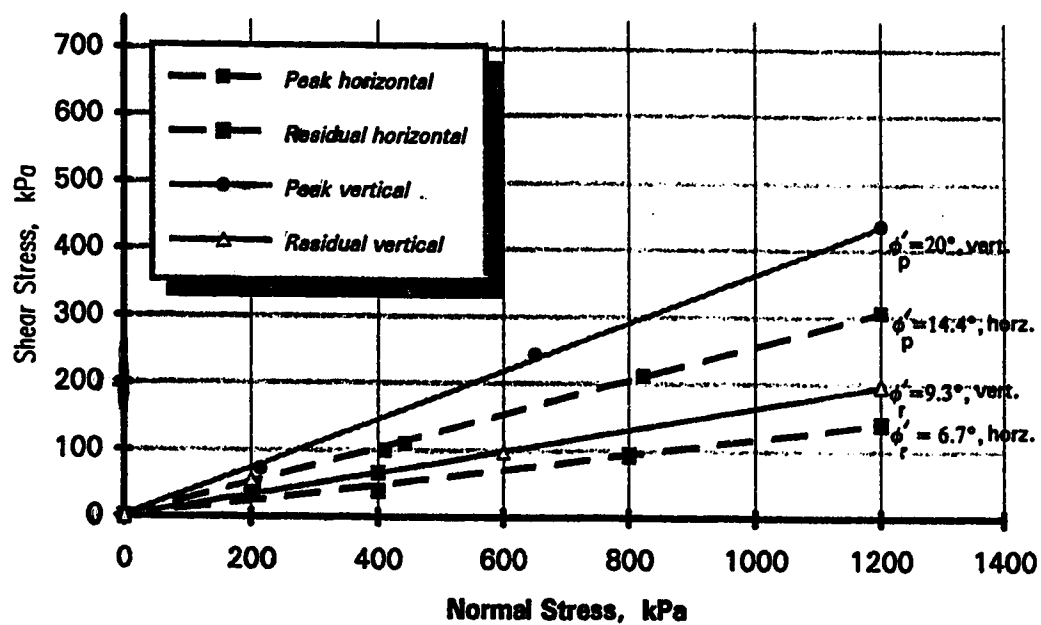


Figure 6.3 Mohr diagram for preglacial lake clay.

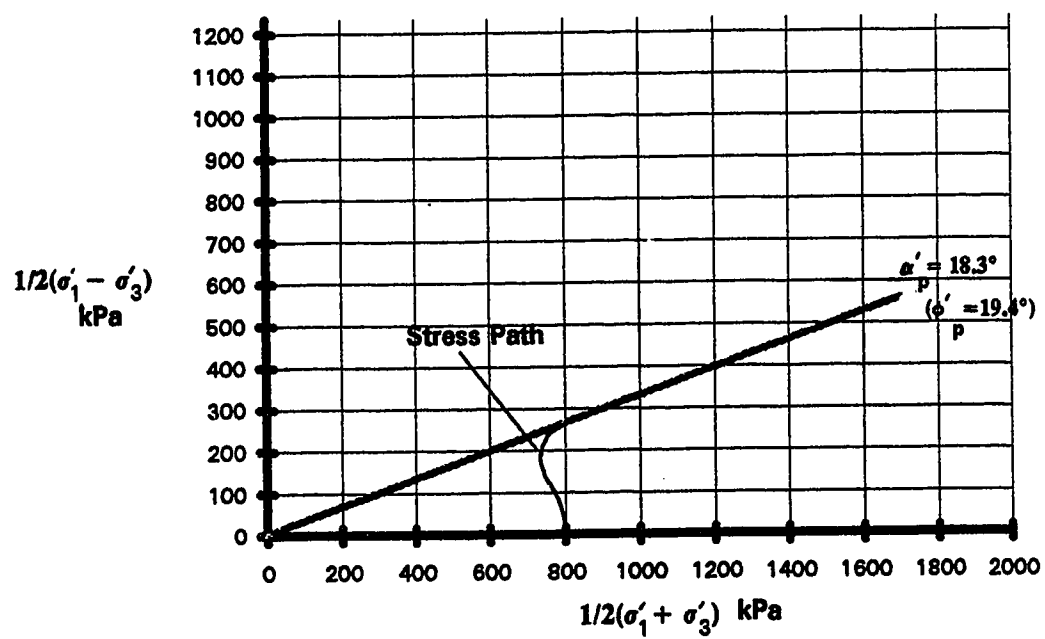


Figure 6.4 Stress path for consolidated undrained triaxial compression test on preglacial lake clay.

CHAPTER 7: STABILITY ANALYSIS

7.1 Introduction

This chapter studies the mechanics of the Rycroft Landslide using limit equilibrium analyses of the reconstructed pre-slide slope and the post-slide displaced mass. It is the aim of the chapter to conduct a back analysis of the stability of the pre-slide slope, to establish the difference in factor of safety between the two- and three-dimensional cases, to evaluate the relative effect that changes to the influencing conditions have on the pre-slide stability and to assess the stability of the post-slide slope both before and after the removal of the dam by erosion. To accomplish the analyses of the pre-slide and post-slide slopes requires a reasonably accurate reconstruction of the conditions which existed just prior to the reactivation and retrogression of the landslide and a conservative estimate of the conditions that exist or will exist after the movement. These conditions include the geometry of the slope and rupture surface, the mechanism of the landslide, the available soil strengths and the pore pressure distribution. Each condition is treated separately in Sections 7.2 to 7.5 and used in the following analytical sections. All limit equilibrium stability analyses are conducted using the software package CLARA (Hung, 1988) which has the added capability of calculating three-dimensional stability. The back analysis of the pre-slide slope discussed in Section 7.6 is primarily a check on assumptions made in the reconstruction of the slope. Confidence gained from the back analysis may be useful in furthering understanding, prediction and control of slope instability in the region. The geometry of this landslide suggests there is a three-dimensional influence on the stability of the pre-slide slope so a comparative analysis to determine the order of magnitude of the influence that three-dimensional effects have on the factor of safety is presented in Section 7.7. In Section 7.8 a sensitivity analysis is presented to demonstrate the effect that variation in any of these conditions had on the stability and is used to assess the most likely change in conditions which led to the Rycroft Landslide. A stability analysis of the post-slide displaced mass presented in Section 7.9 is useful in assessing the potential for further movements of the disturbed mass, particularly when the toe material is removed by the inevitable erosion of the dam.

At the onset of this chapter it should be noted that there are a number of assumptions inherent in the choice of phreatic and rupture surfaces and variations

contained in the soil parameters. It is, therefore, not possible, and it is not the intent in this study, to accurately model the conditions of the slope and obtain specific values. It is possible, and is the intent of this study, to test assumptions regarding the phreatic and rupture surfaces and evaluate methods of estimating soil parameters and obtain information from investigation of trends. All values quoted in this chapter are to be considered relative.

7.2 Geometry

The first step in the back analysis is to use the geometry to reconstruct a model of the pre-slide slope and rupture surface. Sources of information used in the reconstruction are airphoto mapping of the site before and after the landslide, 1:20,000 Provincial base maps of the site based on aerial photography flown in 1981 (Alberta Forestry, 1985), post-slide field mapping of the landslide, a post-slide EDM land survey and testholes RS 1 and RS 2.

In plan the Rycroft Landslide (Figure 7.1) extends for a considerable distance along the slope perpendicular to the direction of movement, suggesting that much of the rupture surface may approach the shape of a sector of an elliptical cylinder (Varnes, 1978). Transversely, the landslide is truncated by sub-vertical and parallel lateral margins.

In the head area the back-dipping blocks (0 to 20°) and steep scarps suggest the movement here is more or less rotational on a rupture surface cutting through the glacial lake deposits and the till.

The lack of rotation in the main body of the slide mass, as described in Section 2.3, suggests the movement here was translational on a planar or gently undulating rupture surface. This is supported by assuming that the rupture surface is contained in the weaker, flat lying preglacial lake clay layer.

The distortion at the toe, which includes uplift, thrusting and rotation, suggests this area is a pressure ridge forced upwards as the slide mass encountered the right bank of the river.

The main scarp B and a minor scarp A extending across the head of the slide (Figure 7.1), are used to introduce the hypothesis that the initial rupture surface formed at A and then retrogressed to form the main scarp at B.

The line A-A' on Figure 7.1 was initially assigned perpendicular to the new scarp features at an azimuth from true north of 147° in the centre of the landslide so that it would parallel the direction of movement of the landslide. This was confirmed in the field when the trend of the striations, which are lineation features on shear planes, measured along A-A' were within $\pm 5^{\circ}$ of A-A'.

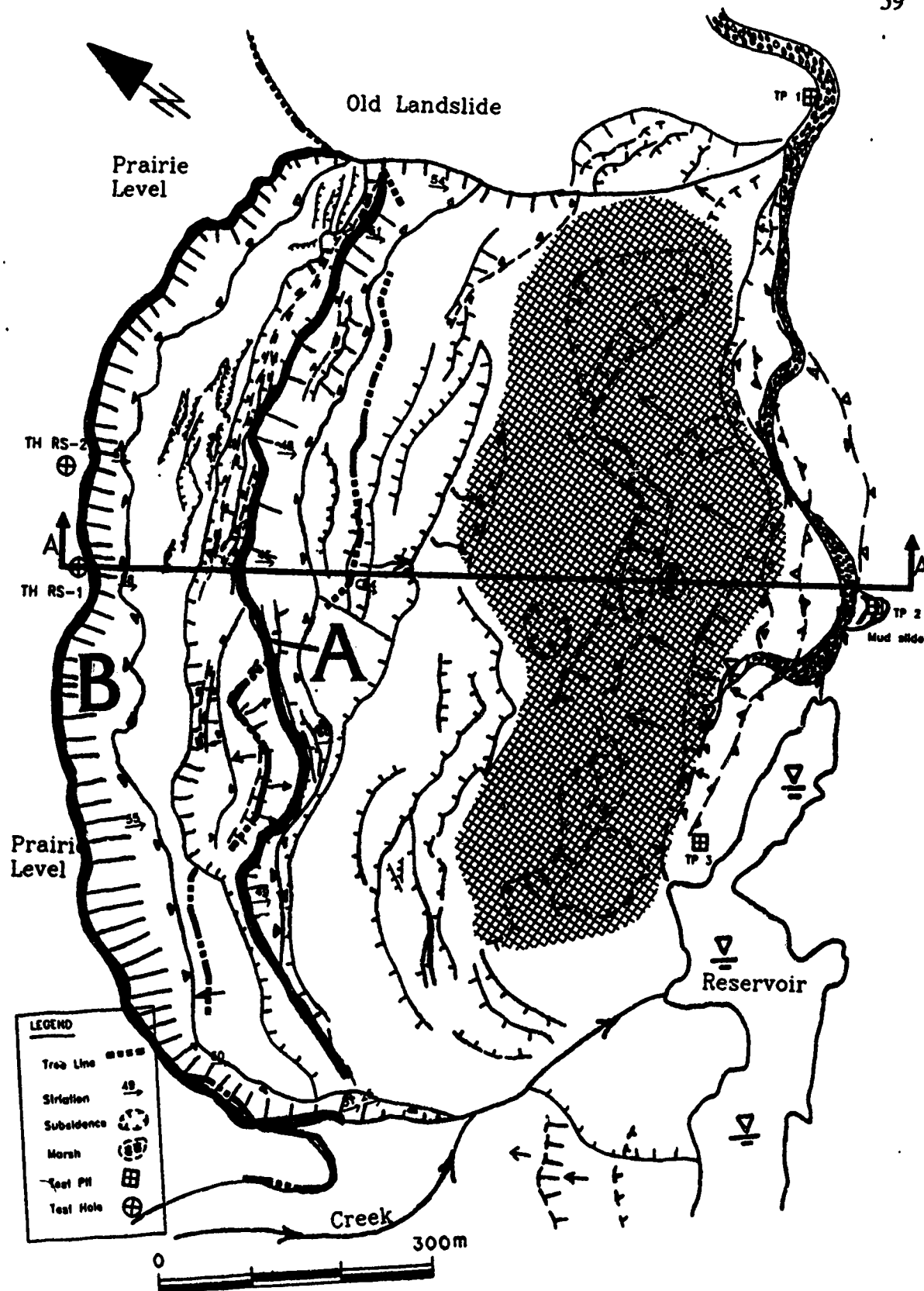


Figure 7.1 Pre-slide plan view of the slide area from an overlay on Alberta Government panchromatic air photo taken at a nominal scale of 1:5000 in October, 1990.

The section along A-A' was chosen as the key section for the analysis because of the approximate symmetry on either side of this line and because it is the section furthest away from the shear resistance along the flanks. Figure 7.2 illustrates the reconstruction of the slope and rupture surface accomplished by first breaking up the surveyed, post-slide section A-A' into a series of wedges (Figure 7.2). Where available, the field mapped crack orientations are extended downward into the slide mass. Using AutoCAD, the wedges are then picked up, moved and rotated back to their assumed original positions. Tree inclinations, bedding dips, tilted cultivated land and comparisons between post-slide and pre-slide air photos are used to estimate the proper rotations for the wedges. The original profile for the slope plus the river location, taken from the 1:20,000 provincial base map (Alberta Forestry, 1985), are used as an outline to position the wedges.

Where it is necessary to rotate wedges to suit constraints or to match rotation implied by inclined trees or bedding, the interwedge faults are curved to facilitate the rotation using the known rotation angle and the relative distance each wedge moved. For example, this exercise showed that the largest intact wedge, 13, had been rotated back four degrees by the slide movement. Since the distance this block moved is 85 m, and the rupture surface is exposed at the toe in the pre-slide river bed, it is possible to reconstruct the curved rupture surface beneath this block as shown in Figure 7.2. The rupture surface behind Wedge 13 is extrapolated using the approximate depth where the main cracks coalesce and is assumed to be contained in the preglacial lake clay. Figure 7.2 (b) illustrates the reconstructed slope profile and rupture surface used in the back analysis. Note that the pre-existing slips on the pre-slide slope were apparently not remobilized during the recent movement. This reconstruction, identifies an additional major scarp with a downward extension labeled as Rupture Surface A on Figure 7.2(b). This scarp is continuous across the slide (Figure 7. 1) and it may be the first scarp to have formed when the movement was initiated.

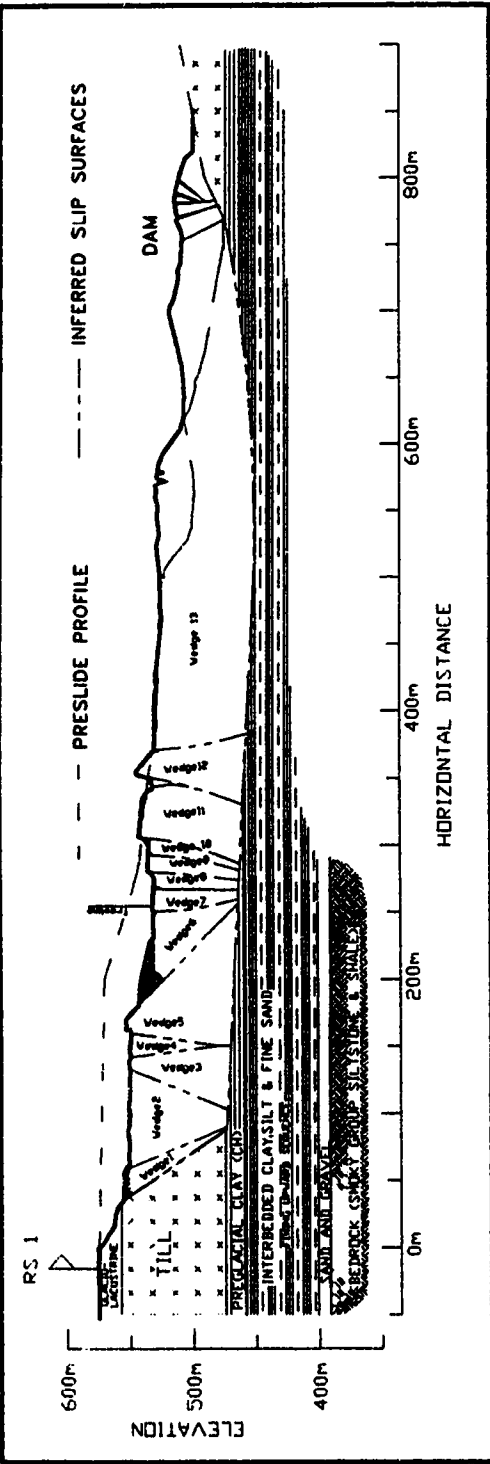


Figure 7.2 (a) Post-slide configuration along A-A'.

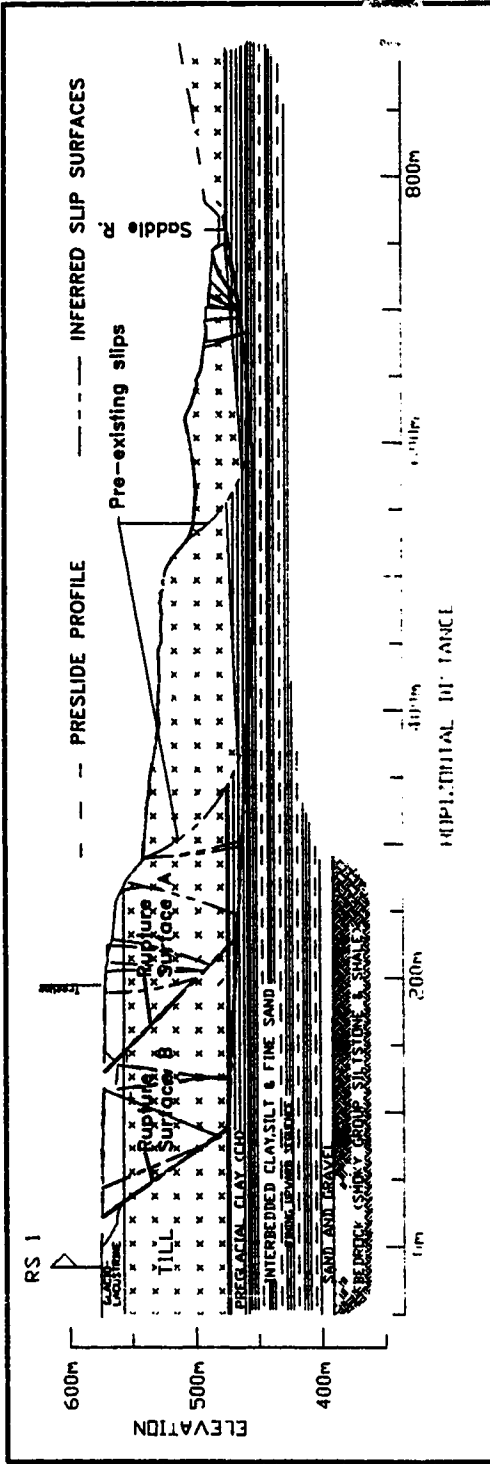


Figure 7.2 (b) Interpreted pre-slide configuration along A-A'.

7.3 Mechanism

The observations discussed in Section 5.3, suggest that the pre-slide slope is in a transition from a minimum slope angle governed by the available shear strength in the till to a minimum slope angle governed by the lower available shear strength in the preglacial lake clay. The pre-existing scarps in the pre-slide slope, which are thought to extend to the rupture surface in the preglacial lake clay, are indication that the transition of the slope had already begun. It is assumed that the 1 in 50 year rainstorm, that occurred on 11 and 12 of June, 1990, set into motion a change of conditions that crossed over the transition, resulting in the large movement. Geometry changes at the toe due to lateral or downward erosion or changes in the water pressure distribution due to the accumulation of water on the pre-slide slope were possible changes that occurred.

There were two likely changes in geometry at the toe of the landslide after the rainstorm and prior to the movement. The first was the assumed significant bank erosion on the outside of meanders at the toe of the slide resulting from approximately 50 Mm³ of flood volume that flowed past the landslide in the four or five days preceding the movement. Because of the disturbance at the toe of the landslide by the slide movement, an estimate of the magnitude of the erosion at the landslide is not possible. However, there is significant evidence of severe river bank erosion downstream of the landslide as described in Section 5.3. The second change in geometry at the toe prior to the movement was an apparent downcutting of the river bed of about one to two metres following the 1 in 50 year flood described in Section 5.3. The effect of removing material at the toe of the slide is investigated in the sensitivity analysis in Section 7.8.

There was ample source of surface water on the pre-slide slope following the 1 in 50 rainstorm event. Because the pre-slide slope was a dormant landslide, it is possible that open cracks were present in the slide mass. If these cracks filled with water, the resulting water forces would increase the driving forces and reduce the stability of the slope. If the cracks extended to the rupture surface, the increased water pressure would decrease the effective normal stress on a portion of the rupture surface reducing the resisting forces which would again reduce the stability. It is possible that the effects from the erosion at the toe and the accumulated water on the slope were coupled in the sense that the erosion at the toe caused displacement in the lower slope which opened pre-existing and new cracks which subsequently filled with water. The

effect of fluctuating water pressures in the slope is investigated by varying the equivalent phreatic surface in the sensitivity analysis in Section 7.8.

From the exercise in geometry (Section 7.2) it is evident that the rupture surface is markedly non-circular and that the movement of the slide mass was mainly translational on a gently curved basal rupture surface (Figure 7.2). The downward projections of the two main scarps, A and B in Figure 7.2, are rupture surfaces which formed at the rear of the slide. The geometry suggests that the rupture surface extended from a pre-existing rupture surface in the preglacial clays along Rupture Surface A to form the initial scarp. With the downslope mass movement and support gone, the slide then retrogressed to Rupture Surface B forming the present main scarp. To evaluate this hypothesis, the stability of both of these configurations is considered in subsequent analyses (Figure 7.3). The pre-existing rupture surfaces shown in Figure 7.3 are assumed from the observed scarps left from earlier failures. Although there was little or no additional movement observed on these scarps during the latest slide, their locations are important as they indicate the minimum distance back from the toe that the rupture surface existed prior to the slide.

With regards to the behavior of the slide mass after initiation it is of some use to look at the slide mass in terms of lateral earth pressures. It is inferred that the upslope zone of the slide mass which underwent longitudinal stretching, had earth pressures less than before the movement started and approached the limiting active (or minimum) pressure breaking into a number of horsts and grabens with faults at dips of close to $45^\circ + \phi/2$. Similarly, the downslope zone of shortening-ground near the toe had earth pressures higher than before the movement started and approached the limiting passive (or maximum) pressure and showed significant distortion through thrusting as shears formed at approximately $45^\circ - \phi/2$. The middle portion of the slide, between the zones of stretching and shortening remained near the at-rest state and remained relatively undeformed (Baum and Fleming, 1991).

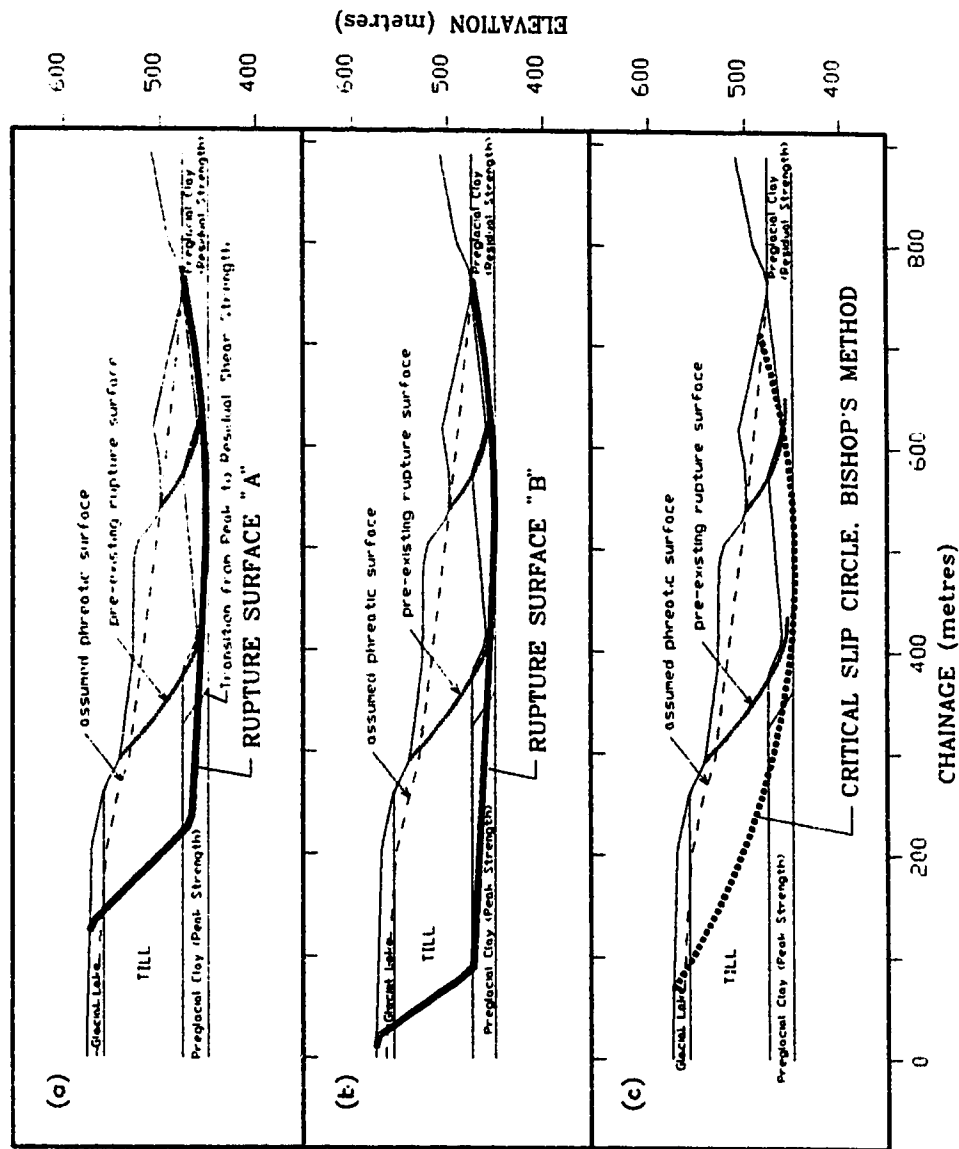


Figure 7.3 Configuration along A-A' used in stability analysis of the pre-slide slope.

7.4 Strength Parameters

Table 7.1 summarizes the soil properties initially used in the stability analysis. The materials in Table 7.1 are numbered from the bottom up as is the convention in the stability analysis program. The majority of the slide mass is comprised of till while the basal rupture surface is contained in the preglacial lake clay (Figure 7.2). The strengths for the till (material 4) and Preglacial lake clay (material 2 & 3) were taken directly from the laboratory test results presented in Section 6.3. The strength of the till is assumed to be isotropic while the shear strength of the preglacial lake clay was shown to be anisotropic. Properties of the silt and clay (material 1) which underlies the preglacial lake clay is assumed to have a strength similar to the preglacial lake clay. This is based on the poorly defined lower contact of the preglacial lake clay and the similar signatures of the two materials apparent in the geophysical log (Appendix B). The glacial lake deposits (material 5) were estimated based on their index properties and physical appearance using an inventory of test results on Alberta soils kept by Larry Kolody of Alberta Environment. Materials 1 and 5 are assumed to have a minor influence on the stability of the slope so they were not tested.

All materials except the till are initially assumed to have zero cohesion in the analysis. For the preglacial clays, using zero cohesion stems directly from the test results as both peak and residual strength envelopes indicate zero cohesion (Figure 6.2). Several test results discussed in Section 6.3 indicate the preglacial lake clay behaves like a normally consolidated clay. The effective strength envelope for the till yields a cohesion intercept of 45 kPa and a $\phi'_p = 15.5$ which is used initially in the analysis for the pre-slide slope. This is appropriate because, in the slope model, this strength parameter is meant to represent soil strengths for a range of effective overburden pressures from approximately 900 kPa to zero and thus a best fit line through all tests is a better strength representation for the stress range experienced in the slope. This assumes that the maximum preconsolidation pressure vertical profile, which would have occurred prior to the post-glacial incising of the river, was the same up and down slope. The sensitivity analysis (Section 7.8) tests the effect the mobilized strength of the till has on stability. For the post-slide stability numerous shears are known to exist within the till and its residual strength of $\phi'_r = 10.5^\circ$ is used.

In the preglacial lake clay, the maximum mobilized strength along the pre-existing basal rupture surface is assumed to be its residual strength due to previous large shear strain movements. At some point beyond the pre-existing slip it is assumed

Table 7.1 Summary of soil properties used in stability analysis

Material Number	Soil	Unit Weight (kN/m ³)	Cohesion	C'	Friction	φ
			Horizontal kPa	Vertical kPa	Horizontal (deg.)	Vertical (deg.)
<i>Pre-slide Stability</i>						
1	Silt and Clay	19.78	-	-	7	10
2	<u>Preglacial Lake Clay</u> Clay(CH)-Peak	19.06	-	-	14.4	20
3	Clay(CH)-Residual	19.06	-	-	6.7	9.3
4	Clay Till	20.39	45	45	15.5	15.5
5	Glacial Lake Deposits	18.80	-	-	15	15
<i>Post-slide Stability</i>						
1	Silt and Clay	19.78	-	-	7	10
2	<u>Preglacial lake clay</u> Clay(CH)-Peak	19.06	-	-	6.7	9.3
3	Clay(CH)-Residual	19.06	-	-	6.7	9.3
4	Clay Till -Residual	20.39	-	-	10.9	10.9
5	Glacial Lake Deposits	18.80	-	-	15	15

the available shear strength increases to the measured peak strength for the clay. The point of transition is initially set at chainage 350 m which is just behind the last recognized pre-existing slip as shown in Figure 7.3. Additional factors which might affect the transition location include ice thrusting, stress release, valley rebound, and progressive failure. In Section 7.8.5, the effect of moving the transition point back will be assessed.

7.5 Pore Pressure Distribution

The piezometric data for the site are very limited. The only indicators of the pre-slide phreatic surface are evidence of seepage and a few sag ponds on the slope. The water level measured in open testhole RS-2 in August, 1991, one month after drilling, was at a depth 12 m below prairie level. At best this is an approximate indicator of the steady state seepage conditions behind the slope crest. Because of the low permeability of the clay soils, it is assumed that seasonal fluctuations in the phreatic surface through the intact soil are insignificant. However, the possibility of cracks in the pre-existing slope would allow rapid build-up of water pressures in the lower slope as discussed in Section 7.3 so a near surface phreatic surface is initially assumed in the lower portion of the slope. The assumed phreatic surface used in the analysis is shown in Figure 7.3 and the effect of varying the level is assessed in the sensitivity analysis in Section 7.8.4.

7.6 Pre-slide Stability

The results of the pre-slide slope stability analysis, based on the assumed conditions developed in the preceding sections, and as shown in Figure 7.3, are summarized in Table 7.2. Because the rupture surface is non-circular, Morgenstern and Price (1965) and Spencer's (1973) methods for a general sliding surface are used to evaluate both possible rupture surfaces A and B. The analysis implies that movement occurred on rupture surface A ($F=0.86$) and that rupture surface B ($F=1.16$) was stable prior to disturbance. A discussion of the low value of F on rupture surface A forms part of Section 7.8. The results support the hypothesis suggested by the geometry that the movement initiated on rupture surface A which, by removing support to the

remaining slope, lowered the factor of safety and initiated the retrogression along rupture surface B forming the final main scarp.

To illustrate the impracticality of applying a slip circle analysis on the given pre-slide slope conditions, Bishop's method is used in a search for the critical slip surface. As shown in Figure 7.3 (c), the critical slip circle obtained, constrained by its circular shape, is forced to pass more through the stronger till layer than the geometry observations indicate, resulting in an analysis which yields a non-conservative result (Table 7.2).

A useful observation of this slope is the way all recent and past scarps extend steeply through the till and coalesce into the sub-horizontal basal rupture surface in the preglacial lake clay. By analyzing a range of potential locations for this scarp on the pre-slide profile using the downward extension of the scarp as the back, steep portion of the rupture surface, a profile of potential scarp (or tension crack) locations is generated as shown in Figure 7.4. The method is analogous to using an auto search technique to determine a critical slip circle. In this case the analysis predicts a critical scarp location at chainage 175 m which is 46 m ahead of where Rupture Surface A daylighted. Given the uncertainty involved in the input parameters for the pre-slide slope, this exercise provides a promising prediction of the initial scarp location. The results also imply that it was unlikely Rupture Surface B preceded Rupture Surface A and partially explains why there was no observed reactivation on the pre-existing scarps downslope. These implications rely on the premise that the profile in Figure 7.4 shifts vertically without significantly changing shape as conditions which affect the stability of the slope change.

Table 7.2 Summary of Stability Analysis of the Rycroft Landslide.

Analysis #	Configuration		Analysis Method	F	Remarks
	Ground Surface	Rupture Surface			
<u>Pre-slide Stability</u>					
1	Preslide Profile	"A"	General Surface: Morg. & Price	0.86	See Figure 7.3 (a)
2	Preslide Profile	"A"	General Surface: Spencer's	0.86	
3	Preslide Profile	"B"	General Surface: Morg. & Price	1.16	See Figure 7.3 (b)
4	Preslide Profile	"B"	General Surface: Spencer's	1.16	
5	Preslide Profile	Critical Circle	Auto Search: Bishop's	0.96	See Figure 7.3 (c)
<u>3-D Analysis</u>					
6	3-D Preslide Surface	A* (with lateral margins)	General Surface: Bishop's	0.90	See Figure 7.5
7	2-D Profile from 3-D Preslide Surface	"A"	General Surface: Bishop's	0.84	6% higher F resulting from 3-D end effects
<u>Post-slide Stability</u>					
8	Postslide Profile	"B"	General Surface: Morg. & Price	1.72	See Figure 7.11 (a)
9	Postslide Profile	"B"	General Surface: Spencer's	1.72	
10	Postslide Profile	Critical Circle	Auto Search: Bishop's	1.58	
11	Postslide Profile with Toe Removed	"B"	General Surface: Morg. & Price	1.39	See Figure 7.11 (b)
12	Postslide Profile with Toe Removed	"B"	General Surface: Spencer's	1.38	
13	Postslide Profile with Toe Removed	Critical Circle	Auto Search: Bishop's	1.35	

Note: Strength parameters used in above analyses are listed in Table 7.1

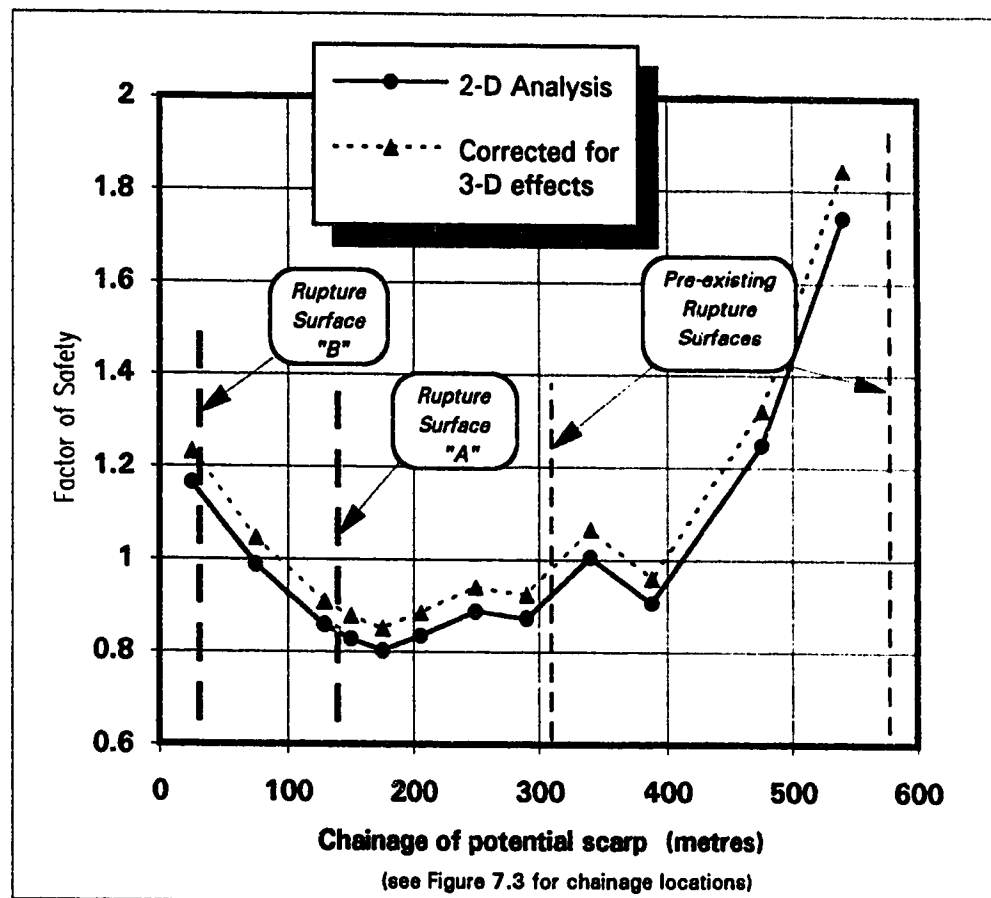


Figure 7.4 Stability analysis of various potential initial scarp locations for the pre-slide configuration.

7.7 Three-Dimensional Analysis

The lateral margins of the slide mass, as described in Section 7.2, represent a transverse change in the resistance to movement which is not accounted for in a two-dimensional plane strain analysis as presented in Section 7.5. This additional resistance may partially explain the low factor of safety ($F=0.86$) obtained for rupture surface A using the two-dimensional analysis. To evaluate an order of magnitude effect the lateral margins have on stability of the slope, a simplified three-dimensional configuration is created as illustrated in Figure 7.5. The pre-slide ground surface used in the model and not shown in Figure 7.5 is the pre-slide slope profile along section A-A' extrapolated across the width of the model. Rupture surface A is also extrapolated laterally from Section A-A' to form the three-dimensional rupture surface terminated by the lateral margins. The lateral margins are downward extensions of the lateral scarps at an average dip of 60° as measured in the field. The analysis is conducted using the software package CLARA (Hung, 1988, 1989) implementing the three-dimensional slope geometry module. The analysis uses Bishop's method to analyze the general slip surface shown in Figure 7.5 in both three- and two-dimensions. The results presented in Table 7.2 show, an order of magnitude, 6% increase in the factor of safety when the lateral margins are accounted for. When applied to $F=0.86$, obtained using Morgenstern and Price (1965) analysis on the two dimensional model for rupture surface A, the result becomes $F=0.91$. The upper profile in Figure 7.4 is the result of increasing the factors of safety by 6% to account for the 3-D effect. This value is closer to the expected result but does not fully explain why the minimum value for the factor of safety is lower than unity. The sensitivity analysis in Section 7.8 will investigate each relevant input parameter separately to determine the most likely unrealistic parameter in the analysis.

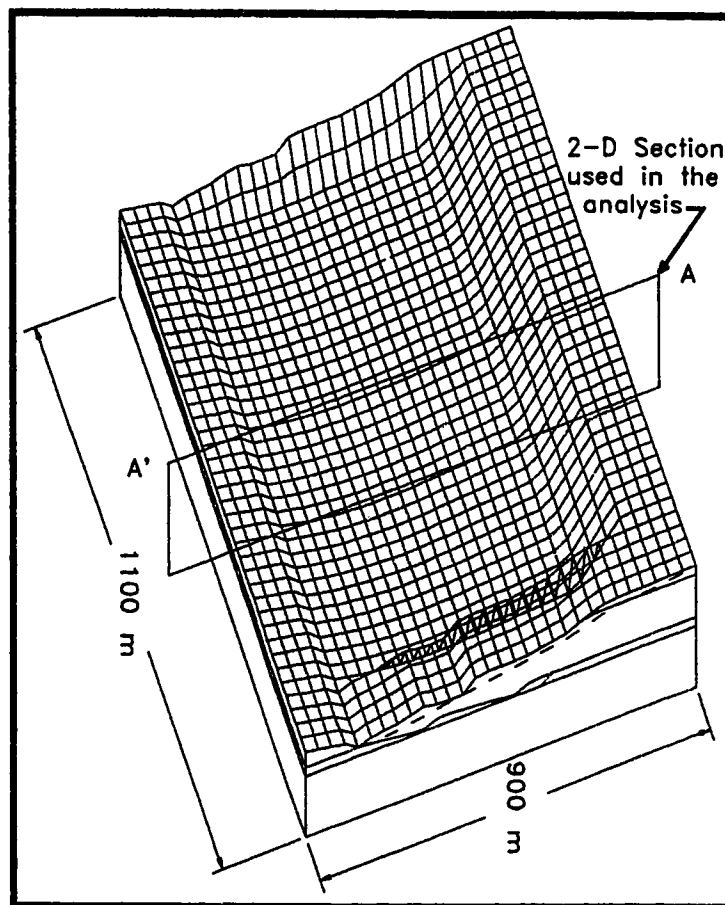


Figure 7.5 Simplified three-dimensional configuration of the rupture surface for the 3-D stability analysis.

7.8 Sensitivity Analysis

The objective of the sensitivity analysis is to test the sensitivity of the factor of safety obtained from the limit equilibrium stability analysis to changes in key input parameters to determine why the factor of safety is less than unity, which factors are most likely part of the initiation of the movement and which factors are part of the mechanism of the landslide.. Morgenstern and Price's analysis is used to analyze rupture surface A on Section A-A' throughout the exercise. All factors of safety are scaled up 6% to account for three dimensional effects determined in Section 7.7. The conditions varied in the sensitivity analysis and discussed in the following sections are the erosion of material at the toe, the residual shear strength in the preglacial lake clay, the effective shear strength in the till, the phreatic surface and the location of the transition from peak to residual strength in the preglacial lake clay.

7.8.1 Erosion of Material at the Toe

The exercise of removing material at the toe (Figure 7.6) is based on to the observations of toe erosion both downward and laterally as discussed in Section 7.3 and the hypothesis that this triggered the movement.. There is no effect on the factor of safety along the existing rupture surface due to downcutting the river bed by as much as 5 m below its original level. Figure 7.6 is the result of removing material laterally at the toe. The figure indicates that although there is a minor effect the stability is relatively unaffected by the removal of material at the toe alone.

The erosion of material at the toe, on its own, has a minimal effect on the stability of the overall slope. If the pre-slide slope had been weakened such that it was on the verge of failure ($F=1$) then the removal of material at the toe may have been enough to initiate the movement. Another possibility is that the erosion of material at the toe initiated deformations in the lower slope which caused new and pre-existing cracks to open in the lower slope. These cracks subsequently filled with water causing a change in the stress regime of the slope and movement was initiated. In other words, the erosion at the toe may have been the indirect trigger for the landslide.

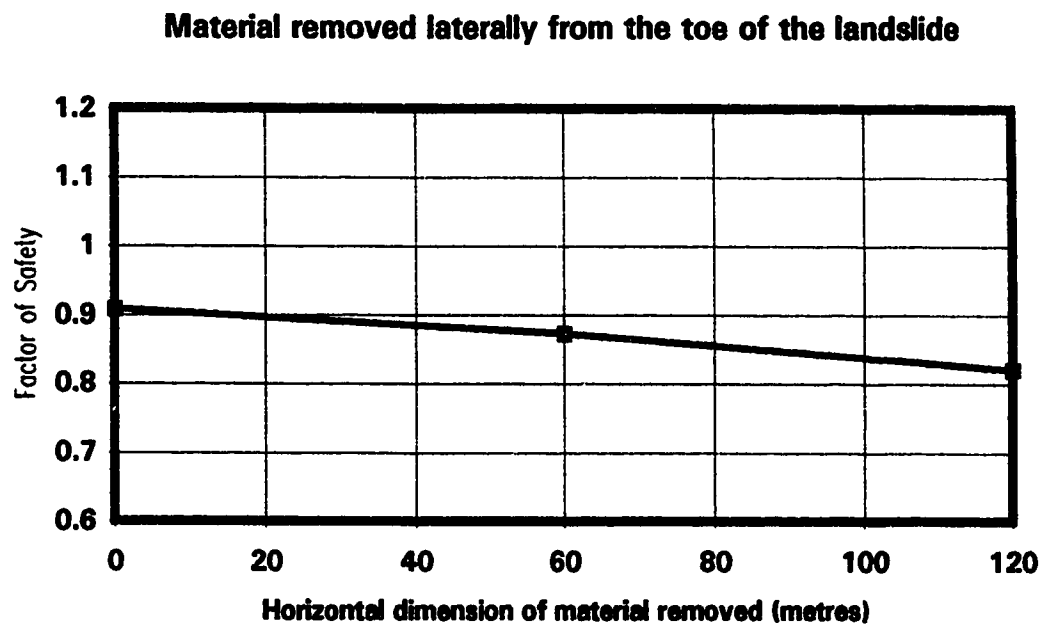


Figure 7.6 Sensitivity analysis: lateral removal of material at the toe.

7.8.2 The Residual Shear Strength in the Preglacial Lake Clay

The effective strength parameters for the residual strength of the preglacial lake clay is tested to see if the strength obtained from laboratory tests is representative of the strength mobilized at the initiation of the movement (Figure 7.7). The results indicate that ϕ_r' has an effect on the factor of safety however the required increase in ϕ_r' to increase the factor of safety from 0.91 to 1.0 is in the order 2° (30% increase in terms of $\tan\phi_r'$) is considered to be unlikely for reasons explained below.

Lupini et al.(1981) showed that soils with high clay content and high plasticity index, like the preglacial lake clay, have a consistent residual strength not significantly affected by subsequent stress history or strain rate. It is affected by fundamental changes in mineralogy, particle shape, grading and pore water chemistry. Since there is little deviation in the index characteristics of the numerous preglacial lake clay samples tested (Section 6.2), both from block and core samples, it is unlikely that changes in the latter characteristics occurred affecting the test results. Studies by Hawkins and Privett (1986) showed that ϕ_r' , which is dependent on the stress range, reaches a lowest constant value at stress values greater than 200 kPa (> 20 m of overburden) and that the 60 mm reversing direct shear test used here gives a higher ϕ_r' than the more reliable ring shear and 100 mm direct shear box. As a result, a discrepancy in the residual shear strength of 30% lower, determined from the laboratory tests, than mobilized in the landslide is unlikely.

7.8.3 Effective Shear Strength in the Till

The shear strength in the till affects the factor of safety in the Morgenstern and Price (1965) analysis by changing the shear strength available along the rupture surface and within the slide mass in the till. The ϕ' used in the till has an apparently small effect on the factor of safety (Figure 7.8). Thomson and Tweedie (1978), in studying the Edgerton Slide, discovered that the factor of safety was relatively insensitive to cohesion in the backscarp, a discovery supported by Figure 7.8 which shows the effect of using or not using cohesion in the strength is small.

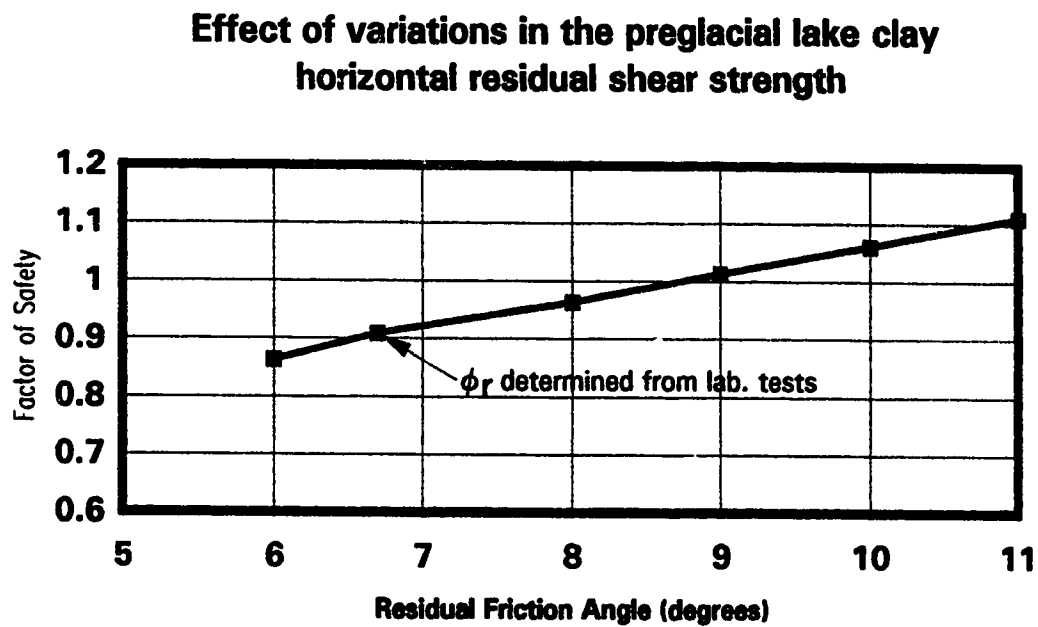


Figure 7.7 Sensitivity analysis: preglacial lake clay, horizontal residual shear strength

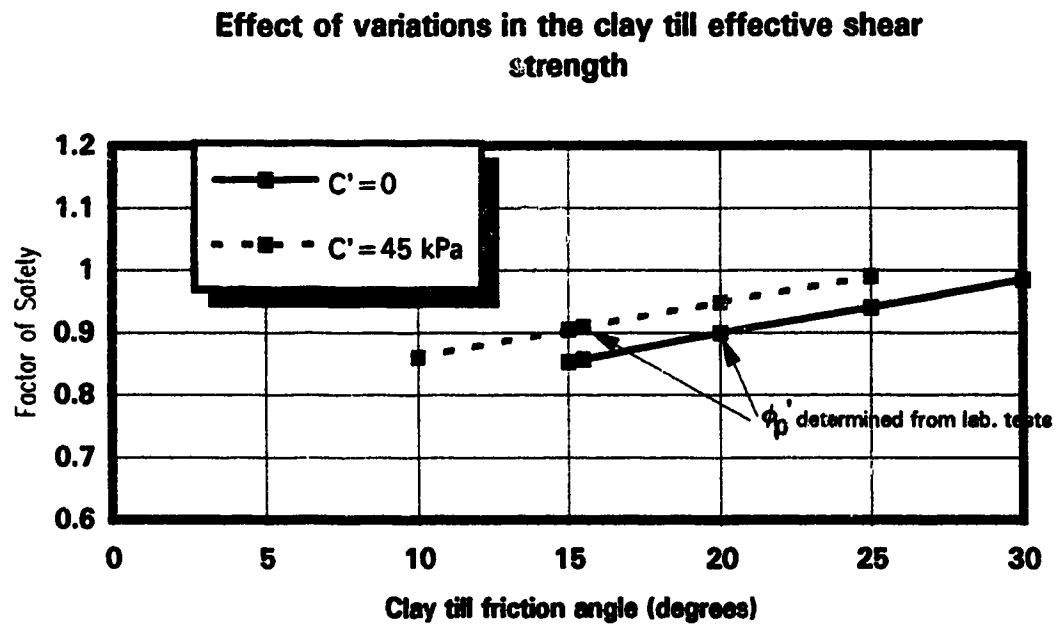


Figure 7.8 Sensitivity analysis: till, effective shear strength

7.8.4 The Phreatic Surface

Changes in the phreatic surface have a significant effect on the factor of safety (Figure 7.9). As discussed in Section 7.5, there is considerable uncertainty regarding the flow regime in the pre-slide slope and the use of a single phreatic surface is an over simplified model of the flow regime in the pre-slide slope. Given the uncertainty, it is reasonable to adjust the assumed equivalent phreatic surface down 10 m and obtain a factor of safety of unity. The sensitivity of the stability to changes in the equivalent phreatic surface in the slope supports the hypothesis that filling of cracks with water in the lower slope (Section 7.3) contributed to the trigger for the movement.

7.8.5 Location of the Transition from Peak to Residual Strength in the Preglacial Lake Clay

Figure 7.10 shows the effect on the factor of safety by moving the transition between peak and residual strength in the preglacial lake clay, back into the slope. Chainage 375 m is the downslope limit of the transition because it marks the start of the pre-existing rupture surface (Figure 7.3) . There is an apparently accelerated reduction in the factor of safety as the transition point is moved back of the assumed chainage (Figure 7.10).

The process of the transition point moving back from its original position may be considered a type of progressive failure made possible by the strain softening characteristic of the preglacial lake clay and is considered as part of the mechanism for the movement. It is hypothesized that changes in the stress state in the upper slope, brought on by stress changes in the lower slope, initiated concentrated shear strains in the weak preglacial lake clay at the transition point. The shear strains caused a drop in shear strength from the fully softened peak strength to the residual strength in the preglacial lake clay. This process, once initiated, is self propagating since a reduction in strength causes a transfer in stress resulting in additional shear strains. As the transition point moved back, the stability along Rupture Surface A decreased at an accelerated rate (Figure 7.10) resulting in mobilization of the retrogressive portion of the landslide. Possible changes in the stress state of the lower slope, which initiated this

process, include a build-up of water pressures in cracks, creep resulting from erosion at the toe or a coupling of the two effects as discussed in Section 7.3.

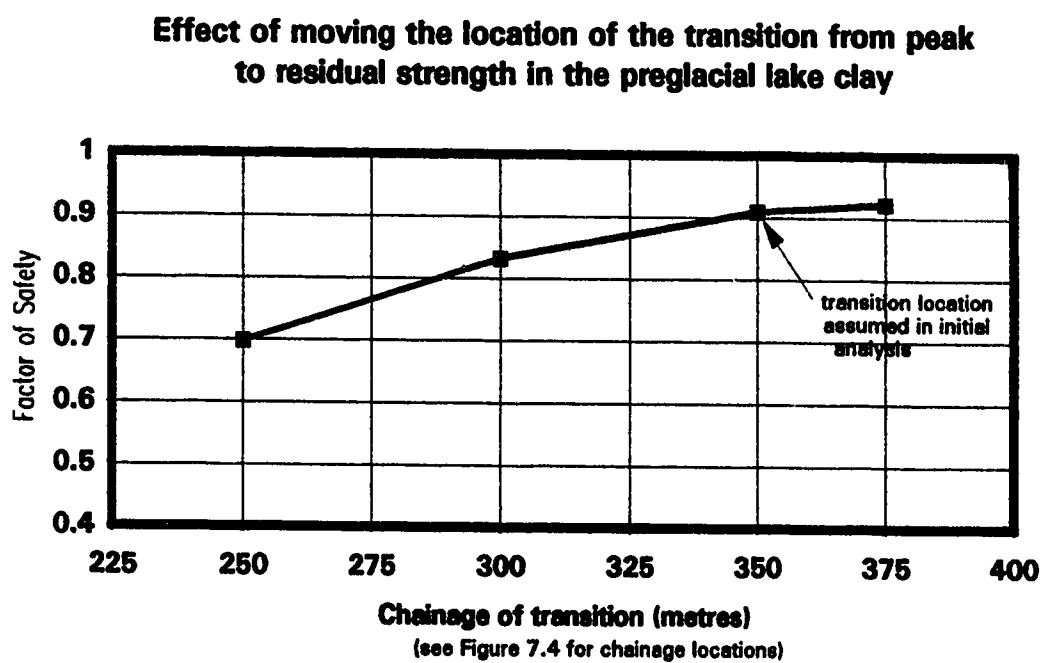


Figure 7.9 Sensitivity analysis: variation of the phreatic surface

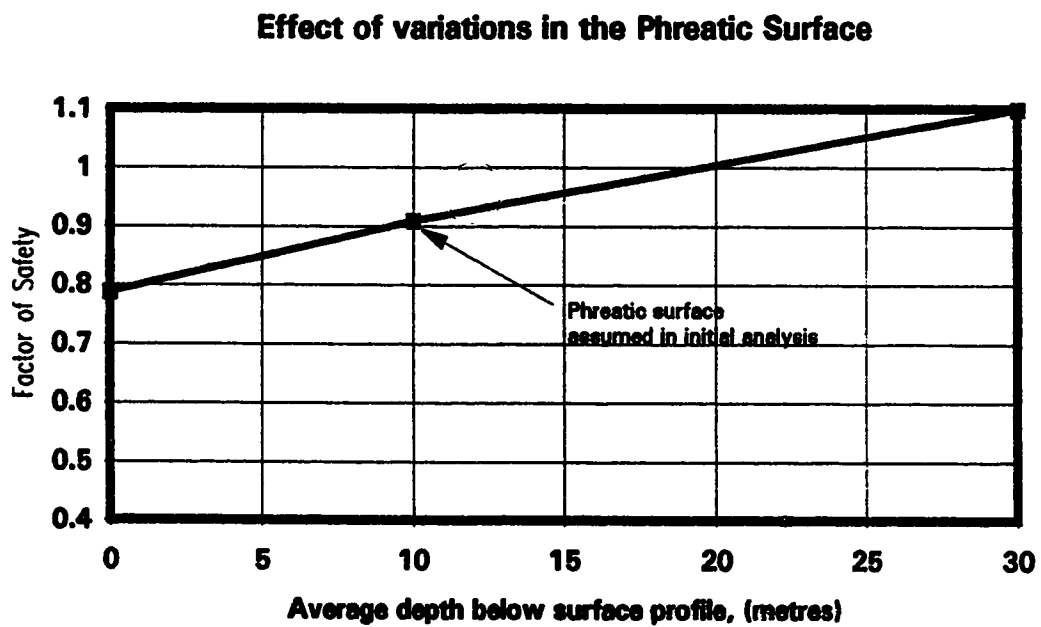


Figure 7.10 Sensitivity analysis: location of the transition from peak to residual strength in the preglacial lake clay.

7.9 Post-slide Stability

Unlike the pre-slide slope the conditions of the post-slide displaced mass are reasonably well understood. The surface profile was surveyed (Appendix D) and the rupture surfaces can be extrapolated with relative ease. With numerous cracks acting as conduits to the rupture surface a worst case scenario of the phreatic surface close to the ground surface can be assumed. The shear strength available along the rupture surface and within the slide mass can be assumed to be the residual strength. And finally, observed separation of the slide mass away from the lateral scarps, significantly reduces the three-dimensional effect and the slope can be analyzed two-dimensionally.

The strength parameters used in the post-slide analysis are summarized in Table 7.2 and the configuration of the present post-slide slope is illustrated in Figure 7.11(a). For this configuration, the analysis yields $F=1.58$ from the critical slip circle analysis implying the displaced slide mass is considerably more stable after the slide. The effect of toe unloading caused by the inevitable river erosion of the dam to the original river level (Figure 7.11 (b)) is evaluated using a similar analysis. This analysis yields a drop in the factor of safety to $F=1.35$. This implies the displaced slide mass will continue to be stable when the river initially re-establishes itself. This does not preclude the possibility of localized slope movements near the toe of the slide or creep but based on the size of the intact wedge 13 (Figure 7.2) retrogression of the instability seems unlikely. Instability will likely reoccur as the river cuts below its original level.

The stability of the displaced mass could be explained by considering momentum, generated by the slide movement, carried the slide mass past its equilibrium point. This has two effects on the factor of safety formula. The resisting forces are increased due to the buttressing of the displaced mass against the right bank of the river. The driving forces are reduced when the average slope angle dropped from 11° to 5° after the movement. Both effects result in a rise in the factor of safety above unity. Removal of the toe material to the original river level (Figure 7.11b) would reduce the resisting forces by removing some buttressing but the driving forces are still low because the resulting average slope is still low at 7° . It is felt that as the river cuts below its original level the factor of safety of the overall slope will again drop below unity and the main scarp will retrogress. Eventually the slope will maintain a constant 8° average slope angle, as seen downstream.

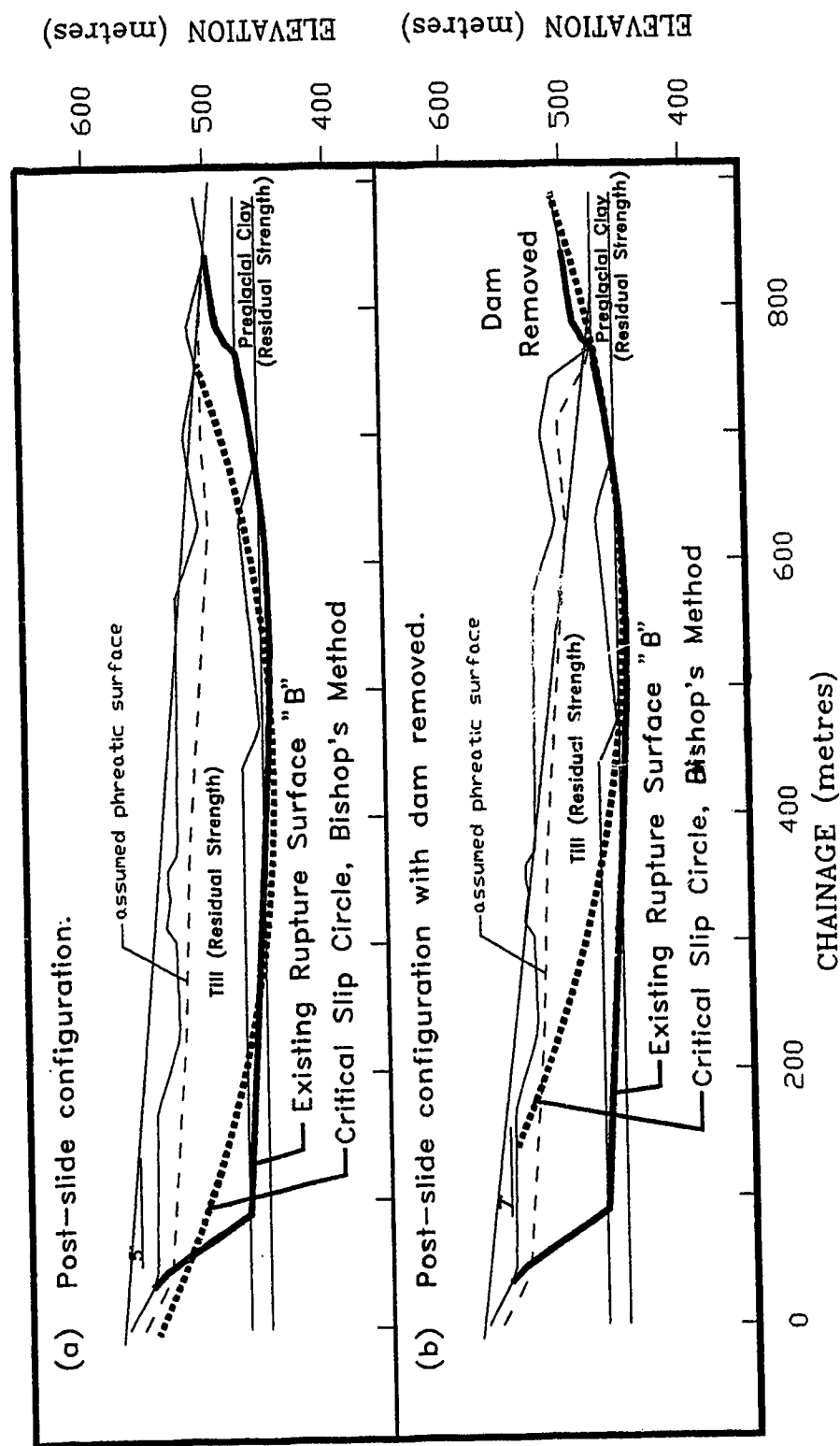


Figure 7.11 Configuration along A-A' for stability analysis of the post-slide displaced mass.

7.10 Summary

An investigation of the mechanics of the Rycroft Landslide involves a stability analysis of the reconstruction of the pre-slide slope and post-slide displaced mass using available information about the geometry, the slide mechanism, the strength parameters and the pore pressure distribution.

The rupture surface of the Rycroft Landslide is considered to approach the shape of a sector of an elliptical cylinder truncated by sub-vertical and parallel lateral margins. In the head area the movement is more or less rotational on a rupture surface cutting through the glacial lake deposits and the till. In the main body the movement is translational on a planar or gently undulating rupture surface contained in the flat-lying preglacial lake clay. The toe is a pressure ridge forced upwards as the slide mass encountered the right bank of the river. The slope and rupture surfaces are reconstructed along A-A' using the available information from the pre- and post-slide slopes.

With regard to the mechanism of the landslide, it is assumed that the 1 in 50 year rainstorm set in motion a change of conditions that crossed over the transition, discussed in Section 5.3, from a slope angle governed by the available shear strength in the till to a slope angle governed by the lower available shear strength in the preglacial lake clay, resulting in mobilization of the large landslide. The changed conditions include lateral or downward erosion at the toe and increases in the water pressure distribution due to the accumulation of water on the lower pre-slide slope. A hypothesis is introduced that the initial rupture surface formed along Rupture Surface A then retrogressed to form the present main scarp along Rupture Surface B. The way in which the slide mass behaved after mobilization is explained using lateral earth pressures in Section 7.3.

For the analysis, the strengths in terms of effective stress of the till and preglacial lake clay are taken from the laboratory test results. Properties of the silt and clay (material 1) and glacial lake deposits (material 5) were estimated based on their index properties and physical appearance. A point of transition is recognized between the residual and peak strengths of the preglacial lake clay and initially set at chainage 350 m, just behind the last recognized pre-existing rupture surface. The uncertain flow regime for the slope is modelled assuming an equivalent phreatic surface high in the lower slope to account for water-filled cracks.

Once the assumed configuration of the slope, the rupture surface and the physical conditions is completed, it is analyzed using Morgenstern and Price's (1965) and Spencer's (1967, 1973) methods for analysis of a general slip surface in two dimensions. The analysis yields $F=0.86$ on Rupture Surface A and $F=1.12$ on Rupture Surface B supporting the hypothesis that the movement initiated on Rupture Surface A then retrogressed along Rupture Surface B to form the final main scarp. This hypothesis is further supported by a profile generated by testing the stability of a range of possible initial back scarp locations. The profile indicates that the scarp formed by Rupture Surface A observed in the field is close to the most likely location for the initial scarp to form using the assumed pre-slide conditions in a general slip surface limit equilibrium analysis. An order of magnitude, three-dimensional analysis shows there is a 6% increase in the factor of safety when the lateral margins are accounted for. Applying this three-dimensional correction to the results of the two-dimensional Morgenstern and Price analysis, yields $F=0.91$ on Rupture Surface A.

In the sensitivity analysis, conditions believed to have an influence on the stability of the pre-slide slope, are individually varied to determine their effect on the factor of safety. The stability is relatively unaffected by the removal of material at the toe on its own. The residual shear strength of the preglacial lake clay has an effect on the stability but a 30% discrepancy in the ϕ_r' , to obtain $F=1$, is considered unlikely. Within the confidence range of uncertainty in the test results, the ϕ' and C' values used in the till have an apparently small effect on the stability. Of all the conditions considered, changes to the phreatic surface have the most dynamic effect on the stability supporting the hypothesis that the filling of cracks in the lower slope with water contributed to initiating movement. Considering the uncertainty of the assumed phreatic surface, it is also not unreasonable that the phreatic surface was, on average, 10 m lower than the assumed level, raising the factor of safety on Rupture Surface A from 0.91 to 1.0. There is an accelerated reduction in the factor of safety as the transition between the peak and residual shear strength in the preglacial lake clay is moved back of the assumed chainage. The progressive movement of this transition back in the preglacial lake clay, essentially a strain softening effect, is coincident with the retrogression of the rupture surface and is considered a significant factor in the mechanism for the movement.

A post-slide stability of $F=1.58$ for the displaced mass as it exists now, and $F=1.35$ after the river regains its original level, suggest that the displaced slide mass gained some stability during the slide movement. This stability is explained by considering that the momentum, generated by the slide movement, carried the slide

mass past its equilibrium point. As the river cuts below its original level the factor of safety of the overall slope will again drop below unity and the main scarp may retrogress. Eventually the slope will maintain a constant 8° average slope angle as seen downstream.

CHAPTER 8. CONCLUSION

8.1 General

The Rycroft Landslide is a reactivated, retrogressive compound earth-slide. The occurrence of the Rycroft Landslide emphasizes the significant impact that buried channels have on the stability of valley walls in the Peace River Lowlands physiographic region. Of particular importance to stability is the presence of preglacial lake clays beneath the glacial deposits.

The timing of the large-scale landslides, like the Rycroft Landslide, appears to be dependent on the variable and infrequent flood flows of the Saddle River and is therefore difficult to predict or control. It is the 1 in 50 year storm that occurred on June 11 and 12, 1990, that initiated a change in conditions that led to the Rycroft Landslide, 4 or 5 days later.

The landslide occurred at a location where the Saddle River was cutting through the overlying till and into preglacial lake clay marking the start of a transition from a slope angle governed by the available shear strength in the till to a slope angle governed by the lower available shear strength in the preglacial lake clay. If the stratigraphy downstream of the landslide is similar to the stratigraphy at the site the average slope angle will eventually stabilize at approximately 8° .

It is considered that the triggers for the landslide were the accelerated erosion of the Saddle River and the filling of pre-existing cracks in the dormant landslide with water, both caused by the severe flood in June, 1990. These two effects may be coupled in the sense that the erosion at the toe causes displacements in the lower slope which opens new or pre-existing cracks that subsequently fill with water.

General slip surface limit equilibrium stability analyses confirm the assumed parameters of the pre-slide slope by indicating the right order of magnitude factor of safety of near unity for the initial rupture surface. The initial rupture surface formed a scarp 50 m back of the valley crest and then retrogressed to form the present main scarp. The lateral margins of the landslide represent a lateral resistance to movement or a three-dimensional effect that results in an order of magnitude 6% increase in the factor of safety.

Changes to the phreatic surface have the most important effect on the stability of any of the conditions considered in the sensitivity analysis and are postulated as the

primary reason the stability analysis returned a factor of safety of less than unity. This result also supports the hypothesis that the filling of cracks in the lower slope with water contributed to initiating movement.

The post-slide stability analysis indicates that the forces driving the movement of the displaced mass decreased as a result of the movement and forces resisting movement increased. Some of the resisting forces are removed with the removal of the dam to the original level of the river but the factor of safety is still greater than unity, suggesting the displaced mass will remain relatively stable in the near future. As the river cuts below its original level the factor of safety of the overall slope will again drop below unity and the main scarp may retrogress. Eventually the slope will maintain a constant 8° average slope angle as seen downstream.

Over a period of years, the river will erode through the toe mass until it reaches its original level. As the river cuts below its original level exposing more preglacial lake clay, similar large scale landslides are anticipated upstream.

8.2 Further Work

This work points to a number of conditions which, in combination, resulted in the Rycroft Landslide Dam. The dominant conditions relate to the river cutting into preglacial buried channel deposits and in particular into the preglacial lake clay. Because of the regionally similar pre- and post-glacial drainage patterns and glacial history of the Peace River Lowlands it is likely that similar geologic settings are present in other tributaries to the Peace River and an investigation to locate similar settings in the Peace River Lowlands might prove useful in predicting instability. A stability analysis, as presented in this work, may prove useful in that prediction.

The long term observation of the overall slope during and following the removal of the dam by erosion is a rare opportunity to enhance our knowledge of these phenomena which may play significant roles in the cutting of deep valleys that dominate the northern part of the Interior Plains of Canada. The survey information in Appendix D is left for future researchers of the Landslide to monitor the movement of the displaced mass. In addition, the Peace River office of Alberta Environment, Development and Operations Branch, keeps an ongoing record of the reservoir level behind the Rycroft Landslide Dam which provides a useful though indirect indicator of the performance of the dam. Qualitative information on the performance of the dam

may be available from Nova Pipelines as they periodically fly over the landslide during routine inspections of their pipeline crossing upstream of the Rycroft Landslide Dam.

Not mentioned thus far in the thesis is the presence of a standpipe piezometer, left in testhole RS 2, sealed off in the preglacial lake clay behind the present main scarp. The reading of this piezometer may shed useful information on the largely unknown pore pressure distribution in the slope.

References

- ALBERTA ENVIRONMENT** 1991. Water Management in Alberta, Background Paper, Vol. 1.
- ALBERTA FORESTRY** 1985. 1:20,000 Provincial base maps 83M/ 16 SW, 16 NE, 10 NE & 10 SW. Compiled from aerial photographs taken in 1981. Produced by Alberta Bureau of Surveying and Mapping.
- BAUM, R.L. and FLEMING, R.W.** 1991. Use of longitudinal strain in identifying driving and resisting elements of landslides. Geological Society of America Bulletin, 103:p. 1121-1132.
- BOULTON, G.S. and PAUL, M.A.** 1976. The influence of genetic processes on some geotechnical properties of glacial tills. Quarterly Journal of Engineering Geology, 9:pp. 159-194.
- CARLSON, V.A. and HACKBARTH, D.A.** 1974. Bedrock topography of the Grande Prairie Area, NTS 83 M, Alberta. Alberta Research Council Map 1:250,000 scale.
- CASAGRANDE, A.** 1948. Classification and identification of soils. American Society of Civil Engineers, ASCE Journal for Soil Mechanics and Foundation Engineering, Transactions, Vol. 113, pp. 901-930.
- COSTA, J.E. and SCHUSTER, R.L.** 1988. The formation and failure of natural dams, Bulletin Geological Society of America, 100:1054- 1068.
- CRUDEN, D.M., REUL, M. and THOMSON, S.** 1990. Landslide along the Peace River, Alberta, Proceedings, 43rd Canadian Geotechnical Conference, 1:61-67.
- DEARMAN, W.R., et al.** 1972. The preparation of maps and plans in terms of engineering geology. Quarterly Journal of Engineering Geology, 5:293-382.
- FENTON, M.** 1984. Quaternary Stratigraphy of the Canadian Prairies. In Quaternary Stratigraphy of Canada, Edited by R.J. Fulton. Geological Survey of Canada Paper 84-10, pp. 57-68.

- FISHER, D.A., REEH, N. and LANGLEY, K. 1985. Objective reconstruction of the Late Wisconsin Laurentide ice sheet, and the significance of deformable beds. *Geographie physique et Quaternaire*, 39:229-238.
- FULTON, R.J., and PREST, V.K. 1987. The Laurentide Ice Sheet and its significance. *Geographie physique et Quaternaire*, XLI:181-186.
- HACKBARTH, D. 1977. Hydrogeology of the Grande Prairie area. Alberta Research Council report 76-4.
- HAWKINS, A.B. and PRIVETT, K.D. 1986. Measurement and use of residual shear strength of cohesive soils. *Ground Engineering*, March: 1986.
- HUNGR, O. 1981. Dynamics of Rock Avalanches and Other Types of Slope Movements. Ph.D. Thesis, Dept. of Civil Eng., University of Alberta.
- HUNGR, O. 1988. CLARA slope stability analysis in two or three dimensions for IBM compatible microcomputers. User's manual.
- HUNGR, O., SALGADO, F.M. and BYRNE, P.M. 1989. Evaluation of a three-dimensional method of slope stability analysis. *Canadian Geotechnical Journal* 26-4.
- LAMBE, T.W. 1951. *Soil Testing for Engineers*, John Wiley and Sons, New York.
- LAMBE, T.W. and WHITMAN, R.V. 1969. *Soil Mechanics*, John Wiley and Sons, New York
- LIVERMAN, D.G.E. 1989. Quaternary geology of the Grande Prairie area, Alberta. Ph.D. thesis, Dept. of Geology, University of Alberta, Edmonton, 360 p.
- LIVERMAN, D.G.E., CATTO, N.R. and RUTTER, N.W. 1989. Laurentide glaciation in west-central Alberta: A single (Late Wisconsinan) event. *Canadian Journal of Earth Sciences*, 26:266-274.
- LUPINI, J.F., SKINNER, A.E. and VAUGHAN, P.R. 1981. The drained residual strength of cohesive soils. *Geotechnique*, 31: pp. 181-213.
- MATHEWSON, D.S. and THOMSON, S. 1973. Geological implications of valley rebound. *Canadian Journal of Earth Sciences*. 10:961-978.

- MATHEWS, W.H. 1980. Retreat of the last ice sheets in northeastern British Columbia and adjacent Alberta. Geological Survey of Canada Bulletin 331.**
- McCLUNG, J.S. 1990. Ry croft Landslide geotechnical report December 1990, Location 29 and 30-78-3-W6. Alberta Environment internal report, file no: 8040 - 5 - 1.**
- MORGENSTERN, N.R. and PRICE, V.E. 1965. The analysis of the stability of general slip surfaces, Geotechnique, 15-1:79-93.**
- QUIGLEY, R. M. 1980. Geology, mineralogy, and geochemistry of Canadian soft soils: a geotechnical perspective. Canadian Geotechnical Journal, 17- 4:514 - 526.**
- RAINS, B. and WELCH, J. 1988. Out-of phase Holocene terraces in part of the North Saskatchewan River basin, Alberta. Canadian Journal of Earth Sciences, 25-3: 454-464.**
- RAINS, B., KVILL, D. and SHAW, J. 1990, Evidence and some implications of coalescent Cordilleran and Laurentide glacial systems in western Alberta. In A World of Real Places, edited by P.J. Smith and E.L. Jackson, pp. 147-161.**
- RUTTER, N.W. 1976. Multiple glaciation in the Canadian Rocky Mountains with special emphasis on northeastern British Columbia. In Quaternary Stratigraphy of North America. Edited by W.C. Mahaney. Dowden, Hutchinson and Ross. Stroudsburg, Pennsylvania, pp. 409-440.**
- RUTTER, N.W. 1977a. Multiple Glaciation in the area of Williston Lake, British Columbia. Geological Survey of Canada, Bulletin 273.**
- SKEMPTON, A.W. 1953. The colloidal activity of clays. Proceedings 3rd International Conference on Soil Mechanics and Foundation Engineering, Switzerland, I: 57.**
- SPENCER, E. 1967. A method of analysis of the stability of embankments assuming parallel inter-slice forces, Geotechnique, 17-1:11-26.**
- SPENCER, E. 1973. The thrust line criterion in embankment stability analysis, Geotechnique, 23:85-101.**

- THOMSON, S. and HAYLEY, D.W. 1975. The Little Smoky Landslide. Canadian Geotechnical Journal. 12:379-392.**
- THOMSON, S. and MORGENSTERN, N.R. 1977. Factors affecting distribution of landslides along rivers in southern Alberta, Canadian Geotechnical Journal, 14:508-523.**
- THOMSON, S. and TWEEDIE, R.W. 1978. The Edgerton Landslide. Canadian Geotechnical Journal, 15: 510-521.**
- WESTGATE, J.A., FRITZ, P., MATHEWS, J.V., KALAS, L., DELORME, L.D., GREEN, R., and AARIO, R. 1972. Geochronology and paleoecology of mid-Wisconsin sediments in west-central Alberta. International Geological Congress, 24th Session, Abstracts, p. 380.**
- WHITE, J.M., MATHEWES, R.W. and MATHEWS, W.H. 1979. Late Pleistocene chronology and environment of the "ice free corridor" of northwestern Alberta. Quaternary Research, 24: 173-186.**
- WP/WLI (International Geotechnical Societies' UNESCO Working Party on World Landslide Inventory) 1990. A Suggested Method of Reporting Landslide, Bulletin International Association for Engineering Geology, 41:5-12.**
- VARNES, D.J. 1978. Slope movement and types and processes. In Landslides : Analysis and Control. Edited by R.L. Schuster and R.J. Krizek. Transportation Research Board, National Academy of Science, Washington, Special Report 176: 11- 33**
- YOSHIDA, N., MORGENSTERN, N.R., and CHAN, D.H. 1990. A failure criterion for stiff soils and rocks exhibiting softening. Canadian Geotechnical Journal, 27:195-202.**

Appendix A: Detailed log of testholes RS-1 and RS-2

Page 4 of 31

TEST RESULTS	DEPTH (m)	SYMBOL	DESCRIPTION	SAMPLE	OTHER INFORMATION
			TOPSOIL		RIG: AUGER TYPE:
	1				
	2				
	3		Cl-stiff-v stiff, dk-lt gry, sand pkts, slicks, cal.		PP= 192 Rec= .30m/.35m
	4				
	5				
	6		as above, med br-dk gry, slicks.		

0 20 40 60 80 100

1000 1500 2000 2500 3000


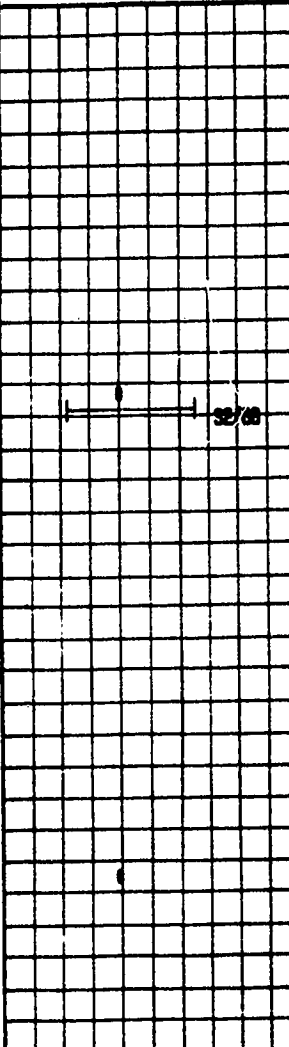
DEPTH SCALE

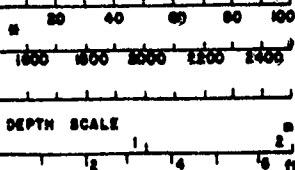
0 1 2 3 4 5 6 ft

TOPSOIL OR NO SAMPLE	GRAVEL	SAND OR SANDSTONE	CLAY OR SHALE	SILT OR SILTSTONE	UNDISTURBED SAMPLE	DISTURBED SAMPLE

w - MOISTURE CONTENT (%), G - DRY UNIT WEIGHT (kg/m³), K - PERMEABILITY (cm/s), RA - PLUGGY AVERAGE
 NCA - HOLLOW CORE AVERAGE, V OR S.P.T. - STANDARD PENETRATION TEST BLOW COUNT,
 PR - POCKET PENETROMETER (kPa), Cu - UNCONSOLIDATED COMPRESSION (kPa)
 Wp - PLASTIC LIMIT (%), Lp - LIQUID LIMIT (%), --- CORE RECOVERY (%),
 12-0.075-25 - 12.5% RETAINED ON No. 4 SIEVE, 0.075-0.25 - 0.075-0.25 No. 200 SIEVE,
 40 = 40% CLAY, ♡ - WATER LEVEL NOT TAKEN.


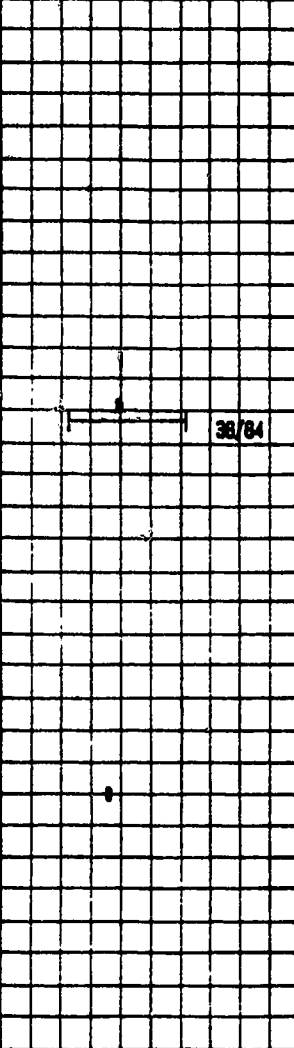


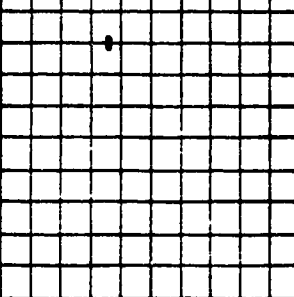


GS-104-86

 DEVELOPMENT & OPERATIONS DIVISION GEOTECHNICAL SERVICES LABORATORY		PROJECT <u>RYCROFT SLIDE</u> SITE _____ HOLE No. <u>RS 1</u> ELEV. _____ LOCATION _____ TECHNOLOGIST <u>JS AS JB</u> DATE DRILLED <u>16 Jul 1991</u>	
BOREHOLE AND TEST LOG			
TEST RESULTS	DEPTH (m)	DESCRIPTION	OTHER INFORMATION
	7	as above.	
	8		
	9	CH-dk gry-med br, blk, slicks, odd pebble.	X
	10		
	11		
	12	as above.	X
	13		



TOPSOIL OR NO SAMPLE	GRAVEL	SAND OR SANDSTONE	CLAY OR SHALE	SILT OR SILTSTONE	UNDISTURBED SAMPLE	DISTURBED SAMPLE

G-MOISTURE CONTENT (%), W-WET UNIT WEIGHT (kg/m³), K-PERMEABILITY (cm/s), P.A.-PLASTIC NUMBER,
 NCA-NOLLOW CORE AUGER, V OR S.P.T.-STANDARD PENETRATION TEST BLOW COUNT,
 P.P.-POCKET PENETROMETER (kPa), Q_u-UNCONFINED COMPRESSION (kPa)
 W_p-PLASTIC LIMIT (%), L_u-LIQUID LIMIT (%), --- CORE RECOVERY (%),
 12-0.075-20-12.5% RETAINED ON No. 4 SIEVE, 0.075-0.425-20-2.0% No. 200 SIEVE,
 20 = % SILT, 25 = % CLAY, ∇-WATER LEVEL








 Alberta ENVIRONMENT DEVELOPMENT & OPERATIONS DIVISION GEOTECHNICAL SERVICES LABORATORY		PROJECT <u>RYCROFT SLIDE</u> SITE _____ HOLE No. <u>RS 1</u> ELEV. _____ LOCATION _____ TECHNOLOGIST <u>JS AS JB</u> DATE DRILLED <u>16 Jul 1991</u>			
BOREHOLE AND TEST LOG					
TEST RESULTS	DEPTH (m)	SYMBOL	DESCRIPTION	SAMPLE	OTHER INFORMATION
	14		as above.		
	15				
	16				
	17				
	18				
	18		as above.		
	19				

0 20 40 60 80 100

1600 1800 2000 2200 2400

DEPTH SCALE


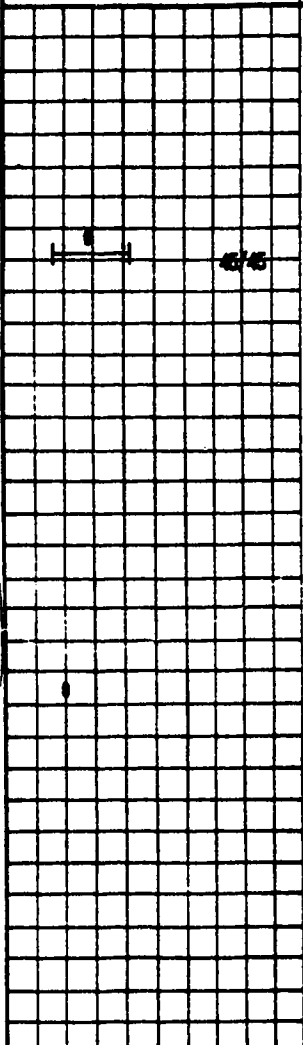
1 2 3 4 5 6

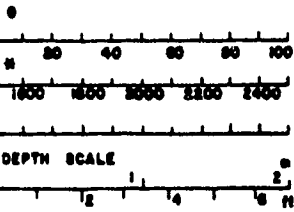
						
TOPSOIL OR NO SAMPLE	GRAVEL	SAND OR SANDSTONE	CLAY OR SHALE	SILT OR SILTSTONE	UNDISTURBED SAMPLE	DISTURBED SAMPLE

w - MOISTURE CONTENT (%), γ - WET UNIT WEIGHT (kg/m^3), k - PERMEABILITY (cm/s), P.A. - FLIGHT AUGER,
 HCA - HOLLOW CORE AUGER, V OR S.P.T. - STANDARD PENETRATION TEST BLOW COUNT,
 P.P. - POCKET PENETROMETER (SPa), q_u - UNCONFINED COMPRESSION (SPa)
 w_p - PLASTIC LIMIT (%), w_L - LIQUID LIMIT (%), --- CORE RECOVERY (%),
 12-0.075-22 - 12% RETAINED ON No. 4 SIEVE, 0.075-0.425 - 22% No. 200 SIEVE,
 40 = % SILT, 30 = % CLAY, ∇ - WATER LEVEL

GS-104-95

Page 4 of 31

 DEVELOPMENT & OPERATIONS DIVISION GEOTECHNICAL SERVICES LABORATORY		PROJECT <u>RYCROFT SLIDE</u> SITE _____ HOLE No. <u>RS 1</u> ELEV. _____ LOCATION _____ TECHNOLOGIST <u>JS AS JB</u> DATE DRILLED <u>16 Jul 1991</u>			
BOREHOLE AND TEST LOG					
TEST RESULTS	DEPTH (m)	SYMBOL	DESCRIPTION	SAMPLE	OTHER INFORMATION
	20	[Symbol]	as above.		
	21	[Symbol]	CI(TILL)-dk gry-med br, pab, cal, SS frags.	X	
	22	[Symbol]			
	23	[Symbol]			
	24	[Symbol]	as above, stiff.	X	PP= 115 Rec= .30m/.40m
	25	[Symbol]			
	26	[Symbol]			



TOPSOIL OR NO SAMPLE	GRAVEL	SAND OR SANDSTONE	CLAY OR SHALE	SILT OR SILTSTONE	UNDISTURBED SAMPLE	DISTURBED SAMPLE
----------------------	--------	-------------------	---------------	-------------------	--------------------	------------------

w - MOISTURE CONTENT (%), γ - WET UNIT WEIGHT (kg/m^3), k - PERMEABILITY (cm/s), P.A. - PLIGHT AUGER,
 HCA - HOLLOW CORE AUGER, V OR S.P.T. - STANDARD PENETRATION TEST BLOW COUNT,
 P.P. - POCKET PENETROMETER (kPa), q_u - UNCONFINED COMPRESSION (kPa)
 w_p - PLASTIC LIMIT (%), w_L - LIQUID LIMIT (%), --- CORE RECOVERY (%),
 12-0.05-25 - 12% RETAINED ON No. 40 SIEVE, 0.05-0.25 mm, 25% No. 200 SIEVE,
 SS = SILT, CL = CLAY, ∇ - WATER LEVEL

Page 1 of 2

Aberta
ENVIRONMENT

DEVELOPMENT & OPERATIONS DIVISION
GEOTECHNICAL SERVICES LABORATORY

PROJECT RYCROFT SLIDE

SITE _____

HOLE No. RS 1 ELEV. _____

LOCATION _____

TECHNOLOGIST JS AS JB DATE DRILLED 16 Jul 1991

BOREHOLE AND TEST LOG

TEST RESULTS

0

10

20

30

40

50

60

70

80

90

100

110

120

130

140

150

160

170

180

190

200

210

220

230

240

250

260

270

280

290

300

310

320

330

DEPTH (m)

SYMBOL

as above, sand pkts, rust stains.

X

OTHER INFORMATION

TOPSOIL OR NO SAMPLE

GRAVEL

SAND OR SANDSTONE

CLAY OR SHALE


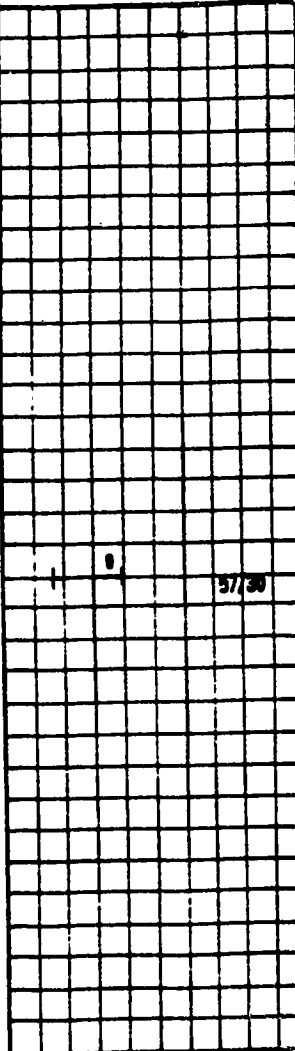


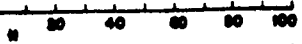

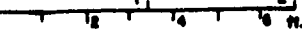

SHALE OR SILTSTONE

UNDISTURBED SAMPLE

DISTURBED SAMPLE


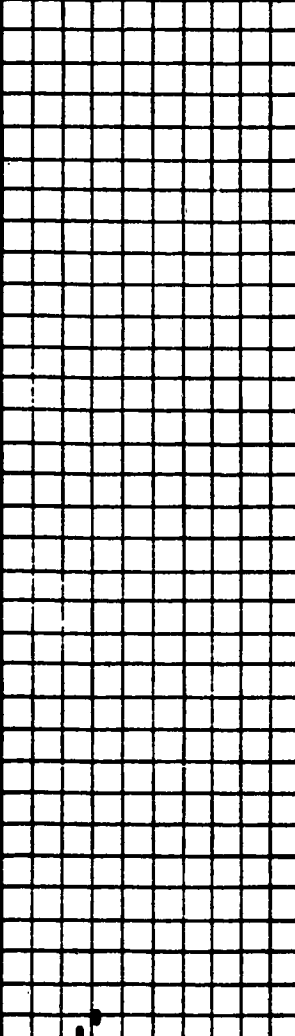
G - MOISTURE CONTENT (%), W - WET UNIT WEIGHT (kg/m^3), K - PERMEABILITY (cm/d), P.A. - PLANT AUGER
MCA - MELLOW CORE AUGER, V or S.P.T. - STANDARD PENETRATION TEST BLOW COUNT,
PP - POCKET PENETROMETER (kPa), Cu - UNCONFINED COMPRESSION (kPa)
w_p - PLASTIC LIMIT (%), L.L. - LIQUID LIMIT (%), --- CURVE RECOVERY (%),
IE-GCS-22 = IE-% RETAINED ON No. 4 sieve, G.S. + S_m, SIZE mm, ZZ = % No. 200 sieve,
40 = % CLY, ∇ - WATER LEVEL

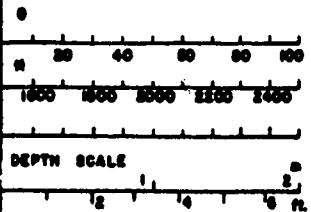
CS-104-86

 DEVELOPMENT & OPERATIONS DIVISION GEOTECHNICAL SERVICES LABORATORY		PROJECT <u>RYCROFT SLIDE</u>			
		SITE _____			
		HOLE No. <u>RS 1</u>		ELEV. _____	
		LOCATION _____			
		TECHNOLOGIST <u>JS AS JB</u> DATE DRILLED <u>16 Jul 1991</u>			
BOREHOLE AND TEST LOG					
TEST RESULTS	DEPTH (E)	SYMBOL	DESCRIPTION	SAMPLE	OTHER INFORMATION
	34		as above, med br, rust stains.		
	35				
	36				
	37				
	38				
	39				
<div style="display: flex; justify-content: space-between;"> <div>   DEPTH SCALE  </div> <div>  <p> TOPSOIL OR NO SAMPLE GRAVEL SAND OR SANDSTONE CLAY OR SHALE SILT OR SILTSTONE UNDISTURBED SAMPLE DISTURBED SAMPLE 0 - MOISTURE CONTENT (%), w - WET UNIT WEIGHT (lb/m³), k - PERMEABILITY (cm/s), RA - FLIGHT AUGER, HCA - HOLLOW CORE AUGER, V OR S.P.T. - STANDARD PENETRATION TEST BLOW COUNT, P.H. - POCKET PENETROMETER (lbf/in²), Cu - UNCONFINED COMPRESSION (lbf/in²) W_p - PLASTIC LIMIT (%), L - LIQUID LIMIT (%), --- CORE RECOVERY (%), 12-0.075-2.0 - 12% RETAINED ON No. 40 SIEVE, 0.075-0.425 No. 200 SIEVE, 0.425-2.0 = % CLAY, ∇ - WATER LEVEL </p> </div> </div>					

GS-104-86

Page 7 of 31

 Alberta ENVIRONMENT DEVELOPMENT & OPERATIONS DIVISION GEOTECHNICAL SERVICES LABORATORY		PROJECT <u>RYCROFT SLIDE</u> SITE <u> </u> HOLE No. <u>RS 1</u> ELEV. <u> </u> LOCATION <u> </u> TECHNOLOGIST <u>JS AS JB</u> DATE DRILLED <u>16 Jul 1991</u>			
BOREHOLE AND TEST LOG					
TEST RESULTS	DEPTH (m)	SYMBOL	DESCRIPTION	SAMPLE	OTHER INFORMATION
	10	[Symbol]			
	41	[Symbol]			
	42	[Symbol]			
	43	[Symbol]			
	44	[Symbol]			
	45	[Symbol]			
	46	[Symbol]	as above, soft-firm. as above, soft-firm. CH(TILL)-soft, dk gry, Peb. sand pkts.		PP= 48 Rec= .33m/.45m PP= 29
	47	[Symbol]			
	48	[Symbol]			
	49	[Symbol]			










0 20 40 60 80 100
cm

0 100 200 300 400
cm

DEPTH SCALE


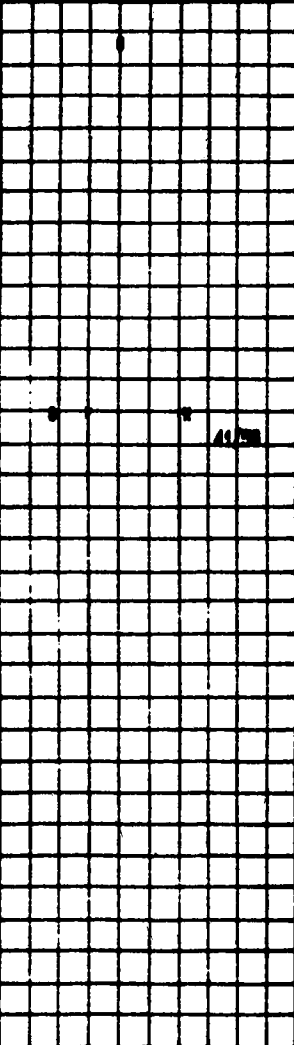
0 1 2 3 4 5 6 ft

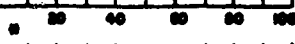

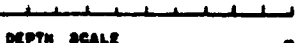
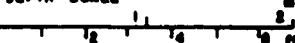
						
TOPSOIL OR NO SAMPLE	GRAVEL	SAND OR SANDSTONE	CLAY OR SHALE	SILT OR SILTSTONE	UNDISTURBED SAMPLE	DISTURBED SAMPLE


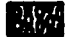





w - MOISTURE CONTENT (%), G - WET UNIT WEIGHT (kg/m³), K - PERMEABILITY (cm/s), FA - FLIGHT AUGER,
 HCA - HOLLOW CORE AUGER, V OR S.P.T. - STANDARD PENETRATION TEST BLOW COUNT,
 PR - POCKET PENETROMETER (kPa), Cu - UNCONFINED COMPRESSION (kPa),
 W_p - PLASTIC LIMIT (%), L - LIQUID LIMIT (%), --- CORE RECOVERY (%),
 15-20-25 - 15% RETAINED ON No. 40 SIEVE, 0.075-0.425-0.850-1.75-3.0-6.0-12.5-25-50-100-200-400-800-1600-3200-6300-12500-25000-50000-100000-200000-400000-800000-1600000-3200000-6400000-12800000-25600000-51200000-102400000-204800000-409600000-819200000-1638400000-3276800000-6553600000-13107200000-26214400000-52428800000-104857600000-209715200000-419430400000-838860800000-1677721600000-3355443200000-6710886400000-13421772800000-26843545600000-53687091200000-107374182400000-214748364800000-429496729600000-858993459200000-1717986918400000-3435973836800000-6871947673600000-13743895347200000-27487790694400000-54975581388800000-109951162777600000-219902325555200000-439804651110400000-879609302220800000-1759218604441600000-3518437208883200000-7036874417766400000-14073748835532800000-28147497671065600000-56294995342131200000-112589990684262400000-225179981368524800000-450359962737049600000-900719925474099200000-1801439850948198400000-3602879701896396800000-7205759403792793600000-14411518807585587200000-28823037615171174400000-57646075230342348800000-115292150460684697600000-230584300921369395200000-461168601842738790400000-922337203685477580800000-1844674407370955161600000-3689348814741910323200000-7378697629483820646400000-14757395258967641292800000-29514790517935282585600000-59029581035870565171200000-118059162071741130342400000-236118324143482260684800000-472236648286964521369600000-944473296573929042739200000-1888946593147858085478400000-3777893186295716170956800000-7555786372591432341913600000-15111572745182864683827200000-30223145490365729367654400000-60446290980731458735308800000-120892581961462917470617600000-241785163922925834941235200000-483570327845851669882470400000-967140655691703339764940800000-1934281311383406679529881600000-3868562622766813359059763200000-7737125245533626718119526400000-15474250491067253436239052800000-30948500982134506872478105600000-61897001964269013744956211200000-123794003928538027489912422400000-247588007857076054979824844800000-495176015714152109959649689600000-990352031428304219919299379200000-1980704062856608439838598758400000-3961408125713216879677197516800000-7922816251426433759354395033600000-15845632502852867518708790067200000-31691265005705735037417580134400000-63382530011411470074835160268800000-126765060022822940149670320537600000-253530120045645880299340641075200000-507060240091291760598681282150400000-1014120480182583521197362564300800000-2028240960365167042394725128601600000-4056481920730334084789450257203200000-8112963841460668169578900514406400000-16225927682921336339157801028812800000-32451855365842672678315602057625600000-64903710731685345356631204115251200000-129807421463370690713262408230502400000-259614842926741381426524816461004800000-519229685853482762853049632922009600000-1038459371706965525706099265844019200000-2076918743413931051412198531688038400000-4153837486827862102824397063376076800000-8307674973655724205648794126752153600000-16615349947311448411297588253504307200000-33230699894622896822595176507008614400000-66461399789245793645190353014017228800000-132922799578491587290380706028034457600000-265845599156983174580761412056068915200000-531691198313966349161522824112137830400000-1063382396627932698323045648224275660800000-2126764793255865396646091296448551321600000-4253529586511730793292182592897102643200000-8507059173023461586584365185794205286400000-17014118346046923173168730371588410572800000-34028236692093846346337460743176821145600000-68056473384187692692674921486353642291200000-136112946768375385385349842972707284582400000-272225893536750770770699685945414569164800000-544451787073501541541399371890829138329600000-1088903574147003083082798743781658276659200000-2177807148294006166165597487563316553318400000-4355614296588012332331194975126633106636800000-8711228593176024664662389950253266213273600000-17422457186352049329324779900506532426547200000-34844914372704098658649559801013064853094400000-69689828745408197317299119602026129706188800000-139379657490816394634598239204052259412377600000-278759314981632789269196478408104518824755200000-557518629963265578538392956816209037649510400000-1115037259926531157076785913632418075299020800000-2230074519853062314153571827264836150598041600000-4460149039706124628307143654529672301196083200000-8920298079412249256614287309059344602392166400000-17840596158824498513228574618118689204784332800000-35681192317648997026457149236237378409568665600000-71362384635297994052914298472474756819137331200000-142724769270595988105828596944949513638274662400000-285449538541191976211657193889899027276549324800000-570899077082383952423314387779798054553098649600000-1141798154164767904846628775559596109106197299200000-2283596308329535809693257551119192218212394598400000-4567192616659071619386515102238384436424789196800000-9134385233318143238773030204476768872849578393600000-18268770466636286477546060408953537745699156787200000-36537540933272572955092120817907075491398313574400000-73075081866545145910184241635814150982796627148800000-146150163733090291820368483271628301965593254297600000-292300327466180583640736966543256603931186508595200000-584600654932361167281473933086513207862373017190400000-1169201309864722334562947866173026415724746034380800000-2338402619729444669125895732346052831449492068761600000-4676805239458889338251791464692105662898984137523200000-9353610478917778676503582929384211325797968275046400000-18707220957835557353007165858768422651595936550092800000-37414441915671114706014331717536845303191873100185600000-74828883831342229412028663435073690606383746200371200000-149657767662684458824057326870147381212767492400742400000-299315535325368917648114653740294762425534984801484800000-598631070650737835296229307480589524851069969602969600000-1197262141301475670592458614961179049702139939205939200000-2394524282602951341184917229922358099404279878411878400000-4789048565205902682369834459844716198808559756823756800000-9578097130411805364739668919689432397617119513647513600000-19156194260823610729479337839378864795234239027295027200000-38312388521647221458958675678757729590468478054590054400000-76624777043294442917917351357515459180936956109180108800000-153249554086588885835834702715030918361873912218360217600000-306499108173177771671669405430061836723747824436720435200000-612998216346355543343338810860123673447495648873440867200000-1225996432692711086686677621720247346894991297746881734400000-2451992865385422173373355243440494693789982595493763468800000-4903985730770844346746710486880989387579965190987526937600000-9807971461541688693493420973761978775159930381975053875200000-19615942923083377386986841947523957550319860763950107750400000-39231885846166754773973683895047915100639721527900215500800000-78463771692333509547947367790095830201279443055800431001600000-156927543384667019095894735580191660402558886111600862003200000-313855086769334038191789471160383320805117772223201724006400000-627710173538668076383578942320766641610235544446403448012800000-1255420347077336152767157884641533283220471088892806896025600000-2510840694154672305534315769283066566440942177785613792051200000-5021681388309344611068631538566133132881884355571227584102400000-10043362776618689222137263077132266265763768711142455168204800000-20086725553237378444274526154264532531527537422284910336409600000-40173451106474756888549052308529065063055074844569820672819200000-80346902212949513777098104617058130126110149689139641345638400000-160693804425899027554196209234116260252220299378279282691276800000-321387608851798055108392418468232520504440598756558565382553600000-642775217703596110216784836936465041008881197513117130765107200000-1285550435407192220433569673872930082017762395026234261530214400000-2571100870814384440867139347745860164035524790052468523060428800000-5142201741628768881734278695491720328071049580104937046120857600000-10284403483257537763468557390983440656142099160209874092241715200000-20568806966515075526937114781966881312284198320419748184483430400000-41137613933030151053874229563933762624568396640839496368966860800000-82275227866060302107748459127867525249136793281678992737933721600000-164550455732120604215496918255735050498273586563357985475867443200000-329100911464241208430993836511470100996547173126715970951734886400000-658201822928482416861987673022940201993094346253431941903469772800000-1316403645856964833723975346045880403986188692506863883806939545600000-2632807291713929667447950692091760807972377385013727767613879091200000-5265614583427859334895901384183521615944754770027455535227758182400000-10531229166855718669791802768367043231889509540054911070455516364800000-21062458333711437339583605536734086463779019080109822140911032729600000-42124916667422874679167211073468172927558038160219644281822065459200000-84249833334845749358334422146936345855116076320439288563644130918400000-168499666669691498716668844293872691710232152640878577127288261836800000-336999333339382997433337688587745383420464305281757154254576523673600000-673998666678765994866675377175490766840928610563514308509153047347200000-1347997333357531989733350754350981533681857221127028617018306094694400000-2695994666715063979466701508701963067363714442254057234036612189388800000-5391989333430127958933403017403926134727428884508114468073224378777600000-10783978666860255917866806034807852269454857769016228936146448757555200000-21567957333720511835733612069615704538909715538032457872292897515110400000-43135914667441023671467224139231409077819431076064915744585795030220800000-86271829334882047342934448278462818155638862152129831489171590060441600000-172543658669764094685868896556925636311277724304259662978343180120883200000-345087317339528189371737793113851272622555448608519325956686360241766400000-690174634679056378743475586227702545245110897217038651913372720483532800000-1380349269358112757486951172455405090490221794434077303826745440967065600000-2760698538716225514973902344910810180980443588868154607653490881934131200000-5521397077432451029947804689821620361960887177736309215306981763868262400000-11042794154864902059895609379643240723921774355472618430613963527736524800000-22085588309729804119791218759286481447843548710945236861227927055473049600000-44171176619459608239582437518572962895687097421890473722455854110946099200000-88342353238919216479164875037145925791374194843780947444911708221892198400000-176684706477838432958329750074291851582748389687561894889823416443784396800000-353369412955676865916659500148583703165496779375123789779646832887568793600000-706738825911353731833319000297167406330993558750247579559293665775137587200000-1413477651822707463666

GS-104-86

Page 8 of 31

 Alberta ENVIRONMENT DEVELOPMENT & OPERATIONS DIVISION GEOTECHNICAL SERVICES LABORATORY		PROJECT <u>RYCROFT SLIDE</u> SITE _____ HOLE No. <u>RS 1</u> ELEV. _____ LOCATION _____ TECHNOLOGIST <u>JS AS JB</u> DATE DRILLED <u>16 Jul 1991</u>		
BOREHOLE AND TEST LOG				
TEST RESULTS	DEPTH (m)	SYMBOL	DESCRIPTION	OTHER INFORMATION
			as above, med br.	
	47			
	48			
	48		as above, hard, cal. sand pkts, SS frags.	FP= 383+ Rec= .45m/.45m
	49		as above, dk br, slicks.	Soft @ 48.8-54.9m.
	50			
	51			
	52			

						
TOPSOIL OR NO SAMPLE	GRAVEL	SAND OR SANDSTONE	CLAY OR SHALE	SILT OR SILTSTONE	UNDISTURBED SAMPLE	DISTURBED SAMPLE

W - MOISTURE CONTENT (%), G - WET UNIT WEIGHT (kg/m³), K - PERMEABILITY (cm/s), RA - PLANT AUGER,
 NCA - HOLLOW CORE AUGER, V OR S.P.T. - STANDARD PENETRATION TEST BLOW COUNT,
 R.R. - POCKET PENETROMETER (kPa), Cu - UNCONSOLIDATED COMPRESSION (kPa)
 W_p - PLASTIC LIMIT (%), L_p - LIQUID LIMIT (%), --- CORE RECOVERY (%),
 12-0.05-25 - 12.5% RETAINED ON No. 4 SIEVE, 0.05-0.25 - 0.075 No. 200 SIEVE,
 25 = % SILT, 75 = % CLAY, ∇ - WATER LEVEL


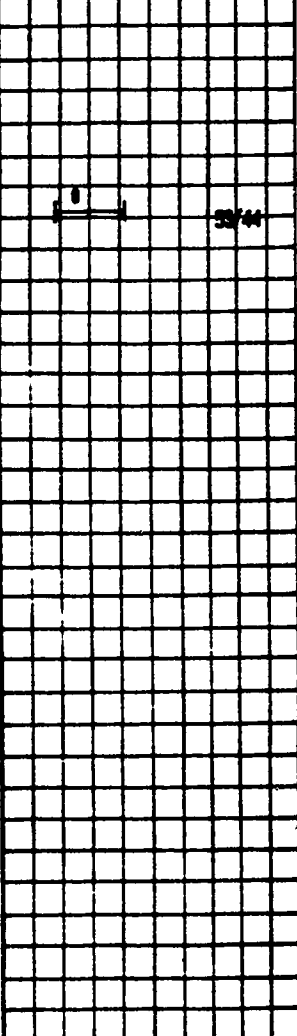

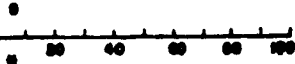

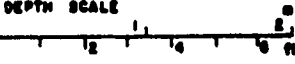





















Page 8 of 31

BOREHOLE AND TEST LOG

0-MOISTURE CONTENT (%), 0-WET UNIT WEIGHT (lb/ft³), K-PERMEABILITY (cm/s), P.A-PLASTY AUMER
H.CA-HOLLOW CORE AUGER, V OR S.P.T-STANDARD PENETRATION TEST BLOW COUNT,
P-POCKET PENETROMETER (lbf), Gc-UNSPECIFIED COMPRESSION (lbf)
Wp-PLASTIC LIMIT (%), WL-LIQUID LIMIT (%), --- CORE RECOVERY (%),
10-0.075 - 10 - 10% RETAINED ON NO. 4 SIEVE, 0.075 - 200 SIEVE NO. 200 SIEVE,
20 = 20 MIN. 7-WATER LEVEL


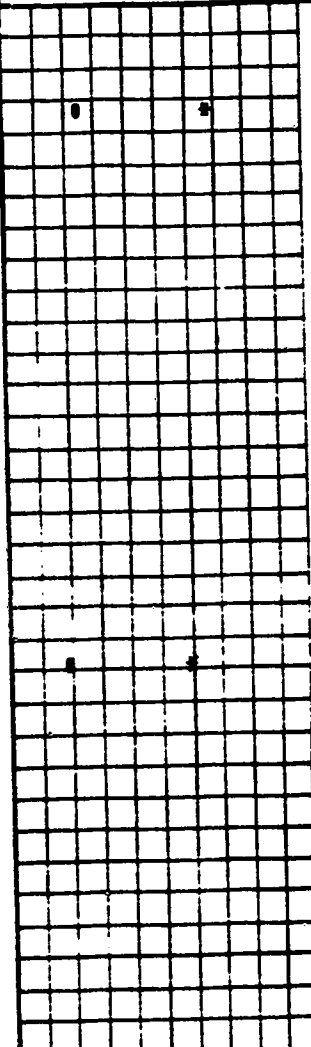

GS-104-86

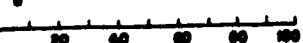

Page 10 of 21








 Alberta ENVIRONMENT DEVELOPMENT & OPERATIONS DIVISION GEOTECHNICAL SERVICES LABORATORY		PROJECT <u>RYCROFT SLIDE</u> SITE _____ HOLE No. <u>RS 1</u> ELEV. _____ LOCATION _____ TECHNOLOGIST <u>JS AS JB</u> DATE DRILLED <u>16 Jul 1991</u>																
BOREHOLE AND TEST LOG																		
TEST RESULTS	DEPTH (m)	SYMBOL	DESCRIPTION	OTHER INFORMATION														
	80 81 82 83 84 85 86		CI(TILL)-v stiff, dk br, peb silty cal, sand pkts, SS frags.	FP= 211 Rec= .20m/.20m Odd rock from 60.7m.														
<div style="display: flex; justify-content: space-between;"> <div style="width: 30%;">   DEPTH SCALE  </div> <div style="width: 70%;"> <table border="0" style="width: 100%;"> <tr> <td></td> <td></td> <td></td> <td></td> <td></td> <td></td> <td></td> </tr> <tr> <td>TOPSOIL OR NO SAMPLE</td> <td>GRAVEL</td> <td>SAND OR SANDSTONE</td> <td>CLAY OR SHALE</td> <td>SILT OR SILTSTONE</td> <td>UNDISTURBED SAMPLE</td> <td>DISTURBED SAMPLE</td> </tr> </table> <p style="font-size: small;"> w - MOISTURE CONTENT (%), G - DRY UNIT WEIGHT (kg/m³), K - PERMEABILITY (cm/s), RA - FLIGHT AUGER, HSA - HOLLOW CORE AUGER, V OR S.P.T. - STANDARD PENETRATION TEST BLOW COUNT, PP - POCKET PENETROMETER (MPa), Cu - UNCONSOLIDATED COMPRESSION (MPa) W_p - PLASTIC LIMIT (%), L_p - LIQUID LIMIT (%), --- CORE RECOVERY (%), 12-0.075-25 - 12-0.075% RETAINED ON No. 100 SIEVE, 0.075-0.425-0.850-1.75-3.0-6.0-12.5-25-50-100-200-425-850-1750-3000-6000-12500-25000-50000-100000-200000-400000-800000-1600000-3200000-6400000-12800000-25600000-51200000-102400000-204800000-409600000-819200000-1638400000-3276800000-6553600000-13107200000-26214400000-52428800000-104857600000-209715200000-419430400000-838860800000-1677721600000-3355443200000-6710886400000-13421772800000-26843545600000-53687091200000-107374182400000-214748364800000-429496729600000-858993459200000-1717986918400000-3435973836800000-6871947673600000-13743895347200000-27487790694400000-54975581388800000-109951162777600000-219902325555200000-439804651110400000-879609302220800000-1759218604441600000-3518437208883200000-7036874417766400000-14073748835532800000-28147497671065600000-56294995342131200000-112589990684262400000-225179981368524800000-450359962737049600000-900719925474099200000-1801439850948198400000-3602879701896396800000-7205759403792793600000-14411518807585587200000-28823037615171174400000-57646075230342348800000-115292150460684697600000-230584300921369395200000-461168601842738790400000-922337203685477580800000-1844674407370955161600000-3689348814741910323200000-7378697629483820646400000-14757395258967641292800000-29514790517935282585600000-59029581035870565171200000-118059162071741130342400000-236118324143482260684800000-472236648286964521369600000-944473296573929042739200000-1888946593147858085478400000-3777893186295716170956800000-7555786372591432341913600000-15111572745182864683827200000-30223145490365729367654400000-60446290980731458735308800000-120892581961462917470617600000-241785163922925834941235200000-483570327845851669882470400000-967140655691703339764940800000-1934281311383406679529881600000-3868562622766813359059763200000-7737125245533626718119526400000-15474250491067253436239052800000-30948500982134506872478105600000-61897001964269013744956211200000-123794003928538027489912422400000-247588007857076054979824844800000-495176015714152109959649689600000-990352031428304219919299379200000-1980704062856608439838598758400000-3961408125713216879677197516800000-7922816251426433759354395033600000-15845632502852867518708790067200000-31691265005705735037417580134400000-63382530011411470074835160268800000-126765060022822940149670320537600000-253530120045645880299340641075200000-507060240091291760598681282150400000-1014120480182583521197362564300800000-2028240960365167042394725128601600000-4056481920730334084789450257203200000-8112963841460668169578900514406400000-16225927682921336339157801028812800000-32451855365842672678315602057625600000-64903710731685345356631204115251200000-129807421463370690713262408230502400000-259614842926741381426524816461004800000-519229685853482762853049632922009600000-1038459371706965525706099265844019200000-2076918743413931051412198531688038400000-4153837486827862102824397063376076800000-8307674973655724205648794126752153600000-16615349947311448411297588253504307200000-33230699894622896822595176507008614400000-66461399789245793645190353014017228800000-132922799578491587290380706028034457600000-265845599156983174580761412056068915200000-531691198313966349161522824112137830400000-1063382396627932698323045648224275660800000-2126764793255865396646091296448551321600000-4253529586511730793292182592897102643200000-8507059173023461586584365185794205286400000-17014118346046923173168730371588410572800000-34028236692093846346337460743176821145600000-68056473384187692692674921486353642291200000-136112946768375385385349842972707284582400000-27222589353675077077069968594541456915200000-54445178707350154154139937189082913830400000-108890357414700308308279874378165827660800000-217780714829400616616559748756331655321600000-435561429658801233233119497512663310643200000-871122859317602466466238995025326621286400000-1742245718635204932932477990050653242572800000-3484491437270409865864955980101306485145600000-6968982874540819731729911960202612970291200000-13937965749081639463459823920405225940582400000-27875931498163278926919647840810451881164800000-55751862996326557853839295681620903762329600000-111503725992653115707678591363241807524659200000-223007451985306231415357182726483615049318400000-446014903970612462830714365452967230098636800000-892029807941224925661428730905934460197273600000-1784059615882449851322857461811868920394547200000-3568119231764899702645714923623737840789094400000-7136238463529799405291429847247475681578188800000-14272476927059598810582859694494951363156377600000-28544953854119197621165719388989902726312755200000-57089907708238395242331438777979805452625510400000-114179815416476790484662877555959610905251020800000-228359630832953580969325755111919221810502041600000-456719261665907161938651510223838443621004083200000-913438523331814323877303020447676887242008166400000-1826877046663628647754606040895353774484016332800000-3653754093327257295509212081790707548968032665600000-7307508186654514591018424163581415097936065331200000-14615016373309029182036848327162830195872130662400000-29230032746618058364073696654325660391744261324800000-58460065493236116728147393308651320783488522649600000-116920130986472233456294786617302641566977045299200000-233840261972944466912589573234605283133954090598400000-467680523945888933825179146469210566267908181196800000-935361047891777867650358292938421132535816362393600000-1870722095783555735300716585876842265071632724787200000-3741444191567111470601433171753684530143265449574400000-7482888383134222941202866343507369060286530899148800000-14965776766268445882405732687014738120573061798297600000-29931553532536891764811465374029476241146123596595200000-59863107065073783529622930748058952482292247193190400000-119726214130147567059245861496117904964584494386380800000-239452428260295134118491722992235809929168988772761600000-478904856520590268236983445984471619858337977545523200000-957809713041180536473966891968943239716675955091046400000-1915619426082361072947933783937886479433351910182092800000-3831238852164722145895867567875772958866703820364185600000-7662477704329444291791735135751545917733407640728371200000-15324955408658888583583470271503091835466815281456742400000-30649910817317777167166940543006183670933630562913484800000-61299821634635554334333881086012367341867261125826969600000-122599643269271108668667762172024734683734522251653939200000-245199286538542217337335524344049469367469044503307878400000-490398573077084434674671048688098938734938089006615756800000-980797146154168869349342097376197877469876178013231513600000-1961594292308337738698684194752395754939752356026463027200000-3923188584616675477397368389504791509879504712052926444800000-7846377169233350954794736779009583019759009424105852889600000-15692754338466701909589473558019166039518018848211705779200000-31385508676933403819178947116038332079036037696423411558400000-62771017353866807638357894232076664158072075392846823116800000-125542034707733615276715788464153328316144150785693646233600000-251084069415467230553431576928306656632288301571387292467200000-502168138830934461106863153856613313264576603142774593934400000-1004336277661868922213726307713226626529153206285549187868800000-2008672555323737844427452615426453253058306412571098375737600000-4017345110647475688854905230852906506116612825142196751475200000-8034690221294951377709810461705813012233225650284393502950400000-16069380442589902755419620923411626024466451300568787005900800000-32138760885179805510839241846823252048932902601137574011801600000-64277521770359611021678483693646504097865805202275148023603200000-128555043540719222043356967387293008195731610404550296047206400000-257110087081438444086713934774586016391463220809100592094412800000-514220174162876888173427869549172032782926441618201184188825600000-1028440348325753776346855739098344065565852883236402368377651200000-2056880696651507552693711478196688131131705766472804736755302400000-4113761393303015105387422956393376262263411532945609473510604800000-8227522786606030210774845912786752524526823065891218947021209600000-16455045573212060421549691825573505049053646131782437894042419200000-32910091146424120843099383651147010098107292263564875788084838400000-65820182292848241686198767302294020196214584527129751576169676800000-131640364585696483372397534604588040392429169054259503152339353600000-263280729171392966744795069209176080784858338108519006304678707200000-526561458342785933489590138418352161569716676217038012609357414400000-1053122916685571866979180276836704323139433352434076025218714828800000-2106245833371143733958360553673408646278866704868152050437429657600000-4212491666742287467916721107346817292557733409736304100874859315200000-8424983333484574935833442214693634585115466819472608201749718630400000-16849966666969149871666884429387269170230933638945201603499437260800000-33699933333938299743333768858774538340461867277890403206998874521600000-67399866667876599486667537717549076680923734555780806413997749043200000-134799733335753198973335075435098153361847469111561612827995498086400000-269599466671506397946670150870196306723694938223123225655990996172800000-539198933343012795893340301740392613447389876446246451311981992345600000-1078397866686025591786680603480785226894779752892492902623963984691200000-2156795733372051183573361206961570453789559505784985805247927969382400000-4313591466744102367146722413923140907579119011569971604495855938764800000-8627182933488204734293444827846281815158238023139943208991711877529600000-17254365866976409468586889655692563630316476046279886417983423755059200000-34508731733952818937173779311385127260632952092559772835966847510118400000-69017463467905637874347558622770254521265904185119545671933695020236800000-138034926935811275748695117245540509042531808370239091343867390040473600000-276069853871622551497390234491081018085063616740478182687734780080947200000-552139707743245102994780468982162036170127233480956365375469560161894400000-1104279415486490205989560937964324072340254466961912730750939120323788800000-2208558830972980411979121875928648144680508933923825461501878240647577600000-4417117661945960823958243751857296289361017867847650923003756481295155200000-8834235323891921647916487503714592578722035735695301846007512962590310400000-17668470647783843295832975007429185157444071471390603692015025925180620800000-35336941295567686591665950014858370314888142942781207384030051850361241600000-70673882591135373183331900029716740629776258845562414768060103700722483200000-141347765182270746366663800059433481259552517691124829536120207401444966400000-282695530364541492733327600118866962519105035382249659072240414802889932800000-565391060729082985466655200237733925038210070764499318144480829605779865600000-1130782121458165970933310400475467850076420141528998636288961659211559731200000-2261564242916331941866620800950935700152840283057997272577923318423119462400000-4523128485832663883733241601901871400305680566115994545155846636846238924800000-904625697166532776746648320380374280061136113223198909031169327</p></div></div>												TOPSOIL OR NO SAMPLE	GRAVEL	SAND OR SANDSTONE	CLAY OR SHALE	SILT OR SILTSTONE	UNDISTURBED SAMPLE	DISTURBED SAMPLE
																		
TOPSOIL OR NO SAMPLE	GRAVEL	SAND OR SANDSTONE	CLAY OR SHALE	SILT OR SILTSTONE	UNDISTURBED SAMPLE	DISTURBED SAMPLE												

GS-04-86

Page 11 of 31

 DEVELOPMENT & OPERATIONS DIVISION GEOTECHNICAL SERVICES LABORATORY		PROJECT <u>RYCROFT SLIDE</u>				
		SITE _____				
		HOLE No. <u>RS 1</u>		ELEV. _____		
		LOCATION _____				
		TECHNOLOGIST <u>JS AS JB</u> DATE DRILLED <u>16 Jul 1991</u>				
BOREHOLE AND TEST LOG						
TEST RESULTS	DEPTH (m)	SYMBOL	DESCRIPTION	SAMPLE	OTHER INFORMATION	
	87		as above.	/	PP= 211 Rec= .25m/.50m	
	88					
	89					
	70			as above.	/	PP= 287-306 Rec= .30m/.45m
	71					
	72					


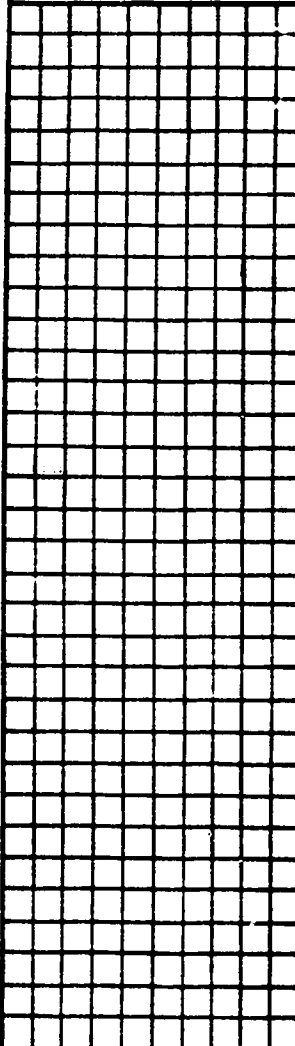




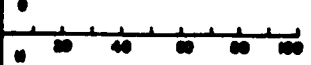

						
TOPSOIL OR NO SAMPLE	GRAVEL	SAND OR SANDSTONE	CLAY OR SHALE	SILT OR SILTSTONE	UNDISTURBED SAMPLE	DISTURBED SAMPLE


w - MOISTURE CONTENT (%), u - WET UNIT WEIGHT (kg/m³), k - PERMEABILITY (cm/s), RA - FLIGHT AUGER,
 HCA - HOLLOW CORE AUGER, v ON S.P.T. - STANDARD PENETRATION TEST BLOW COUNT,
 RP - POCKET PENETROMETER (MPa), Cu - UNCONFINED COMPRESSION (MPa),
 w_p - PLASTIC LIMIT (%), w_L - LIQUID LIMIT (%), --- CORE RECOVERY (%),
 12-0.075-25 - 12.5% RETAINED ON No. 4 SIEVE, 0.075-0.425 mm, 25.0% No. 200 SIEVE,
 25 = 25% SALT, ∇ - WATER LEVEL


GS-04-86


Page 12 of 31


 DEVELOPMENT & OPERATIONS DIVISION GEOTECHNICAL SERVICES LABORATORY		PROJECT <u>RYCROFT SLIDE</u> SITE _____ HOLE No. <u>RS 1</u> ELEV. _____ LOCATION _____ TECHNOLOGIST <u>JS AS JB</u> DATE DRILLED <u>16 Jul 1991</u>			
BOREHOLE AND TEST LOG					
TEST RESULTS	DEPTH (m)	SYMBOL	DESCRIPTION	SAMPLE	OTHER INFORMATION
	73				Stiffer from 76.2m.
	74				
	75				
	76				
	77				
	78				
	79				






 TOPSOIL OR NO SAMPLE


 GRAVEL

 SAND OR SANDSTONE

 CLAY OR SHALE

 SILT OR SILTSTONE

 UNDISTURBED SAMPLE

 DISTURBED SAMPLE


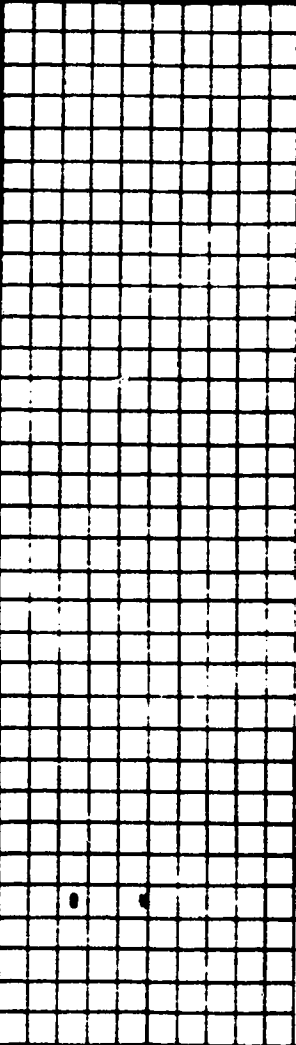

G - MOISTURE CONTENT (%), U - DRY UNIT WEIGHT (kg/m^3), K - PERMEABILITY (cm/s), RA - FLIGHT AUGER
 RRA - ROLLER AUGER, V OR S.P.T. - STANDARD PENETRATION TEST BLOW COUNT,
 RP - POCKET PENETROMETER (kPa), Cu - UNCONFINED COMPRESSION (kPa),
 Wp - PLASTIC LIMIT (%), Lp - LIQUID LIMIT (%), --- CORE RECOVERY (%),
 15-200-25 - 15% RETAINED ON No. 10 sieve, 0.075 mm size, 25% No. 200 sieve,
 25 = 25% RETAINED ON No. 4 sieve, 0.075 mm size, 25% No. 200 sieve,
 25 = 25% RETAINED ON No. 4 sieve, 0.075 mm size, 25% No. 200 sieve,
 25 = 25% RETAINED ON No. 4 sieve, 0.075 mm size, 25% No. 200 sieve,



Page 13 of 31








3


25-K4-96

Page 94 of 31

 DEVELOPMENT & OPERATIONS DIVISION GEOTECHNICAL SERVICES LABORATORY		PROJECT <u>RYCROFT SLIDE</u> SITE _____ HOLE No. <u>RS 1</u> ELEV. _____ LOCATION _____ TECHNOLOGIST <u>JS AS JB</u> DATE DRILLED <u>16 Jul 1991</u>		
BOREHOLE AND TEST LOG				
TEST RESULTS	DEPTH (m)	SYMBOL	DESCRIPTION	OTHER INFORMATION
	86		as above.	PP= 287 Rec= .35m/.48m
	87			
	88			
	89			
	90			
	91			
	92			


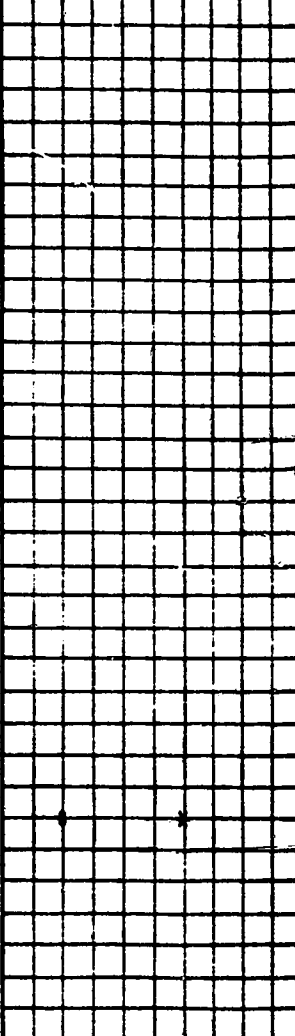


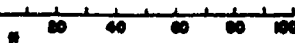

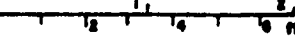
























 TOPSOIL OR NO SAMPLE
  GRAVEL
  SAND OR SANDSTONE
  CLAY OR SHALE
  SALT OR SALTSTONE
  UNDISTURBED SAMPLE
  DISTURBED SAMPLE

w - MOISTURE CONTENT (%), G - WET UNIT WEIGHT (kg/m³), K - PERMEABILITY (cm/s), RA - FLIGHT AUGER,
 HCA - HOLLOW CORE AUGER, V ON S.P.T. - STANDARD PENETRATION TEST BLOW COUNT,
 RP - POCKET PENETROMETER (kPa), Cu - UNCONFINED COMPRESSION (kPa)
 W_p - PLASTIC LIMIT (%), L_p - LIQUID LIMIT (%), --- CORE RECOVERY (%),
 15-0.05-22 = 15% RETAINED ON No. 40 sieve, 0.05-0.25 = 0.05-0.25 sieve, 22 = % No. 200 sieve,
 25 = % CLAY  - WATER LEVEL


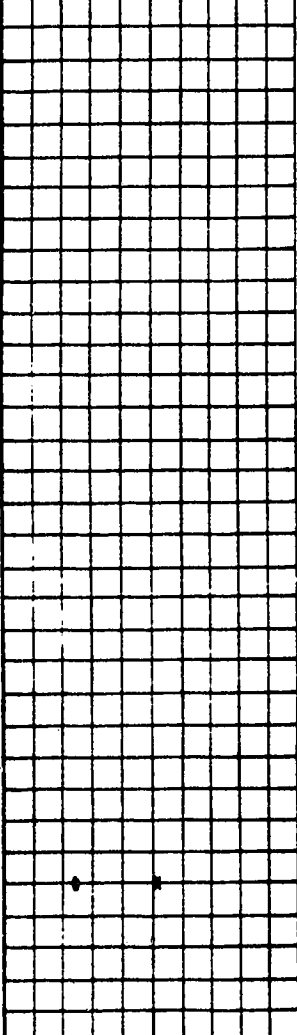

GS-Q4-86








Page 15 of 31

 Albera ENVIRONMENT DEVELOPMENT & OPERATIONS DIVISION GEOTECHNICAL SERVICES LABORATORY		PROJECT <u>RYCROFT SLIDE</u> SITE _____ HOLE No. <u>RS 1</u> ELEV. _____ LOCATION _____ TECHNOLOGIST <u>JS AS JB</u> DATE DRILLED <u>16 Jul 1991</u>																	
BOREHOLE AND TEST LOG																			
TEST RESULTS	DEPTH (m)	SYMBOL	DESCRIPTION	SAMPLE	OTHER INFORMATION														
	93		as above, hard.		FP= 383+ Rec= .30m/.45m														
	94																		
	95																		
	96																		
	97																		
	98																		
	99																		
<div style="display: flex; justify-content: space-between; align-items: flex-start;"> <div style="width: 30%;">   DEPTH SCALE  </div> <div style="width: 70%;"> <table style="width: 100%; border: none;"> <tr> <td style="text-align: center;"></td> <td style="text-align: center;"></td> <td style="text-align: center;"></td> <td style="text-align: center;"></td> <td style="text-align: center;"></td> <td style="text-align: center;"></td> <td style="text-align: center;"></td> </tr> <tr> <td style="text-align: center;">TOPSOIL OR NO SAMPLE</td> <td style="text-align: center;">GRAVEL</td> <td style="text-align: center;">SAND OR SANDSTONE</td> <td style="text-align: center;">CLAY OR SHALE</td> <td style="text-align: center;">SILT OR SILTY CLAY</td> <td style="text-align: center;">UNDISTURBED SAMPLE</td> <td style="text-align: center;">DISTURBED SAMPLE</td> </tr> </table> <p style="font-size: small;"> w - MOISTURE CONTENT (%), d - DRY UNIT WEIGHT (kg/m³), k - PERMEABILITY (cm/s), RA - FLIGHT AUGER, HCA - HOLLOW CORE AUGER, V OR S.P.T. - STANDARD PENETRATION TEST BLOW COUNT, RR - POCKET PENETROMETER (kPa), Cu - UNCONFINED COMPRESSION (kPa) w_p - PLASTIC LIMIT (%), L_p - LIQUID LIMIT (%), --- CORE RECOVERY (%), 12-0.075-2.0 - 12% RETAINED ON No. 4 SIEVE, 0.075-0.425 - 75% No. 40 SIEVE, 0.425-0.850 - 100% No. 20 SIEVE, 0.850-2.0 - 100% No. 10 SIEVE, 2.0-4.75 - 100% No. 4 SIEVE, 4.75-9.5 - 100% No. 20 SIEVE, 9.5-19 - 100% No. 10 SIEVE, 19-37.5 - 100% No. 5 SIEVE, 37.5-75 - 100% No. 2 SIEVE, 75-150 - 100% No. 1 SIEVE, 150-300 - 100% No. 0.85 SIEVE, 300-600 - 100% No. 0.425 SIEVE, 600-1200 - 100% No. 0.25 SIEVE, 1200-2400 - 100% No. 0.15 SIEVE, 2400-4800 - 100% No. 0.075 SIEVE, 4800-9600 - 100% No. 0.0425 SIEVE, 9600-19200 - 100% No. 0.025 SIEVE, 19200-38400 - 100% No. 0.015 SIEVE, 38400-76800 - 100% No. 0.0075 SIEVE, 76800-153600 - 100% No. 0.00425 SIEVE, 153600-307200 - 100% No. 0.0025 SIEVE, 307200-614400 - 100% No. 0.0015 SIEVE, 614400-1228800 - 100% No. 0.00075 SIEVE, 1228800-2457600 - 100% No. 0.000425 SIEVE, 2457600-4915200 - 100% No. 0.00025 SIEVE, 4915200-9830400 - 100% No. 0.00015 SIEVE, 9830400-19660800 - 100% No. 0.000075 SIEVE, 19660800-39321600 - 100% No. 0.0000425 SIEVE, 39321600-78643200 - 100% No. 0.000025 SIEVE, 78643200-157286400 - 100% No. 0.000015 SIEVE, 157286400-314572800 - 100% No. 0.0000075 SIEVE, 314572800-629145600 - 100% No. 0.00000425 SIEVE, 629145600-1258291200 - 100% No. 0.0000025 SIEVE, 1258291200-2516582400 - 100% No. 0.0000015 SIEVE, 2516582400-5033164800 - 100% No. 0.00000075 SIEVE, 5033164800-10066329600 - 100% No. 0.000000425 SIEVE, 10066329600-20132659200 - 100% No. 0.00000025 SIEVE, 20132659200-40265318400 - 100% No. 0.00000015 SIEVE, 40265318400-80530636800 - 100% No. 0.000000075 SIEVE, 80530636800-161061273600 - 100% No. 0.0000000425 SIEVE, 161061273600-322122547200 - 100% No. 0.000000025 SIEVE, 322122547200-644245094400 - 100% No. 0.000000015 SIEVE, 644245094400-1288490188800 - 100% No. 0.0000000075 SIEVE, 1288490188800-2576980377600 - 100% No. 0.00000000425 SIEVE, 2576980377600-5153960755200 - 100% No. 0.0000000025 SIEVE, 5153960755200-10307921510400 - 100% No. 0.0000000015 SIEVE, 10307921510400-20615843020800 - 100% No. 0.00000000075 SIEVE, 20615843020800-41231686041600 - 100% No. 0.000000000425 SIEVE, 41231686041600-82463372083200 - 100% No. 0.00000000025 SIEVE, 82463372083200-164926744166400 - 100% No. 0.00000000015 SIEVE, 164926744166400-329853488332800 - 100% No. 0.000000000075 SIEVE, 329853488332800-659706976665600 - 100% No. 0.0000000000425 SIEVE, 659706976665600-1319413953331200 - 100% No. 0.000000000025 SIEVE, 1319413953331200-2638827906662400 - 100% No. 0.000000000015 SIEVE, 2638827906662400-5277655813324800 - 100% No. 0.0000000000075 SIEVE, 5277655813324800-10555311626649600 - 100% No. 0.00000000000425 SIEVE, 10555311626649600-21110623253299200 - 100% No. 0.0000000000025 SIEVE, 21110623253299200-42221246506598400 - 100% No. 0.0000000000015 SIEVE, 42221246506598400-84442493013196800 - 100% No. 0.00000000000075 SIEVE, 84442493013196800-168884986026393600 - 100% No. 0.000000000000425 SIEVE, 168884986026393600-337769972052787200 - 100% No. 0.00000000000025 SIEVE, 337769972052787200-675539944105574400 - 100% No. 0.00000000000015 SIEVE, 675539944105574400-1351079888211148800 - 100% No. 0.000000000000075 SIEVE, 1351079888211148800-2702159776422297600 - 100% No. 0.0000000000000425 SIEVE, 2702159776422297600-5404319552844595200 - 100% No. 0.000000000000025 SIEVE, 5404319552844595200-10808639105689190400 - 100% No. 0.000000000000015 SIEVE, 10808639105689190400-21617278211378380800 - 100% No. 0.0000000000000075 SIEVE, 21617278211378380800-43234556422756761600 - 100% No. 0.00000000000000425 SIEVE, 43234556422756761600-86469112845513523200 - 100% No. 0.0000000000000025 SIEVE, 86469112845513523200-172938225691027046400 - 100% No. 0.0000000000000015 SIEVE, 172938225691027046400-345876451382054092800 - 100% No. 0.00000000000000075 SIEVE, 345876451382054092800-691752902764108185600 - 100% No. 0.000000000000000425 SIEVE, 691752902764108185600-1383505805528216371200 - 100% No. 0.00000000000000025 SIEVE, 1383505805528216371200-2767011611056432742400 - 100% No. 0.00000000000000015 SIEVE, 2767011611056432742400-5534023222112865484800 - 100% No. 0.000000000000000075 SIEVE, 5534023222112865484800-11068046444225730969600 - 100% No. 0.0000000000000000425 SIEVE, 11068046444225730969600-22136092888451461939200 - 100% No. 0.000000000000000025 SIEVE, 22136092888451461939200-44272185776902923878400 - 100% No. 0.000000000000000015 SIEVE, 44272185776902923878400-88544371553805847756800 - 100% No. 0.0000000000000000075 SIEVE, 88544371553805847756800-177088743107611695513600 - 100% No. 0.00000000000000000425 SIEVE, 177088743107611695513600-354177486215223391027200 - 100% No. 0.0000000000000000025 SIEVE, 354177486215223391027200-708354972430446782054400 - 100% No. 0.0000000000000000015 SIEVE, 708354972430446782054400-1416709944860893564108800 - 100% No. 0.00000000000000000075 SIEVE, 1416709944860893564108800-2833419889721787128217600 - 100% No. 0.000000000000000000425 SIEVE, 2833419889721787128217600-5666839779443574256435200 - 100% No. 0.00000000000000000025 SIEVE, 5666839779443574256435200-11333679558887148512870400 - 100% No. 0.00000000000000000015 SIEVE, 11333679558887148512870400-22667359117774297025740800 - 100% No. 0.000000000000000000075 SIEVE, 22667359117774297025740800-45334718235548594051481600 - 100% No. 0.0000000000000000000425 SIEVE, 45334718235548594051481600-90669436471097188102963200 - 100% No. 0.000000000000000000025 SIEVE, 90669436471097188102963200-181338872942194376205926400 - 100% No. 0.000000000000000000015 SIEVE, 181338872942194376205926400-362677745884388752411852800 - 100% No. 0.0000000000000000000075 SIEVE, 362677745884388752411852800-725355491768777504823705600 - 100% No. 0.00000000000000000000425 SIEVE, 725355491768777504823705600-1450710983537555009647411200 - 100% No. 0.0000000000000000000025 SIEVE, 1450710983537555009647411200-2901421967075110019294822400 - 100% No. 0.0000000000000000000015 SIEVE, 2901421967075110019294822400-5802843934150220038589644800 - 100% No. 0.00000000000000000000075 SIEVE, 5802843934150220038589644800-11605687868300440077179289600 - 100% No. 0.000000000000000000000425 SIEVE, 11605687868300440077179289600-23211375736600880154358579200 - 100% No. 0.00000000000000000000025 SIEVE, 23211375736600880154358579200-46422751473201760308717158400 - 100% No. 0.00000000000000000000015 SIEVE, 46422751473201760308717158400-92845502946403520617434316800 - 100% No. 0.000000000000000000000075 SIEVE, 92845502946403520617434316800-185691005892807041234868633600 - 100% No. 0.0000000000000000000000425 SIEVE, 185691005892807041234868633600-371382011785614082469737267200 - 100% No. 0.000000000000000000000025 SIEVE, 371382011785614082469737267200-742764023571228164939474534400 - 100% No. 0.000000000000000000000015 SIEVE, 742764023571228164939474534400-1485528047142456329878949068800 - 100% No. 0.0000000000000000000000075 SIEVE, 1485528047142456329878949068800-2971056094284912659757898137600 - 100% No. 0.00000000000000000000000425 SIEVE, 2971056094284912659757898137600-5942112188569825319515796275200 - 100% No. 0.0000000000000000000000025 SIEVE, 5942112188569825319515796275200-11884224377139650639031592550400 - 100% No. 0.0000000000000000000000015 SIEVE, 11884224377139650639031592550400-23768448754279301278063185100800 - 100% No. 0.00000000000000000000000075 SIEVE, 23768448754279301278063185100800-47536897508558602556126370201600 - 100% No. 0.000000000000000000000000425 SIEVE, 47536897508558602556126370201600-95073795017117205112252740403200 - 100% No. 0.00000000000000000000000025 SIEVE, 95073795017117205112252740403200-190147590034234410224505480806400 - 100% No. 0.00000000000000000000000015 SIEVE, 190147590034234410224505480806400-380295180068468820449010961612800 - 100% No. 0.000000000000000000000000075 SIEVE, 380295180068468820449010961612800-760590360136937640898021923225600 - 100% No. 0.0000000000000000000000000425 SIEVE, 760590360136937640898021923225600-1521180720273875281796043846451200 - 100% No. 0.000000000000000000000000025 SIEVE, 1521180720273875281796043846451200-3042361440547750563592087692902400 - 100% No. 0.000000000000000000000000015 SIEVE, 3042361440547750563592087692902400-6084722881095501127184175385804800 - 100% No. 0.0000000000000000000000000075 SIEVE, 6084722881095501127184175385804800-12169445762191002254368350771609600 - 100% No. 0.00000000000000000000000000425 SIEVE, 12169445762191002254368350771609600-24338891524382004508736701543219200 - 100% No. 0.0000000000000000000000000025 SIEVE, 24338891524382004508736701543219200-48677783048764009017473403086438400 - 100% No. 0.0000000000000000000000000015 SIEVE, 48677783048764009017473403086438400-97355566097528018034946806172876800 - 100% No. 0.00000000000000000000000000075 SIEVE, 97355566097528018034946806172876800-194711132195056036069893612345753600 - 100% No. 0.000000000000000000000000000425 SIEVE, 194711132195056036069893612345753600-389422264390112072139787224691507200 - 100% No. 0.00000000000000000000000000025 SIEVE, 389422264390112072139787224691507200-778844528780224144279574449383014400 - 100% No. 0.00000000000000000000000000015 SIEVE, 778844528780224144279574449383014400-1557689057560448288559148898766028800 - 100% No. 0.000000000000000000000000000075 SIEVE, 1557689057560448288559148898766028800-3115378115120896577118297797532057600 - 100% No. 0.0000000000000000000000000000425 SIEVE, 3115378115120896577118297797532057600-6230756230241793154236595595064115200 - 100% No. 0.000000000000000000000000000025 SIEVE, 6230756230241793154236595595064115200-12461512460483586308473191190128230400 - 100% No. 0.000000000000000000000000000015 SIEVE, 12461512460483586308473191190128230400-24923024920967172616946382380256460800 - 100% No. 0.0000000000000000000000000000075 SIEVE, 24923024920967172616946382380256460800-49846049841934345233892764760512921600 - 100% No. 0.00000000000000000000000000000425 SIEVE, 49846049841934345233892764760512921600-99692099683868690467785529521025843200 - 100% No. 0.0000000000000000000000000000025 SIEVE, 99692099683868690467785529521025843200-199384199367737380935571059042051686400 - 100% No. 0.0000000000000000000000000000015 SIEVE, 199384199367737380935571059042051686400-398768398735474761871142118084103372800 - 100% No. 0.00000000000000000000000000000075 SIEVE, 398768398735474761871142118084103372800-797536797470949523742284236168206745600 - 100% No. 0.000000000000000000000000000000425 SIEVE, 797536797470949523742284236168206745600-1595073594941899047484568472336413491200 - 100% No. 0.00000000000000000000000000000025 SIEVE, 1595073594941899047484568472336413491200-3190147189883798094969136944672826982400 - 100% No. 0.00000000000000000000000000000015 SIEVE, 3190147189883798094969136944672826982400-6380294379767596189938273889345653964800 - 100% No. 0.000000000000000000000000000000075 SIEVE, 6380294379767596189938273889345653964800-12760588759535192379876547778691307929600 - 100% No. 0.0000000000000000000000000000000425 SIEVE, 12760588759535192379876547778691307929600-25521177519070384759753095557382615859200 - 100% No. 0.000000000000000000000000000000025 SIEVE, 25521177519070384759753095557382615859200-51042355038140769519506191114765231718400 - 100% No. 0.000000000000000000000000000000015 SIEVE, 51042355038140769519506191114765231718400-102084710076281539039012382229530463436800 - 100% No. 0.0000000000000000000000000000000075 SIEVE, 102084710076281539039012382229530463436800-204169420152563078078024764459060926873600 - 100% No. 0.00000000000000000000000000000000425 SIEVE, 204169420152563078078024764459060926873600-408338840305126156156049528918121853747200 - 100% No. 0.0000000000000000000000000000000025 SIEVE, 408338840305126156156049528918121853747200-8166776806102523123120990578</p></div></div>													TOPSOIL OR NO SAMPLE	GRAVEL	SAND OR SANDSTONE	CLAY OR SHALE	SILT OR SILTY CLAY	UNDISTURBED SAMPLE	DISTURBED SAMPLE
																			
TOPSOIL OR NO SAMPLE	GRAVEL	SAND OR SANDSTONE	CLAY OR SHALE	SILT OR SILTY CLAY	UNDISTURBED SAMPLE	DISTURBED SAMPLE													

GS-104-BE

Page 18 of 31


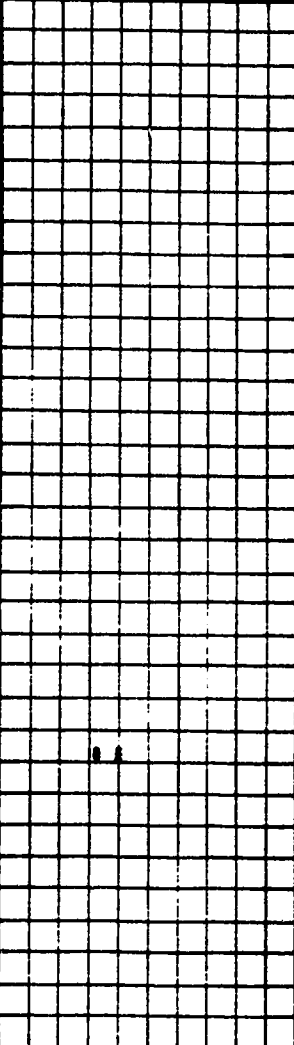
 DEVELOPMENT & OPERATIONS DIVISION GEOTECHNICAL SERVICES LABORATORY		PROJECT <u>RYCROFT SLIDE</u> SITE _____ HOLE No. <u>RS 1</u> ELEV. _____ LOCATION _____ TECHNOLOGIST <u>JS AS JB</u> DATE DRILLED <u>16 Jul 1991</u>			
		BOREHOLE AND TEST LOG			
TEST RESULTS	DEPTH (m)	SYMBOL	DESCRIPTION	SAMPLE	OTHER INFORMATION
	100		as above, hard.		
	101				
	102				
	103				
	104				
	105		CN-dk gry, ML partings & pkts, odd pebble, ML layers @ 105.5m & 106.7m.		Cored @ 104.6-107.15m. Rec= 2.00m/2.55m

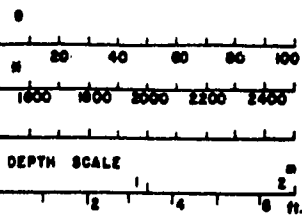
 TOPSOIL OR NO SAMPLE  GRAVEL  SAND OR SANDSTONE  CLAY OR SHALE  SILT OR SILTSTONE  UNDISTURBED SAMPLE  DISTURBED SAMPLE	w - MOISTURE CONTENT (%), γ - WET UNIT WEIGHT (kg/m^3), K - PERMEABILITY (cm/s), P.A. - PLINT AUGER, HCA - HOLLOW CORE AUGER, V OR S.P.T. - STANDARD PENETRATION TEST BLOW COUNT, R.R. - POCKET PENETROMETER (tpe), q_u - UNCONFINED COMPRESSION (tpe) W _p - PLASTIC LIMIT (%), L - LIQUID LIMIT (%), --- CORE RECOVERY (%), 12-0.075-25 - 12-25% RETAINED ON No. 40 sieve, 0.075-0.25 mm, 25-200 sieve, 20 = % SILT, 50 = % CLAY, ∇ - WATER LEVEL
---	---

0 20 40 60 80 100
 1000 1500 2000 2500 3000
 DEPTH SCALE m
 1 2 3 4 5 6 7 8 9 10 11

GS-104-BE

Page 17 of 31

 Alberta ENVIRONMENT DEVELOPMENT & OPERATIONS DIVISION GEOTECHNICAL SERVICES LABORATORY		PROJECT <u>RYCROFT SLIDE</u> SITE _____ HOLE No. <u>RS 1</u> ELEV. _____ LOCATION _____ TECHNOLOGIST <u>JS AS JB</u> DATE DRILLED <u>16 Jul 1991</u>			
BOREHOLE AND TEST LOG					
TEST RESULTS	DEPTH (m)	SYMBOL	DESCRIPTION	SAMPLE	OTHER INFORMATION
	106	[Symbol]			
	107	[Symbol]			
	108	[Symbol]			
	109	[Symbol]			
	110	[Symbol]	as above, slicks.		Cored @ 110.35-113.10m Rec = .25m/2.75m
	111	[Symbol]			
	112	[Symbol]			
	113	[Symbol]			
	114	[Symbol]			
	115	[Symbol]			



TOPSOIL OR NO SAMPLE

GRAVEL

SAND OR SANDSTONE

CLAY OR SHALE

SILT OR SILTSTONE
























UNDISTURBED SAMPLE

DISTURBED SAMPLE

w - MOISTURE CONTENT (%), γ - WET UNIT WEIGHT (kg/m^3), k - PERMEABILITY (cm/s), R_a - PLIGHT AUGER
 MCA - HOLLOW CORE AUGER, γ OR S.P.T. - STANDARD PENETRATION TEST BLOW COUNT,
 R.P. - POCKET PENETROMETER (SPe), q_u - UNCONFINED COMPRESSION (SPe)
 w_p - PLASTIC LIMIT (%), w_L - LIQUID LIMIT (%), --- CORE RECOVERY (%),
 12-0.075-2.0 - 12% RETAINED ON No. 40 SIEVE, 0.075-0.425 - 2.0-4.75 mm, 2.0-4.75 - 4.75-7.5 mm, 4.75-7.5 - 7.5-12.5 mm, 12.5-12.5 - 12.5-25.0 mm, 25.0-25.0 - 25.0-50.0 mm, 50.0-50.0 - 50.0-100.0 mm, 100.0-100.0 - 100.0-200.0 mm, 200.0-200.0 - 200.0-400.0 mm, 400.0-400.0 - 400.0-800.0 mm, 800.0-800.0 - 800.0-1600.0 mm, 1600.0-1600.0 - 1600.0-3200.0 mm, 3200.0-3200.0 - 3200.0-6400.0 mm, 6400.0-6400.0 - 6400.0-12800.0 mm, 12800.0-12800.0 - 12800.0-25600.0 mm, 25600.0-25600.0 - 25600.0-51200.0 mm, 51200.0-51200.0 - 51200.0-102400.0 mm, 102400.0-102400.0 - 102400.0-204800.0 mm, 204800.0-204800.0 - 204800.0-409600.0 mm, 409600.0-409600.0 - 409600.0-819200.0 mm, 819200.0-819200.0 - 819200.0-1638400.0 mm, 1638400.0-1638400.0 - 1638400.0-3276800.0 mm, 3276800.0-3276800.0 - 3276800.0-6553600.0 mm, 6553600.0-6553600.0 - 6553600.0-13107200.0 mm, 13107200.0-13107200.0 - 13107200.0-26214400.0 mm, 26214400.0-26214400.0 - 26214400.0-52428800.0 mm, 52428800.0-52428800.0 - 52428800.0-104857600.0 mm, 104857600.0-104857600.0 - 104857600.0-209715200.0 mm, 209715200.0-209715200.0 - 209715200.0-419430400.0 mm, 419430400.0-419430400.0 - 419430400.0-838860800.0 mm, 838860800.0-838860800.0 - 838860800.0-1677721600.0 mm, 1677721600.0-1677721600.0 - 1677721600.0-3355443200.0 mm, 3355443200.0-3355443200.0 - 3355443200.0-6710886400.0 mm, 6710886400.0-6710886400.0 - 6710886400.0-13421772800.0 mm, 13421772800.0-13421772800.0 - 13421772800.0-26843545600.0 mm, 26843545600.0-26843545600.0 - 26843545600.0-53687091200.0 mm, 53687091200.0-53687091200.0 - 53687091200.0-107374182400.0 mm, 107374182400.0-107374182400.0 - 107374182400.0-214748364800.0 mm, 214748364800.0-214748364800.0 - 214748364800.0-429496729600.0 mm, 429496729600.0-429496729600.0 - 429496729600.0-858993459200.0 mm, 858993459200.0-858993459200.0 - 858993459200.0-1717986918400.0 mm, 1717986918400.0-1717986918400.0 - 1717986918400.0-3435973836800.0 mm, 3435973836800.0-3435973836800.0 - 3435973836800.0-6871947673600.0 mm, 6871947673600.0-6871947673600.0 - 6871947673600.0-13743895347200.0 mm, 13743895347200.0-13743895347200.0 - 13743895347200.0-27487790694400.0 mm, 27487790694400.0-27487790694400.0 - 27487790694400.0-54975581388800.0 mm, 54975581388800.0-54975581388800.0 - 54975581388800.0-109951162777600.0 mm, 109951162777600.0-109951162777600.0 - 109951162777600.0-219902325555200.0 mm, 219902325555200.0-219902325555200.0 - 219902325555200.0-439804651110400.0 mm, 439804651110400.0-439804651110400.0 - 439804651110400.0-879609302220800.0 mm, 879609302220800.0-879609302220800.0 - 879609302220800.0-1759218604441600.0 mm, 1759218604441600.0-1759218604441600.0 - 1759218604441600.0-3518437208883200.0 mm, 3518437208883200.0-3518437208883200.0 - 3518437208883200.0-7036874417766400.0 mm, 7036874417766400.0-7036874417766400.0 - 7036874417766400.0-14073748835532800.0 mm, 14073748835532800.0-14073748835532800.0 - 14073748835532800.0-28147497671065600.0 mm, 28147497671065600.0-28147497671065600.0 - 28147497671065600.0-56294995342131200.0 mm, 56294995342131200.0-56294995342131200.0 - 56294995342131200.0-112589990684262400.0 mm, 112589990684262400.0-112589990684262400.0 - 112589990684262400.0-225179981368524800.0 mm, 225179981368524800.0-225179981368524800.0 - 225179981368524800.0-450359962737049600.0 mm, 450359962737049600.0-450359962737049600.0 - 450359962737049600.0-900719925474099200.0 mm, 900719925474099200.0-900719925474099200.0 - 900719925474099200.0-1801439850948198400.0 mm, 1801439850948198400.0-1801439850948198400.0 - 1801439850948198400.0-3602879701896396800.0 mm, 3602879701896396800.0-3602879701896396800.0 - 3602879701896396800.0-7205759403792793600.0 mm, 7205759403792793600.0-7205759403792793600.0 - 7205759403792793600.0-14411518807585587200.0 mm, 14411518807585587200.0-14411518807585587200.0 - 14411518807585587200.0-28823037615171174400.0 mm, 28823037615171174400.0-28823037615171174400.0 - 28823037615171174400.0-57646075230342348800.0 mm, 57646075230342348800.0-57646075230342348800.0 - 57646075230342348800.0-115292150460684697600.0 mm, 115292150460684697600.0-115292150460684697600.0 - 115292150460684697600.0-230584300921369395200.0 mm, 230584300921369395200.0-230584300921369395200.0 - 230584300921369395200.0-461168601842738790400.0 mm, 461168601842738790400.0-461168601842738790400.0 - 461168601842738790400.0-922337203685477580800.0 mm, 922337203685477580800.0-922337203685477580800.0 - 922337203685477580800.0-1844674407370955161600.0 mm, 1844674407370955161600.0-1844674407370955161600.0 - 1844674407370955161600.0-3689348814741910323200.0 mm, 3689348814741910323200.0-3689348814741910323200.0 - 3689348814741910323200.0-7378697629483820646400.0 mm, 7378697629483820646400.0-7378697629483820646400.0 - 7378697629483820646400.0-14757395258967641292800.0 mm, 14757395258967641292800.0-14757395258967641292800.0 - 14757395258967641292800.0-29514790517935282585600.0 mm, 29514790517935282585600.0-29514790517935282585600.0 - 29514790517935282585600.0-59029581035870565171200.0 mm, 59029581035870565171200.0-59029581035870565171200.0 - 59029581035870565171200.0-118059162071741130342400.0 mm, 118059162071741130342400.0-118059162071741130342400.0 - 118059162071741130342400.0-236118324143482260684800.0 mm, 236118324143482260684800.0-236118324143482260684800.0 - 236118324143482260684800.0-472236648286964521369600.0 mm, 472236648286964521369600.0-472236648286964521369600.0 - 472236648286964521369600.0-944473296573929042739200.0 mm, 944473296573929042739200.0-944473296573929042739200.0 - 944473296573929042739200.0-1888946593147858085478400.0 mm, 1888946593147858085478400.0-1888946593147858085478400.0 - 1888946593147858085478400.0-3777893186295716170956800.0 mm, 3777893186295716170956800.0-3777893186295716170956800.0 - 3777893186295716170956800.0-7555786372591432341913600.0 mm, 7555786372591432341913600.0-7555786372591432341913600.0 - 7555786372591432341913600.0-15111572745182864683827200.0 mm, 15111572745182864683827200.0-15111572745182864683827200.0 - 15111572745182864683827200.0-30223145490365729367654400.0 mm, 30223145490365729367654400.0-30223145490365729367654400.0 - 30223145490365729367654400.0-60446290980731458735308800.0 mm, 60446290980731458735308800.0-60446290980731458735308800.0 - 60446290980731458735308800.0-120892581961462917470617600.0 mm, 120892581961462917470617600.0-120892581961462917470617600.0 - 120892581961462917470617600.0-241785163922925834941235200.0 mm, 241785163922925834941235200.0-241785163922925834941235200.0 - 241785163922925834941235200.0-483570327845851669882470400.0 mm, 483570327845851669882470400.0-483570327845851669882470400.0 - 483570327845851669882470400.0-967140655691703339764940800.0 mm, 967140655691703339764940800.0-967140655691703339764940800.0 - 967140655691703339764940800.0-1934281311383406679529881600.0 mm, 1934281311383406679529881600.0-1934281311383406679529881600.0 - 1934281311383406679529881600.0-3868562622766813359059763200.0 mm, 3868562622766813359059763200.0-3868562622766813359059763200.0 - 3868562622766813359059763200.0-7737125245533626718119526400.0 mm, 7737125245533626718119526400.0-7737125245533626718119526400.0 - 7737125245533626718119526400.0-15474250491067253436239052800.0 mm, 15474250491067253436239052800.0-15474250491067253436239052800.0 - 15474250491067253436239052800.0-30948500982134506872478105600.0 mm, 30948500982134506872478105600.0-30948500982134506872478105600.0 - 30948500982134506872478105600.0-61897001964269013744956211200.0 mm, 61897001964269013744956211200.0-61897001964269013744956211200.0 - 61897001964269013744956211200.0-123794003928538027489912422400.0 mm, 123794003928538027489912422400.0-123794003928538027489912422400.0 - 123794003928538027489912422400.0-247588007857076054979824844800.0 mm, 247588007857076054979824844800.0-247588007857076054979824844800.0 - 247588007857076054979824844800.0-495176015714152109959649689600.0 mm, 495176015714152109959649689600.0-495176015714152109959649689600.0 - 495176015714152109959649689600.0-990352031428304219919299379200.0 mm, 990352031428304219919299379200.0-990352031428304219919299379200.0 - 990352031428304219919299379200.0-1980704062856608439838598758400.0 mm, 1980704062856608439838598758400.0-1980704062856608439838598758400.0 - 1980704062856608439838598758400.0-3961408125713216879677197516800.0 mm, 3961408125713216879677197516800.0-3961408125713216879677197516800.0 - 3961408125713216879677197516800.0-7922816251426433759354395033600.0 mm, 7922816251426433759354395033600.0-7922816251426433759354395033600.0 - 7922816251426433759354395033600.0-15845632502852867518708790067200.0 mm, 15845632502852867518708790067200.0-15845632502852867518708790067200.0 - 15845632502852867518708790067200.0-31691265005705735037417580134400.0 mm, 31691265005705735037417580134400.0-31691265005705735037417580134400.0 - 31691265005705735037417580134400.0-63382530011411470074835160268800.0 mm, 63382530011411470074835160268800.0-63382530011411470074835160268800.0 - 63382530011411470074835160268800.0-126765060022822940149670320537600.0 mm, 126765060022822940149670320537600.0-126765060022822940149670320537600.0 - 126765060022822940149670320537600.0-253530120045645880299340641075200.0 mm, 253530120045645880299340641075200.0-253530120045645880299340641075200.0 - 253530120045645880299340641075200.0-507060240091291760598681282150400.0 mm, 507060240091291760598681282150400.0-507060240091291760598681282150400.0 - 507060240091291760598681282150400.0-1014120480182583521197362564300800.0 mm, 1014120480182583521197362564300800.0-1014120480182583521197362564300800.0 - 1014120480182583521197362564300800.0-2028240960365167042394725128601600.0 mm, 2028240960365167042394725128601600.0-2028240960365167042394725128601600.0 - 2028240960365167042394725128601600.0-4056481920730334084789450257203200.0 mm, 4056481920730334084789450257203200.0-4056481920730334084789450257203200.0 - 4056481920730334084789450257203200.0-8112963841460668169578900514406400.0 mm, 8112963841460668169578900514406400.0-8112963841460668169578900514406400.0 - 8112963841460668169578900514406400.0-16225927682921336339157801028812800.0 mm, 16225927682921336339157801028812800.0-16225927682921336339157801028812800.0 - 16225927682921336339157801028812800.0-32451855365842672678315602057625600.0 mm, 32451855365842672678315602057625600.0-32451855365842672678315602057625600.0 - 32451855365842672678315602057625600.0-64903710731685345356631204115251200.0 mm, 64903710731685345356631204115251200.0-64903710731685345356631204115251200.0 - 64903710731685345356631204115251200.0-129807421463370690713262408230502400.0 mm, 129807421463370690713262408230502400.0-129807421463370690713262408230502400.0 - 129807421463370690713262408230502400.0-259614842926741381426524816461004800.0 mm, 259614842926741381426524816461004800.0-259614842926741381426524816461004800.0 - 259614842926741381426524816461004800.0-519229685853482762853049632922009600.0 mm, 519229685853482762853049632922009600.0-519229685853482762853049632922009600.0 - 519229685853482762853049632922009600.0-1038459371706965525706099265844019200.0 mm, 1038459371706965525706099265844019200.0-1038459371706965525706099265844019200.0 - 1038459371706965525706099265844019200.0-2076918743413931051412198531688038400.0 mm, 2076918743413931051412198531688038400.0-2076918743413931051412198531688038400.0 - 2076918


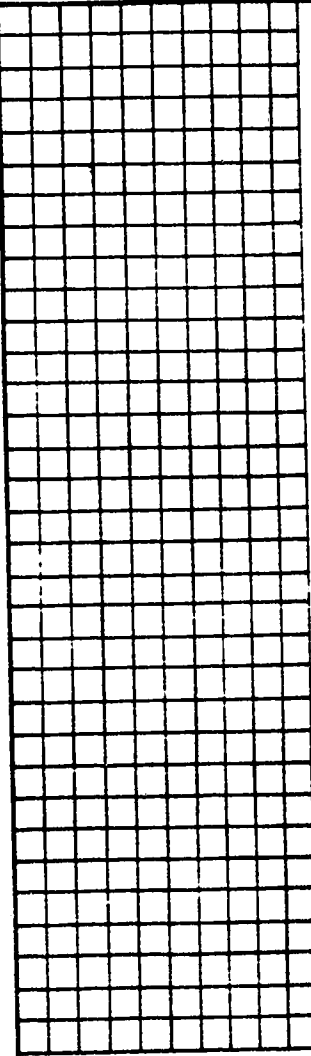




GS-106-86

Page 18 of 31

 DEVELOPMENT & OPERATIONS DIVISION GEOTECHNICAL SERVICES LABORATORY		PROJECT <u>RYCROFT SLIDE</u> SITE _____ HOLE No. <u>RS 1</u> ELEV. _____ LOCATION _____ TECHNOLOGIST <u>JS AS JB</u> DATE DRILLED <u>16 Jul 1991</u>																
BOREHOLE AND TEST LOG																		
TEST RESULTS	DEPTH (m)	SYMBOL	DESCRIPTION	OTHER INFORMATION														
<div style="display: flex; align-items: center;"> <div style="width: 100px; height: 100px; border: 1px solid black; background: repeating-linear-gradient(45deg, transparent, transparent 2px, black 2px, black 4px);"></div> <div style="margin-left: 10px;"> <p>113</p> <p>114</p> <p>115</p> <p>116</p> <p>117</p> <p>118</p> </div> </div>			<p>as above.</p>	<p>Rec = .15m/.15m</p>														
<div style="display: flex; justify-content: space-between;"> <div style="width: 30%;"> <p>0 20 40 60 80 100</p> <p>1800 1600 1400 1200 1000</p> <p>DEPTH SCALE</p> <p>0 2 4 6 ft.</p> </div> <div style="width: 65%;"> <table border="0" style="width: 100%;"> <tr> <td></td> <td></td> <td></td> <td></td> <td></td> <td></td> <td></td> </tr> <tr> <td>TOPSOIL OR NO SAMPLE</td> <td>GRAVEL</td> <td>SAND OR SANDSTONE</td> <td>CLAY OR SHALE</td> <td>SILT OR SILTSTONE</td> <td>UNDISTURBED SAMPLE</td> <td>DISTURBED SAMPLE</td> </tr> </table> <p> w - MOISTURE CONTENT (%), ρ - WET UNIT WEIGHT (kg/m^3), k - PERMEABILITY (cm/s), FA - FLIGHT AUGER, HCA - HOLLOW CORE AUGER, P OR S.P.T. - STANDARD PENETRATION TEST BLOW COUNT, PP - POCKET PENETROMETER (kPa), q_u - UNCONFINED COMPRESSION (kPa) w_p - PLASTIC LIMIT (%), w_L - LIQUID LIMIT (%), --- CORE RECOVERY (%), 12-0.075-25 - 12.5% RETAINED ON No. 40 SIEVE, 0.075-0.425 SIZE 25, 25% No. 200 SIEVE, 40 = % SILT, 25 = % CLAY, ∇ - WATER LEVEL </p> </div> </div>												TOPSOIL OR NO SAMPLE	GRAVEL	SAND OR SANDSTONE	CLAY OR SHALE	SILT OR SILTSTONE	UNDISTURBED SAMPLE	DISTURBED SAMPLE
																		
TOPSOIL OR NO SAMPLE	GRAVEL	SAND OR SANDSTONE	CLAY OR SHALE	SILT OR SILTSTONE	UNDISTURBED SAMPLE	DISTURBED SAMPLE												


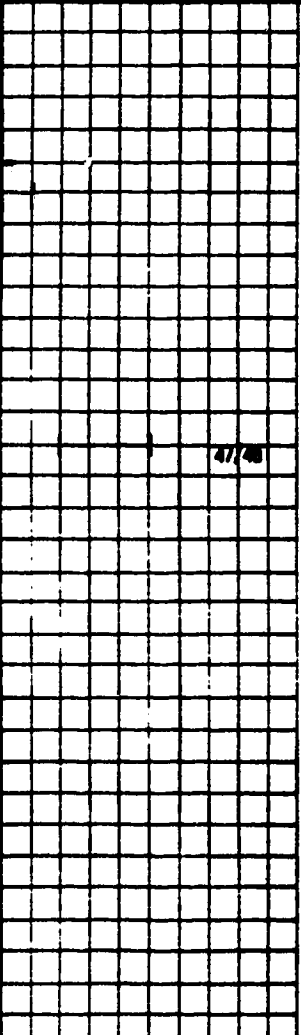


GS-104-B6


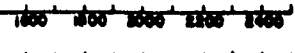

Page 18 of 31








 DEVELOPMENT & OPERATIONS DIVISION GEOTECHNICAL SERVICES LABORATORY		PROJECT <u>RYCROFT SLIDE</u>			
		SITE _____			
		HOLE No. <u>RS 1</u>		ELEV. _____	
		LOCATION _____			
		TECHNOLOGIST <u>JS AS JB</u> DATE DRILLED <u>16 Jul 1991</u>			
BOREHOLE AND TEST LOG					
TEST RESULTS	DEPTH (ft)	SYMBOL	DESCRIPTION	SAMPLE	OTHER INFORMATION
	118				
	120				
	121				
	122				
	123				
	124				
	125				
<div style="display: flex; justify-content: space-between;"> <div>   DEPTH SCALE </div> <div>  <p> TOPSOIL OR NO SAMPLE GRAVEL SAND OR SANDSTONE CLAY OR SHALE SILT OR SILTSTONE UNDISTURBED SAMPLE DISTURBED SAMPLE </p> <p> w - MOISTURE CONTENT (%), γ - WET UNIT WEIGHT (lb/ft^3), k - PERMEABILITY (cm/s), P.A. - FLIGHT AUGER, HCA - HOLLOW CORE AUGER, V OR S.P.T. - STANDARD PENETRATION TEST BLOW COUNT, RR - POCKET PENETROMETER (SPe), q_u - UNCONFINED COMPRESSION (SPe) w_p - PLASTIC LIMIT (%), w_L - LIQUID LIMIT (%), --- CORE RECOVERY (%), 12-0.075-2.0 - 15% RETAINED ON No. 40 SIEVE, 0.075-0.425 mm, 25% No. 200 SIEVE, 40 = 75% SILT, 25 = 75% CLAY, ∇ - WATER LEVEL </p> </div> </div>					

CS-G4-96

Page 20 of 31

 Abena ENVIRONMENT DEVELOPMENT & OPERATIONS DIVISION GEOTECHNICAL SERVICES LABORATORY		PROJECT <u>RYCROFT SLIDE</u> SITE _____ HOLE No. <u>RS 1</u> ELEV. _____ LOCATION _____ TECHNOLOGIST <u>JS AS JB</u> DATE DRILLED <u>16 Jul 1991</u>			
BOREHOLE AND TEST LOG					
TEST RESULTS	DEPTH (ft)	SYMBOL	DESCRIPTION	SAMPLE	OTHER INFORMATION
	126		CR-dk gry, thin ML layers.		
	127				
	128				
	129				
	130				
	131				
	132				


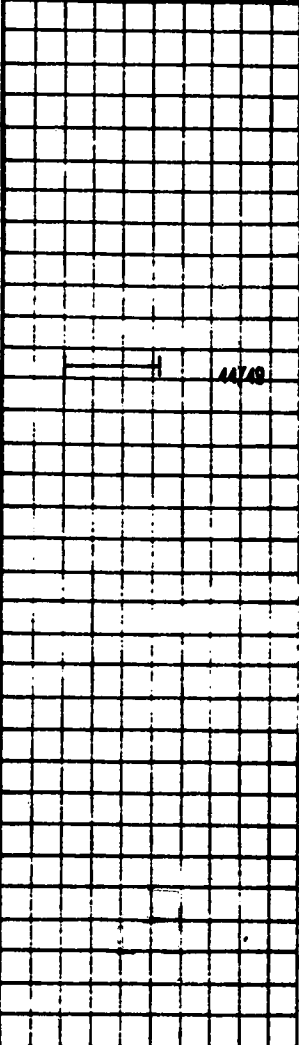







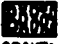





 TOPSOIL OR NO SAMPLE	 GRAVEL	 SAND OR SANDSTONE	 CLAY OR SHALE	 SILT OR SILTSTONE	 UNDISTURBED SAMPLE	 DISTURBED SAMPLE
--	--	---	---	--	--	--

w - MOISTURE CONTENT (%), G - DRY UNIT WEIGHT (lb/ft³), K - PERMEABILITY (cm/s), F.A. - FLIGHT AUGER,
 HSA - HOLLOW CORE AUGER, V OR S.P.T. - STANDARD PENETRATION TEST BLOW COUNT,
 R.R. - POCKET PENETROMETER (lbf/in²), C_u - UNCONSOLIDATED COMPRESSION (lbf/in²),
 W_p - PLASTIC LIMIT (%), L_u - LIQUID LIMIT (%), --- CORE RECOVERY (%),
 12-0.075-2.0 - 12.5% RETAINED ON No. 40 SIEVE, 0.075-0.425 mm, 25% No. 200 SIEVE,
 0.425-0.850 mm, 25% No. 100 SIEVE, 0.850-2.0 mm, 25% No. 60 SIEVE,
 2.0-4.75 mm, 25% No. 40 SIEVE, 4.75-9.5 mm, 25% No. 20 SIEVE, 9.5-19 mm, 25% No. 10 SIEVE, 19-37.5 mm, 25% No. 5 SIEVE, 37.5-75 mm, 25% No. 2 SIEVE, 75-150 mm, 25% No. 1 SIEVE, 150-300 mm, 25% No. 0.5 SIEVE, 300-600 mm, 25% No. 0.25 SIEVE, 600-1200 mm, 25% No. 0.125 SIEVE, 1200-2400 mm, 25% No. 0.0625 SIEVE, 2400-4800 mm, 25% No. 0.03125 SIEVE, 4800-9600 mm, 25% No. 0.015625 SIEVE, 9600-19200 mm, 25% No. 0.0078125 SIEVE, 19200-38400 mm, 25% No. 0.00390625 SIEVE, 38400-76800 mm, 25% No. 0.001953125 SIEVE, 76800-153600 mm, 25% No. 0.0009765625 SIEVE, 153600-307200 mm, 25% No. 0.00048828125 SIEVE, 307200-614400 mm, 25% No. 0.000244140625 SIEVE, 614400-1228800 mm, 25% No. 0.0001220703125 SIEVE, 1228800-2457600 mm, 25% No. 0.00006103515625 SIEVE, 2457600-4915200 mm, 25% No. 0.000030517578125 SIEVE, 4915200-9830400 mm, 25% No. 0.0000152587890625 SIEVE, 9830400-19660800 mm, 25% No. 0.00000762939453125 SIEVE, 19660800-39321600 mm, 25% No. 0.000003814697265625 SIEVE, 39321600-78643200 mm, 25% No. 0.0000019073486328125 SIEVE, 78643200-157286400 mm, 25% No. 0.00000095367431640625 SIEVE, 157286400-314572800 mm, 25% No. 0.000000476837158203125 SIEVE, 314572800-629145600 mm, 25% No. 0.0000002384185791015625 SIEVE, 629145600-1258291200 mm, 25% No. 0.00000011920928955078125 SIEVE, 1258291200-2516582400 mm, 25% No. 0.000000059604644775390625 SIEVE, 2516582400-5033164800 mm, 25% No. 0.0000000298023223876953125 SIEVE, 5033164800-10066329600 mm, 25% No. 0.00000001490116119384765625 SIEVE, 10066329600-20132659200 mm, 25% No. 0.000000007450580596923828125 SIEVE, 20132659200-40265318400 mm, 25% No. 0.0000000037252902984619140625 SIEVE, 40265318400-80530636800 mm, 25% No. 0.00000000186264514923095703125 SIEVE, 80530636800-161061273600 mm, 25% No. 0.000000000931322574615478515625 SIEVE, 161061273600-322122547200 mm, 25% No. 0.0000000004656612873077392578125 SIEVE, 322122547200-644245094400 mm, 25% No. 0.00000000023283064365386962890625 SIEVE, 644245094400-1288490188800 mm, 25% No. 0.000000000116415321826934814453125 SIEVE, 1288490188800-2576980377600 mm, 25% No. 0.0000000000582076609134674072265625 SIEVE, 2576980377600-5153960755200 mm, 25% No. 0.00000000002910383045673370361328125 SIEVE, 5153960755200-10307921510400 mm, 25% No. 0.000000000014551915228366851806640625 SIEVE, 10307921510400-20615843020800 mm, 25% No. 0.0000000000072759576141834259033203125 SIEVE, 20615843020800-41231686041600 mm, 25% No. 0.00000000000363797880709171295166015625 SIEVE, 41231686041600-82463372083200 mm, 25% No. 0.000000000001818989403545856475830078125 SIEVE, 82463372083200-164926744166400 mm, 25% No. 0.0000000000009094947017729282379150390625 SIEVE, 164926744166400-329853488332800 mm, 25% No. 0.00000000000045474735088646411895751953125 SIEVE, 329853488332800-659706976665600 mm, 25% No. 0.000000000000227373675443232059478759765625 SIEVE, 659706976665600-1319413953331200 mm, 25% No. 0.0000000000001136868377216160297393798828125 SIEVE, 1319413953331200-2638827906662400 mm, 25% No. 0.00000000000005684341886080801486968994140625 SIEVE, 2638827906662400-5277655813324800 mm, 25% No. 0.000000000000028421709430404007434844970703125 SIEVE, 5277655813324800-10555311626649600 mm, 25% No. 0.0000000000000142108547152020037174224853515625 SIEVE, 10555311626649600-21110623253299200 mm, 25% No. 0.00000000000000710542735760100185871124267578125 SIEVE, 21110623253299200-42221246506598400 mm, 25% No. 0.000000000000003552713678800500929355621337890625 SIEVE, 42221246506598400-84442493013196800 mm, 25% No. 0.0000000000000017763568394002504646778106689453125 SIEVE, 84442493013196800-168884986026393600 mm, 25% No. 0.00000000000000088817841970012523233890533447265625 SIEVE, 168884986026393600-337769972052787200 mm, 25% No. 0.000000000000000444089209850062616169452667236328125 SIEVE, 337769972052787200-675539944105574400 mm, 25% No. 0.0000000000000002220446049250313080847263336181640625 SIEVE, 675539944105574400-1351079888211148800 mm, 25% No. 0.0000000000000001110223024625156540423631668090625 SIEVE, 1351079888211148800-2702159776422297600 mm, 25% No. 0.00000000000000005551115123125782702118158340453125 SIEVE, 2702159776422297600-5404319552844595200 mm, 25% No. 0.000000000000000027755575615628913510590791702265625 SIEVE, 5404319552844595200-10808639105689190400 mm, 25% No. 0.0000000000000000138777878078144567552953958511328125 SIEVE, 10808639105689190400-21617278211378380800 mm, 25% No. 0.00000000000000000693889390390722837764769792556640625 SIEVE, 21617278211378380800-43234556422756761600 mm, 25% No. 0.000000000000000003469446951953614188823848962783203125 SIEVE, 43234556422756761600-86469112845513523200 mm, 25% No. 0.0000000000000000017347234759768070944119244813916015625 SIEVE, 86469112845513523200-172938225691027046400 mm, 25% No. 0.00000000000000000086736173798840354720559622406953078125 SIEVE, 172938225691027046400-345876451382054092800 mm, 25% No. 0.000000000000000000433680868994201773602798112034765390625 SIEVE, 345876451382054092800-691752902764108185600 mm, 25% No. 0.0000000000000000002168404344971008868013990560173826953125 SIEVE, 691752902764108185600-1383505805528216371200 mm, 25% No. 0.00000000000000000010842021724855044340069952800869134765625 SIEVE, 1383505805528216371200-2767011611056432742400 mm, 25% No. 0.000000000000000000054210108624275221700349764004345673828125 SIEVE, 2767011611056432742400-5534023222112865484800 mm, 25% No. 0.0000000000000000000271050543121376108501748820021728369140625 SIEVE, 5534023222112865484800-11068046444225730969600 mm, 25% No. 0.00000000000000000001355252715606880542508744100108641845703125 SIEVE, 11068046444225730969600-22136092888451461939200 mm, 25% No. 0.000000000000000000006776263578034402712543720500543209228515625 SIEVE, 22136092888451461939200-44272185776902923878400 mm, 25% No. 0.0000000000000000000033881317890172013562718602500271604642890625 SIEVE, 44272185776902923878400-88544371553805847756800 mm, 25% No. 0.00000000000000000000169406589450860067813593012501358023214453125 SIEVE, 88544371553805847756800-177088743107611695513600 mm, 25% No. 0.000000000000000000000847032947254350033906796506250679011607265625 SIEVE, 177088743107611695513600-354177486215223391027200 mm, 25% No. 0.0000000000000000000004235164736271750169533982531253395055811328125 SIEVE, 354177486215223391027200-708354972430446782054400 mm, 25% No. 0.00000000000000000000021175823681358750847669912656266975279056640625 SIEVE, 708354972430446782054400-1416709944860893564108800 mm, 25% No. 0.00000000000000000000010587911840679375423834956328133487639533203125 SIEVE, 1416709944860893564108800-2833419889721787128217600 mm, 25% No. 0.000000000000000000000052939559203396877119174778140667438197666015625 SIEVE, 2833419889721787128217600-5666839779443574256435200 mm, 25% No. 0.0000000000000000000000264697796016984385595873890703337190988330078125 SIEVE, 5666839779443574256435200-11333679558887148512870400 mm, 25% No. 0.00000000000000000000001323488980084921927797936953516668594941650390625 SIEVE, 11333679558887148512870400-22667359117774297025740800 mm, 25% No. 0.000000000000000000000006617444900424609638989684767583342974708251953125 SIEVE, 22667359117774297025740800-45334718235548594051481600 mm, 25% No. 0.0000000000000000000000033087224502123048194948423837916714738541259765625 SIEVE, 45334718235548594051481600-90669436471097188102963200 mm, 25% No. 0.00000000000000000000000165436122510615240974742119189583573692706298828125 SIEVE, 90669436471097188102963200-181338872942194376205926400 mm, 25% No. 0.000000000000000000000000827180612553076204873710595947917868463531494140625 SIEVE, 181338872942194376205926400-362677745884388752411852800 mm, 25% No. 0.0000000000000000000000004135903062765381024368552979739589342317657470703125 SIEVE, 362677745884388752411852800-725355491768777504823705600 mm, 25% No. 0.00000000000000000000000020679515313826905121842764898697946711588287353515625 SIEVE, 725355491768777504823705600-1450710983537555009647411200 mm, 25% No. 0.000000000000000000000000103397576569134525609213824493489733557941436767578125 SIEVE, 1450710983537555009647411200-2901421967075110019294822400 mm, 25% No. 0.0000000000000000000000000516987882845672628046069122467448667789707183837890625 SIEVE, 2901421967075110019294822400-5802843934150220038589644800 mm, 25% No. 0.00000000000000000000000002584939414228363140230345612337243338948535919169453125 SIEVE, 5802843934150220038589644800-11605687868300440077179289600 mm, 25% No. 0.000000000000000000000000012924697071141815701151728061686216694742679595847265625 SIEVE, 11605687868300440077179289600-23211375736600880154358579200 mm, 25% No. 0.0000000000000000000000000064623485355709078505758640308431084737213397979236328125 SIEVE, 23211375736600880154358579200-46422751473201760308717158400 mm, 25% No. 0.00000000000000000000000000323117426778545392528793201542155423686166989896181640625 SIEVE, 46422751473201760308717158400-92845502946403520617434316800 mm, 25% No. 0.00000000000000000000000000161558713389272696264396600771077711843083494948090625 SIEVE, 92845502946403520617434316800-185691005892807041234868633600 mm, 25% No. 0.000000000000000000000000000807793566946363481321983003855388589215421974742453125 SIEVE, 185691005892807041234868633600-371382011785614082469737267200 mm, 25% No. 0.000000000000000000000000000403896783473181740660991501927719259609373737265625 SIEVE, 371382011785614082469737267200-742764023571228164939474534400 mm, 25% No. 0.000000000000000000000000000201948391736590870330495750963859398046886868686328125 SIEVE, 742764023571228164939474534400-1485528047142456329878949068800 mm, 25% No. 0.0000000000000000000000000001009741958682954351652478754819296990234434343431640625 SIEVE, 1485528047142456329878949068800-2971056094284912659757898137600 mm, 25% No. 0.00000000000000000000000000005048709793414771758262393774096484951172171717168203125 SIEVE, 2971056094284912659757898137600-5942112188569825319515796275200 mm, 25% No. 0.000000000000000000000000000025243548967073858791311968870482424755860858585841015625 SIEVE, 5942112188569825319515796275200-11884224377139650639031592550400 mm, 25% No. 0.0000000000000000000000000000126217744835369293956559844352412237779304292929205078125 SIEVE, 11884224377139650639031592550400-23768448754279301278063185100800 mm, 25% No. 0.00000000000000000000000000000631088724176846469782799222176061188896521464646025390625 SIEVE, 23768448754279301278063185100800-47536897508558602556126370201600 mm, 25% No. 0.000000000000000000000000000003155443620884232348913996110880305944482607323230126953125 SIEVE, 47536897508558602556126370201600-95073795017117205112252740403200 mm, 25% No. 0.0000000000000000000000000000015777218104421161744569980554401529722413036615150634765625 SIEVE, 95073795017117205112252740403200-190147590034234410224505480806400 mm, 25% No. 0.00000000000000000000000000000078886090522105808722784940272007648612065183075753173828125 SIEVE, 190147590034234410224505480806400-380295180068468820449010961612800 mm, 25% No. 0.000000000000000000000000000000394430452610529043613924701360038243060325915378765869140625 SIEVE, 380295180068468820449010961612800-760590360136937640898021923225600 mm, 25% No. 0.0000000000000000000000000000001972152263052645218069623506800191215301629576893829345703125 SIEVE, 760590360136937640898021923225600-1521180720273875281796043846451200 mm, 25% No. 0.00000000000000000000000000000009860761315263226090348117534000956076508147884469146728515625 SIEVE, 1521180720273875281796043846451200-3042361440547750563592087692902400 mm, 25% No. 0.000000000000

GS-1-1-84

Page 21 of 31


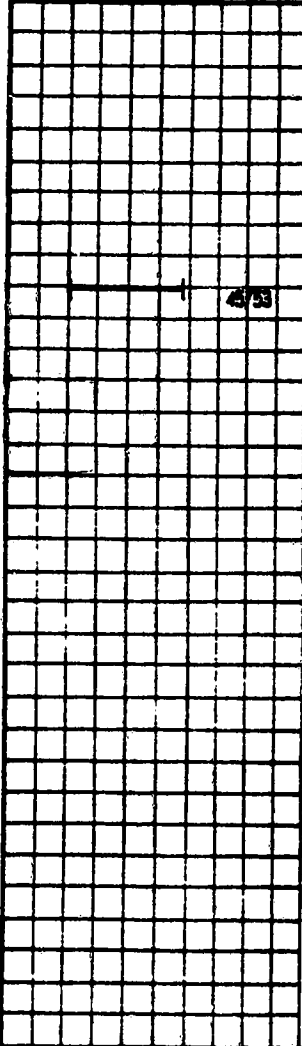
 DEVELOPMENT & OPERATIONS DIVISION GEOTECHNICAL SERVICES LABORATORY		PROJECT <u>RYCROFT SLIDE</u> SITE _____ HOLE No. <u>RS 1</u> ELEV. _____ LOCATION _____ TECHNOLOGIST <u>JS AS JB</u> DATE DRILLED <u>16 Jul 1991</u>			
		BOREHOLE AND TEST LOG			
TEST RESULTS	DEPTH (m)	SYMBOL	DESCRIPTION	SAMPLE	OTHER INFORMATION
	133		as above.		
	134				
	135				
	136				
	137				
	138		CR-dk gry, interbedded sand & ML layers.		

0 20 40 60 80 100 1200 1400 1600 1800 2000 2200 2400 DEPTH SCALE 1 2 3 4 5 6 7 8 9 10 ft	 TOPSOIL OR NO SAMPLE  GRAVEL  SAND OR SANDSTONE  CLAY OR SHALE  SILT OR SILTSTONE  UNDISTURBED SAMPLE  DISTURBED SAMPLE
--	---

w - MOISTURE CONTENT (%), ρ - WET UNIT WEIGHT (kg/m^3), k - PERMEABILITY (cm/s), RA - FLIGHT AUGER
 NCA - HOLLOW CORE AUGER, γ OR S.P.T. - STANDARD PENETRATION TEST BLOW COUNT,
 R.R. - POCKET PENETROMETER (SPe), q_u - UNCONFINED COMPRESSION (SPe)
 w_p - PLASTIC LIMIT (%), w_L - LIQUID LIMIT (%), --- CORE RECOVERY (%),
 12-0.075-25 - 12 = % RETAINED ON No. 4 SIEVE, 0.075-0.425 mm, 25 = % No. 200 SIEVE,
 12 = % SILT, 25 = % CLAY, ∇ - WATER LEVEL

GS-G4-BE

Page 22 of 31

 DEVELOPMENT & OPERATIONS DIVISION GEOTECHNICAL SERVICES LABORATORY		PROJECT <u>RYCROFT SLIDE</u> SITE _____ HOLE No. <u>RS 1</u> ELEV. _____ LOCATION _____ TECHNOLOGIST <u>JS AS JB</u> DATE DRILLED <u>16 Jul 1991</u>			
BOREHOLE AND TEST LOG					
TEST RESULTS	DEPTH (E)	SYMBOL	DESCRIPTION	SAMPLE	OTHER INFORMATION
	.39	[Symbol]	as above.	[Symbol]	
	140	[Symbol]			
	141	[Symbol]			
	142	[Symbol]			
	143	[Symbol]			
	144	[Symbol]			
	145	[Symbol]			
	146	[Symbol]			
	147	[Symbol]			
	148	[Symbol]			

0 20 40 60 80 100

1000 1500 2000 2500 3000

DEPTH SCALE


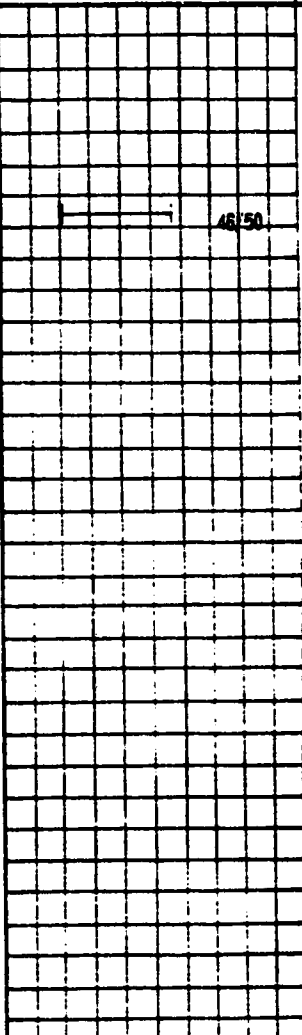


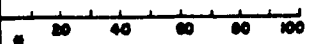

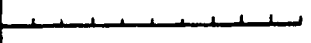





















1 2 3 4 5 ft

[Symbol]	[Symbol]	[Symbol]	[Symbol]	[Symbol]	[Symbol]	[Symbol]
TOPSOIL OR NO SAMPLE	GRAVEL	SAND OR SANDSTONE	CLAY OR SHALE	SILT OR SILTSTONE	UNDISTURBED SAMPLE	DISTURBED SAMPLE

w - MOISTURE CONTENT (%), u - WET UNIT WEIGHT (lb/ft³), k - PERMEABILITY (cm/s), RA - FLIGHT AUGER
 HCA - HOLLOW CORE AUGER, v ON S.P.T. - STANDARD PENETRATION TEST BLOW COUNT,
 RP - POCKET PENETROMETER (lbf), q_u - UNCONFINED COMPRESSION (lbf)
 w_p - PLASTIC LIMIT (%), L_u - LIQUID LIMIT (%), --- CORE RECOVERY (%),
 12-0.075-20 - 12% RETAINED ON No. 40 SIEVE, 0.075-0.25 - 20% No. 200 SIEVE,
 20-0.25-425 - 42% No. 40 SIEVE, 42-0.25-425 - 42% No. 200 SIEVE,
 42-0.25-425 - 42% No. 40 SIEVE, 42-0.25-425 - 42% No. 200 SIEVE,
 42-0.25-425 - 42% No. 40 SIEVE, 42-0.25-425 - 42% No. 200 SIEVE,


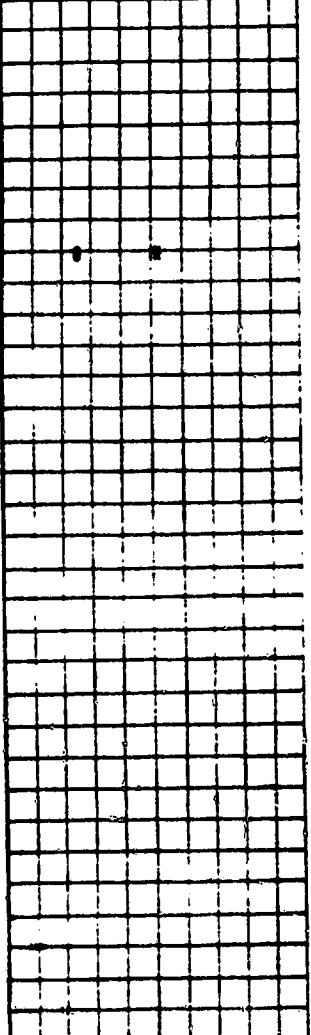


GS-C4-Bc

Page 23 of 31

 DEVELOPMENT & OPERATIONS DIVISION GEOTECHNICAL SERVICES LABORATORY		PROJECT <u>RYCROFT SLIDE</u>																	
		SITE _____																	
		HOLE No. <u>RS 1</u>		ELEV. _____															
		LOCATION _____																	
		TECHNOLOGIST <u>JS AS JB</u>		DATE DRILLED <u>16 Jul 1991</u>															
BOREHOLE AND TEST LOG																			
TEST RESULTS	DEPTH (m)	SYMBOL	DESCRIPTION	SAMPLE	OTHER INFORMATION														
	146		as above.																
	147																		
	148																		
	149																		
	150																		
	151																		
					Slower noisier drilling from 150.9m.														
   DEPTH SCALE		<table border="0"> <tr> <td></td> <td></td> <td></td> <td></td> <td></td> <td></td> <td></td> </tr> <tr> <td>TOPSOIL OR NO SAMPLE</td> <td>GRAVEL</td> <td>SAND OR SANDSTONE</td> <td>CLAY OR SHALE</td> <td>SILT OR SILTSTONE</td> <td>UNDISTURBED SAMPLE</td> <td>DISTURBED SAMPLE</td> </tr> </table> <p> w - MOISTURE CONTENT (%), γ - WET UNIT WEIGHT (kg/m^3), k - PERMEABILITY (cm/s), RA - FLIGHT AUGER, NCA - HOLLOW CORE AUGER, V OR S.P.T. - STANDARD PENETRATION TEST BLOW COUNT, RP - POCKET PENETROMETER (kPa), q_u - UNCONFINED COMPRESSION (kPa) w_p - PLASTIC LIMIT (%), w_L - LIQUID LIMIT (%), --- CORE RECOVERY (%), $12-0.075-20$ - 12% RETAINED ON No. 4 SIEVE, 0.075 \times 20 SIZE NO. 20 SIEVE, $20 = \frac{\% \text{ SALT}}{\% \text{ CLAY}}$ ∇ - WATER LEVEL </p>											TOPSOIL OR NO SAMPLE	GRAVEL	SAND OR SANDSTONE	CLAY OR SHALE	SILT OR SILTSTONE	UNDISTURBED SAMPLE	DISTURBED SAMPLE
																			
TOPSOIL OR NO SAMPLE	GRAVEL	SAND OR SANDSTONE	CLAY OR SHALE	SILT OR SILTSTONE	UNDISTURBED SAMPLE	DISTURBED SAMPLE													


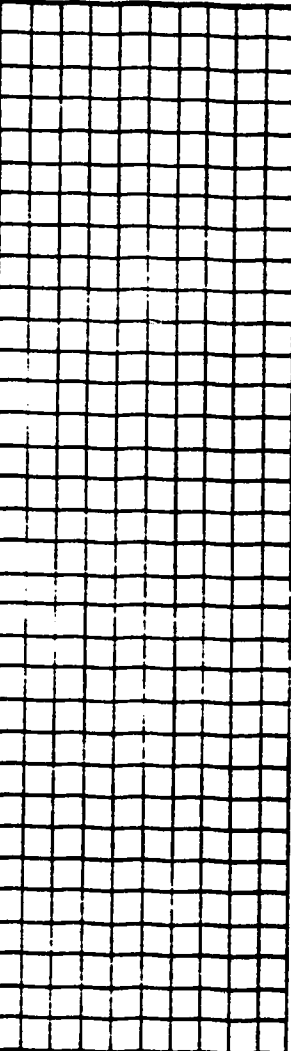

25-04-96

Page 24 of 31

 DEVELOPMENT & OPERATIONS DIVISION GEOTECHNICAL SERVICES LABORATORY		PROJECT <u>RYCROFT SLIDE</u>			
		SITE _____			
HOLE No. <u>RS 1</u> ELEV. _____		LOCATION _____			
TECHNOLOGIST <u>JS AS JB</u> DATE DRILLED <u>16 Jul 1991</u>					
BOREHOLE AND TEST LOG					
TEST RESULTS	DEPTH (m)	SYMBOL	DESCRIPTION	SAMPLE	OTHER INFORMATION
	152		Interbedded clay, silt & sand layers, (interpreted from geophysical logs).		
	153				
	154				
	155				
	156				
	157		Interbedded silt & clay, occ thin sand seams, (interpreted from geophysical logs).		
	158				
	159				
	160				
	161				
	162				
	163				
	164				
	165				
	166				
	167				
	168				
	169				
	170				
	171				
	172				
	173				
	174				
	175				
	176				
	177				
	178				
	179				
	180				
	181				
	182				
	183				
	184				
	185				
	186				
	187				
	188				
	189				
	190				
	191				
	192				
	193				
	194				
	195				
	196				
	197				
	198				
	199				
	200				
	201				
	202				
	203				
	204				
	205				
	206				
	207				
	208				
	209				
	210				
	211				
	212				
	213				
	214				
	215				
	216				
	217				
	218				
	219				
	220				
	221				
	222				
	223				
	224				
	225				
	226				
	227				
	228				
	229				
	230				
	231				
	232				
	233				
	234				
	235				
	236				
	237				
	238				
	239				
	240				
	241				
	242				
	243				
	244				
	245				
	246				
	247				
	248				
	249				
	250				
	251				
	252				
	253				
	254				
	255				
	256				
	257				
	258				
	259				
	260				
	261				
	262				
	263				
	264				
	265				
	266				
	267				
	268				
	269				
	270				
	271				
	272				
	273				
	274				
	275				
	276				
	277				
	278				
	279				
	280				
	281				
	282				
	283				
	284				
	285				
	286				
	287				
	288				
	289				
	290				
	291				
	292				
	293				
	294				
	295				
	296				
	297				
	298				
	299				
	300				

GS-C4-86

Page 25 of 31








 DEVELOPMENT & OPERATIONS DIVISION GEOTECHNICAL SERVICES LABORATORY		PROJECT <u>RYCROFT SLIDE</u>			
		SITE _____			
HOLE No. <u>RS 1</u> ELEV. _____		LOCATION _____			
TECHNOLOGIST <u>JS AS JB</u> DATE DRILLED <u>16 Jul 1991</u>					
BOREHOLE AND TEST LOG					
TEST RESULTS	DEPTH (m)	SYMBOL	DESCRIPTION	SAMPLE	OTHER INFORMATION
	158		as above.		
	159				
	160				
	161				
	162				
	163				
	164				
	165				
	166				
	167				

0 20 40 60 80 100

1000 1500 2000 2500 3000

DEPTH SCALE


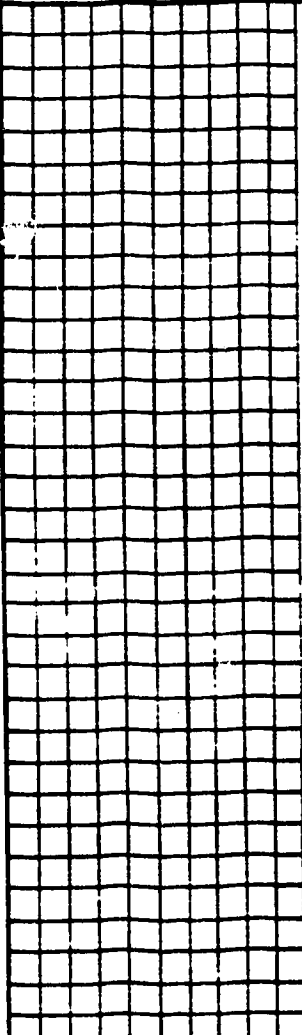

0 1 2 3 4 5 6 ft.








						
TOPSOIL OR NO SAMPLE	GRAVEL	SAND OR SANDSTONE	CLAY OR SHALE	SILT OR SILTSTONE	UNDISTURBED SAMPLE	DISTURBED SAMPLE

w - MOISTURE CONTENT (%), γ - WET UNIT WEIGHT (kg/m^3), k - PERMEABILITY (cm/s), RA - FLIGHT AUGER,
 HCA - HOLLOW CORE AUGER, γ OR S.P.T. - STANDARD PENETRATION TEST BLOW COUNT,
 R.R. - POCKET PENETROMETER (SPe), q_u - UNCONFINED COMPRESSION (SPe)
 W_p - PLASTIC LIMIT (%), w_L - LIQUID LIMIT (%), --- CORE RECOVERY (%),
 10-200-25 = 10-20% RETAINED ON No. 10 sieve, 200-25 = 20-25% No. 200 sieve,
 25 = % SILT, 25 = % CLAY, ∇ - WATER LEVEL

CS-G4-96

Page 26 of 31


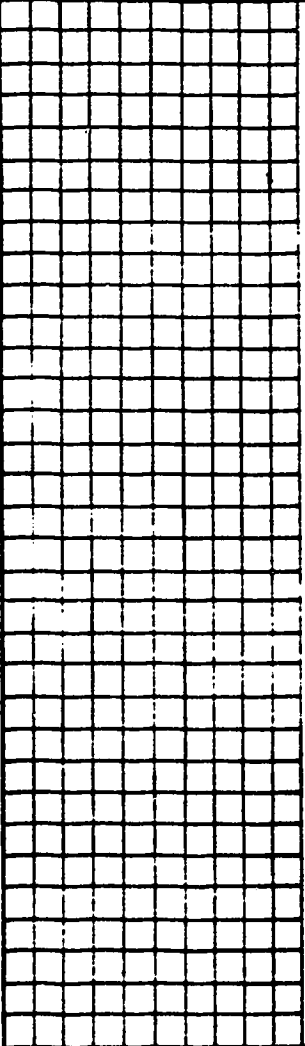



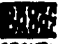





 DEVELOPMENT & OPERATIONS DIVISION GEOTECHNICAL SERVICES LABORATORY		PROJECT <u>RYCROFT SLIDE</u> SITE _____ HOLE No. <u>RS 1</u> ELEV. _____ LOCATION _____ TECHNOLOGIST <u>JS AS JB</u> DATE DRILLED <u>16 Jul 1991</u>			
		BOREHOLE AND TEST LOG			
TEST RESULTS	DEPTH (m)	SYMBOL	DESCRIPTION	SAMPLE	OTHER INFORMATION
	166		as above.		
	167				
	168				
	169				
	170				
	171		GRAVEL		

 TOPSOIL OR NO SAMPLE  GRAVEL  SAND OR SANDSTONE  CLAY OR SHALE  SILT OR SILTSTONE  UNDEVELOPED SAMPLE  DISTURBED SAMPLE	G - MOISTURE CONTENT (%), S - WET UNIT WEIGHT (kg/m^3), K - PERMEABILITY (cm/s), P.A. - FLIGHT AUGER, HCA - HOLLOW CORE AUGER, V OR S.P.T. - STANDARD PENETRATION TEST BLows/30cm, RR - POCKET PENETROMETER (MPa), C _u - UNCONFINED COMPRESSION (kPa) W _p - PLASTIC LIMIT (%), W _L - LIQUID LIMIT (%), --- CORE RECOVERY (%), 15-200-25 = 15% RETAINED ON No. 4 SIEVE, 600-200 SIZE 20, 25% ON 200 SIEVE, 25 = 25% SILT, ∇ - WATER LEVEL
--	--

DEPTH SCALE: 0 to 100 m


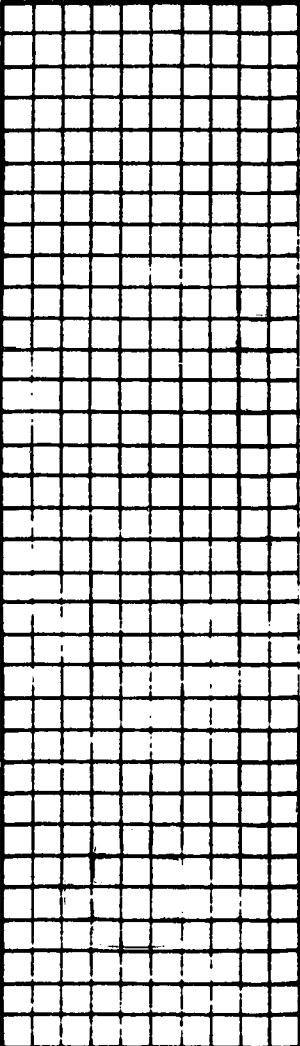







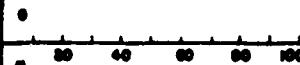

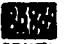






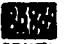






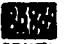





GS-104-BE

Page 27 of 31

 DEVELOPMENT & OPERATIONS DIVISION GEOTECHNICAL SERVICES LABORATORY		PROJECT <u>RYCROFT SLIDE</u> SITE _____ HOLE No. <u>RS 1</u> ELEV. _____ LOCATION _____ TECHNOLOGIST <u>JS AS JB</u> DATE DRILLED <u>16 Jul 1991</u>			
		BOREHOLE AND TEST LOG			
TEST RESULTS	DEPTH (m)	SYMBOL	DESCRIPTION	SAMPLE	OTHER INFORMATION
	172		as above.		
	173				
	174				
	175				
	176				
	177				
	178				
<p style="text-align: right;">Rough drilling @ 176.83m.</p>					
<div style="display: flex; justify-content: space-between;"> <div> <p>0 20 40 60 80 100</p> <p>1000 1500 2000 2500 3000</p> <p>DEPTH SCALE</p> <p>0 2 4 6 ft</p> </div> <div> <div style="display: flex; justify-content: space-around;"> <div> TOPSOIL OR NO SAMPLE</div> <div> GRAVEL</div> <div> SAND OR SANDSTONE</div> <div> CLAY OR SHALE</div> <div> SILT OR SILTSTONE</div> <div> UNDISTURBED SAMPLE</div> <div> DISTURBED SAMPLE</div> </div> <p> w - MOISTURE CONTENT (%), d - DRY UNIT WEIGHT (kg/m³), k - PERMEABILITY (cm/s), RA - FLIGHT AUGER HCA - HOLLOW CORE AUGER, V OR S.P.T. - STANDARD PENETRATION TEST BLOW COUNT, PP - POCKET PENETROMETER (MPa), Qu - UNCONFINED COMPRESSION (MPa) W_p - PLASTIC LIMIT (%), L - LIQUID LIMIT (%), --- - CORE RECOVERY (%), 12-0.075-25 - 12% RETAINED ON No. 4 SIEVE, 0.075-0.425 - No. 40-100 SIEVE, 0.425-2.0 - No. 10-40 SIEVE, 2.0 - 75mm - No. 10 SIEVE, 75-150mm - No. 10 SIEVE, 150-300mm - No. 10 SIEVE, 300-600mm - No. 10 SIEVE, 600-1200mm - No. 10 SIEVE, 1200-2400mm - No. 10 SIEVE, 2400-4800mm - No. 10 SIEVE, 4800-9600mm - No. 10 SIEVE, 9600-19200mm - No. 10 SIEVE, 19200-38400mm - No. 10 SIEVE, 38400-76800mm - No. 10 SIEVE, 76800-153600mm - No. 10 SIEVE, 153600-307200mm - No. 10 SIEVE, 307200-614400mm - No. 10 SIEVE, 614400-1228800mm - No. 10 SIEVE, 1228800-2457600mm - No. 10 SIEVE, 2457600-4915200mm - No. 10 SIEVE, 4915200-9830400mm - No. 10 SIEVE, 9830400-19660800mm - No. 10 SIEVE, 19660800-39321600mm - No. 10 SIEVE, 39321600-78643200mm - No. 10 SIEVE, 78643200-157286400mm - No. 10 SIEVE, 157286400-314572800mm - No. 10 SIEVE, 314572800-629145600mm - No. 10 SIEVE, 629145600-1258291200mm - No. 10 SIEVE, 1258291200-2516582400mm - No. 10 SIEVE, 2516582400-5033164800mm - No. 10 SIEVE, 5033164800-10066329600mm - No. 10 SIEVE, 10066329600-20132659200mm - No. 10 SIEVE, 20132659200-40265318400mm - No. 10 SIEVE, 40265318400-80530636800mm - No. 10 SIEVE, 80530636800-161061273600mm - No. 10 SIEVE, 161061273600-322122547200mm - No. 10 SIEVE, 322122547200-644245094400mm - No. 10 SIEVE, 644245094400-1288490188800mm - No. 10 SIEVE, 1288490188800-2576980377600mm - No. 10 SIEVE, 2576980377600-5153960755200mm - No. 10 SIEVE, 5153960755200-10307921510400mm - No. 10 SIEVE, 10307921510400-20615843020800mm - No. 10 SIEVE, 20615843020800-41231686041600mm - No. 10 SIEVE, 41231686041600-82463372083200mm - No. 10 SIEVE, 82463372083200-164926744166400mm - No. 10 SIEVE, 164926744166400-329853488332800mm - No. 10 SIEVE, 329853488332800-659706976665600mm - No. 10 SIEVE, 659706976665600-1319413953331200mm - No. 10 SIEVE, 1319413953331200-2638827906662400mm - No. 10 SIEVE, 2638827906662400-5277655813324800mm - No. 10 SIEVE, 5277655813324800-10555311626649600mm - No. 10 SIEVE, 10555311626649600-21110623253299200mm - No. 10 SIEVE, 21110623253299200-42221246506598400mm - No. 10 SIEVE, 42221246506598400-84442493013196800mm - No. 10 SIEVE, 84442493013196800-168884986026393600mm - No. 10 SIEVE, 168884986026393600-337769972052787200mm - No. 10 SIEVE, 337769972052787200-675539944105574400mm - No. 10 SIEVE, 675539944105574400-1351079888211148800mm - No. 10 SIEVE, 1351079888211148800-2702159776422297600mm - No. 10 SIEVE, 2702159776422297600-5404319552844595200mm - No. 10 SIEVE, 5404319552844595200-10808639105689190400mm - No. 10 SIEVE, 10808639105689190400-21617278211378380800mm - No. 10 SIEVE, 21617278211378380800-43234556422756761600mm - No. 10 SIEVE, 43234556422756761600-86469112845513523200mm - No. 10 SIEVE, 86469112845513523200-172938225691027046400mm - No. 10 SIEVE, 172938225691027046400-345876451382054092800mm - No. 10 SIEVE, 345876451382054092800-691752902764108185600mm - No. 10 SIEVE, 691752902764108185600-1383505805528216371200mm - No. 10 SIEVE, 1383505805528216371200-2767011611056432742400mm - No. 10 SIEVE, 2767011611056432742400-5534023222112865484800mm - No. 10 SIEVE, 5534023222112865484800-11068046444225730969600mm - No. 10 SIEVE, 11068046444225730969600-22136092888451461939200mm - No. 10 SIEVE, 22136092888451461939200-44272185776902923878400mm - No. 10 SIEVE, 44272185776902923878400-88544371553805847756800mm - No. 10 SIEVE, 88544371553805847756800-177088743107611695513600mm - No. 10 SIEVE, 177088743107611695513600-354177486215223391027200mm - No. 10 SIEVE, 354177486215223391027200-708354972430446782054400mm - No. 10 SIEVE, 708354972430446782054400-1416709944860893564108800mm - No. 10 SIEVE, 1416709944860893564108800-2833419889721787128217600mm - No. 10 SIEVE, 2833419889721787128217600-5666839779443574256435200mm - No. 10 SIEVE, 5666839779443574256435200-11333679558887148512870400mm - No. 10 SIEVE, 11333679558887148512870400-22667359117774297025740800mm - No. 10 SIEVE, 22667359117774297025740800-45334718235548594051481600mm - No. 10 SIEVE, 45334718235548594051481600-90669436471097188102963200mm - No. 10 SIEVE, 90669436471097188102963200-181338872942194376205926400mm - No. 10 SIEVE, 181338872942194376205926400-362677745884388752411852800mm - No. 10 SIEVE, 362677745884388752411852800-725355491768777504823705600mm - No. 10 SIEVE, 725355491768777504823705600-1450710983537555009647411200mm - No. 10 SIEVE, 1450710983537555009647411200-2901421967075110019294822400mm - No. 10 SIEVE, 2901421967075110019294822400-5802843934150220038589644800mm - No. 10 SIEVE, 5802843934150220038589644800-11605687868300440077179289600mm - No. 10 SIEVE, 11605687868300440077179289600-23211375736600880154358579200mm - No. 10 SIEVE, 23211375736600880154358579200-46422751473201760308717158400mm - No. 10 SIEVE, 46422751473201760308717158400-92845502946403520617434316800mm - No. 10 SIEVE, 92845502946403520617434316800-185691005892807041234868633600mm - No. 10 SIEVE, 185691005892807041234868633600-371382011785614082469737267200mm - No. 10 SIEVE, 371382011785614082469737267200-742764023571228164939474534400mm - No. 10 SIEVE, 742764023571228164939474534400-1485528047142456329878949068800mm - No. 10 SIEVE, 1485528047142456329878949068800-2971056094284912659757898137600mm - No. 10 SIEVE, 2971056094284912659757898137600-5942112188569825319515796275200mm - No. 10 SIEVE, 5942112188569825319515796275200-11884224377139650639031592550400mm - No. 10 SIEVE, 11884224377139650639031592550400-23768448754279301278063185100800mm - No. 10 SIEVE, 23768448754279301278063185100800-47536897508558602556126370201600mm - No. 10 SIEVE, 47536897508558602556126370201600-95073795017117205112252740403200mm - No. 10 SIEVE, 95073795017117205112252740403200-190147590034234410224505480806400mm - No. 10 SIEVE, 190147590034234410224505480806400-380295180068468820449010961612800mm - No. 10 SIEVE, 380295180068468820449010961612800-760590360136937640898021923225600mm - No. 10 SIEVE, 760590360136937640898021923225600-1521180720273875281796043846451200mm - No. 10 SIEVE, 1521180720273875281796043846451200-3042361440547750563592087692902400mm - No. 10 SIEVE, 3042361440547750563592087692902400-6084722881095501127184175385804800mm - No. 10 SIEVE, 6084722881095501127184175385804800-12169445762191002254368350771609600mm - No. 10 SIEVE, 12169445762191002254368350771609600-24338891524382004508736701543219200mm - No. 10 SIEVE, 24338891524382004508736701543219200-48677783048764009017473403086438400mm - No. 10 SIEVE, 48677783048764009017473403086438400-97355566097528018034946806172876800mm - No. 10 SIEVE, 97355566097528018034946806172876800-194711132195056036069893612345753600mm - No. 10 SIEVE, 194711132195056036069893612345753600-389422264390112072139787224691507200mm - No. 10 SIEVE, 389422264390112072139787224691507200-778844528780224144279574449383014400mm - No. 10 SIEVE, 778844528780224144279574449383014400-1557689057560448288559148898766028800mm - No. 10 SIEVE, 1557689057560448288559148898766028800-3115378115120896577118297797532057600mm - No. 10 SIEVE, 3115378115120896577118297797532057600-6230756230241793154236595595064115200mm - No. 10 SIEVE, 6230756230241793154236595595064115200-12461512460483586308473191190128230400mm - No. 10 SIEVE, 12461512460483586308473191190128230400-24923024920967172616946382380256460800mm - No. 10 SIEVE, 24923024920967172616946382380256460800-49846049841934345233892764760512921600mm - No. 10 SIEVE, 49846049841934345233892764760512921600-99692099683868690467785529521025843200mm - No. 10 SIEVE, 99692099683868690467785529521025843200-199384199367737380935571059042051686400mm - No. 10 SIEVE, 199384199367737380935571059042051686400-398768398735474761871142118084103372800mm - No. 10 SIEVE, 398768398735474761871142118084103372800-797536797470949523742284236168206745600mm - No. 10 SIEVE, 797536797470949523742284236168206745600-1595073594941899047484568472336413491200mm - No. 10 SIEVE, 1595073594941899047484568472336413491200-3190147189883798094969136944672826982400mm - No. 10 SIEVE, 3190147189883798094969136944672826982400-6380294379767596189938273889345653964800mm - No. 10 SIEVE, 6380294379767596189938273889345653964800-12760588759535192379876547778691307929600mm - No. 10 SIEVE, 12760588759535192379876547778691307929600-25521177519070384759753095557382615859200mm - No. 10 SIEVE, 25521177519070384759753095557382615859200-51042355038140769519506191114765231718400mm - No. 10 SIEVE, 51042355038140769519506191114765231718400-102084710076281539039012382229530463436800mm - No. 10 SIEVE, 102084710076281539039012382229530463436800-204169420152563078078024764459060926873600mm - No. 10 SIEVE, 204169420152563078078024764459060926873600-408338840305126156156049528918121853747200mm - No. 10 SIEVE, 408338840305126156156049528918121853747200-816677680610252312312099057836243707494400mm - No. 10 SIEVE, 816677680610252312312099057836243707494400-1633355361220504624624198115672487414988800mm - No. 10 SIEVE, 1633355361220504624624198115672487414988800-3266710722441009249248396231344974829977600mm - No. 10 SIEVE, 3266710722441009249248396231344974829977600-6533421444882018498496792462689949659955200mm - No. 10 SIEVE, 6533421444882018498496792462689949659955200-13066842889764036996993584925379899319910400mm - No. 10 SIEVE, 13066842889764036996993584925379899319910400-26133685779528073993987169850759798639820800mm - No. 10 SIEVE, 26133685779528073993987169850759798639820800-52267371559056147987974339701519597279641600mm - No. 10 SIEVE, 52267371559056147987974339701519597279641600-104534743118112295975948679403039194559283200mm - No. 10 SIEVE, 104534743118112295975948679403039194559283200-209069486236224591951897358806078389118566400mm - No. 10 SIEVE, 209069486236224591951897358806078389118566400-418138972472449183903794717612156778237132800mm - No. 10 SIEVE, 418138972472449183903794717612156778237132800-836277944944898367807589435224313556474265600mm - No. 10 SIEVE, 836277944944898367807589435224313556474265600-1672555889889796735615178870448627112948531200mm - No. 10 SIEVE, 1672555889889796735615178870448627112948531200-3345111779779593471230357740897254225897062400mm - No. 10 SIEVE, 3345111779779593471230357740897254225897062400-6690223559559186942460715481794508451794124800mm - No. 10 SIEVE, 6690223559559186942460715481794508451794124800-13380447119118373884921430963589016903588249600mm - No. 10 SIEVE, 13380447119118373884921430963589016903588249600-26760894238236747769842861927178033807176499200mm - No. 10 SIEVE, 26760894238236747769842861927178033807176499200-53521788476473495539685723854356067614352998400mm - No. 10 SIEVE, 53521788476473495539685723854356067614352998400-107043576952946991079371447708712135228705996800mm - No. 10 SIEVE, 107043576952946991079371447708712135228705996800-214087153905893982158742895417424270457411993600mm - No. 10 SIEVE, 214087153905893982158742895417424270457411993600-428174307811787964317485790834848540914823987200mm - No. 10 SIEVE, 428174307811787964317485790834848540914823987200-856348615623575928634971581669697081829647974400mm - No. 10 SIEVE, 856348615623575928634971581669697081829647974400-1712697231247151857269943163339394163659295948800mm - No. 10 SIEVE, 1712697231247151857269943163339394163659295948800-3425394462494303714539886326678788327318591897600mm - No. 10 SIEVE, 3425394462494303714539886326678788327318591897600-6850788924988607429079772653357576654637183795200mm - No. 10 SIEVE, 6850788924988607429079772653357576654637183795200-13701577849977214858159545306715153309274367590400mm - No. 10 SIEVE, 13701577849977214858159545306715153309274367590400-27403155699954429716319090613430306618548735180800mm - No. 10 SIEVE, 27403155699954429716319090613430306618548735180800-54806311399908859432638181226860613237097470361600mm - No. 10 SIEVE, 54806311399908859432638181226860613237097470361600-1096126227998177188652763624537212264741944072230400mm - No. 10 SIEVE, 1096126227998177188652763624537212264741944072230400-2192252455996354377305527249074424529483888144460800mm - No. 10 SIEVE, 2192252455996354377305527249074424529483888144460800-4384504911992708754611054498148849059767776288921600mm - No. 10 SIEVE, 4384504911992708754611054498148849059767776288921600-8769009823985417509222108996297690119535552577843200mm - No. 10 SIEVE, 8769009823985417509222108996297690119535552577843200-1753801964797</p></div></div>					

CS-C4-96

Page 28 of 31

 DEVELOPMENT & OPERATIONS DIVISION GEOTECHNICAL SERVICES LABORATORY		PROJECT <u>RYCROFT SLIDE</u>																	
		SITE _____																	
		HOLE No. <u>RS 1</u>		ELEV. _____															
		LOCATION _____																	
		TECHNOLOGIST <u>JS AS JB</u>		DATE DRILLED <u>16 Jul 1991</u>															
BOREHOLE AND TEST LOG																			
TEST RESULTS	DEPTH (m)	SYMBOL	DESCRIPTION	SAMPLE	OTHER INFORMATION														
			as above.																
	178																		
	180																		
	181																		
	182																		
	183																		
	184		GRAVEL-with sand & rocks, as above. BEDROCK-CS & MS of Smokey group, (from field observations).		Smoother easier drilling from 184.1m.														
 DEPTH SCALE		<table border="0"> <tr> <td></td> <td></td> <td></td> <td></td> <td></td> <td></td> <td></td> </tr> <tr> <td>TOPSOIL OR NO SAMPLE</td> <td>GRAVEL</td> <td>SAND OR SANDSTONE</td> <td>CLAY OR SHALE</td> <td>SILT OR SILTSTONE</td> <td>UNDISTURBED SAMPLE</td> <td>DISTURBED SAMPLE</td> </tr> </table> <p> w - MOISTURE CONTENT (%), γ - WET UNIT WEIGHT (kg/m^3), k - PERMEABILITY (cm/s), RA - FLIGHT AUGER MEA - HOLLOW CORE AUGER, N OR S.P.T. - STANDARD PENETRATION TEST BLOW COUNT, RP - POCKET PENETROMETER (kPa), q_u - UNCONFINED COMPRESSION (kPa) w_p - PLASTIC LIMIT (%), w_L - LIQUID LIMIT (%), ----- CORE RECOVERY (%), $15-0.075-25$ - 15% RETAINED ON No. 4 SIEVE, 0.075-0.425 SIEVE NO. 25 - % No. 200 SIEVE, $25 = \frac{\% \text{SILT}}{\% \text{CLAY}}$, ∇ - WATER LEVEL </p>											TOPSOIL OR NO SAMPLE	GRAVEL	SAND OR SANDSTONE	CLAY OR SHALE	SILT OR SILTSTONE	UNDISTURBED SAMPLE	DISTURBED SAMPLE
																			
TOPSOIL OR NO SAMPLE	GRAVEL	SAND OR SANDSTONE	CLAY OR SHALE	SILT OR SILTSTONE	UNDISTURBED SAMPLE	DISTURBED SAMPLE													

GS-04-86

Page 29 of 31

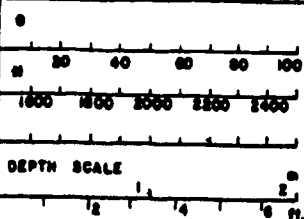


DEVELOPMENT & OPERATIONS DIVISION
GEOTECHNICAL SERVICES LABORATORY

PROJECT RYCROFT SLIDE
SITE _____
HOLE No. RS 1 ELEV. _____
LOCATION _____
TECHNOLOGIST JS AS JB DATE DRILLED 16 Jul 1991


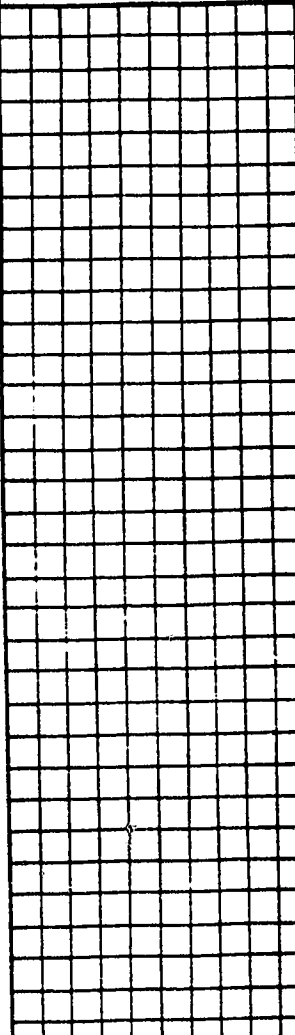

BOREHOLE AND TEST LOG

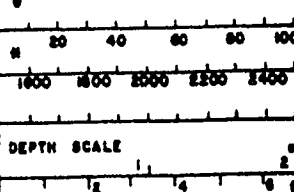
TEST RESULTS	DEPTH (m)	SYMBOL	DESCRIPTION	SAMPLE	OTHER INFORMATION
	185		as above.		
	186				
	187				
	188				
	189				
	190				
	191				










w - MOISTURE CONTENT (%), γ - WET UNIT WEIGHT (kg/m^3), k - PERMEABILITY (cm/s), L - FLIGHT AUGER
 HCA - HOLLOW CORE AUGER, γ OR S.P.T. - STANDARD PENETRATION TEST BLOW COUNT,
 R.P. - POCKET PENETROMETER (kPa), q_c - UNSATURATED COMPRESSION (kPa)
 w_p - PLASTIC LIMIT (%), w_L - LIQUID LIMIT (%), --- CORE RECOVERY (%),
 15-0.05-22 - 15% RETAINED ON No. 4 SIEVE, 0.05-0.075 SIZE MM, 22% No. 200 SIEVE,
 22 = % SILT, 22 = % CLAY, ∇ - WATER LEVEL

GS-104-86

 DEVELOPMENT & OPERATIONS DIVISION GEOTECHNICAL SERVICES LABORATORY		PROJECT <u>RYCROFT SLIDE</u> SITE _____ HOLE No. <u>RS 1</u> ELEV. _____ LOCATION _____ TECHNOLOGIST <u>JS AS JB</u> DATE DRILLED <u>16 Jul 1991</u>			
		BOREHOLE AND TEST LOG			
TEST RESULTS	DEPTH (m)	SYMBOL	DESCRIPTION	SAMPLE	OTHER INFORMATION
	192		as above.		
	193				
	194				
	195				
	196				
	197				
	198				



0 20 40 60 80 100
1000 1500 2000 2500 3000
DEPTH SCALE

						
TOPSOIL OR NO SAMPLE	GRAVEL	SAND OR SANDSTONE	CLAY OR SHALE	SILT OR SILTSTONE	UNDISTURBED SAMPLE	DISTURBED SAMPLE

w - MOISTURE CONTENT (%), γ - WET UNIT WEIGHT (kg/m^3), k - PERMEABILITY (cm/s), P.A. - PLANNET AUGER,
 MCA - MOLLOW CORE AUGER, v OR S.P.T. - STANDARD PENETRATION TEST BLOW COUNT,
 R.P. - POCKET PENETROMETER (SPa), q_u - UNCONFINED COMPRESSION (SPa)
 w_p - PLASTIC LIMIT (%), w_L - LIQUID LIMIT (%), --- CORE RECOVERY (%),
 12-0.05-22 - 12% RETAINED ON No. 40 SIEVE, 0.05 = 0.075 mm, 22 = % No. 200 SIEVE,
 40 = % SILT, 22 = % CLAY, ∇ - WATER LEVEL

GS-104-86



DEVELOPMENT & OPERATIONS DIVISION
GEOTECHNICAL SERVICES LABORATORY

PROJECT RYCROFT SLIDESITE HOLE No. RS 1 ELEV. LOCATION TECHNOLOGIST JS AS JB DATE DRILLED 16 Jul 1991

BOREHOLE AND TEST LOG

TEST RESULTS	DEPTH (m)	SYMBOL	DESCRIPTION	SAMPLE	OTHER INFORMATION
	199		END OF HOLE		
	200				
	201				
	202				
	203				
	204				

0 20 40 60 80 100
1600 1800 2000 2200 2400

DEPTH SCALE

0 2 4 6 8

TOPSOIL OR NO SAMPLE

GRAVEL

SAND OR SANDSTONE

CLAY OR SHALE


SILT OR SILTSTONE

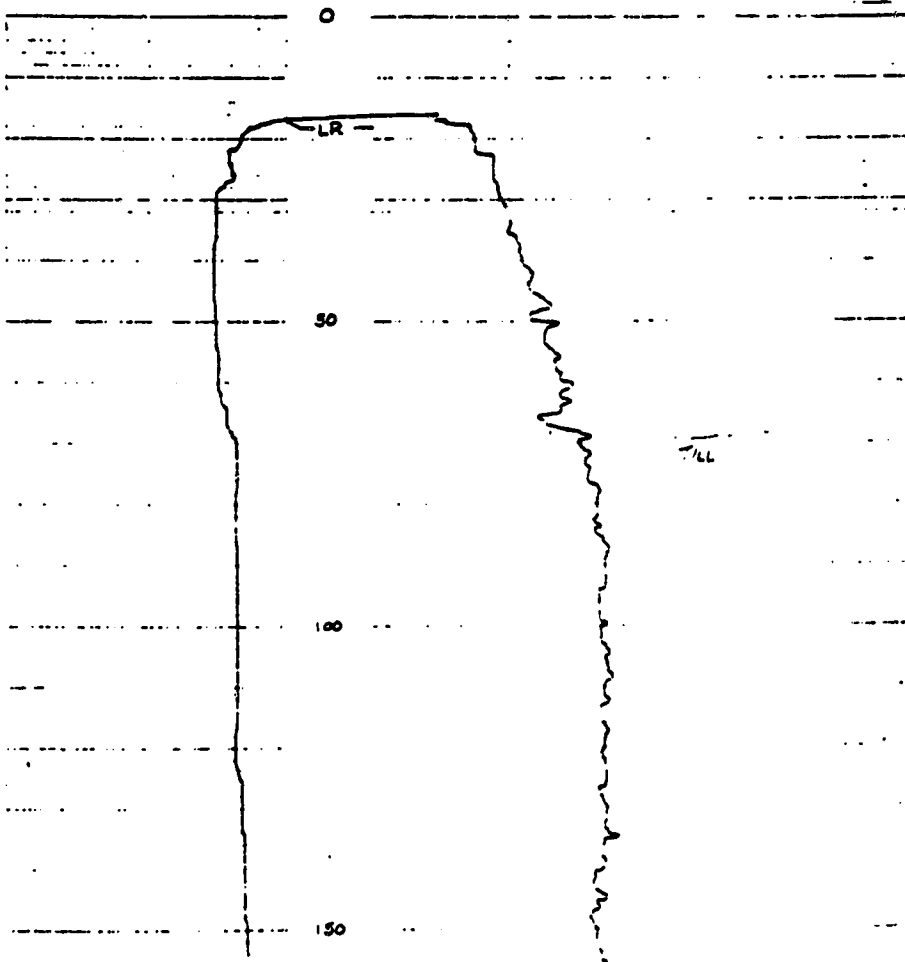
UNDISTURBED SAMPLE

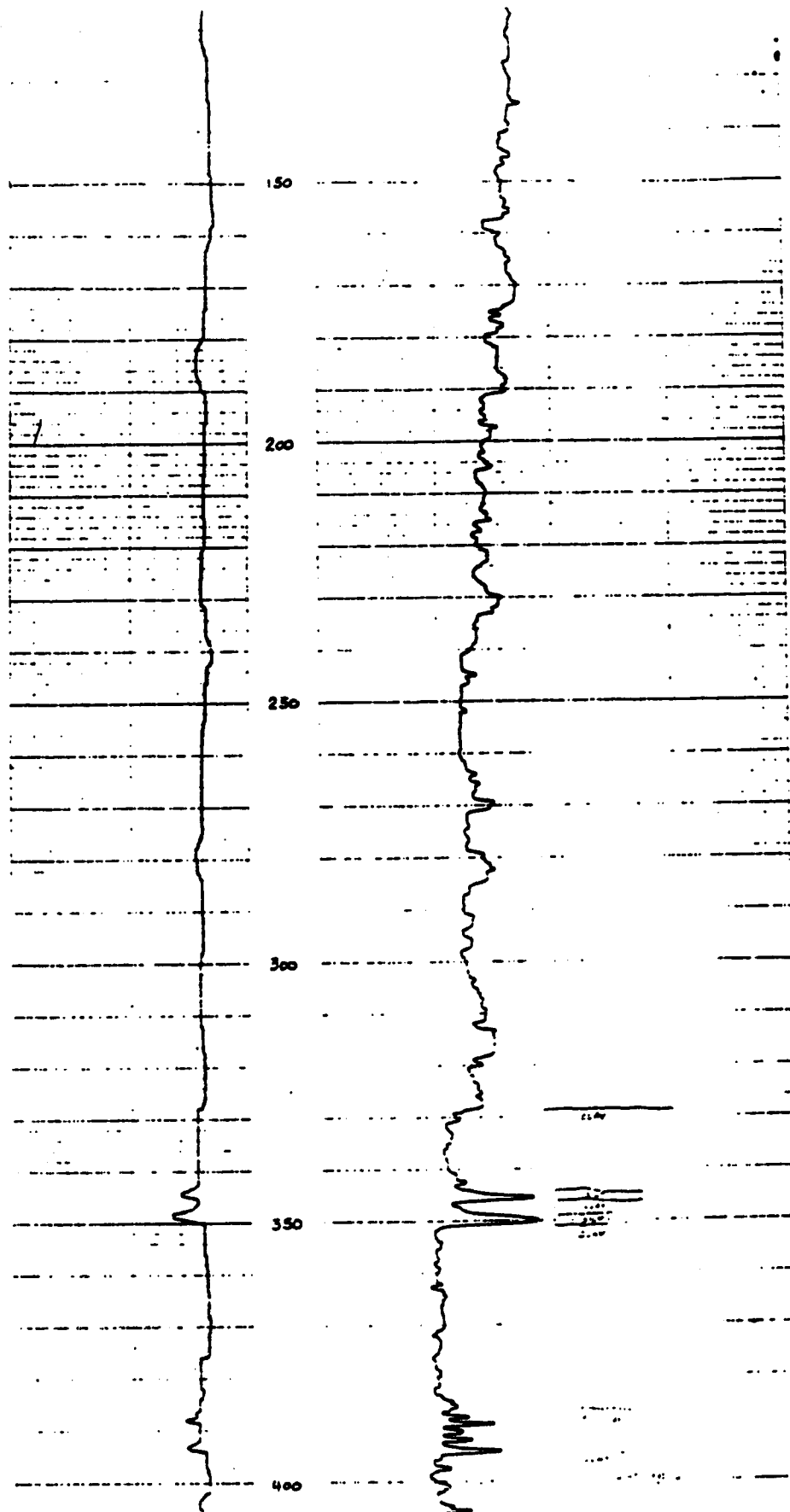
DISTURBED SAMPLE

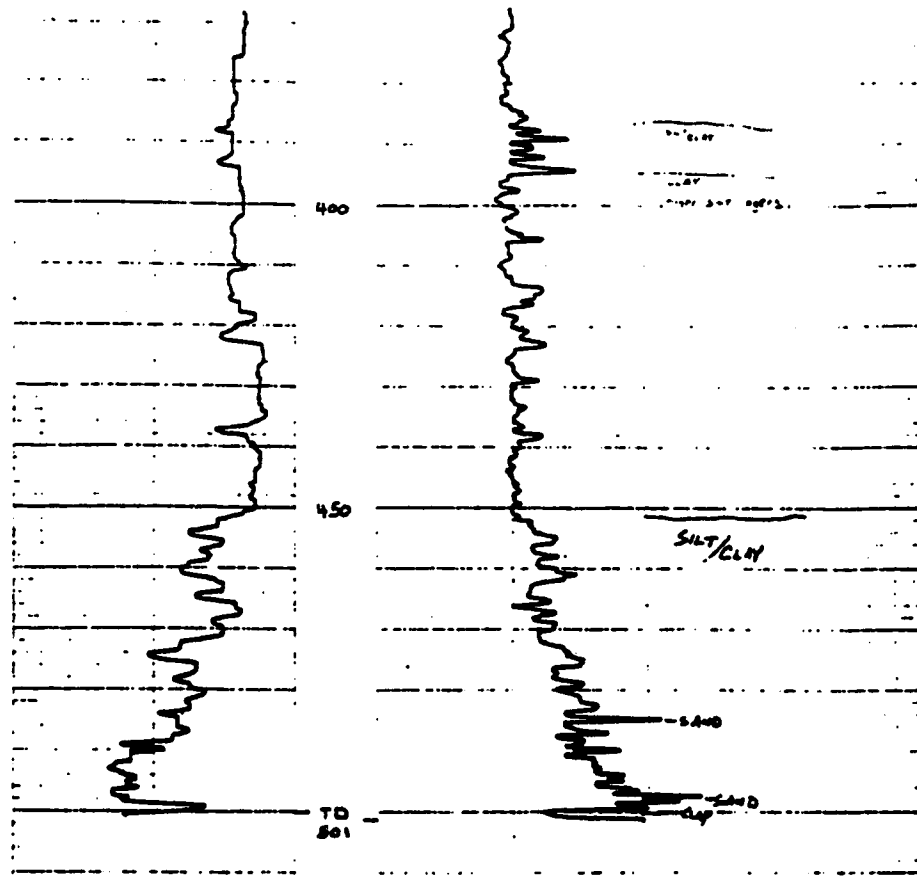
w - MOISTURE CONTENT (%), G - WET UNIT WEIGHT (kg/m^3), K - PERMEABILITY (cm/s), P.A. - FLIGHT AUGER,
 HCA - HOLLOW CORE AUGER, V OR S.P.T. - STANDARD PENETRATION TEST BLOW COUNT,
 P.P. - POCKET PENETROMETER (SPa), Cu - UNCONFINED COMPRESSION (SPa)
 Wp - PLASTIC LIMIT (%), L - LIQUID LIMIT (%), --- CORE RECOVERY (%),
 12-0.075-2.0 - 12% RETAINED ON No. 40 SIEVE, 0.075-0.425 SIZE No. 200 SIEVE,
 40 = % SILT, 20 = % CLAY, V - WATER LEVEL


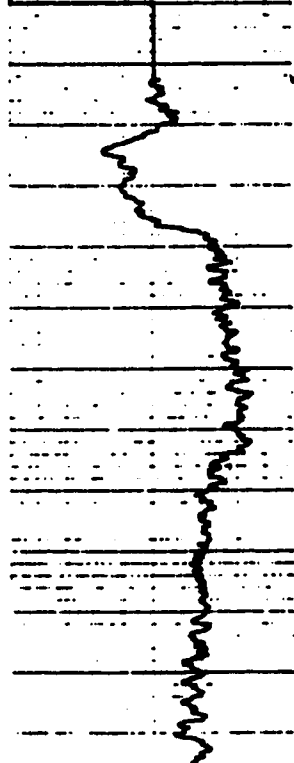
APPENDIX B: Geophysical log testhole RS-1

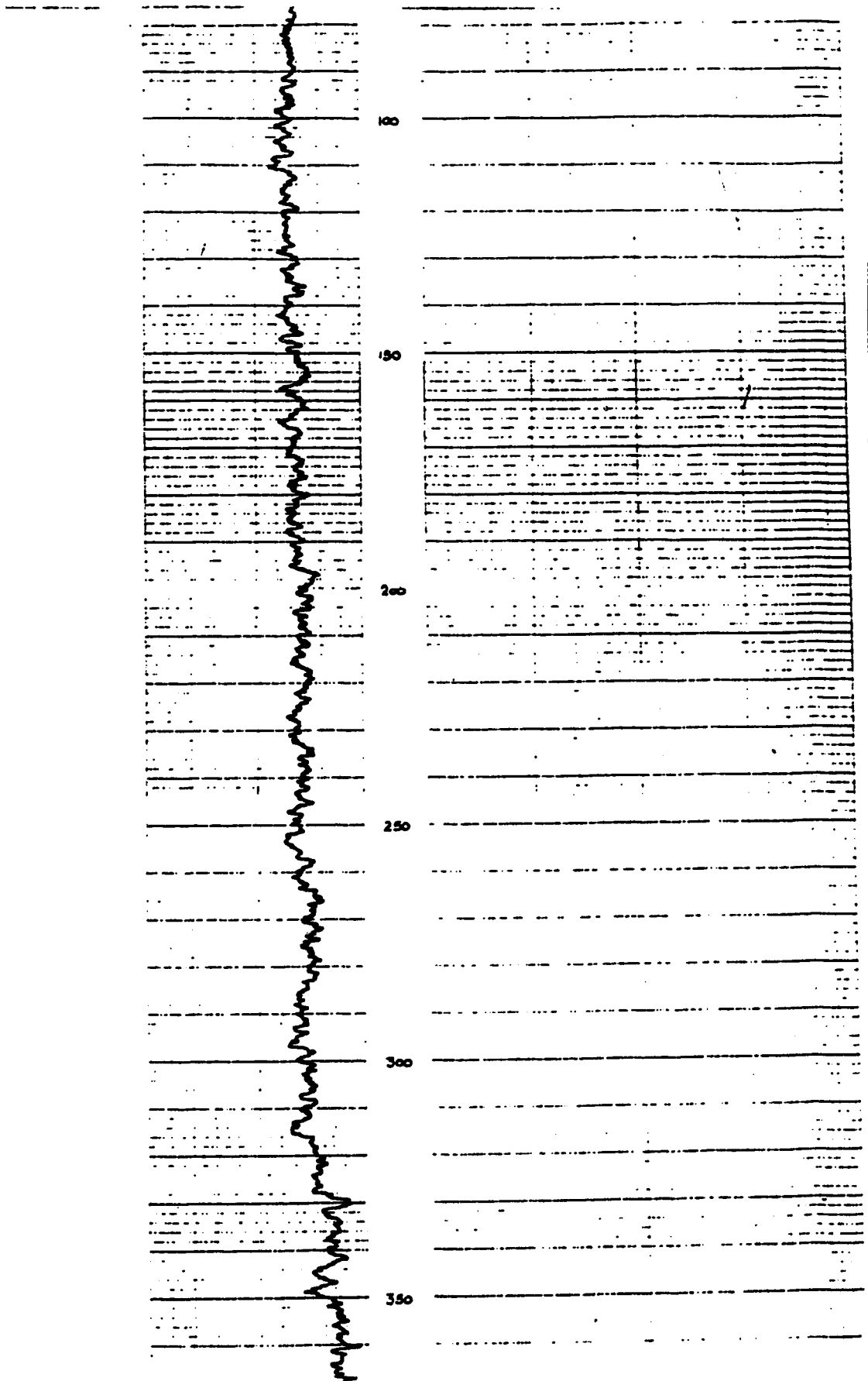
GEOPHYSICAL LOG		 ENVIRONMENT EARTH SCIENCES DIVISION 3900-116th Street S.E.		PROJECT: RYCKROFT SLIDE DATE: RYCKROFT, ALBERTA TEST HOLE NO. 2637E LOCATION: SE 1/4-30-78-3W6	
LOGGING SPEED: 60 fpm SPONTANEOUS POTENTIAL 2 MV/50		RESISTANCE 8000/50		PROJECT: RYCKROFT SLIDE DATE: 2637E LOCATION: SE 1/4-30-78-3W6 83M 1667 FT. QUICK GEL DON HOEP TIM HERRAN	

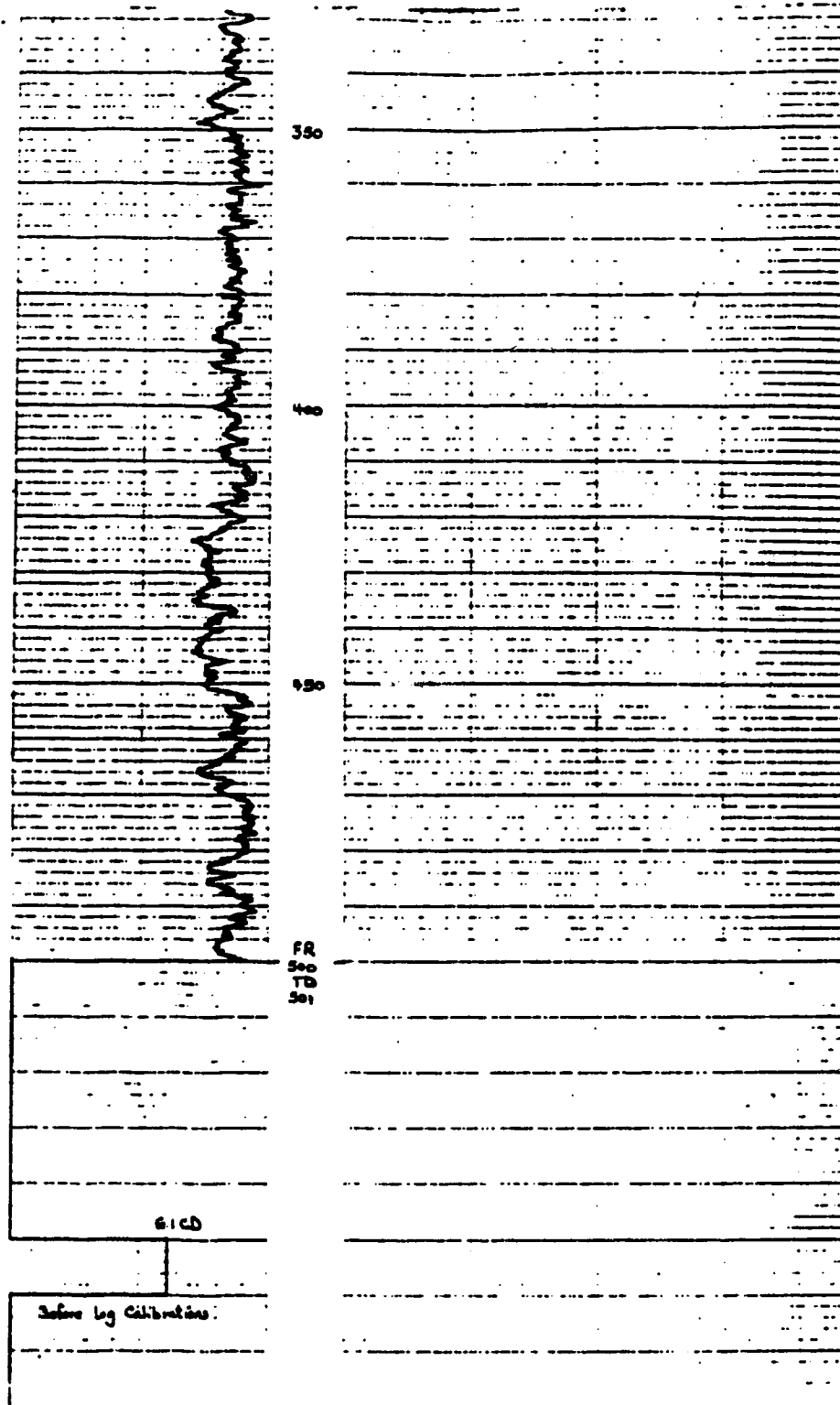




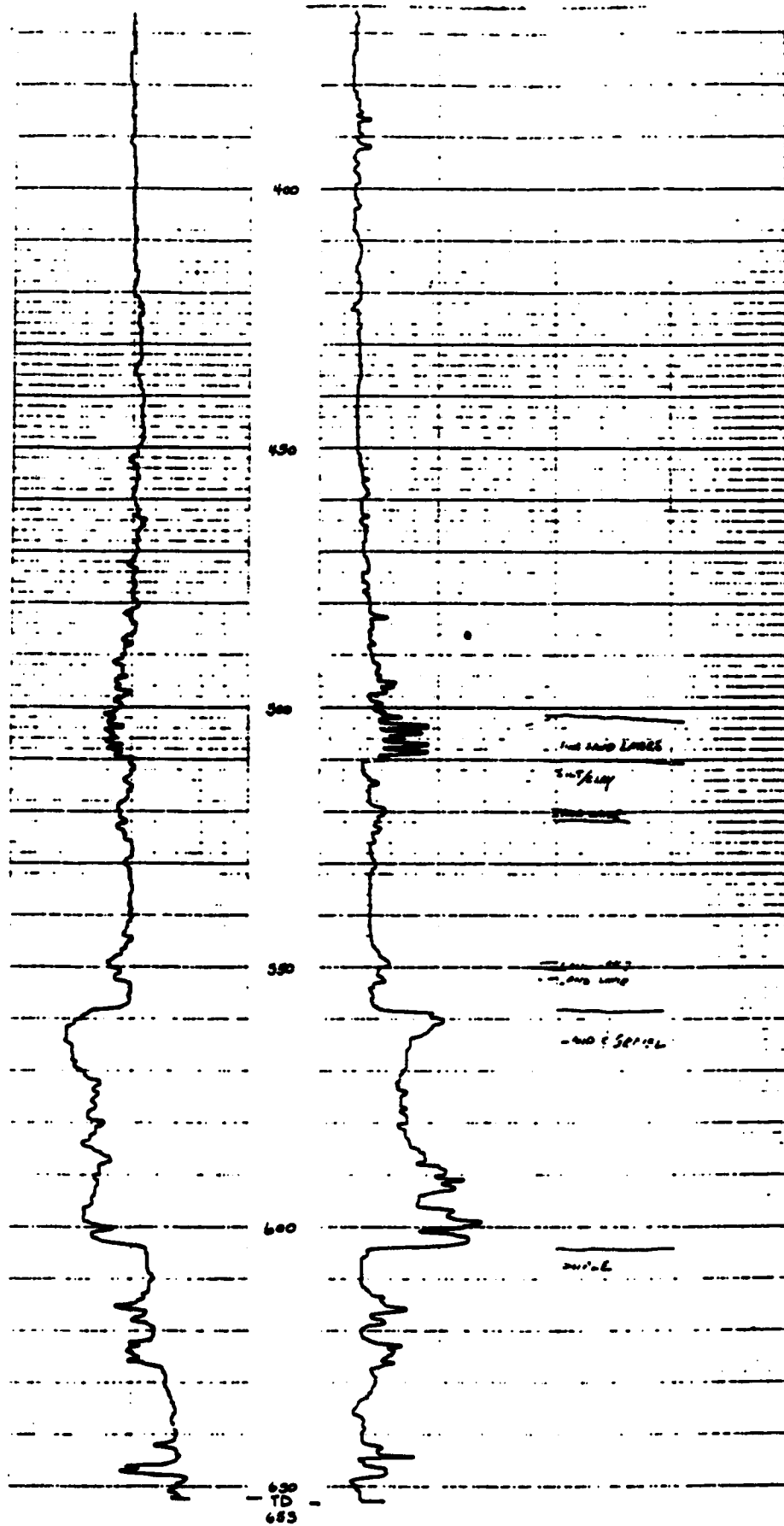


GEOPHYSICAL LOG		 Alberta ENVIRONMENT EARTH SCIENCES DIVISION GROUNDWATER BRANCH		POINT OF CONTACT "SUBMITTER'S" REPORT NO. SPECIAL REPORT NO. DATE "SUBMITTER'S" REPORT NO. DATE "SUBMITTER'S" REPORT NO. DATE		PROJECT: RYKROFT SLIDE WELL: 8637E LOCATION: 50°N-30°W-30°E	
RYKROFT SLIDE RYKROFT, ALBERTA TEST HOLE NO. 2637E 50°N-30°W-30°E				85 M 1967 FT.			
DATE	TIME	LOGGERS	LOG NO.	WELL NO.	WELL DEPTH	WELL TYPE	WELL STATUS
July 19, 1991							
1st Reading	500 FT.						
2nd Reading	3 FT.						
3rd Reading	447 FT.						
4th Reading	500 FT.						
5th Reading	504 IN.						
6th Reading	7 FT.						
7th Reading	1875 to Surface						
8th Reading	875 IN.						
9th Reading	OPEN HOLE						
LOGGING SPEED: 18 fpm TC: 3				LOGGED BY: Bob MAPP CHECKED BY: Tom KERRAN			
GAMMA RAY 19APR/90							
APPEL Log CR1.100.000							
5160							
							






[illegible]



GEOPHYSICAL LOG

PROJECT: RYCKROFT SLIDE
 AREA: RYCKROFT, ALBERTA
 WELL: TEST HOLE NO. 2637E
 LOCATION: 58 1/4 - 30 - 70 - 30W6



Alberta
 ENVIRONMENT
 EARTH SCIENCES DIVISION
 GROUNDWATER BRANCH

WELL DEPTH: 1887 FT.
 DATE: 1991

DATE	TIME	LOGGERS	WELL NO.	WELL DEPTH	WELL TYPE	WELL STATUS
July 12, 1991	10:00	Tom Kegan	2637E	1887 FT.	Test Hole	Active
July 21, 1991	10:00	Tom Kegan	2637E	1887 FT.	Test Hole	Active

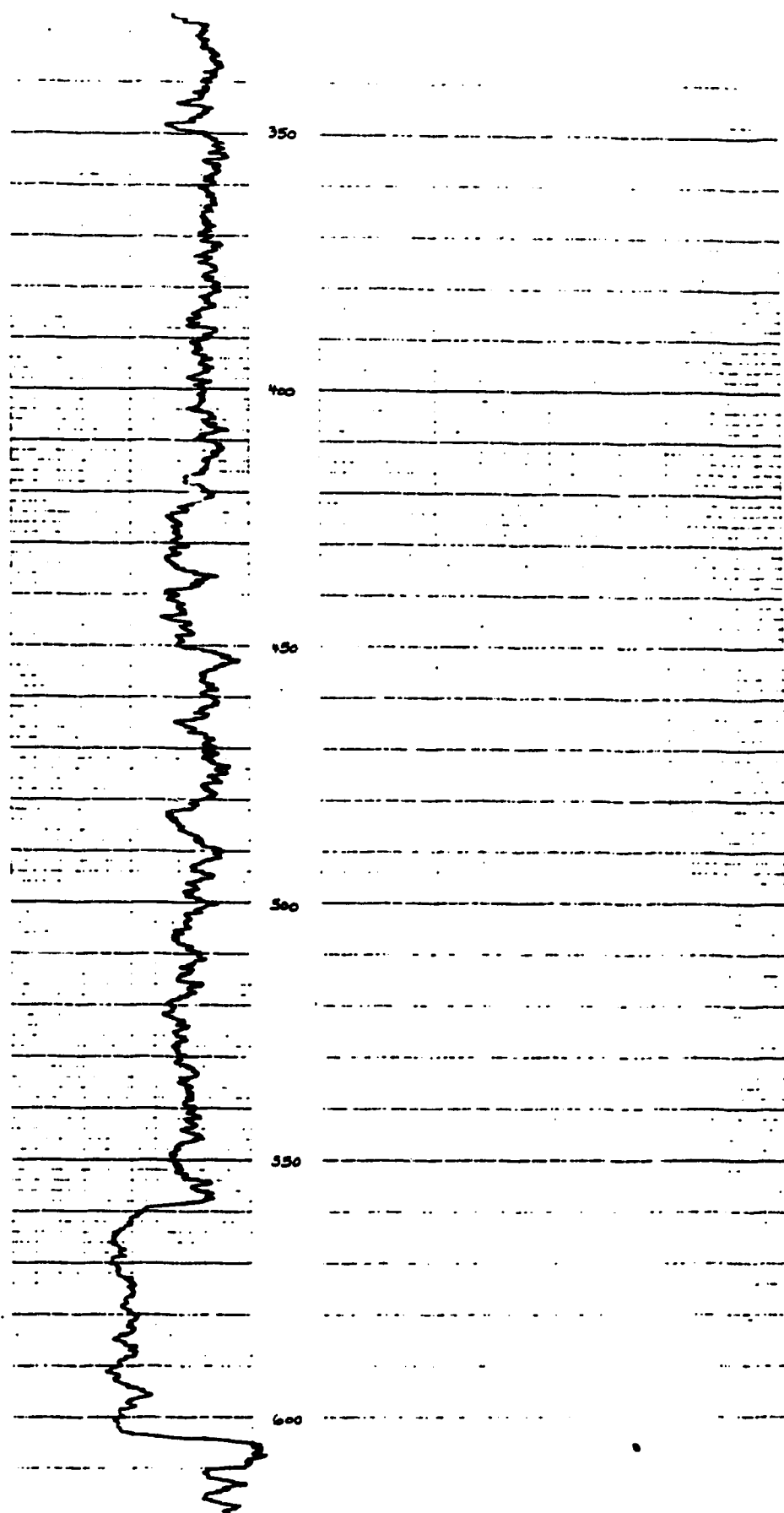
LOGGING SPEED: 150
 TS: 3

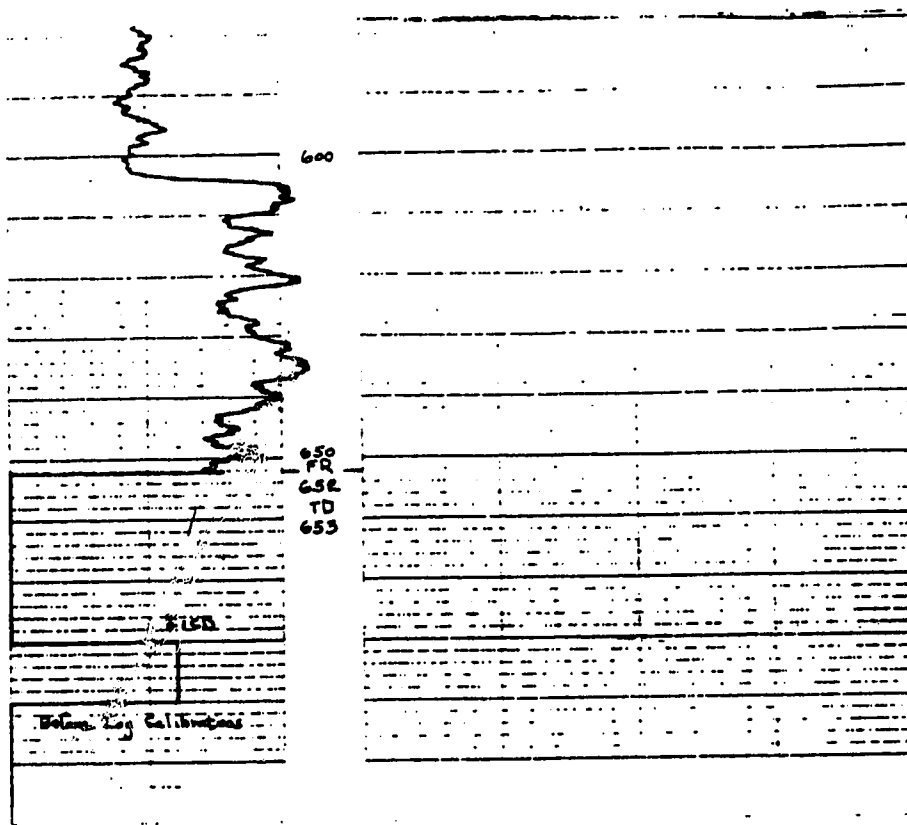
ANNOT: Signal attenuated in surface casing

GAMMA RAY
 LEAD/CS

After Log Calibration

0 LR -
 50
 100





APPENDIX C: Flood Frequency Analysis, Saddle River.

HYDROLOGY
REPORT
7FD
90-232

Flood Frequency Analysis
Saddle River 30-78-3-W6M

Prepared for

Development and Operations Division

Prepared by:


Dave Siemonsen
Hydrology Technologist

Reviewed by:


John Taggart, P. Eng.
Peace River Basin Hydrologist

Alberta HYDROLOGY Branch
ENVIRONMENT

EDMONTON

OCTOBER 1990

FLOOD FREQUENCY ANALYSIS
SADDLE RIVER 30-78-3-W6M

The Geotechnical Branch has requested that a flood frequency analysis be carried out for the Saddle River at 30-78-3-W6M. The information is to be used to assess the safety of a natural dam at this site. The drainage basin is shown in Figure 1.

Hydrometric data are available for the Saddle River Near Woking from 1967 to present providing 24 years of record. For 1987 where the annual peak flow is not available, but the maximum mean daily flow is identified, the peak flow is obtained based on a regression relationship between Q_1 and Q_2 . Table 1 presents the Saddle River data set void filled for 1987.

Table 1: Maximum Annual Discharges For Saddle River Near Woking
W.S.C. Station 07FD006

Year	Maximum Mean Daily Discharge (cms)	Maximum Instantaneous Discharge (cms)
1967	64.8	80.1
1968	150	439
1969	32.3	57.2
1970	9.46	10.2
1971	56.4	78.4
1972	43.3	61.4
1973	27.6	37.4
1974	60.9	80.1
1975	13.1	22.5
1976	47.6	60.9
1977	43.0	86.1
1978	15.7	18.4
1979	30.0	54.3
1980	2.27	8.22
1981	6.20	7.31
1982	14.3	26.1
1983	20.8	37.3
1984	27.9	34.5
1985	5.31	8.48
1986	21.7	26.1
1987	17.0	26.8 e
1988	6.04	9.38
1989	20.4	35.1
1990	338	436

e - estimated

A modified Pearson Type III frequency distribution is used to define the maximum instantaneous discharges for the Saddle River. The results of the frequency analysis are presented in Table 2.

Table 2 : Flood Frequency Analysis for Saddle River Near Woking W.S.C. Stn. 07FD006

Return Period (Years)	Maximum Instantaneous Discharge (cms)
100	548
50	439
25	335
20	302
10	205
5	116
2	26

The drainage area measured to the hydrometric station on the Saddle is approximately 538 square kilometers and the drainage area to the project site is estimated at 907 square kilometers. The peak discharges at Saddle River near Woking are transposed to the project site using Equation 2.

$$Q_p = Q_s (D.A._{proj}/D.A._s)^{0.8} \quad \text{..... Equation 2}$$

Where : Q_p is the estimated discharge at the project site

Q_s is the discharge at the Saddle River at the hydrometric site

$D.A._{proj}$ is the drainage area measured to the project site

$D.A._s$ is the drainage area measured to the hydrometric site

The results of the frequency analysis for the Saddle River at 30-78-3-W6 are presented in Table 3.

Table 3 : Flood Frequency Analysis for Saddle River at 30-78-3-W6

Return Period (Years)	Maximum Instantaneous Discharge (cms)
100	832
50	667
25	509
20	459
10	311
5	176
2	39.5

The volume analysis is carried out using annual maximum 12 day volumes for the Saddle River Near Woking and applying a Pearson Type III frequency distribution to this data set. The 12 day maximum volumes for the Saddle River Near Woking are presented in Table 4. The results of the frequency analysis of volumes are presented in Table 5.

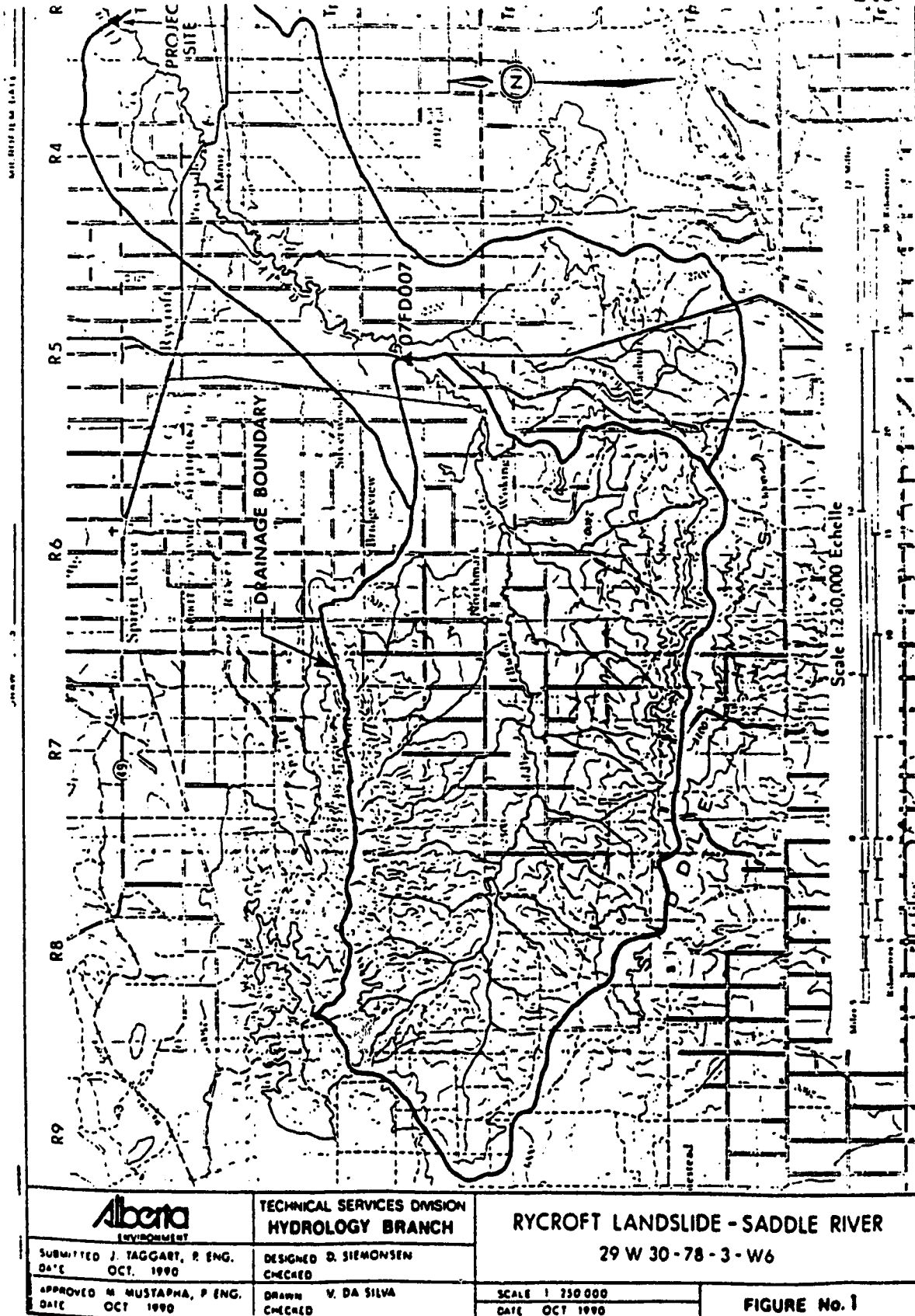
Table 4 : Annual Maximum 12 Day Volumes for the Saddle River at Woking - W.S.C. Stn 07FD006

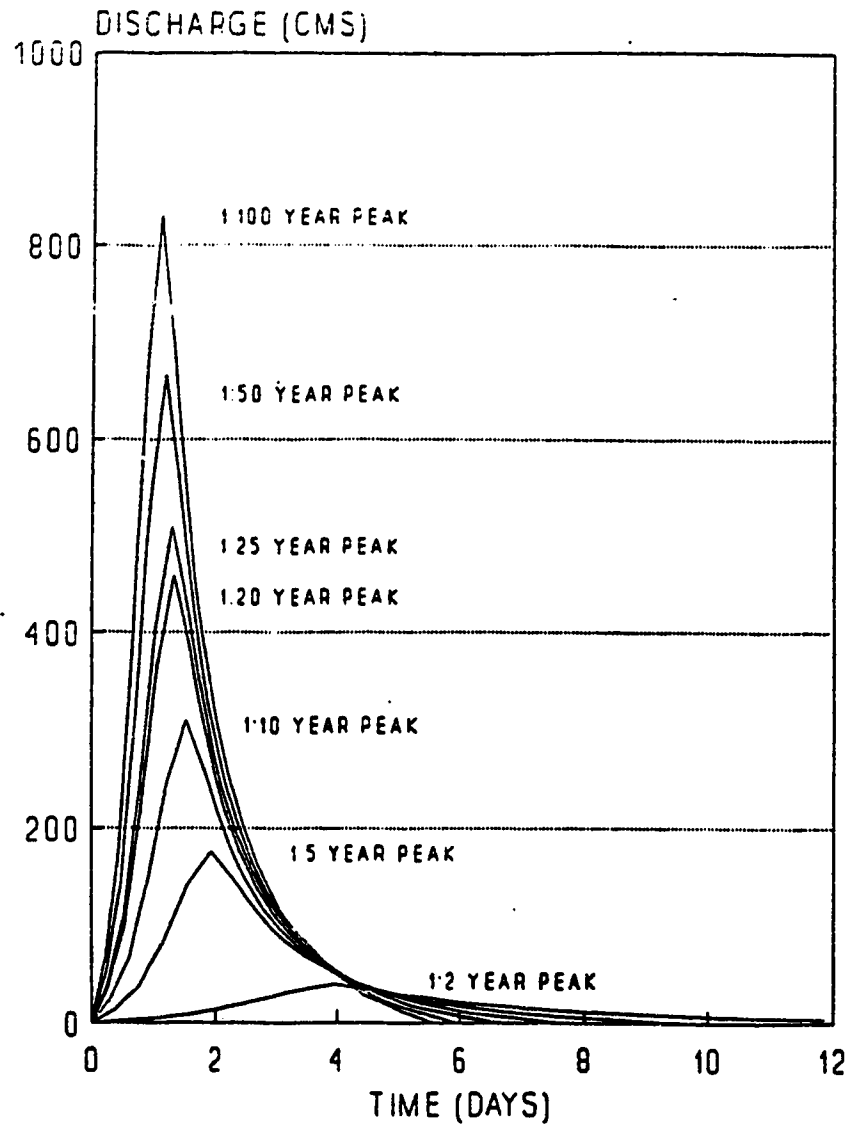
Year	Maximum 12 Day Volume (Dam ³)
1967	31251
1968	34733
1969	17135
1970	7420
1971	16002
1972	19507
1973	17287
1974	46284
1975	6652
1976	12346
1977	17473
1978	7165
1979	14997
1980	756
1981	5201
1982	6186
1983	10859
1984	7656
1985	3884
1986	9007
1987	5308
1988	2044
1989	4440
1990	54709

Table 5 : Volume Frequency Analysis for Saddle River
Near Woking W.S.C. Stn 07FD006

Return Period (Years)	Flood Volume (Dams)
100	64195
50	54876
25	45527
20	42510
10	33101
5	23618
2	10847

The flood volumes are transposed linearly using drainage area ratios to estimate the flood volumes for floods of various returnperiods at the Rycroft Project Site. The flood hydrographs are developed using a dimensionless hydrograph program and are presented in Tables 6 to 12 and illustrated in Figure 2.






	Technical Services Division HYDROLOGY BRANCH	RYCROFT LANDSLIDE PROJECT SITE INFLOW HYDROGRAPHS	
SUBMITTED John Toppert, P.Eng. DATE October 1990	DESIGNED B. Gieseler DATE October 1990	SCALE DATE	
APPROVED S. Majed Mousheh, P. Eng. DATE October 1990	DRAWN CHECKED	FIGURE No. 2	

Table 6 : FLOOD HYDROGRAPH ANALYSIS

100 YEAR RETURN PERIOD	
TIME (DAYS)	DISCHARGE (CMS)
0.000	0.0
0.111	33.3
0.222	66.6
0.333	124.8
0.444	178.0
0.555	291.2
0.666	394.4
0.778	528.3
0.889	665.6
1.000	748.8
1.111	832.0
1.222	761.3
1.333	688.9
1.444	603.2
1.555	530.8
1.666	459.3
1.777	402.7
1.999	317.0
2.222	253.8
2.444	203.8
2.666	166.4
2.888	134.8
3.110	108.2
3.332	91.5
3.888	54.9
4.443	29.1
4.999	14.1
5.554	0.0

HYDROGRAPH VOLUMES	
TIME (DAYS)	VOLUME (CUBIC DECAMETERS)
5.6 (TOTAL)	108225.0

Table 7 : FLOOD HYDROGRAPH ANALYSIS

50 YEAR RETURN PERIOD	
TIME (DAYS)	DISCHARGE (CMS)
0.000	0.0
0.118	26.7
0.237	53.4
0.355	100.1
0.474	142.7
0.592	233.4
0.711	316.2
0.829	423.5
0.948	533.6
1.066	600.3
1.184	667.0
1.303	610.3
1.421	552.3
1.540	483.6
1.658	425.5
1.777	368.2
1.895	322.8
2.132	254.1
2.369	203.4
2.606	163.4
2.843	133.4
3.080	108.1
3.316	86.7
3.553	73.4
4.146	44.0
4.738	23.3
5.330	11.3
5.922	0.0

HYDROGRAPH VOLUMES	
TIME (DAYS)	VOLUME (CUBIC DECAMETERS)
5.9 (TOTAL)	92514.0

Table 8 : FLOOD HYDROGRAPH ANALYSIS

25 YEAR RETURN PERIOD	
TIME (DAYS)	DISCHARGE (CMS)
0.000	0.0
0.130	20.4
0.261	40.7
0.391	76.4
0.522	108.9
0.652	178.1
0.783	241.3
0.913	323.2
1.044	407.2
1.174	458.1
1.304	509.0
1.435	465.7
1.565	421.5
1.696	369.0
1.826	324.7
1.957	281.0
2.087	246.4
2.348	193.9
2.609	155.2
2.870	124.7
3.131	101.8
3.392	82.5
3.653	66.2
3.913	56.0
4.566	33.6
5.218	17.8
5.870	8.7
6.522	0.0

HYDROGRAPH VOLUMES	
TIME (DAYS)	VOLUME (CUBIC DECAMETERS)
6.5 (TOTAL)	77753.0

Table 9 : FLOOD HYDROGRAPH ANALYSIS

20 YEAR RETURN PERIOD	
TIME (DAYS)	DISCHARGE (CMS)
0.000	0.0
0.133	18.4
0.267	36.7
0.400	68.9
0.533	98.2
0.667	160.6
0.800	217.6
0.933	291.5
1.067	367.2
1.200	413.1
1.333	459.0
1.467	420.0
1.600	380.1
1.733	332.8
1.867	292.8
2.000	253.4
2.133	222.2
2.400	174.9
2.667	140.0
2.933	112.5
3.200	91.8
3.467	74.4
3.734	59.7
4.000	50.5
4.667	30.3
5.334	16.1
6.000	7.8
6.667	0.0

HYDROGRAPH VOLUMES	
TIME (DAYS)	VOLUME (CUBIC DECAMETERS)
6.7 (TOTAL)	71670.0

Table 10 : FLOOD HYDROGRAPH ANALYSIS

10 YEAR RETURN PERIOD	
TIME (DAYS)	DISCHARGE (CMS)
0.000	0.0
0.153	12.4
0.306	24.9
0.460	46.7
0.613	66.6
0.766	108.8
0.919	147.4
1.073	197.5
1.226	248.8
1.379	279.9
1.532	311.0
1.685	284.6
1.839	257.5
1.992	225.5
2.145	198.4
2.298	171.7
2.451	150.5
2.758	118.5
3.064	94.9
3.371	76.2
3.677	62.2
3.984	50.4
4.290	40.4
4.597	34.2
5.363	20.5
6.129	10.9
6.895	5.3
7.661	0.0

HYDROGRAPH VOLUMES	
TIME (DAYS)	VOLUME (CUBIC DECAMETERS)
7.7 (TOTAL)	55800.0

Table 11 : FLOOD HYDROGRAPH ANALYSIS

5 YEAR RETURN PERIOD

TIME (DAYS)	DISCHARGE (CMS)
0.000	0.0
0.193	7.0
0.386	14.1
0.580	26.4
0.773	37.7
0.966	61.6
1.159	83.4
1.352	111.8
1.546	140.8
1.739	158.4
1.932	176.0
2.125	161.0
2.318	145.7
2.512	127.6
2.705	112.3
2.898	97.2
3.091	85.2
3.478	67.1
3.864	53.7
4.251	43.1
4.637	35.2
5.023	28.5
5.410	22.9
5.796	19.4
6.762	11.6
7.728	6.2
8.694	3.0
9.660	0.0

HYDROGRAPH VOLUMES

TIME (DAYS)	VOLUME (CUBIC DECAMETERS)
9.7 (TOTAL)	39820.0

Table 12 : FLOOD HYDROGRAPH ANALYSIS
2 YEAR RETURN PERIOD

TIME (DAYS)	DISCHARGE (CMS)
0.000	0.0
0.395	1.6
0.791	3.2
1.186	5.9
1.582	8.5
1.977	13.8
2.372	18.7
2.768	25.1
3.163	31.6
3.559	35.5
3.954	39.5
4.350	36.1
4.745	32.7
5.140	28.6
5.536	25.2
5.931	21.8
6.327	19.1
7.117	15.0
7.908	12.0
8.699	9.7
9.490	7.9
10.281	6.4
11.072	5.1
11.862	4.3
13.839	2.6
15.817	1.4
17.794	0.7
19.771	0.0

HYDROGRAPH VOLUMES

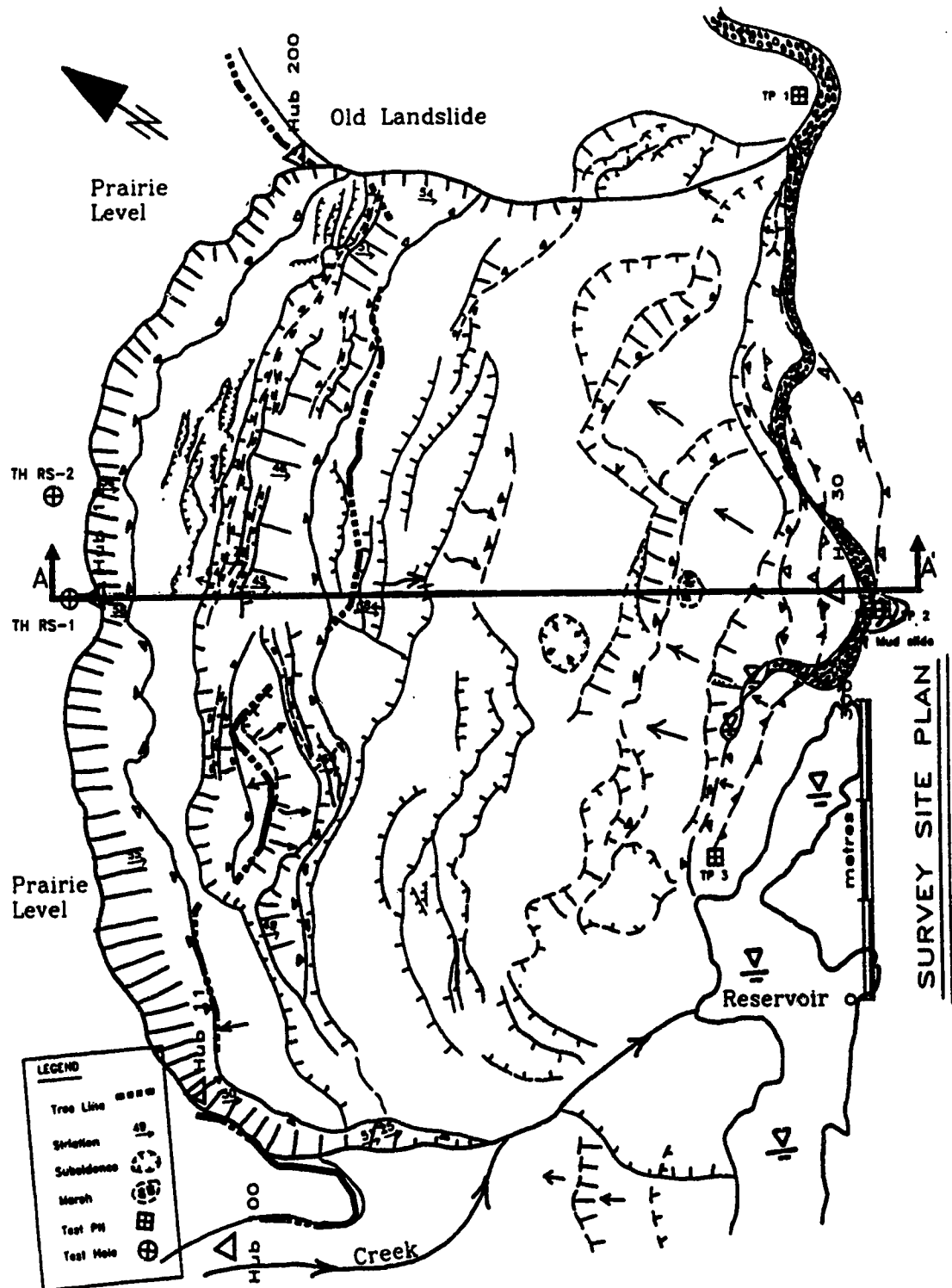
TIME (DAYS)	VOLUME (CUBIC DECAMETERS)
19.8 (TOTAL)	18290.0

The return period for the 1990 flood event for the Saddle River is estimated at 50 years. The volume of the 1990 event is estimated at 54,700 dam³ and the maximum instantaneous discharge is estimated at 662 CMS at the Rycroft Landslide site.

Prepared by: _____


Dave Siemonsen
Hydrology Technologist

APPENDIX D: Topographic survey of the Rycroft Landslide, July 1991.



RYCROFT SLIDE

TAEP
Rod T.K.

No. 3/7
Date JULY 9/91 Page 3/7

No. 3/7
Date JULY 9/91 Page 3/7

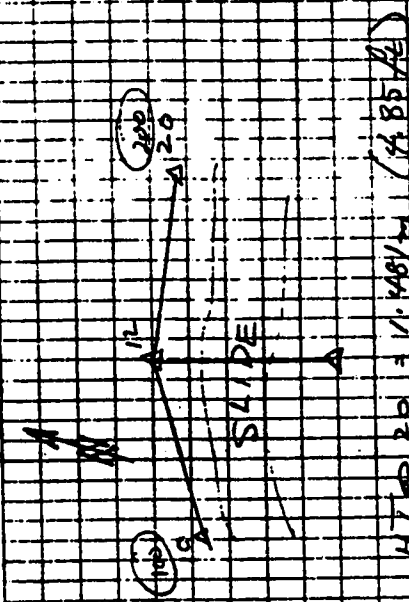
HT	HT = (use 1.47 m of)
HCR	20
10	664.919
20	494.441
20	494.442
10	664.920
	664.920

HT =

HP Calculator Time Checks
from JULY 6/91 - COPY

UTC	4:03:10 + 2DB	(1.5 sec)
HP41CV	22:03:10.10	ΔT = -0.10
UTC	4:04:05 + 2DB	
HP41CV	22:04:05.09	ΔT = -0.11
UTC	4:05:08 + 2DB	
HP41CV	22:05:08.13	ΔT = -0.07

Take ΔT = -0.10 on JULY 6/91



TA.E.P. SOKK SET 2B
 Rod T.K. Ser# 113372
 No.
 Date July 9/91 Page 5/7

RYCROFT SLIDE
 Date July 9/91 Page 5/7

NO	HC	12	HI = 1	477m (4.85ft)
	HC	REP.N	ED	563
20	0.00-00		90-12-07	90-12-18
16	64-10-32	64-10-32	95-03-10	95-03-22
10	142-56-22	142-56-22	89-59-29	89-59-39
10	322-56-31	142-56-35	87-00-11	664-920
20/16	244-10-48	64-10-52	264-58-25	357-243
16	178-59-58		487-47-30	
20	178-59-48		289-47-32	90-12-20
16	244-10-25	64-10-37	84-58-21	357-244
10	322-56-22	142-56-34	370-00-10	664-920
10	142-56-20	142-56-37	87-59-25	
16	64-10-33	64-10-52	95-03-20	357-244
20	359-59-44		90-12-11	
	HC		ED	Slope Dip Rod
20	0.00-00		90-12-07	
10	142-56-34		87-59-31	
16	64-10-51		-	
15	64-10-40		97-37-05	171-287
14	64-10-40		97-51-34	165-129
			-012	

Target Pole @ 1182m

1057m

13.53 ft

HT @ 20 = 1.481m (4.85ft)

HT @ 10 = 1.421m (4.66ft)

HT @ 16 = 1.077m (Target 1.06)

105

105

105

105

105

105

105

105

105

105

105

105

105

105

105

105

105

105

105

Inst SET 2B
Ser # 113372

RAEP
R&A T.K

No
Date..... JULY 9/91..... Page 7/7

RYCROFT SLIDE

No
Date..... JULY 9/91..... Page 7/7

	HT 12	cont
Top	64-10-29	114.38-35 49.093
"	64-10-25	118.47-21 42.750
"	64-10-23	116.12-44 33.768
"	64-10-22	118.57-40 29.405
"	64-10-18	120.55-01 25.933
"	64-10-13	127.55-25 19.108
10	142.56-46	89.57-16 66.479
20	0.00-30	90-11.57 —

JULY 10/91

HT 11 1.581²⁴ (5.194⁴)

HT 12 1.455²⁴ (4.784⁴)

NT2-4207

五九四

SUNSHOT @ HYCROFT SLIDE

No. JUNE 10/19/1910 Page 1/10

Date JULY 10/91 Page 3/10

Date JULY 10/91 Page 3/10

No. 5 Date July 10/91 Page 1/10

Date.....JULY 10/91.....Page 1/10

Date.....JULY 10/91.....Page 1/10

[illegible]

Inst Set 28
Ser # 113372

TREP
R.J. T.K.

Page 2-10

No
Date JULY 10/71

RYC CO. T. SLIDE
Page 2-10

Top 15	HT = 1.424	(56.1")	Δ 112
12	0.00-00	82.30-44	HT = 1.438
Seam	0.19-10	84.04-03	0.41T
Seam	358-50-05	24.58-40	0.41T
Top Slope	0.00-59	84.46-10	0.41T
Seam	355-55-52	86.48-13	0.41T
Seam	355-48-34	87-02-21	0.41T
Top Slope	0.19-24	88.12-16	Top
Top Slope	0.20-08	86.28-59	Top
On Slope	0.46-11	88.53-07	Top
Top	0.57-07	89-11-21	Top
Top	91-17-06	91-14-49	Top
Top	2.38-27	98.53-43	HT = 3.11077
Seam	339-30-59	95-36-00	0.41T
16	178-58-58		
Cont'd	185-03-53	139-46-27	
Top Slope	178-35-08	132-30-10	
Top	182-26-42	112-20-57	
"	180-28-19	108-30-10	
Top Slope	178-23-52	108-35-44	
Top Cont	172-08-59	105-28-29	
"	177-12-22	105-53-57	
"	177-12-08	105-50-42	
Top Cont	177-14-28	104-42-34	
		OVER	

RE-SETLB
115572AEP
Red TK

Page 3/10

Date JULY 10/91

Page 3/10

RYCROFT SLIDE

No. JULY 10/91

Date

	TKP 15 (cont)		
Top Crest	178-52-02	102-33-25	101-233
"	179-17-02	102-34-40	103-132
Top Slope	179-46-06	102-24-29	108-686
Top	180-07-04	100-39-20	113-117
Top Slope	179-43-53	99-00-11	112-965
Top Line	179-54-52	98-39-31	117-298
Top Crest	180-00-57	98-16-32	125-259
"	180-00-57	98-27-56	126-201
Top	180-05-01	98-11-44	131-334
"	180-14-05	98-21-59	136-469
Top Slope	180-04-52	94-41-33	137-186
"	178-33-31	87-30-45	---
16	178-59-49	92-48-21	186-178
12	159-59-52	82-30-52	---

SFT 2B
#113372

KAEP
P.ATK

No
Date

July 10/91

Page 4/10

RYCROFT SLIDE

No
Date

July 10/91

Page 4/10

	AC 16	HI = 1.193m	(4.92ft)
	9.12m Pole HT = 1.077m		
11	0.00-01	86.50-27	86.50-18
12	61.34.58	61.34.57	84.58-12
17	241-11-05	241-11-04	104.15-13
17	61-11-05	241-10-57	255-44-37
12	241-35-00	61-34.52	275-01-57
11	180.00-08	275-07-52	
11	41-34.52		
12	359-59-56		
comp	45-31-49	100-28-44	29.254
Top Slope	37-56-22	116-54-57	19.590
On Slope	39-44-95	126-56-18	20.389
3.41	38-26-39	133-52-04	18.852
0.9m depth	10.3m up from	416	is top slope
Top Curb	244.04-44	115-14-05	23.918
1.8 Top Vent	Drop of	2.13 m	
A. 5.7	240.54-07	113-51-50	33.520
12	179-59-58	273-07-55	Reverse Face.

Isot SE72B
Sect 113372
Page 5/10

TAEP
RMTK

No.

Date July 10/91

RYCPOFT SLIDE

Page 5/10

No.

Date JULY 10/91

16	359.57.57	17	421.35.27	(4.53 ft)	1077	Top H ₂ O	147.0 16 15 0.000m
16	0.00.01		77.0.57	"	0.77.11.07		
17	180.46.42	18	36.41	90.20.36	151.09.00	90.20.51	
17	0.36.52	18	36.57	168.38.56	151.09.44		
16	178.57.55		282.48.43	Top H ₂ O			
16	359.57.55		77.0.52				
Top	180.41.41		91.08.18	144.34.5			
"	180.29.44		90.55.56	135.15.3			
11-A(10)	180.30.40		90.59.05	113.55.0			
Top	180.38.25		91.10.17	124.95.4			
Top	180.33.17		92.53.08	91.01.7			
"	180.33.19		92.37.26	89.6.2.7			
11-A(9)	180.20.13		93.44.51	70.49.3			
Top	180.25.44		95.49.53	57.12.2			
"	180.40.28		94.42.11	19.32.7			
11-A(8)	180.33.20		95.31.10	15.34.6			
Top	180.33.21		102.25.03	5.32.2			
16	359.57.55		77.11.01				

Report uses 147.0 16 15 0.000m

357.4 9.1/14

Inst SET 2B
Ser# 113372
Page 6/10

TRAP
Rod TK

No
Date JULY 10/91

RYCROFT SLIDE
JULY 10/91
Page 6/10

No	Date	HT	HT	HT
17	0-00-01	90.314	90.317	90.317
19	179-25-06	179-25-05	97.0647	21.397
19	359-25-04	179-24-30	243.5317	21.398
17	180-00-34		282.5646	
17	0-00-19			
Top/End	179-53-01		97.3347	18.536
"	179-30-25		97.0334	15.707
Top	179-52-49		95.3237	13.338
Top Cont	181-02-11		101.4603	11.165
"	182-32-14		101-18-38	9.314
Top	182-14-11		94.4205	5.535
Top	173-36-30		116.2107	2.707
Alt				
17	0-00-16		70.0308	

HT 17 = 0.6617 (2.18.42)

HT 19 = 1.5152 (2.18.42)

Inst SET 24
Ser # 113372
Page 7/10

No
Date July 10/91
T/AEP
Ref TR

No RY-CRAFT SLIDE
Date July 10/91
Page 7/10

17	4-00-01	HT =	
		70-05-13	
	TA @ 19	HT = 1.206m (3.96 ft)	
	HT = 0.9	P1.5m	1.077m
18	0-00-05	84-06-49	21.335 (68'4"07")
20	178-58-38	116-05-38	415.451 (1263'45")
20	389-57-11	177-57-06	244.5409 45.448
On Site	359-05-07	245-17-09	12.017
"	358-58-06	256-55-20	2.453
18	180-00-05	275-52-58	21.333
	TA @ 20	HT = 1.388m (54'38")	
	P1.5m	HT = 1.077m	
19	0-00-34	64-23-58	45.259 (148'4"08")
21	180-46-07	10-45-33	51.36-19 76.550 (241'36"12")
21	0-46-11	10-45-26	278-23-54 76.531
Topo	0-48-30	278-25-17	74.446
"	0-21-04	278-25-18	38.389
"	359-28-35	268-08-04	20.379
"	183-14-35	255-44-28	2.442
Top (val)	180-52-17	279-58-56	13.274
19	180-00-05	295-35-43	45.256

Δ 20 = 1.077m

No. RYCROFT SLIDE SET 25
 Date JULY 10/91 Page 8/10
 No. RAEP Page 8/10
 Date JULY 10/91 Page 8/10

20	0-00-00	HI = 1314.2	(51.8")	HT@20 0.614	(8.014)
21	0-00-00	Prism B/c HT = 1077.2		0.71 Prism Rod	
22	0-00-00	99-08-03	-		
23	0-00-00	92-57-25	83.06		
24	0-00-00	87-01-50	83.06		
25	0-00-00	86-58-49	81.84		
26	0-00-00	86-31-25	80.28		
27	0-00-00	86-49-25	71.69		
28	0-00-00	86-05-05	68.77		
29	0-00-00	86-29-22	66.87		
30	0-00-00	86-34-50	62.28		
31	0-00-00	85-12-30	55.26		
32	0-00-00	85-57-37	38.05		
33	0-00-00	85-48-00	27.70		
34	0-00-00	85-14-54	26.69		
35	0-00-00	84-44-42	10.40		
36	0-00-00	85-34-35	2.59		
37	0-00-00	86-57-35			
38	0-00-00	86-12-15	76.64		
39	0-00-00				
40	0-00-00				
41	0-00-00				
42	0-00-00				
43	0-00-00				
44	0-00-00				
45	0-00-00				
46	0-00-00				
47	0-00-00				
48	0-00-00				
49	0-00-00				
50	0-00-00				
51	0-00-00				
52	0-00-00				
53	0-00-00				
54	0-00-00				
55	0-00-00				
56	0-00-00				
57	0-00-00				
58	0-00-00				
59	0-00-00				
60	0-00-00				
61	0-00-00				
62	0-00-00				
63	0-00-00				
64	0-00-00				
65	0-00-00				
66	0-00-00				
67	0-00-00				
68	0-00-00				
69	0-00-00				
70	0-00-00				
71	0-00-00				
72	0-00-00				
73	0-00-00				
74	0-00-00				
75	0-00-00				
76	0-00-00				
77	0-00-00				
78	0-00-00				
79	0-00-00				
80	0-00-00				
81	0-00-00				
82	0-00-00				
83	0-00-00				
84	0-00-00				
85	0-00-00				
86	0-00-00				
87	0-00-00				
88	0-00-00				
89	0-00-00				
90	0-00-00				
91	0-00-00				
92	0-00-00				
93	0-00-00				
94	0-00-00				
95	0-00-00				
96	0-00-00				
97	0-00-00				
98	0-00-00				
99	0-00-00				
100	0-00-00				

Inst. R. SET 26
S# 113372
Page 10/10

No. TAEP
Rod TK
Date JULY 1

No. RYCROFT SLIDE Page 10/10
Date JULY 10/91

10	23	115 @ 43 = 1.25M (49 5/8')
----	----	----------------------------

30	0-00-00	89-23-43	36.897 @ 88.2404
			37.508 @ 107.0814

153-15-15	153-15-13	153-15-12	153-15-11	153-15-10
67-08-22	67-08-22	67-08-22	67-08-22	67-08-22
37.527	37.527	37.527	37.527	37.527

30	177.59.29	271.35.36	36.190
----	-----------	-----------	--------

03/11/2017

Feb: 76.5°C

1971	1972	1973	1974	1975	1976	1977	1978	1979	1980	1981	1982	1983	1984	1985	1986	1987	1988	1989	1990	1991	1992	1993	1994	1995	1996	1997	1998	1999	2000	2001	2002	2003	2004	2005	2006	2007	2008	2009	2010	2011	2012	2013	2014	2015	2016	2017	2018	2019	2020	2021	2022	2023	2024	2025	2026	2027	2028	2029	2030	2031	2032	2033	2034	2035	2036	2037	2038	2039	2040	2041	2042	2043	2044	2045	2046	2047	2048	2049	2050	2051	2052	2053	2054	2055	2056	2057	2058	2059	2060	2061	2062	2063	2064	2065	2066	2067	2068	2069	2070	2071	2072	2073	2074	2075	2076	2077	2078	2079	2080	2081	2082	2083	2084	2085	2086	2087	2088	2089	2090	2091	2092	2093	2094	2095	2096	2097	2098	2099	2100	2101	2102	2103	2104	2105	2106	2107	2108	2109	2110	2111	2112	2113	2114	2115	2116	2117	2118	2119	2120	2121	2122	2123	2124	2125	2126	2127	2128	2129	2130	2131	2132	2133	2134	2135	2136	2137	2138	2139	2140	2141	2142	2143	2144	2145	2146	2147	2148	2149	2150	2151	2152	2153	2154	2155	2156	2157	2158	2159	2160	2161	2162	2163	2164	2165	2166	2167	2168	2169	2170	2171	2172	2173	2174	2175	2176	2177	2178	2179	2180	2181	2182	2183	2184	2185	2186	2187	2188	2189	2190	2191	2192	2193	2194	2195	2196	2197	2198	2199	2200	2201	2202	2203	2204	2205	2206	2207	2208	2209	2210	2211	2212	2213	2214	2215	2216	2217	2218	2219	2220	2221	2222	2223	2224	2225	2226	2227	2228	2229	2230	2231	2232	2233	2234	2235	2236	2237	2238	2239	2240	2241	2242	2243	2244	2245	2246	2247	2248	2249	2250	2251	2252	2253	2254	2255	2256	2257	2258	2259	2260	2261	2262	2263	2264	2265	2266	2267	2268	2269	2270	2271	2272	2273	2274	2275	2276	2277	2278	2279	2280	2281	2282	2283	2284	2285	2286	2287	2288	2289	2290	2291	2292	2293	2294	2295	2296	2297	2298	2299	2300	2301	2302	2303	2304	2305	2306	2307	2308	2309	2310	2311	2312	2313	2314	2315	2316	2317	2318	2319	2320	2321	2322	2323	2324	2325	2326	2327	2328	2329	2330	2331	2332	2333	2334	2335	2336	2337	2338	2339	2340	2341	2342	2343	2344	2345	2346	2347	2348	2349	2350	2351	2352	2353	2354	2355	2356	2357	2358	2359	2360	2361	2362	2363	2364	2365	2366	2367	2368	2369	2370	2371	2372	2373	2374	2375	2376	2377	2378	2379</
------	------	------	------	------	------	------	------	------	------	------	------	------	------	------	------	------	------	------	------	------	------	------	------	------	------	------	------	------	------	------	------	------	------	------	------	------	------	------	------	------	------	------	------	------	------	------	------	------	------	------	------	------	------	------	------	------	------	------	------	------	------	------	------	------	------	------	------	------	------	------	------	------	------	------	------	------	------	------	------	------	------	------	------	------	------	------	------	------	------	------	------	------	------	------	------	------	------	------	------	------	------	------	------	------	------	------	------	------	------	------	------	------	------	------	------	------	------	------	------	------	------	------	------	------	------	------	------	------	------	------	------	------	------	------	------	------	------	------	------	------	------	------	------	------	------	------	------	------	------	------	------	------	------	------	------	------	------	------	------	------	------	------	------	------	------	------	------	------	------	------	------	------	------	------	------	------	------	------	------	------	------	------	------	------	------	------	------	------	------	------	------	------	------	------	------	------	------	------	------	------	------	------	------	------	------	------	------	------	------	------	------	------	------	------	------	------	------	------	------	------	------	------	------	------	------	------	------	------	------	------	------	------	------	------	------	------	------	------	------	------	------	------	------	------	------	------	------	------	------	------	------	------	------	------	------	------	------	------	------	------	------	------	------	------	------	------	------	------	------	------	------	------	------	------	------	------	------	------	------	------	------	------	------	------	------	------	------	------	------	------	------	------	------	------	------	------	------	------	------	------	------	------	------	------	------	------	------	------	------	------	------	------	------	------	------	------	------	------	------	------	------	------	------	------	------	------	------	------	------	------	------	------	------	------	------	------	------	------	------	------	------	------	------	------	------	------	------	------	------	------	------	------	------	------	------	------	------	------	------	------	------	------	------	------	------	------	------	------	------	------	------	------	------	------	------	------	------	------	------	------	------	------	------	------	------	------	------	------	------	------	------	------	------	------	------	------	------	------	------	------	------	------	------	------	------	------	------	--------

PARMIER: 28.25 10.60000

Time Check - July 10/91

1	2	3	4	5	6	7	8	9	10	11	12	13	14	15	16	17	18	19	20	21	22	23	24	25	26	27	28	29	30	31	32	33	34	35	36	37	38	39	40	41	42	43	44	45	46	47	48	49	50	51	52	53	54	55	56	57	58	59	60	61	62	63	64	65	66	67	68	69	70	71	72	73	74	75	76	77	78	79	80	81	82	83	84	85	86	87	88	89	90	91	92	93	94	95	96	97	98	99	100
---	---	---	---	---	---	---	---	---	----	----	----	----	----	----	----	----	----	----	----	----	----	----	----	----	----	----	----	----	----	----	----	----	----	----	----	----	----	----	----	----	----	----	----	----	----	----	----	----	----	----	----	----	----	----	----	----	----	----	----	----	----	----	----	----	----	----	----	----	----	----	----	----	----	----	----	----	----	----	----	----	----	----	----	----	----	----	----	----	----	----	----	----	----	----	----	----	----	----	-----

UTC	3:34:00 + 2.05	AT: - .38
-----	----------------	-----------

HTC	3:35:05 + 2 DA
HTC	3:37:45 + 2 DA

HP41CV	21:35:04.73	DT	-47
--------	-------------	----	-----

UTC	3:36:08 + 2DA	AT - .40
-----	---------------	----------

4750	3:37:08 + 2PB
4741CV	21:36:08

MP416V	21:37:07.70	47-50
--------	-------------	-------

UTC	3:38:11 +20A	07-41
-----	--------------	-------

HP44Cv	21:38:	10:17	$Ay = -0.43$
--------	--------	-------	--------------

10

-0.43 @ 21.5 on July 10/11

W 5150 4111 10/0
10/9 8 20 22 0

$$-0.33/17 = -2.5 = -14.12\%$$

$$-0.33/45.5 = -0.00725453\%$$

127

1. 2. 3. 4. 5. 6. 7. 8. 9. 10. 11. 12. 13. 14. 15. 16. 17. 18. 19. 20. 21. 22. 23. 24. 25. 26. 27. 28. 29. 30. 31. 32. 33. 34. 35. 36. 37. 38. 39. 40. 41. 42. 43. 44. 45. 46. 47. 48. 49. 50. 51. 52. 53. 54. 55. 56. 57. 58. 59. 60. 61. 62. 63. 64. 65. 66. 67. 68. 69. 70. 71. 72. 73. 74. 75. 76. 77. 78. 79. 80. 81. 82. 83. 84. 85. 86. 87. 88. 89. 90. 91. 92. 93. 94. 95. 96. 97. 98. 99. 100. 101. 102. 103. 104. 105. 106. 107. 108. 109. 110. 111. 112. 113. 114. 115. 116. 117. 118. 119. 120. 121. 122. 123. 124. 125. 126. 127. 128. 129. 130. 131. 132. 133. 134. 135. 136. 137. 138. 139. 140. 141. 142. 143. 144. 145. 146. 147. 148. 149. 150. 151. 152. 153. 154. 155. 156. 157. 158. 159. 160. 161. 162. 163. 164. 165. 166. 167. 168. 169. 170. 171. 172. 173. 174. 175. 176. 177. 178. 179. 180. 181. 182. 183. 184. 185. 186. 187. 188. 189. 190. 191. 192. 193. 194. 195. 196. 197. 198. 199. 200. 201. 202. 203. 204. 205. 206. 207. 208. 209. 210. 211. 212. 213. 214. 215. 216. 217. 218. 219. 220. 221. 222. 223. 224. 225. 226. 227. 228. 229. 230. 231. 232. 233. 234. 235. 236. 237. 238. 239. 240. 241. 242. 243. 244. 245. 246. 247. 248. 249. 250. 251. 252. 253. 254. 255. 256. 257. 258. 259. 260. 261. 262. 263. 264. 265. 266. 267. 268. 269. 270. 271. 272. 273. 274. 275. 276. 277. 278. 279. 280. 281. 282. 283. 284. 285. 286. 287. 288. 289. 290. 291. 292. 293. 294. 295. 296. 297. 298. 299. 300. 301. 302. 303. 304. 305. 306. 307. 308. 309. 310. 311. 312. 313. 314. 315. 316. 317. 318. 319. 320. 321. 322. 323. 324. 325. 326. 327. 328. 329. 330. 331. 332. 333. 334. 335. 336. 337. 338. 339. 340. 341. 342. 343. 344. 345. 346. 347. 348. 349. 350. 351. 352. 353. 354. 355. 356. 357. 358. 359. 360. 361. 362. 363. 364. 365. 366. 367. 368. 369. 370. 371. 372. 373. 374. 375. 376. 377. 378. 379. 380. 381. 382. 383. 384. 385. 386. 387. 388. 389. 390. 391. 392. 393. 394. 395. 396. 397. 398. 399. 400. 401. 402. 403. 404. 405. 406. 407. 408. 409. 410. 411. 412. 413. 414. 415. 416. 417. 418. 419. 420. 421. 422. 423. 424. 425. 426. 427. 428. 429. 430. 431. 432. 433. 434. 435. 436. 437. 438. 439. 440. 441. 442. 443. 444. 445. 446. 447. 448. 449. 450. 451. 452. 453. 454. 455. 456. 457. 458. 459. 460. 461. 462. 463. 464. 465. 466. 467. 468. 469. 470. 471. 472. 473. 474. 475. 476. 477. 478. 479. 480. 481. 482. 483. 484. 485. 486. 487. 488. 489. 490. 491. 492. 493. 494. 495. 496. 497. 498. 499. 500. 501. 502. 503. 504. 505. 506. 507. 508. 509. 510. 511. 512. 513. 514. 515. 516. 517. 518. 519. 520. 521. 522. 523. 524. 525. 526. 527. 528. 529. 530. 531. 532. 533. 534. 535. 536. 537. 538. 539. 540. 541. 542. 543. 544. 545. 546. 547. 548. 549. 550. 551. 552. 553. 554. 555. 556. 557. 558. 559. 560. 561. 562. 563. 564. 565. 566. 567. 568. 569. 570. 571. 572. 573. 574. 575. 576. 577. 578. 579. 580. 581. 582. 583. 584. 585. 586. 587. 588. 589. 590. 591. 592. 593. 594. 595. 596. 597. 598. 599. 600. 601. 602. 603. 604. 605. 606. 607. 608. 609. 610. 611. 612. 613. 614. 615. 616. 617. 618. 619. 620. 621. 622. 623. 624. 625. 626. 627. 628. 629. 630. 631. 632. 633. 634. 635. 636. 637. 638. 639. 640. 641. 642. 643. 644. 645. 646. 647. 648. 649. 650. 651. 652. 653. 654. 655. 656. 657. 658. 659. 660. 661. 662. 663. 664. 665. 666. 667. 668. 669. 670. 671. 672. 673. 674. 675. 676. 677. 678. 679. 680. 681. 682. 683. 684. 685. 686. 687. 688. 689. 690. 691. 692. 693. 694. 695. 696. 697. 698. 699. 700. 701. 702. 703. 704. 705. 706. 707. 708. 709. 710. 711. 712. 713. 714. 715. 716. 717. 718. 719. 720. 721. 722. 723. 724. 725. 726. 727. 728. 729. 730. 731. 732. 733. 734. 735. 736. 737. 738. 739. 740. 741. 742. 743. 744. 745. 746. 747. 748. 749. 750. 751. 752. 753. 754. 755. 756. 757. 758. 759. 760. 761. 762. 763. 764. 765. 766. 767. 768. 769. 770. 771. 772. 773. 774. 775. 776. 777. 778. 779. 780. 781. 782. 783. 784. 785. 786. 787. 788. 789. 790. 791. 792. 793. 794. 795. 796. 797. 798. 799. 800. 801. 802. 803. 804. 805. 806. 807. 808. 809. 810. 811. 812. 813. 814. 815. 816. 817. 818. 819. 820. 821. 822. 823. 824. 825. 826. 827. 828. 829. 830. 831. 832. 833. 834. 835. 836. 837. 838. 839. 840. 84

$$V_T = 0.43 + 0.4 = -0.39$$

33

$$4.58 / 17 = -0.41$$
$$4.5 \text{ ft} = 2 \text{ m}$$

No. 1051 SET 20
 Date JUL 12/91
 Page 1/1

Prism Const. Test
 Date JUL 12/91
 Page 1/1

| A-C | | C | |
|-----------------------|----------------------|-------------------|--|
| E | 28.564 @ 90° 34' 35" |) 28.562 | |
| | .582 | | |
| W | 27.274 @ 89° 37' 33" |) 27.273 | |
| | .273 | | |
| A-C W | | 55.835 | |
| E 11 | 55.839 @ 90° 34' 08" | 55.836 Δ = φ | |
| B 12 | 53.838 | 55.833 | |
| | .835 | | |
| F 10 | 55.844 @ 90° 35' 09" | 55.837 Δ = φ | |
| | .838 @ 90° 35' 11" | | |
| SET 20 MET ROD 2 FORM | | | |
| ppm = 278.96 | | -0.2704 x P(2.6) | |
| | | 1 + 0.0001 x T(2) | |
| JUL 9/91 | P = 2792" H | i T = 23°C | |
| | ppm = +25.7 | | |
| JUL 10/91 | P = 2825" H | i T = 26°C | |
| | ppm = +25.3 | | |
| USE | | +25.5 ppm | |

Test done in yard of
Butler Survey Supply
Office in Edmond, OK

Use scale factor
of 1.000155
on all distances

1051 done in report of
 Butler Survey
 Office in Edmonton

Use scale factor
 of 1.000055
 on all distances

No. RECROFT SLIDE

Date

Page

No. 50

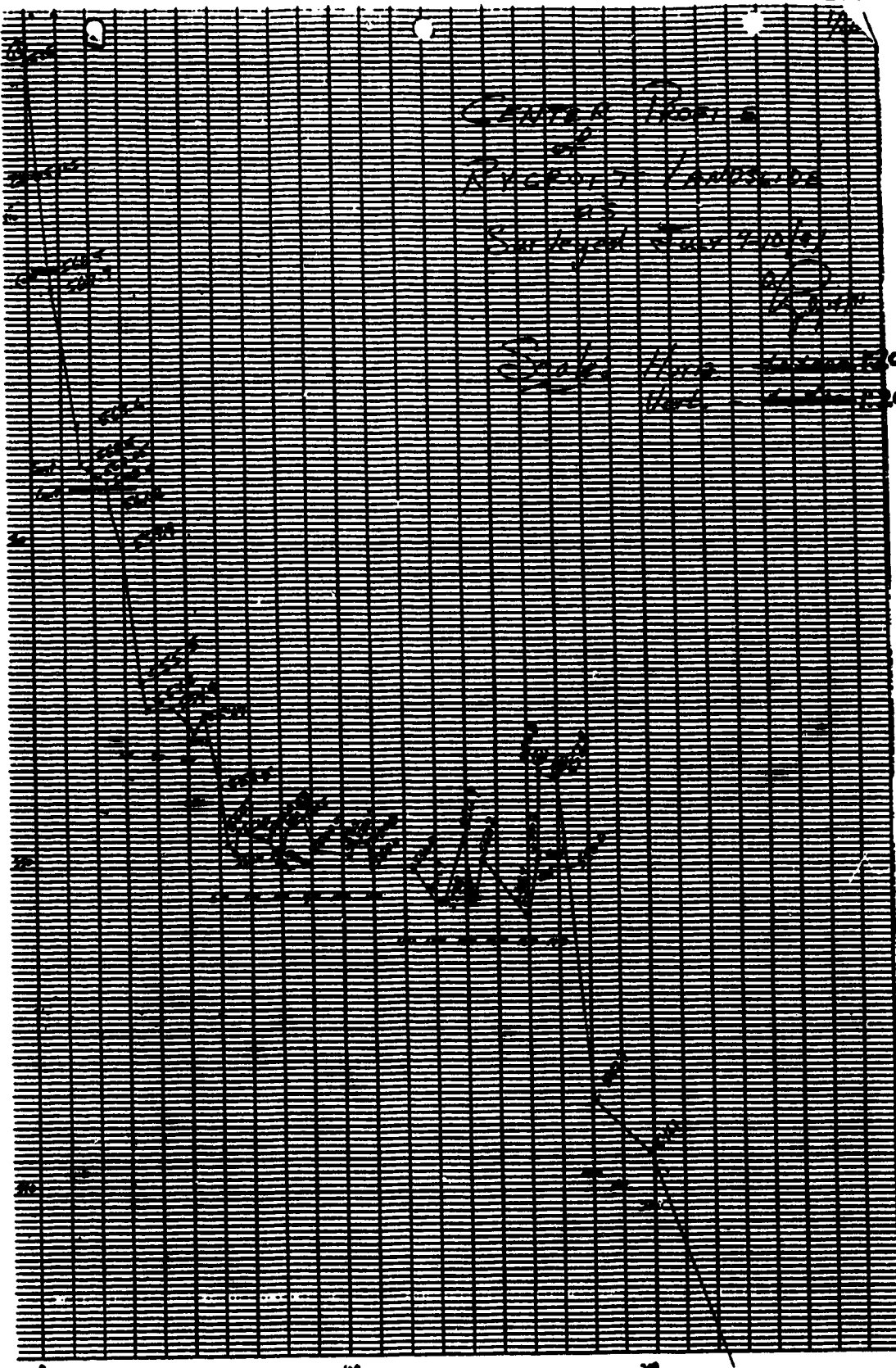
Date

Rotated & Translated Coords

Pt y z H

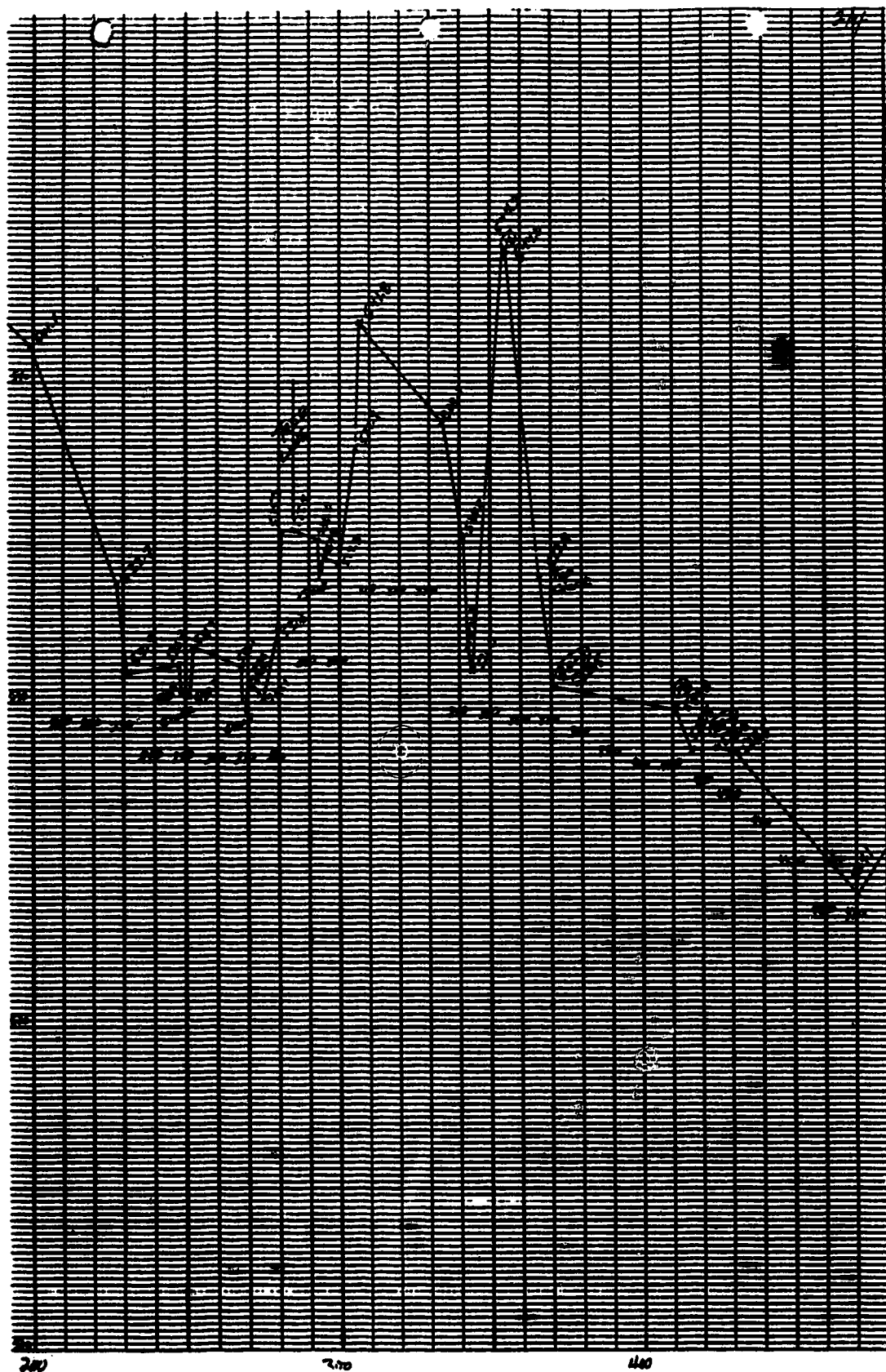
| | | | | |
|-----|--------|--------|--------|-------|
| 100 | 148.73 | 478.88 | 575.17 | AM-2 |
| 101 | 148.73 | 478.88 | 575.17 | AM-15 |
| 102 | 148.73 | 478.88 | 575.17 | AM-5 |
| 103 | 148.73 | 478.88 | 575.17 | AM-5 |
| 104 | 148.73 | 478.88 | 575.17 | AM-13 |
| 105 | 148.73 | 478.88 | 575.17 | AM-14 |
| 106 | 148.73 | 478.88 | 575.17 | AM-16 |
| 107 | 148.73 | 478.88 | 575.17 | AM-16 |
| 108 | 148.73 | 478.88 | 575.17 | AM-16 |
| 109 | 148.73 | 478.88 | 575.17 | AM-16 |
| 110 | 148.73 | 478.88 | 575.17 | AM-16 |
| 111 | 148.73 | 478.88 | 575.17 | AM-16 |
| 112 | 148.73 | 478.88 | 575.17 | AM-16 |
| 113 | 148.73 | 478.88 | 575.17 | AM-16 |
| 114 | 148.73 | 478.88 | 575.17 | AM-16 |
| 115 | 148.73 | 478.88 | 575.17 | AM-16 |
| 116 | 148.73 | 478.88 | 575.17 | AM-16 |
| 117 | 148.73 | 478.88 | 575.17 | AM-16 |
| 118 | 148.73 | 478.88 | 575.17 | AM-16 |
| 119 | 148.73 | 478.88 | 575.17 | AM-16 |
| 120 | 148.73 | 478.88 | 575.17 | AM-16 |
| 121 | 148.73 | 478.88 | 575.17 | AM-16 |
| 122 | 148.73 | 478.88 | 575.17 | AM-16 |
| 123 | 148.73 | 478.88 | 575.17 | AM-16 |
| 124 | 148.73 | 478.88 | 575.17 | AM-16 |
| 125 | 148.73 | 478.88 | 575.17 | AM-16 |
| 126 | 148.73 | 478.88 | 575.17 | AM-16 |
| 127 | 148.73 | 478.88 | 575.17 | AM-16 |
| 128 | 148.73 | 478.88 | 575.17 | AM-16 |
| 129 | 148.73 | 478.88 | 575.17 | AM-16 |
| 130 | 148.73 | 478.88 | 575.17 | AM-16 |
| 131 | 148.73 | 478.88 | 575.17 | AM-16 |
| 132 | 148.73 | 478.88 | 575.17 | AM-16 |
| 133 | 148.73 | 478.88 | 575.17 | AM-16 |
| 134 | 148.73 | 478.88 | 575.17 | AM-16 |
| 135 | 148.73 | 478.88 | 575.17 | AM-16 |
| 136 | 148.73 | 478.88 | 575.17 | AM-16 |
| 137 | 148.73 | 478.88 | 575.17 | AM-16 |
| 138 | 148.73 | 478.88 | 575.17 | AM-16 |
| 139 | 148.73 | 478.88 | 575.17 | AM-16 |
| 140 | 148.73 | 478.88 | 575.17 | AM-16 |
| 141 | 148.73 | 478.88 | 575.17 | AM-16 |
| 142 | 148.73 | 478.88 | 575.17 | AM-16 |
| 143 | 148.73 | 478.88 | 575.17 | AM-16 |
| 144 | 148.73 | 478.88 | 575.17 | AM-16 |
| 145 | 148.73 | 478.88 | 575.17 | AM-16 |
| 146 | 148.73 | 478.88 | 575.17 | AM-16 |
| 147 | 148.73 | 478.88 | 575.17 | AM-16 |
| 148 | 148.73 | 478.88 | 575.17 | AM-16 |
| 149 | 148.73 | 478.88 | 575.17 | AM-16 |
| 150 | 148.73 | 478.88 | 575.17 | AM-16 |
| 151 | 148.73 | 478.88 | 575.17 | AM-16 |
| 152 | 148.73 | 478.88 | 575.17 | AM-16 |
| 153 | 148.73 | 478.88 | 575.17 | AM-16 |
| 154 | 148.73 | 478.88 | 575.17 | AM-16 |
| 155 | 148.73 | 478.88 | 575.17 | AM-16 |
| 156 | 148.73 | 478.88 | 575.17 | AM-16 |
| 157 | 148.73 | 478.88 | 575.17 | AM-16 |
| 158 | 148.73 | 478.88 | 575.17 | AM-16 |
| 159 | 148.73 | 478.88 | 575.17 | AM-16 |
| 160 | 148.73 | 478.88 | 575.17 | AM-16 |
| 161 | 148.73 | 478.88 | 575.17 | AM-16 |
| 162 | 148.73 | 478.88 | 575.17 | AM-16 |
| 163 | 148.73 | 478.88 | 575.17 | AM-16 |
| 164 | 148.73 | 478.88 | 575.17 | AM-16 |
| 165 | 148.73 | 478.88 | 575.17 | AM-16 |
| 166 | 148.73 | 478.88 | 575.17 | AM-16 |
| 167 | 148.73 | 478.88 | 575.17 | AM-16 |
| 168 | 148.73 | 478.88 | 575.17 | AM-16 |
| 169 | 148.73 | 478.88 | 575.17 | AM-16 |
| 170 | 148.73 | 478.88 | 575.17 | AM-16 |
| 171 | 148.73 | 478.88 | 575.17 | AM-16 |
| 172 | 148.73 | 478.88 | 575.17 | AM-16 |
| 173 | 148.73 | 478.88 | 575.17 | AM-16 |
| 174 | 148.73 | 478.88 | 575.17 | AM-16 |
| 175 | 148.73 | 478.88 | 575.17 | AM-16 |
| 176 | 148.73 | 478.88 | 575.17 | AM-16 |
| 177 | 148.73 | 478.88 | 575.17 | AM-16 |
| 178 | 148.73 | 478.88 | 575.17 | AM-16 |
| 179 | 148.73 | 478.88 | 575.17 | AM-16 |
| 180 | 148.73 | 478.88 | 575.17 | AM-16 |
| 181 | 148.73 | 478.88 | 575.17 | AM-16 |
| 182 | 148.73 | 478.88 | 575.17 | AM-16 |
| 183 | 148.73 | 478.88 | 575.17 | AM-16 |
| 184 | 148.73 | 478.88 | 575.17 | AM-16 |
| 185 | 148.73 | 478.88 | 575.17 | AM-16 |
| 186 | 148.73 | 478.88 | 575.17 | AM-16 |
| 187 | 148.73 | 478.88 | 575.17 | AM-16 |
| 188 | 148.73 | 478.88 | 575.17 | AM-16 |
| 189 | 148.73 | 478.88 | 575.17 | AM-16 |
| 190 | 148.73 | 478.88 | 575.17 | AM-16 |
| 191 | 148.73 | 478.88 | 575.17 | AM-16 |
| 192 | 148.73 | 478.88 | 575.17 | AM-16 |
| 193 | 148.73 | 478.88 | 575.17 | AM-16 |
| 194 | 148.73 | 478.88 | 575.17 | AM-16 |
| 195 | 148.73 | 478.88 | 575.17 | AM-16 |
| 196 | 148.73 | 478.88 | 575.17 | AM-16 |
| 197 | 148.73 | 478.88 | 575.17 | AM-16 |
| 198 | 148.73 | 478.88 | 575.17 | AM-16 |
| 199 | 148.73 | 478.88 | 575.17 | AM-16 |
| 200 | 148.73 | 478.88 | 575.17 | AM-16 |

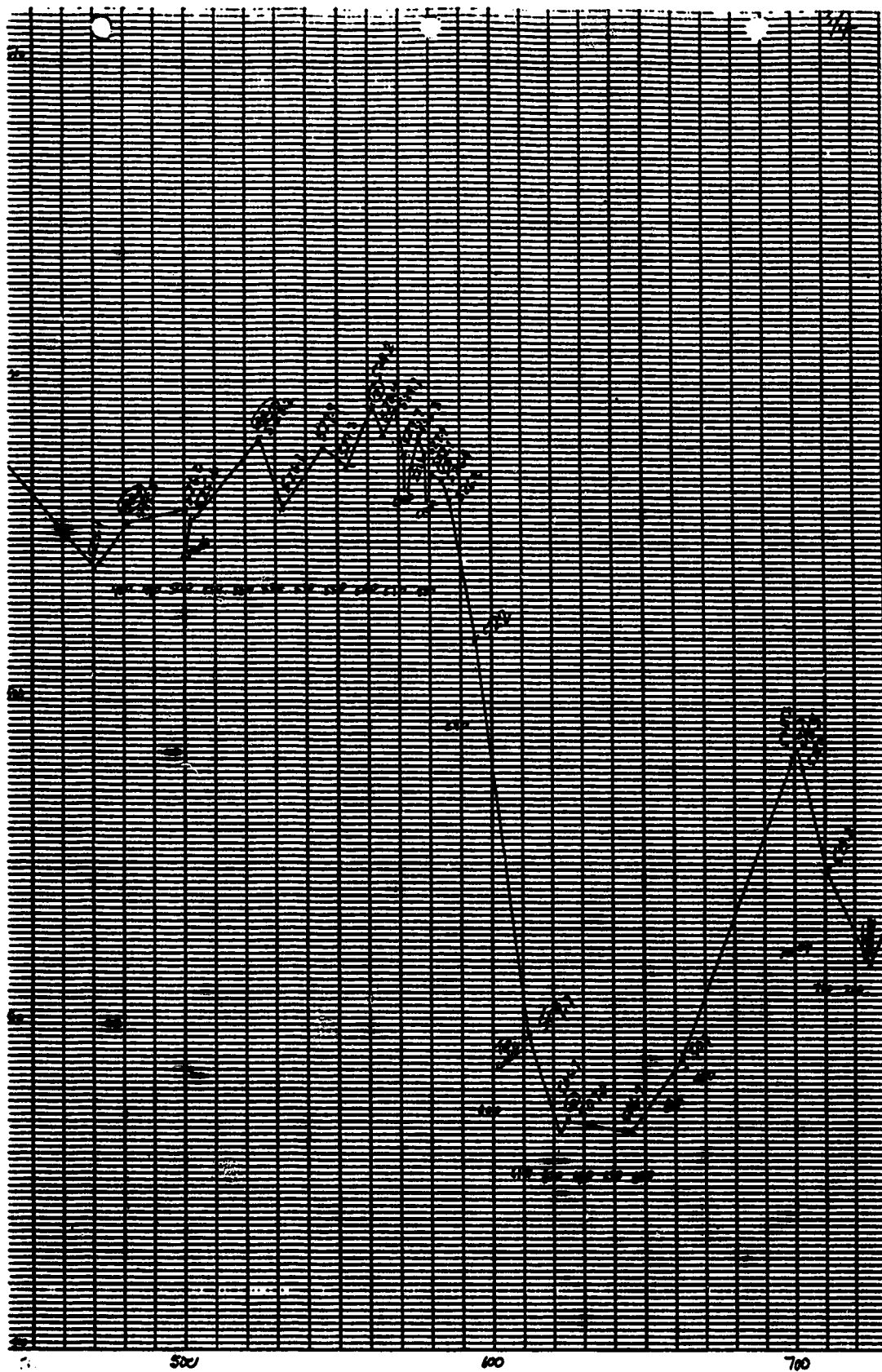
2-4-1968

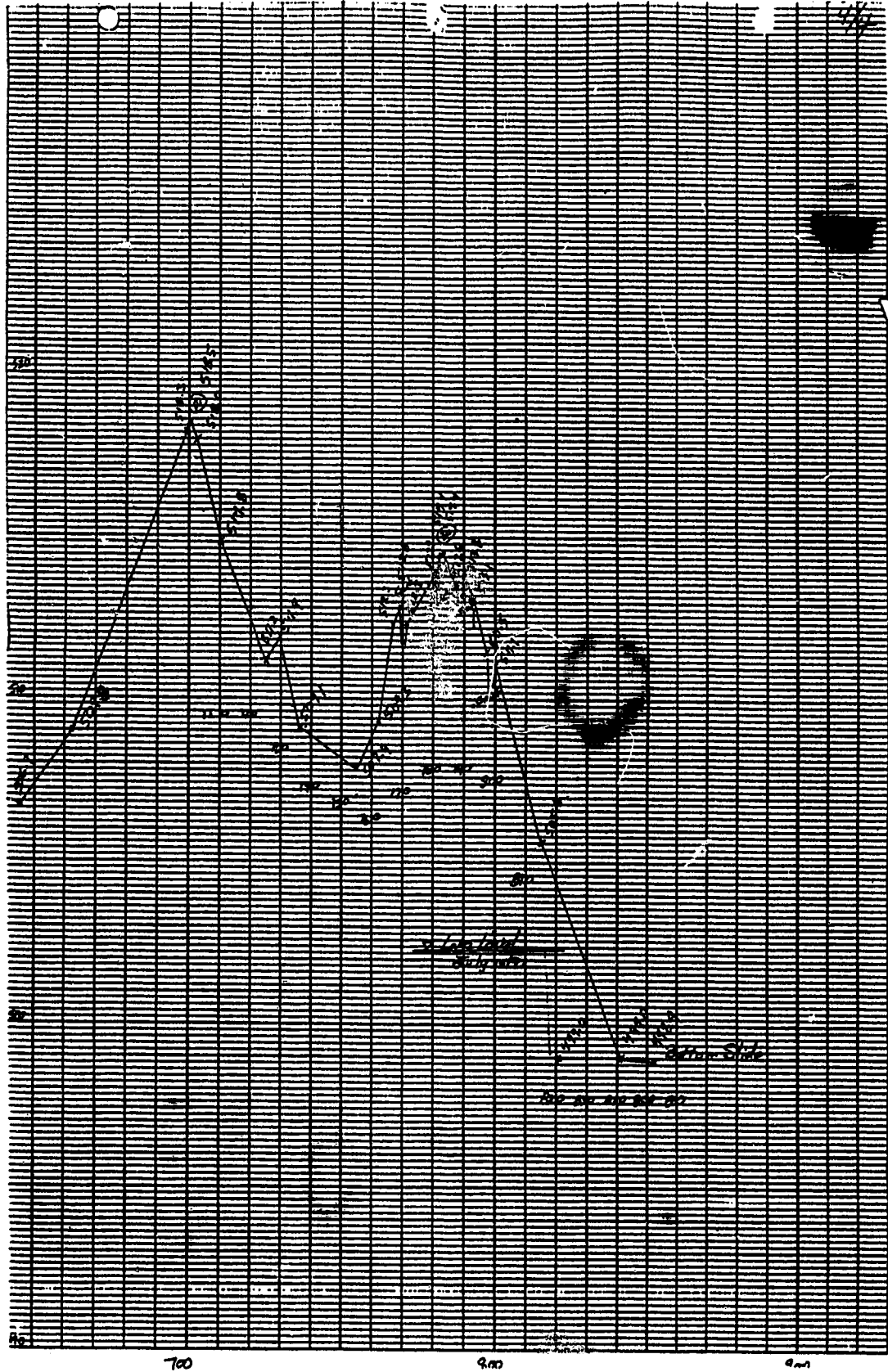


CENTRAL TROPIC
 OF
 RICKS
 SARAJEVO

Scale: 1 inch = 1000
 1/2 inch = 500







APPENDIX E: Laboratory Test Results

**Consolidated Undrained Triaxial test results on till,
Rycroft Landslide**

| Depth
(m) | Effective
Consolidation
Pressure
(kPa) | Peak
Deviator
Stress
(kPa) | Change
in
Pore
Pressure
(kPa) | σ_1
(kPa) | σ_3
(kPa) | Strain
% | A |
|--------------|---|-------------------------------------|---|---------------------|---------------------|-------------|------|
| 48.8-49.25m | 200 | 239 | 62.7 | 376 | 137 | 9.5 | 0.55 |
| 70.2-70.6m | 400 | 227 | 120 | 507 | 280 | 14.4 | 0.73 |
| 70.15-70.6m | Leaky membrane
800 | | 297 | 797 | 503 | 5.7 | 0.67 |
| 91.5-91.95m | 1200 | 672 | 462 | 1415 | 738 | 8.7 | 0.7 |
| 97.6-98.0 | 800 | 601 | 215 | 1180 | 585 | 8.5 | 0.71 |

**Direct shear test result on till,
Rycroft Landslide**

| SHEAR STRESS | | | |
|--------------|---------------------------|---------------|-----------------------------|
| Depth
(m) | NORMAL
STRESS
(kPa) | PEAK
(kPa) | STAGED
RESIDUAL
(kPa) |
| 97.6-98.0m | 800 | | 146 |
| 97.6-98.0m | 800 | 312 | |

**Direct shear tests results on preglacial lake clay,
Rycroft Landslide**

| SHEAR STRESS | | | | | | |
|-----------------------------|----------------------------|-------------------|--------------------------|------------------------------|-------------------|------------------------------|
| Sample # | NORMAL STRESS (kPa) | PEAK (kPa) | STAGED PEAK (kPa) | STAGED RESIDUAL (kPa) | PEAK (kPa) | STAGED RESIDUAL (kPa) |
| | 0 | | | | | |
| 1 | 200 | | | 32 | | |
| 1 | 205 | 46 | | | | |
| 1 | 400 | | | 39 | | |
| 2 | 400 | | | 66 | | |
| 1 | 411 | | 100 | | | |
| 1 | 443 | | 110 | | | |
| 2 | 800 | | | 95 | | |
| 2 | 812 | | 164 | | | |
| 3 | 823 | 212 | | | | |
| 3 | 1117 | | 210 | | | |
| 3 | 800 | | | 93 | | |
| 3 | 1200 | | | 140 | | |
| Cross-bedding tests: | | | | | | |
| C.B.#1 | 214 | | | | 72 | |
| C.B.#1 | 200 | | | | | 55 |
| C.B.#2 | 652 | | | | 243 | |
| C.B.#2 | 600 | | | | | 98 |
| C.B.#3 | 1200 | | | | | 199 |

**Consolidated Undrained Triaxial test results on preglacial lake clay,
Rycroft Landslide**

| Effective Consolidation Pressure (kPa) | Peak Deviator Stress (kPa) | Change in Pore Pressure (kPa) | σ_1 (kPa) | σ_3 (kPa) | Strain % | A |
|---|-----------------------------------|--------------------------------------|------------------------------------|------------------------------------|-----------------|----------|
| 800 | 600 | 200 | 1200 | 600 | 9 | 0.75 |

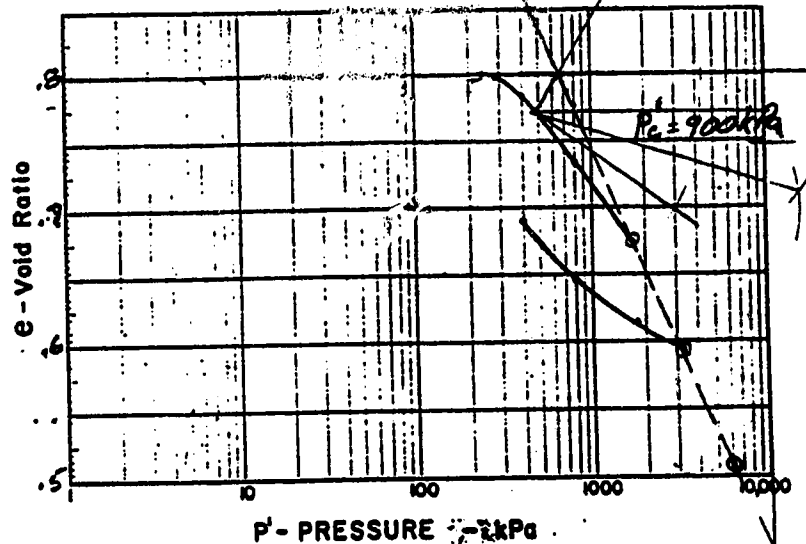
MATTE 1774-A



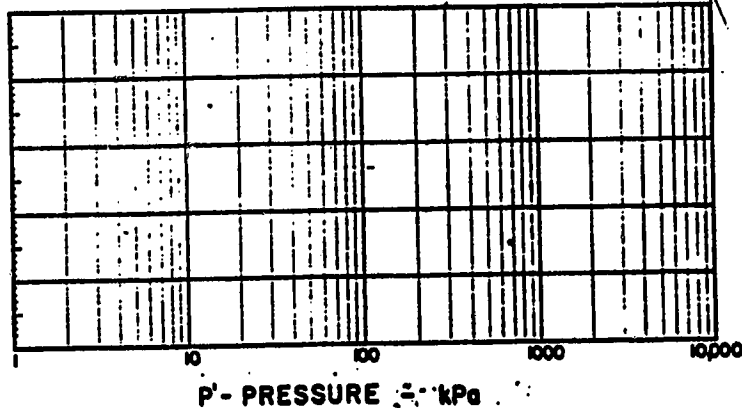
DESIGN AND CONSTRUCTION DIVISION
GEOTECHNICAL BRANCH
MATERIALS TESTING LABORATORY

PROJECT: HYDROFT SLIDE
HOLE No. RS-2 PREGLACIAL LAKE CLAY
DEPTH: 105.8 CORE SAMPLE
TECHNICIAN: LK, JK DATE: SEPT/91

CONSOLIDATION TEST



Cv - Coefficient of Consolidation
x 10 cm²/s
K - Coefficient of Permeability
x 10 cm/s



Soil Type: CH
Liquid Limit: 82.5 % Plastic Limit: 22.6 % Plasticity Index: 52.9 %
Sand: 0 % Silt: 5.6 % Clay: 44 %
Initial Water Content: 29.5 % Saturation: 99.3 %
Final Water Content: 25.9 % Saturation: 100.0 %
Swelling Pressure: 225.0
Compressive Index: .301
Preconsolidation Pressure (P_c): 900 kPa
Approx. Overburden Pressure (P_v):

Remarks:

**WATER RESOURCES DIVISION
EDMONTON, ALBERTA
SOIL MECHANICS LABORATORY
CONSOLIDATION RESULTS**

PROJECT RYCAFT LANDSLIDE
SITE BLOCK SAMPLE TP#3
SAMPLE PREGLACIAL LAKE CLAY
LOCATION _____
HOLE# _____ DEPTH _____
TECHNICIAN TRK DATE OCT 22/91

SPECIFIC GRAVITY OF SOIL SOLIDS $G_s = 2.74$ HEIGHT OF SOIL SOLIDS $H_s = 12244$ mm/cm
VOID RATIO e (start dimensions) = 1.0528 $S\%$ (start) = 97.7 $W\%$ (start) = 38.6
VOID RATIO e (end dimensions) = $W\%$ (end) = 43.1 $S\%$ (end) = 100.0 $W\%$ (end) = 53.98
SOIL TYPE = DefL

[illegible]